Green Ammonia: Optimising Production and Quantifying its Potential as an Energy Vector

Mr Richard Michael Nayak-Luke
New College
University of Oxford

Supervised by
Professor René Bañares-Alcántara

Submitted: 10th October 2019

Submitted with Revisions: 23rd February 2020



This thesis is submitted to the Department of Engineering Science, University of Oxford, in partial fulfilment of the requirements for the degree of Doctor of Philosophy

Declaration

I declare that this thesis is entirely my own work, and except where otherwise stated, describes my own research.

Richard M. Nayak-Luke
Student Number: 397671
New College
University of Oxford

Abstract

The environmental imperative to achieve net-zero emissions quickly to minimise the rise in average global temperature rise due to global warming is clear. To achieve this, variable renewable energy (VRE) needs to substitute existing energy sources in the polluting sectors: electricity, heat, transport and industry. The integration of VRE sources to high levels of penetration however, is difficult: unlike most commodities, supply and demand must be in equilibrium at each moment in time, from the sub-second to inter-annual. This study quantifies the flexibility required by a power network to integrate additional VRE sources as a function of the magnitude and duration of the electrical energy storage required. The original energy storage requirement modelling tool (ESRMT) calculates: 1) the storage magnitude index (SMI), 2) the storage duration index (SDI) and 3) the storage size required. This quantifies the impact of VRE penetration, the mix of VRE sources and the application of other flexibility methods on the storage requirements. The ESRMT is used to consider locations in Japan, the UK, Canada and Australia and shows that, while requirements do increase with VRE penetration, the magnitude and type is location specific and highly dependent on the mix of VRE sources. Medium and long-term storage required at high VRE penetration are difficult to mitigate. The chemical storage of electrical energy, using ammonia, is a promising solution due to its favourable chemical and technical properties. The decarbonisation of the ammonia production is itself an environmental imperative as it accounts for 1.3% of global carbon dioxide emissions and supports over 48% of the global population through nitrogen based fertilisers. The developed islanded ammonia production modelling tool (IAPMT) optimises the mix of VRE sources, plant design and operation to minimise the levelised cost of ammonia (LCOA) at any given location. The IAPMT is used to consider ammonia production at 534 locations in 70 countries. It shows that at the best location a LCOA of $\$473 t^{-1}$ is currently achievable, but this will decrease to $\$310 t^{-1}$ by 2030. Decarbonised production will be highly competitive with conventional production by 2030. Assuming its use for seasonal storage, these

LCOA estimates mean that the levelised cost of electricity (LCOE) of power-to-ammonia-to-power of \$252MWh^{-1} by 2030.

Keywords: Ammonia, Haber-Bosch, LCOA, LCOE, Variable Renewable Energy, Energy Storage, Islanded Production, Decarbonised, Network Flexibility.

Acknowledgements

I would first like to thank my supervisor Professor René Bañares-Alcántara for his continued guidance to give me the opportunity to begin the project, ensure its success and support to me as a colleague and friend. Dr Manojkumar Ramteke's academic contributions prior, during and after my visit to Indian Institute of Technology (IIT) Delhi in January - June 2019 facilitated further development of the models and interesting results. I would also like to thank Ian Wilkinson at Siemens for the opportunity to work on the proof-of-concept power-to-ammonia-to-power plant at Harwell, Oxfordshire.

Sam Collier (and Professor Bañares-Alcántara) supported the energy storage modelling with his 4th year project "Quantifying and Classifying the Need for Energy Storage".

Without financial assistance I would not have been able to conduct this research. For this I am deeply grateful to the Engineering and Physical Sciences Research Council (EPSRC) and Siemens for funding this research under the iCASE Award 1658940, and the British Council and IIT Delhi to support my collaborative work with Dr Ramteke under the Newton-Bhabha Fund. The use of Aspen Plus, Aspen Economic Evaluator and MATLAB (including its numerous applications) were used under a AspenTech and MATLAB academic licences respectively.

All of my teachers and tutors have been invaluable in this journey. Here I would like to highlight a few that have been particularly important to me both academically and personally: Mrs Teresa Dunbar, Mr Graham Dunbar, Dr Ian Gray, Dr Douglas Hamilton, Dr John Huber and Professor René Bañares-Alcántara. Finally I would like to thank my parents, grandparents and sister without whom I would not have been able to get to this point. For their ever-present support and the sacrifices they have made for me I will be forever grateful. I would also like to thank my wife, Sophia, for supporting me in all my endeavours, keeping me sane and consistently putting up with me coding at all hours. I cannot thank you enough.

Nomenclature

\$	United States Dollar
α	Index When the Deficit Has Been Filled
Γ	Cumulative Sum of Δ
γ	Cumulative Sum of δ
Δ	Supply - Demand
Δ^*	Temporary Δ
$\Delta H_{\mathrm{f}}^{\circ}$	Enthalpy of Formation
Δx	Change in the Percentage Change of Cost
Δy	Change in the Percentage Change of the Mass of Ammonia Produced
Δz	Change in the Percentage Change of the Levelised Cost of Ammonia
$\Delta_x z$	Change in the Percentage Change of the Levelised Cost of Ammonia due to the Change in Cost
$\Delta_y z$	Change in the Percentage Change of the Levelised Cost of Ammonia due to the Change in the Mass of Ammonia Produced
δ	Temporary and Constrained Version of Δ
η	Efficiency
η_{H2FC}	Efficiency of the Fuel Cell (Lower Heating Value)
θ	Fraction of Renewable Energy Supplied by Wind
λ	Renewable Penetration: Fraction of Supplied Energy Provided by Renewable Energy Sources

μ	Excess Energy Factor
ρ	Magnitude of Renewable Energy Curtailment as a Fraction of the Total Renewable Energy Supplied
σ	Standard Deviation
τ	Storage Duration (hours)
τ^*	Potential Storage Duration (hours)
τ_{max}	Maximum Storage Duration (hours)
Φ	Storage Matrix
AFOLU	Agriculture, Forestry and Other Land Use
ASU	Air Separation Unit
atm	Atmospheric Pressure
BAT	Best Available Technology
BECCS	Bioenergy with Carbon Capture and Storage
C	Celsius
CAGR	Compound Annual Growth Rate
CAPEX	Capital Expenditure
CAT	Climate Action Tracker
CCGT	Combined Cycle Gas Turbine
CCS	Carbon Capture and Sequestration
CfD	Contracts For Difference
CH_4	Methane
CO_2	Carbon Dioxide
CoMoN	Cobalt Molybdenum Nitride Catalyst
dB	Decibels
DSM	Demand Side Management
E	Energy
E	World's Global Energy Consumption
EF_{Elec}	Electrolyser Excess Factor
ESRMT	Energy Storage Requirement Modelling Tool

EUR	Euro
F	Global CO_2 Emissions Flux from Fossil Fuel Consumption and Industrial Processes
FLH	Full Load Hours Equivalent
G	World's Gross Domestic Product
GBP	Pound Stirling
GDP	Gross Domestic Product
GHG	Greenhouse Gas
$GtCO_2e$	Giga Tonnes of Carbon Dioxide Equivalent
H	Hydrogen
HB	Haber-Bosch Synthesis Process
HHV	Higher Heating Value
HVDC	High Voltage Direct Current
IAPMT	Islanded Ammonia Production Modelling Tool
IEA	International Energy Agency
INDC	Intended Nationally Determined Contribution
IoT	Internet of Things
IPCC	Intergovernmental Panel on Climate Change
IRENA	International Renewable Energy Agency
ISPT	Institute for Sustainable Process Technology
IIT	Indian Institute of Technology
LCOA	Levelised Cost of Ammonia
$LCOA_{Actual}$	Levelised Cost of Ammonia Calculated Using Actual Renewable Energy Profiles
$LCOA_{Ideal}$	Levelised Cost of Ammonia Calculated Using an Ideal Energy Profile
LCOE	Levelised Cost of Electricity
LHV	Lower Heating Value
LNG	Liquified Natural Gas

m	Mass
Mass_{Actual}	Mass of Ammonia Produced Using Actual Renewable Energy Profiles
Mass_{Ideal}	Mass of Ammonia Produced Using Ideal Energy Profile
MCH	Methylcyclohexane
$\text{m}_{H2Consumed}$	Mass of Hydrogen Consumed
MM_{H2}	Molecular Mass of Hydrogen
MM_{NH3}	Molecular Mass of Ammonia
MP-IAMs	Mitigation-Process Integrated Access Models
N_2	Nitrogen
N_2O	Nitrous Oxide
NEA	Nuclear Energy Agency
NH_3	Ammonia
NH_32P	Ammonia-to-Power
NSGA	A Multi-objective Non-dominated Sorting Genetic Algorithm
OPEX	Operational Expenditure
P	Power
P	Global Population
P^*_{Elec}	Trialled Rated Power of the Electrolyser
$P^*_{HB/ASU}$	Trialled Rated Power of the Haber-Bosch Synthesis Process and the Air Separation Unit
P^*_{Plant}	Trialled Rated Power of the Entire Process
p.a.	Per Annum
p/kWh	British pence per Kilowatt Hour
$P2NH_3$	Power-to-Ammonia
P2X	Power-to-X
P_{Elec}	Power of the Electrolyser
$\text{P}_{ElecRated}$	Rated Power of the Electrolyser
$\text{P}_{ElecStoic}$	Stoichiometric Power of the Electrolyser

PEM	Proton Exchange Membrane
$P_{HB/ASU}$	Power of the Haber-Bosch Synthesis Process and the Air Separation Unit
$P_{HB/ASURated}$	Rated Power of the Haber-Bosch Synthesis Process and the Air Separation Unit
$P_{PlantStoic}$	Stoichiometric Power of the Entire Production Plant
PV	Photovoltaic
r	Discount Rate
R&D	Research and Development
RES	Renewable Energy Sources
RFC	Reasons For Concern
Ru	Ruthenium Catalyst
SCF	Supply Capacity Factor
SDI	Storage Duration Index
SMI	Storage Magnitude Index
SMR	Steam Methane Reforming
SOFC	Solid Oxide Fuel Cell
$SpecC_{Elec}$	Specific Energy Consumption of the Electrolyser
$SpecC_{HB}$	Specific Energy Consumption of the Haber-Bosch Synthesis Process
SSAS	Solid State Ammonia Synthesis
t	Metric Tonne
tCO_2/t	Metric Tonnes of Carbon Dioxide per Metric Tonne of Ammonia
t_{First}	First Time Interval
t_{Last}	Last Time Interval
U	Speed (meters per second)
UK	United Kingdom of Great Britain and Northern Ireland
ULG	Unleaded Gasoline
USA	United States of America
V2G	Vehicle-to-Grid

VRE	Variable Renewable Energy
W	Watt
WS	Wind Speed
x	Percentage change of Cost
y	Percentage change of Mass of Ammonia Produced
z	Percentage change of the Levelised Cost of Ammmonia

Contents

Abstract **ii**

Acknowledgements **iv**

Nomenclature **v**

1 Introduction **1**

1.1 Thesis Overview 1

1.2 Environmental Context 7

1.3 Technical Context 20

2 Literature Review **40**

2.1 Network Flexibility Required for Renewable Energy Integration . . . 41

2.2 'Green' Ammonia Production and Use 49

2.3 Importance of Achieving the Research Objectives 55

3 Methodology **62**

3.1 Energy Storage Requirement Modelling Tool (ESRMT) 62

3.2 Islanded Ammonia Production Modelling Tool (IAPMT) 78

4 Calculations **95**

4.1 Energy Storage Requirement Modelling Tool (ESRMT) 95

4.2 Islanded Ammonia Production Modelling Tool (IAPMT) 102

5 Results **109**

5.1 Energy Storage Requirements Due to VRE Integration 109
5.2 Global Potential for Islanded 'Green' Ammonia Production 138

6 Discussion **152**

6.1 Overview of Environmental and Technical Context 152
6.2 Restatement of Research Objectives 153
6.3 Contribution 154
6.4 Discussion of Key Findings 156

7 Conclusion **164**

7.1 Key Findings 164
7.2 Critical Review 166
7.3 Future Work 168

Bibliography **170**

Appendices **192**

Chapter 1

Introduction

1.1 Thesis Overview

1.1.1 Research Hypothesis

There are three interconnected hypotheses in this thesis:

1. The magnitude and duration of energy storage (network 'flexibility') required when integrating variable renewable energy (VRE) supply in an electrical network are quantifiable. A high VRE penetration requires significant seasonal balancing (i.e. seasonal electrical energy storage).

2. Decarbonised 'green' ammonia production (i.e. sourcing hydrogen feedstock from water electrolysis using variable renewable energy instead of fossil fuels) is not only an environmental imperative, but with optimised location selection and process design will be commercially competitive in the medium-term. Industry standard fossil-fuel based ammonia production can therefore be substituted to meet current and future conventional demand (i.e. nitrogen based fertiliser).

3. Green ammonia can be an economically viable energy vector to meet seasonal electrical network balancing requirements (i.e. seasonal electrical energy

storage) by using decarbonised and commercially competitive optimised production.

1.1.2 Research Objectives

- Quantify an electrical network's flexibility requirement (defined as the "ability to... respond [to] the variability and uncertainty of the net load" [1]), both the magnitude and as a function of the duration of energy storage.
- Identify the impact that location, the penetration of renewables and power supply have (both independently and in combination) on the energy storage requirement, with particular focus on seasonal requirements, and how this is mitigated by curtailment.
- Construct a model to identify the optimal design and operation of an islanded 'green' ammonia production process for any given location.
- Identify the range of achievable levelised cost of ammonia (LCOA) for islanded 'green' production, the dominant cost components, the scope and likelihood of future reduction and benchmark this against conventional production.
- Identify the economic viability of using 'green' ammonia to meet seasonal balancing requirements.

1.1.3 Thesis Structure

To demonstrate the importance, novelty, validity and potential impact of the hypothesis, this thesis is formed of seven chapters, the structure and how each chapter meets the research objectives are shown below (see Figure 1.1).

The introduction (Chapter 1) outlines the context, both environmental and technical, and the motivation for this research, demonstrating the research's value. The environmental context shows the paramount importance of achieving net-zero CO_2 emissions quickly and how current CO_2 emission targets and drivers of change are

falling short of the required trajectory to meet this target. The rationale for selecting electrical and chemical (specifically ammonia production) industries is explained (low cost abatement, importance and potential bi-directional synergies). The technical context outlines the problems of achieving decarbonisation in these industries, potential solutions that are being considered and their merits. In summary, the context demonstrates the importance of achieving the research objectives. Objectives one and two would clarify the balancing problems caused by increased VRE penetration, different VRE power sources and location in an electrical network. Policy makers can use this to achieve VRE penetration targets most efficiently. Other stakeholders, such as academia and industry, could use this to understand the magnitude and type of future network flexibility required: enabling them to identify the most beneficial technological improvements or reductions in cost.

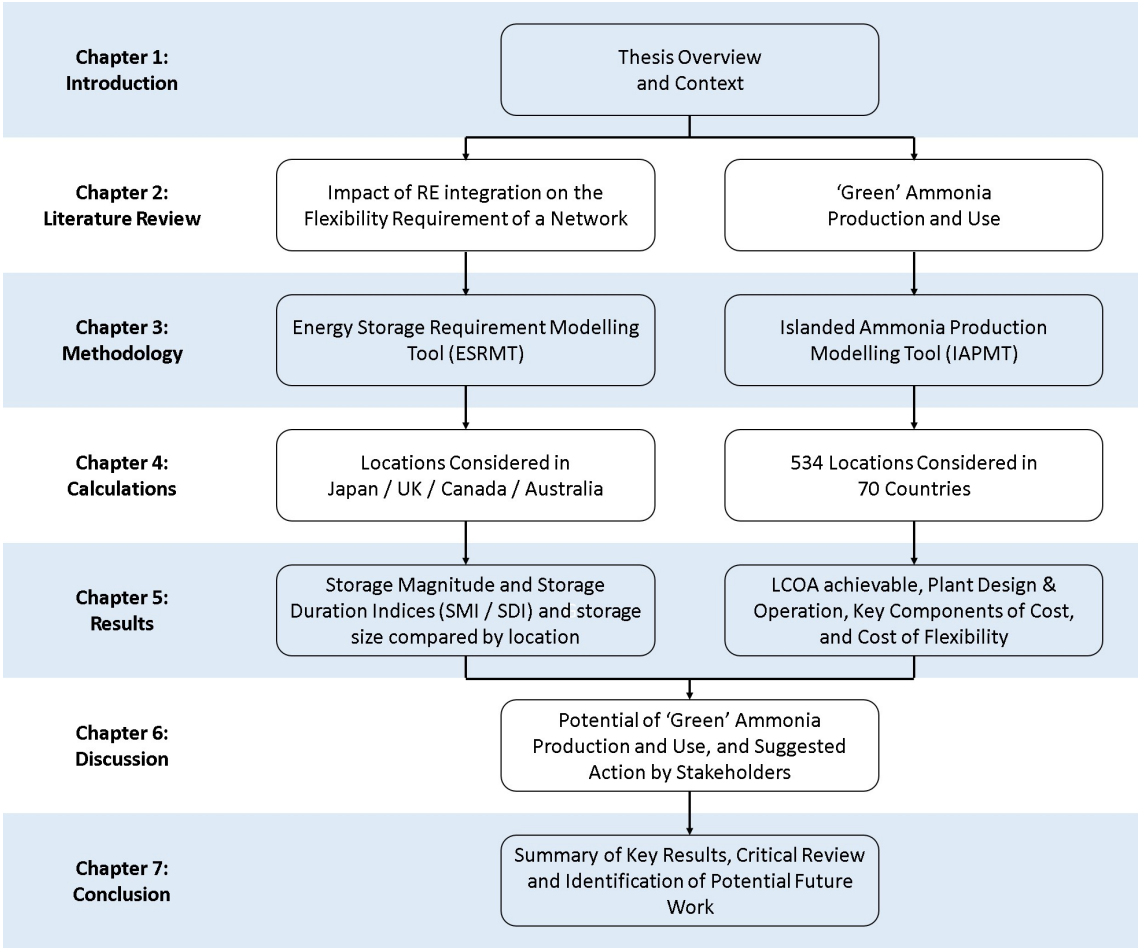

Figure 1.1: Overview of Thesis Structure

Chapter 2 (Literature Review) critically evaluates previous work on decarbonising

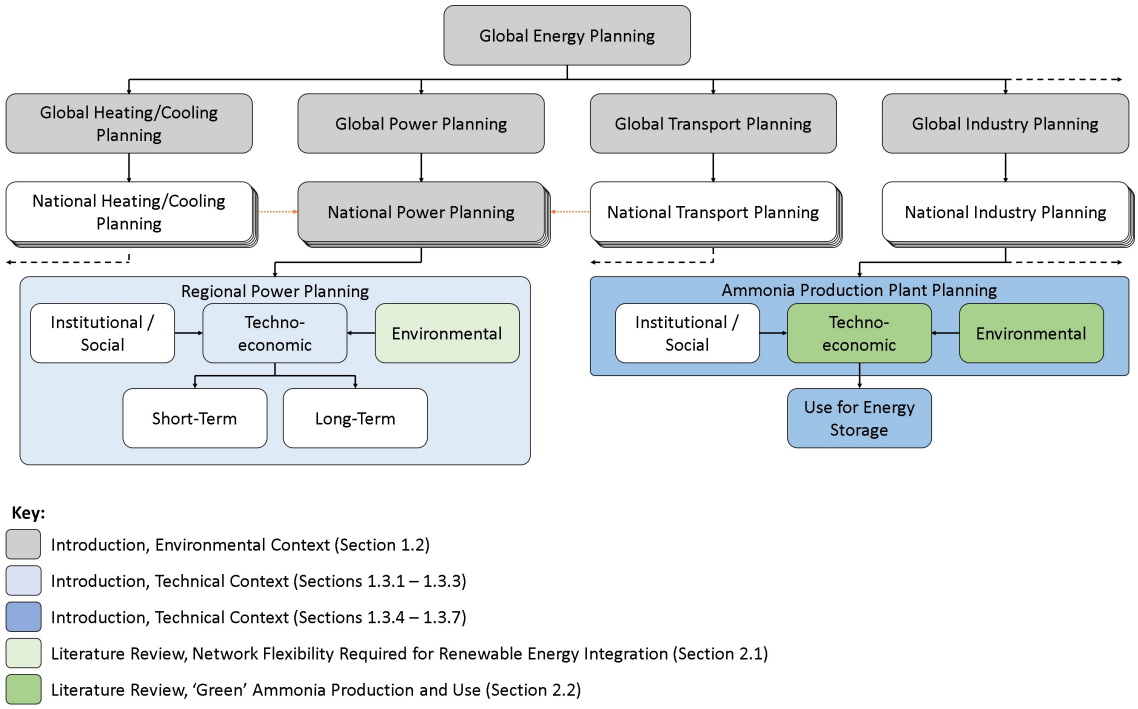

Figure 1.2: Overview of the Context Provided (adapted from [2])

the electrical industry and ammonia production. It identifies the current knowledge gaps and why they need to be filled with novel research. There are two important gaps (Section 1.1.2): quantifying the impact of variable renewable energy integration on the flexibility requirements of electrical networks, and the optimisation of the location, system design (VRE sources and process design) and the operation of islanded 'green' ammonia production. This chapter until Chapter 6 presents the complementary work that fills these independent gaps, as shown in Figure 1.1.

Chapter 3 (Methodology) explains the two MATLAB models and their functionality to provide answer to the knowledge gaps identified earlier. The first, the Energy Storage Requirement Modelling Tool (ESRMT), applies the chemical engineering principle of temporal pinch to quantify the flexibility requirement of a given electrical network. The ESRMT produces two non-dimensional indices (as results) to show the fundamental balancing problem:

1. How much energy needs to be stored (the fraction of total energy demand met by stored energy): the Storage Magnitude Index (SMI);

2. How long the energy needs to be stored (on average): the Storage Duration Index (SDI).

It explains why these two indices (SMI and SDI) are important. They show the impact that individual and multiple decision variables have on the magnitude and duration of flexibility required.

The second (the islanded ammonia production modelling tool's (IAPMT)) objective function is to minimise the levelised cost of ammonia (LCOA). To do this it optimises the decision variables: the variable renewable energy sources, the design of the production process and its operation.

Chapter 4 (Calculations) describes how these two models have been used (i.e. the simulations that have been run) in order to fill the gaps in knowledge identified in Chapter 2 and achieve the research objectives. The ESRMT is used to identify the flexibility needed in electrical power networks at locations in the United Kingdom (UK), Japan, Canada and Australia under different VRE penetrations and mix of renewable power sources (i.e. the ratio of energy provided by wind and solar PV). The IAPMT uses data for 534 locations in 70 countries to find the best areas to locate a plant, the VRE mix of sources to employ, design of the production process, how it should be operated and the achievable LCOA. The IAPMT compares an 'ideal' power profile with realistic wind and solar PV profiles to quantify the process flexibility cost needed for the plant to be technically viable. Sensitivity analyses identify the key technical and economic decision variables and quantify their impact on the achievable LCOA, process design and operation.

Chapter 5 (Results) presents the results from the calculations explained in Chapter 4. Analysis of the ESRMT results for Japan, the UK, Canada and Australia, both as individual countries and comparatively, identifies the flexibility required depending on the VRE penetration and the VRE mix. This highlights common vs. location specific requirements. The magnitude of flexibility requirement increases significantly with the VRE penetration for all locations considered. This is shown

to be mitigable by curtailment to varying degrees depending on location. The impact of the VRE source mix on the magnitude of flexibility and on the duration of flexibility required (i.e. when storage requirements surpass battery storage) depends significantly on country and specific location.

The IAPMT results show that, even without government incentives, islanded 'green' ammonia production will be economically competitive in the best locations, and that more locations will be viable, by 2030 vs. conventional (fossil-fuel based) methods. Green ammonia will be a very economical long-term (seasonal) electrical storage method if the predicted 2030 estimates of LCOA are achieved. IAPMT results show the individual cost components of producing green ammonia (as a fraction of the total LCOA) and the cost of plant flexibility (i.e. to manage VRE intermittency) and show how to achieve, and further reduce, predicted 2030 LCOA estimates.

Chapter 6 (Discussion) explains how the knowledge base gaps (from Chapter 2), and the research objectives (Section 1.1.2) are met by the research in Chapters 3 and 5. Specifically, the ESRMT and the IAPMT achieve research objectives one and three. The results from each meet research objectives two and four respectively. Drawing together these two parallel strands of research, objective five is achieved by identifying how economical 'green' ammonia is / will be to meet seasonal balancing requirements, thereby proving the validity of the research hypothesis (Section 1.1.1). The ESRMT results show that even with optimised power source selection and curtailment in the most favourable location, high VRE penetration requires long-term energy storage. Predictions from the IAPMT show that the green production of ammonia will, by 2030, not only be highly cost competitive with conventional (fossil-fuel) methods but also be a cost effective method of seasonal energy storage.

Chapter 7 (Conclusion) highlights the key findings of the research and explains why the research hypothesis (stated in Chapter 1) is important, novel and valid using this research's models and results. This research is important to the development and implementation of green ammonia production and use. Developments to the ES-

RMT and IAPMT are identified in a critical review and outlined in future work. In conclusion: seasonal energy storage will be increasingly important to achieve emission targets as VRE penetration increases. Producing green ammonia will meet this need requirement cost efficiently and substitute conventional ammonia production.

1.2 Environmental Context

This section provides the operational environment context for this research:

1. Identifying the need to reduce greenhouse gases (GHG) emissions to net-zero
2. The imperative to achieve net-zeo emissions quickly
3. How and why current public and private targets are insufficient to achieve net-zero (either at all or quickly)
4. The most economical actions that could meet the current shortfall.

This section will not present a mix of facts and ethics, but seeks to emulate MacKay's approach in explaining "how the facts constrain the options that are open to us" [3]. The only exception is in recommending where additional action is required (in Section 1.2.3). Here, recommendations are "grounded in", "although not determined by", economics [4].

1.2.1 The Imperative to Achieve Net-Zero CO_2 Emissions Quickly

It is the overwhelming scientific consensus that human GHG emissions into the atmosphere are increasing the average global temperature: "human activities are estimated to have [already] caused approximately 1.0°C of global warming above pre-industrial levels" [6]. Five key economic sectors account for these emissions (Figure 1.3a): industry (32% when combining direct and indirect emissions), agriculture, forestry and other land use (AFOLU) (25%), buildings (18%), transport (14%) and

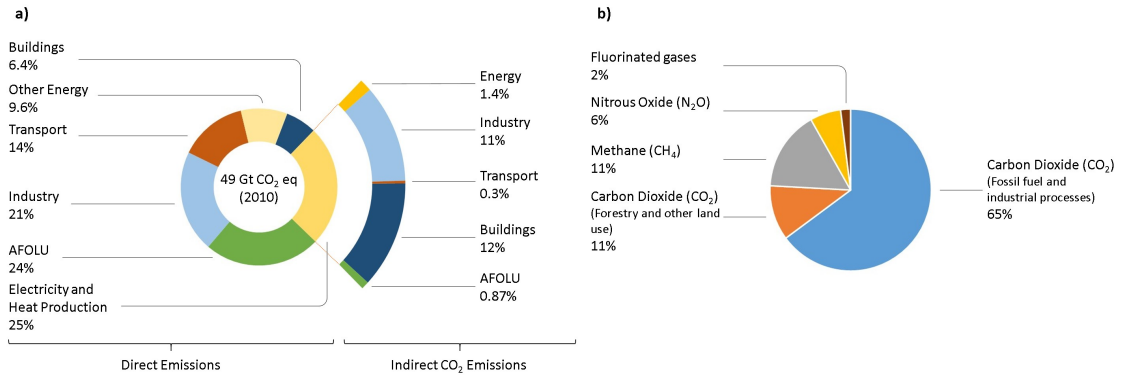

Figure 1.3: Global GHG emissions by a) economic sector and b) gas for 2010 [5]. AFOLU: Agriculture, forestry and other land use. Rounding to two significant figures accounts for arithmetic discrepancies.

other energy demand (11%). Most (over 75%) of GHGs emitted are carbon dioxide (CO_2)(Figure 1.3b).

Prior to human intervention, the 'greenhouse effect' (water vapour and other gases as in Figure 1.3 in the atmosphere retaining heat in the earth's atmosphere) regulated the earth's temperature. The global average CO_2 concentration has fluctuated "between about 180ppm during ice ages and 280ppm during interglacial warm periods" [7], with a maximum of 300ppm for the past 800,000 years (pre-industrial revolution) [8]. In 2018 however, the global average CO_2 concentration reached 407.4ppm [9]. Although the concentration of CO_2 is measured easily, the impact of our emissions is not. Cumulative net CO_2 emissions increasing the concentration of CO_2 contributes to global warming. Negative CO_2 feedback (e.g. additional rock weathering and increased dissolution of CO_2 in seawater) that would mitigate this warming and positive CO_2 feedback (e.g. release of methane in permafrost) that would accelerate are also factors in global warming. Positive feedback provides tipping-points when warming perpetuates warming and could lead to irreversible changes.

The last time that that CO_2 levels were at current levels was over three million years ago, when the "temperature was 2°C - 3°C higher than during the pre-industrial era, and [the] sea level was 15 – 25 meters higher than today" [9]. The most recent IPCC report [6] shows (Figure 1.4) the "impacts / risks" on many systems are stark at a 2°C rise. Even at the present level (shown as the "likely" range of 0.8°C - 1.2°C)

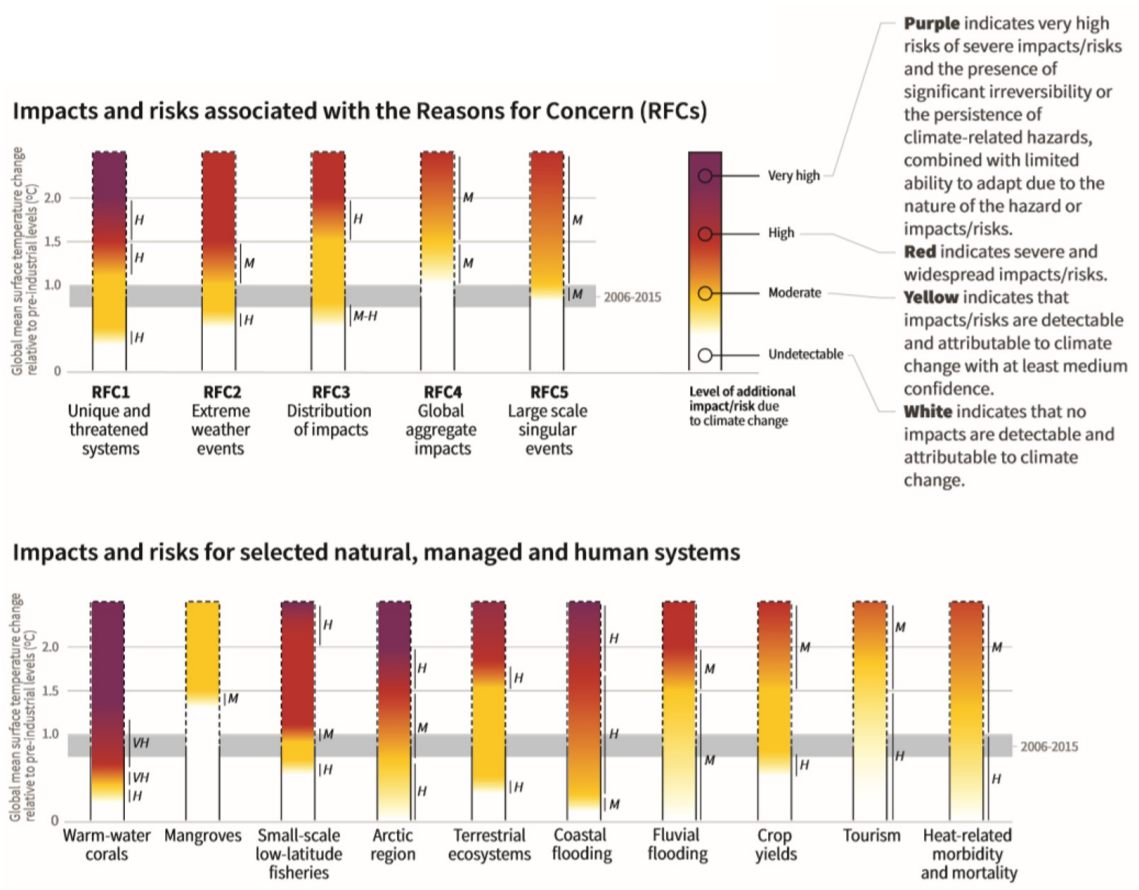

Figure 1.4: The predicted risks from global warming of 2°C for "people, economies, and ecosystems [6]

the consequences are concerning. To avoid these, and worse at higher levels of global warming, global GHG emissions (particularly CO_2) need to decrease (Rogelj [10], Millar [11] and IPCC [6]). Rhetoric that reducing current CO_2 emissions to a low level is sufficient is incorrect. Conservatively assuming that the current global climate is in equilibrium (i.e. the current temperature increase is in a steady-state for the CO_2 concentration and the feedback loops cancel each other out), then the only driving force for an increase in the CO_2 concentration and temperature rise would be an increase in the cumulative net amount of CO_2 emissions. In other words, the average global temperature will only not increase if (and only if) the net emission of CO_2 is less than or equal to 0.

IPCC [6] (building on Millar [11], Krey and Riahi [12] and Bosetti [13]) show that achieving net-zero targets by 2040 (grey in Figure 1.5) or 2055 (in blue) changes the effects of global warming, and therefore the importance to achieve targets quickly.

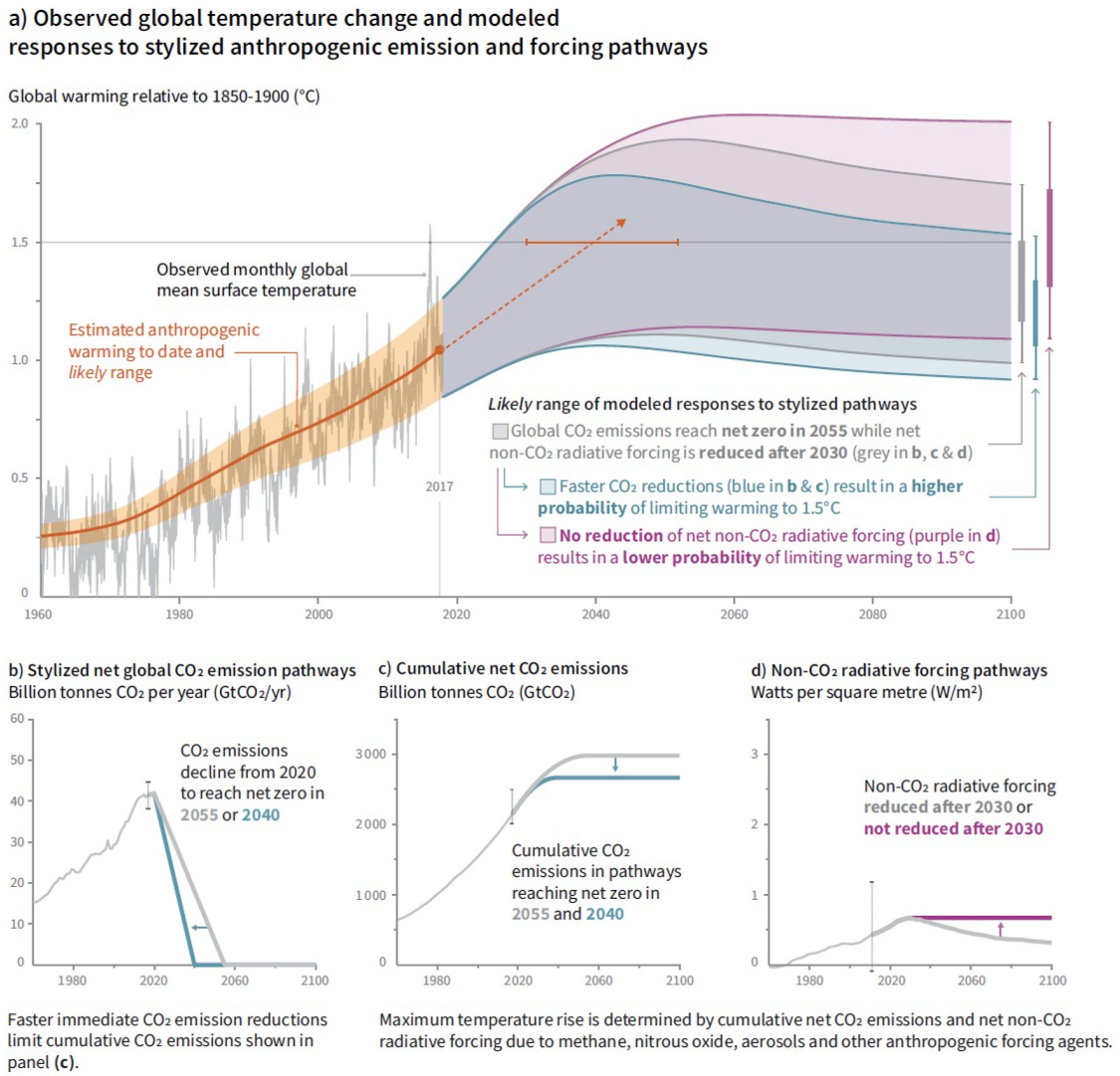

Figure 1.5: The predicted impact of cumulative CO_2 emission levels and non-CO_2 radiative forcing on global warming relative to 1850-1900 [6]

Both scenarios likely keep the maximum temperature rise below 2°C. However, if 'net-zero' is achieved earlier the maximum temperature rise, how quickly the rise decreases and the new steady-state temperature are substantively different.

IPCC set out four pathways to limit global warming to 2 degree, all require net-zero emisisons by "around 2050" (Figure 1.6):

1. Decreasing and decarbonising the energy system and afforestation as the only carbon dioxide removal method.

2. Similar to pathway 1 but with slower energy system decarbonisation and increased afforestation, some BECCS.

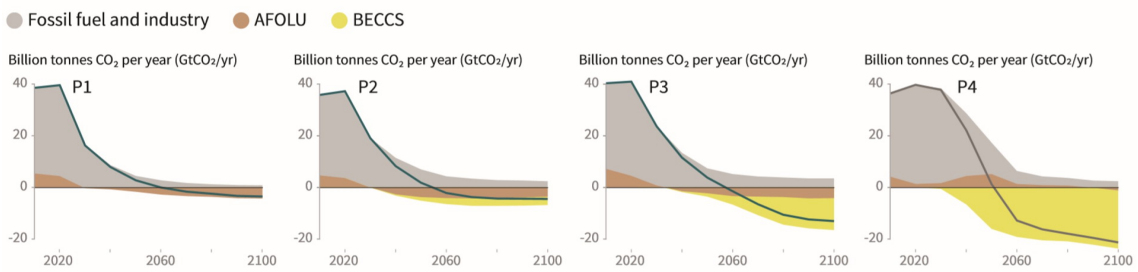

Figure 1.6: Breakdown of contributions to global net CO_2 emissions [6]. AFOLU: Agriculture, forestry and other land use; BECCS: bioenergy with carbon capture and storage.

3. decarbonising energy and production rather than reducing energy demand (through societal and technological development which has historical precedent).

4. Significant BECCS enabling continued "resource- and energy-intensive... GHG-intensive lifestyles".

1.2.2 Present CO_2 Emission Targets and Drivers for Reduction

To limit global warming below 2°C, GHG emissions need to be net-zero by 2050. This section shows efforts to reduce GHG emissions, the future GHG emission targets that have been set, whether the current progress and targets align with meeting the net-zero target by 2050 and other drivers that could help to achieve 'net-zero'.

Targets

The November 2016 'Paris Agreement' agreed to "hold warming well below 2°C, and pursue efforts to limit warming to 1.5°C above pre-industrial levels; and to limit the increase to 1.5°C, since this would substantially reduce the risks and effects of climate change". The USA, China and India and 186 countries signed but are not bound legally to emission targets (intended nationally determined contributions: INDCs). Each country defined its own INDCs. There are no barriers to exiting (e.g. the USA intends to exit in November 2020). The INDCs, together, fall short of what is

required: both in magnitude and timeliness Figure 1.7.

INDCs are insufficient to achieve net-zero CO_2 emissions by 2050. Firstly, INDCs do not account for the costs of decarbonising which decrease a country's economic competitiveness. Secondly, the issue of 'fairness' and how to equitably share the reduction in CO_2 emissions between countries? Many countries' quick development over the past 150 years was fuelled by large scale fossil fuel use. The 2°C target will be missed if even a few countries follow a similar fossil fuelled growth strategy.

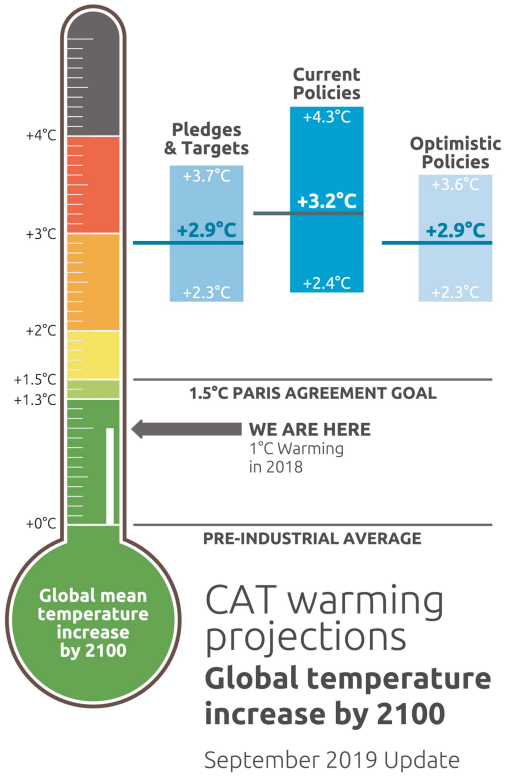

Figure 1.7: The Climate Action Tracker's (CAT) estimate of the global mean temperature rise by 2100 [14]

Developed countries have maintained their high energy consumption per capita (despite some reductions over the last 20 years, Figure 1.9b). For example, up to 2017 the UK has emitted 77.07Bt CO_2 equivalent vs. India's 48.56Bt CO_2, where the UK population is 67M vs. 1.34B. China's total emissions p.a. were largely driven by population growth between 1960 and 2000. Increased demand per capita has driven the recent accelerated emissions (Figure 1.9). If India, Brazil and Indonesia replicated this increase in emissions per capita while other countries retained their emission profiles, global warming targets would not be met. Climate change action needs to account for these countries' development and environmental and socio-economic issues e.g. poverty reduction or water availability [15, 6].

Furthermore, developed countries (e.g. the UK with a net-zero targets by 2050) are offsetting rather than reducing overall carbon emissions i.e. they may meet their

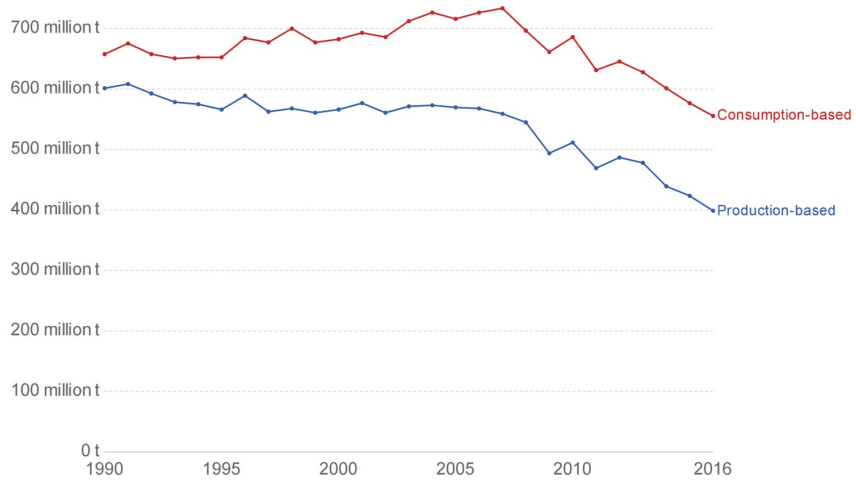

Figure 1.8: Annual production based and consumption based CO_2 emissions for the UK 1990-2016 [16]

carbon budgets but only as carbon consumption is no longer attributable to them under current carbon accounting norms (Figure 1.8).

Current policies to manage these issues would achieve net-zero emissions after 2050 (Figure 1.10). To understand what INDCs need to be and how to achieve them through policy a clear understanding of emissions drivers is needed.

There are four components of global CO_2 emissions in the Kaya identity [18] (Equation 1.1 [19]): global population (P), global mean gross domestic product (GDP) per capita $\left(\frac{G}{P}\right)$, energy intensity of GDP $\left(\frac{E}{G}\right)$ and the carbon intensity of energy $\left(\frac{F}{E}\right)$. Where F represents the "global CO_2 emissions flux from fossil fuel consumption and industrial processes", G the world's gross domestic product (GDP) and E the world's global energy consumption. Most indicators are not moving in the right direction to limit global emissions.

$$F = P \times \left(\frac{G}{P}\right) \times \left(\frac{E}{G}\right) \times \left(\frac{F}{E}\right) \tag{1.1}$$

Global population growth remains above 1% p.a. despite rates declining since the 1962-1963 2.2% p.a. peak. Population is predicted to continue to increase beyond 2100 [20]. The global mean gross domestic product (GDP) per capita has grown at a CAGR of 2.2% (1990-2016), despite slowing from 2014-2016 and the 2008 financial

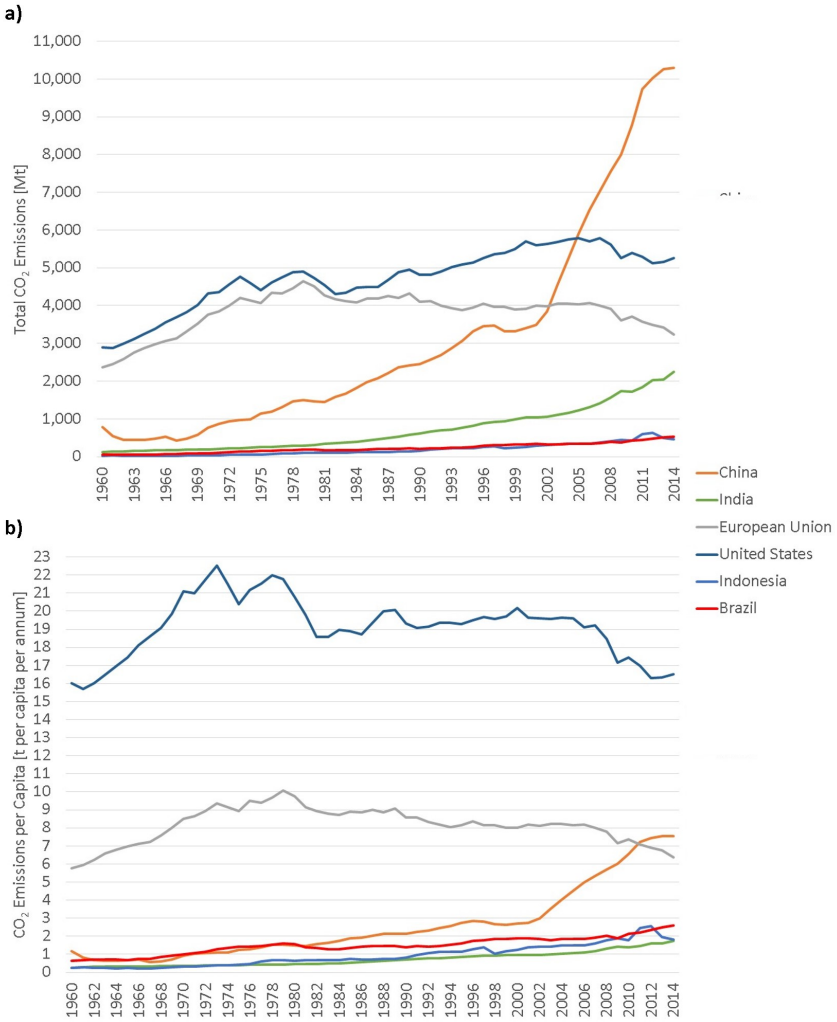

Figure 1.9: CO_2 emissions by country a) total per annum and b) per capita per annum [17]

crisis [21]. The energy intensity of GDP has been decreasing by 1.48% p.a. 1971 to 2014, and by 1.78% since 2010 [22, 21]. The carbon intensity of energy has increased by 1.89% p.a. on average between 2000 and 2017 [23, 22]. Carbon intensity in the power sector, a primary component of energy use, has increased, despite increased VRE penetration (6% growth p.a. since 2010 [24]). Increased demand outstrips new renewable capacity. Off-lining of nuclear power sources has increased fossil-fuel use [24].

With population and the GDP per capita predicted to continue to increase for the foreseeable future, focus should be on securing further reductions in the energy intensity of GDP and reversing the trend in the carbon intensity of energy (primary energy use i.e. not just power sector).

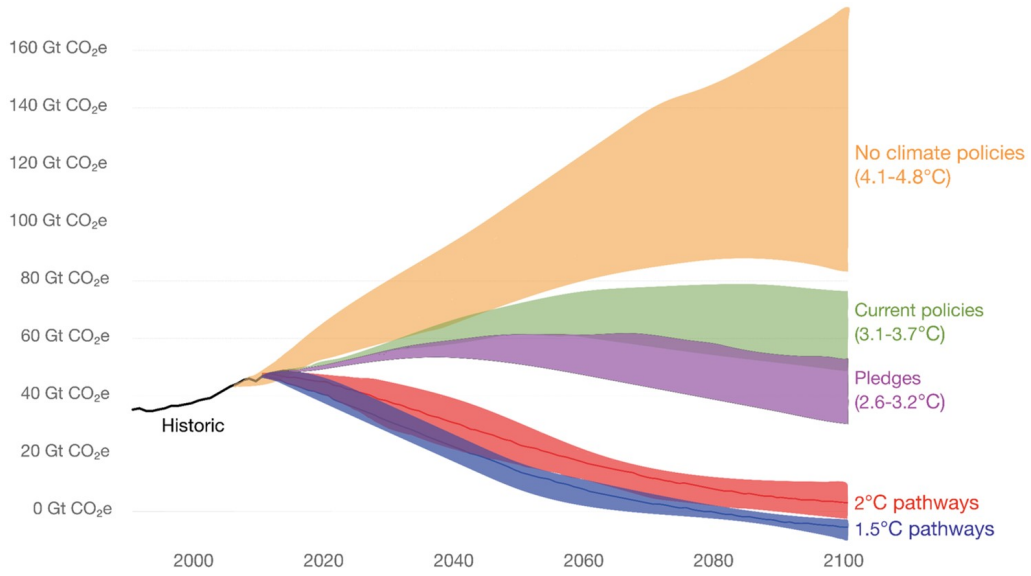

Figure 1.10: The projected impact of current policies and pledges benchmarked against 1.5°C and 2°C consistent pathways [23]

$$LCOE = \frac{\sum_{t=1}^{T} \frac{CAPEX_t + OPEX_t}{(1+r)^t}}{\sum_{t=1}^{T} \frac{Energy_t}{(1+r)^t}} \tag{1.2}$$

The highest carbon producing sectors need to be electrified to enable VRE penetration and therefore reduce primary energy carbon intensity. A key driver of electrification is the levelised cost of electricity (LCOE) from renewable sources (Equation 1.2). LCOE is falling. Lower CAPEX (i.e. installed cost) and an increase in the electricity produced (i.e. capacity factor) per kW is decreasing the LCOE for onshore wind and solar photovoltaic sources (Figures 1.11 and 1.12 respectively). The reduction in solar photovoltaic installed cost per kW since 1976 ($\$100\text{kW}^{-1}$) has been considerable. The module cost per kW compared with cumulative production follows 'Swanson's Law' (akin to Moore's Law for processors): a logarithmic relationship where installed cost falls by 20% for each doubling of global production

[25]. IRENA increased the estimated learning rate for utility scale solar PV between 2010-2020 from 35% to 37% [26].

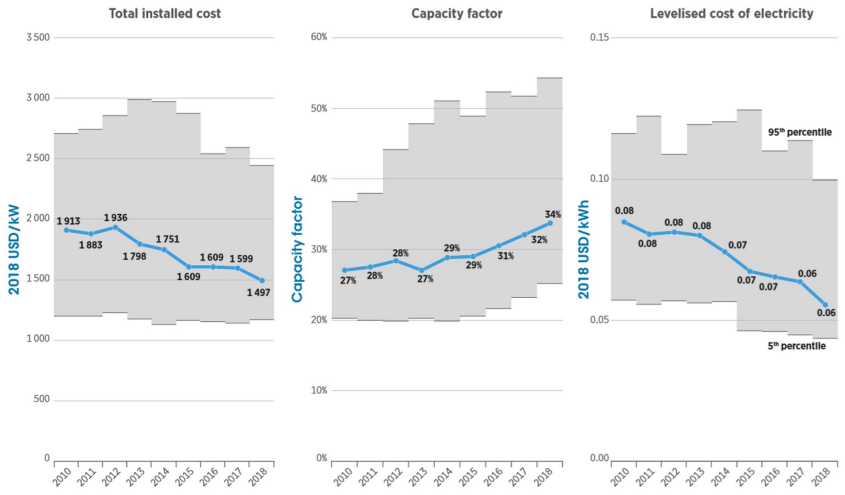

Figure 1.11: The Falling Cost of Onshore Wind [27]

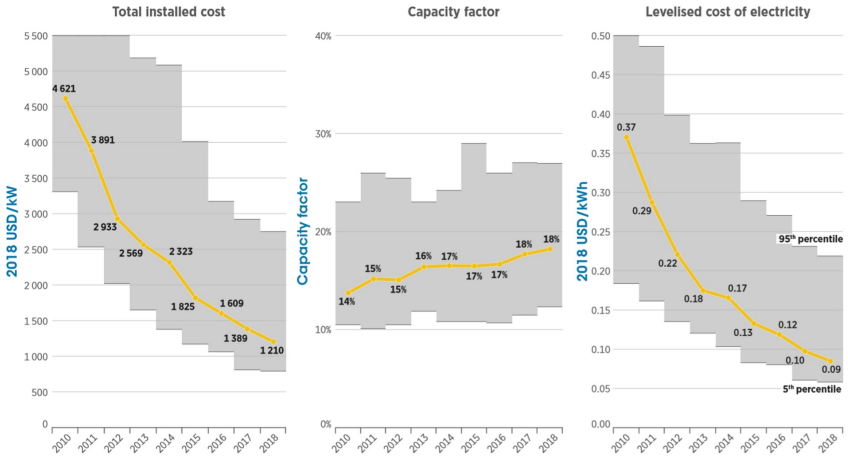

Figure 1.12: The Falling Cost of Solar Photovoltaics [27]

The falling cost and increasing capacity factor of renewable sources means the LCOE is competitive against fossil-fuel sources. For example the successful UK offshore wind strike-price bids for CfD3 (the third Contracts for Difference auction round, September 2019) were £39.65MWh^{-1} vs. c. £120MWh^{-1} in CfD1 (2015) [28].

1.2.3 Which Sectors Can and Should Achieve Even Greater Decarbonisation?

Falling VRE electricity cost is a cost efficient solution to move towards the 2°C pathways (Figure 1.10). The key is to capitalise on falling VRE costs in the main polluting sectors (shown in Figure 1.3b).

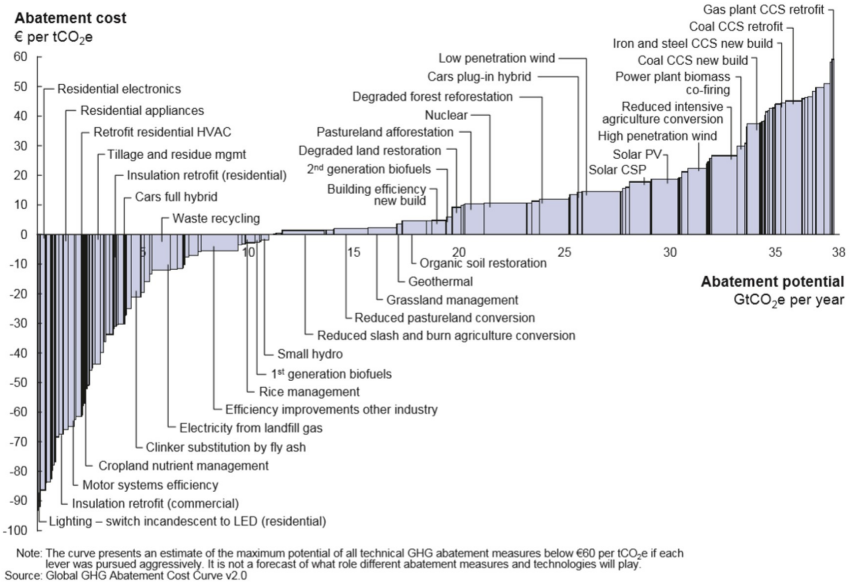

Figure 1.13: The cost of emission abatement [29]

Which sectors and how they decarbonise will contribute to meeting, and the speed of meeting, global warming targets. Emission abatement needs to be efficient as it is an attributable cost which may be met by consumers (including those least able to pay). In many countries the margins are particularly small. Mis-managed de-carbonisation threatens socio-economic development (e.g. India). Figure 1.13 shows McKinsey's analysis of the most cost efficient methods of abatement (without considering implementation complexities). Although sequestration methods shown have significant potential (such as afforestation) to sequester a large amount of CO_2 each year at reasonable cost they will not be sufficient on their own [30, 31].

Most research on the priority sectors to decarbonise assume that to achieve net-zero CO_2 quickly and efficiently we need reduce emissions sectors with the highest current CO_2 emissions and lowest cost abatement potential e.g. IRENA in Figure

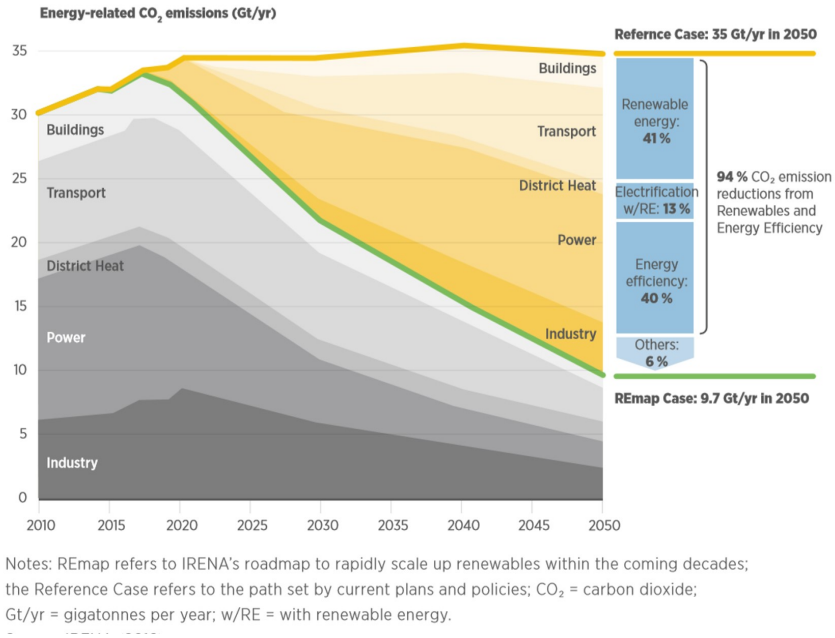

Figure 1.14: Sectors to decarbonise [32]

1.14. Power (including the indirect emissions of other sectors) is the primary target for decarbonisation as industry is either too difficult or expensive to decarbonise (despite being a large proportion of total emissions) [32, 33].

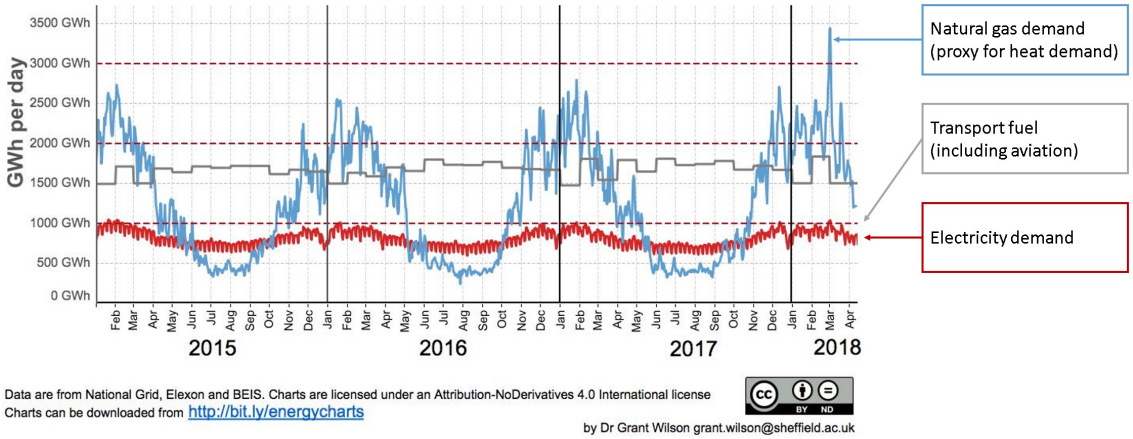

Figure 1.15: UK Daily Energy Demand January 2015 - April 2018 [34, 35]

Integrating VRE into the power sector is crucial to decarbonise other sectors by achieving zero-carbon electrification. However, VRE integration in the power sector needs to consider larger energy balancing issues (Section 1.3). For example, electrifying UK transport would increase the average energy demand that the power sector needs to meet. Electrification of heating would add a huge seasonal and relatively inflexible demand (Figure 1.15).

There is limited research on the electrification of industry and its potential synergies, despite being responsible for a significant proportion of emissions. Research focuses instead on transport, heating / cooling and the power sector. Society relies on industry production and industry energy demand and emissions are high making it a prime target for decarbonisation. Emissions, energy demand, end product and current dependence on fossil-fuels determine which specific industrial process should be prioritised for decarbonisation (Figure 1.16).

	Total primary energy and CO_2 emissions (direct and indirect)		Low – High Estimates of Technical Savings Potential (Primary energy, excludes overlap)	
	EJ per year	Mt CO_2 per year	EJ per year	Mt CO_2 per year
Sectoral improvements*			11.9–16.9	
Chemicals/petrochemicals	33.8	1500	5.0–6.5	370–470
Iron and steel	25.3	2211	2.3–4.5	220–360
Cement	10.1	2000	2.5–3.0	480–520
Pulp and paper[f]	6.9	400	1.3–1.5	52–105
Aluminium[f]	4.1	375	0.3–0.4	20–30
Other (Non-metallic min. and non-ferrous)	59.7	3514	0.5–1.0	40–70

Figure 1.16: Potential to decarbonise heavy industry by adopting the best available technology, improvements in process efficiency and fuel-switching (to less carbon intense fuels, co-firing with waste / biomass, decarbonised energy, or hydrogen) [36]

There are two methods to decarbonise electrical power supply: carbon capture and storage (CCS) or replacing existing generation capacity with non-carbon sources e.g. nuclear fission or VRE (wind, solar, tidal, wave, geothermal, etc.). This research focuses on the integration of VRE, particularly wind and solar photovoltaic, as CCS deployment to date has been slow and nuclear fission is perceived either as too expensive, unsafe or both. Other VRE sources have limited availability and LCOE is relatively high.

Pre/post CCS or process electrification is expected to achieve abatement in the chemicals sector. This research focuses on electrification for three reasons: recent limited appetite for CCS development, the substantial infrastructure overhead to implement CCS and falling VRE LCOE (Figures 1.11 and 1.12).

1.3 Technical Context

The objective of this section is to provide context about the technical environment that this research has been conducted in. This section highlights the problems associated with the integration of VRE in power networks, solutions for additional network flexibility (e.g. energy storage), how to find the optimal combination of solutions, why ammonia is a promising option for long-term electrical energy storage, and the current methods of ammonia production.

1.3.1 Problems of Integrating VRE

Currently electricity networks manage to balance supply and demand over a variety of timescales: seconds, minutes, hours, days and seasons. Throughout history this has been largely managed by varying dispatchable supply sources (i.e. generation that can be turned up / down and on / off when required) to meet a variation in demand. Renewable energy sources (RES) however, specifically VRE sources, unlike the historically dominant fossil-fuelled sources, do not guarantee the delivery of power as and when you need it [37]. As more VRE is integrated into these power networks to achieve the required sustainability, the capacity market and system operator must manage to balance the two other components of the "trilemma": security of supply and affordability [37, 38]. While VRE sources can be seen as a sustainable and secure supplier of energy over long periods of time (i.e. a year or more) the magnitude and speed of their variability (as defined in [39]) and unpredictability over short and medium time periods require networks to have additional flexibility to maintain their ability to balance supply and demand [40]. This flexibility (i.e. ability to manage supply and demand to maintain security of supply) can be provided in many ways but does come at additional cost. In this thesis the impact of VRE integration and the stability of the network considered are discussed from here onwards specifically on the system balancing (i.e. hourly to seasonal balancing). The rationale behind this (as shown in Figure 1.17) is due to "moderate to high" increase in the need for these relative to other methods.

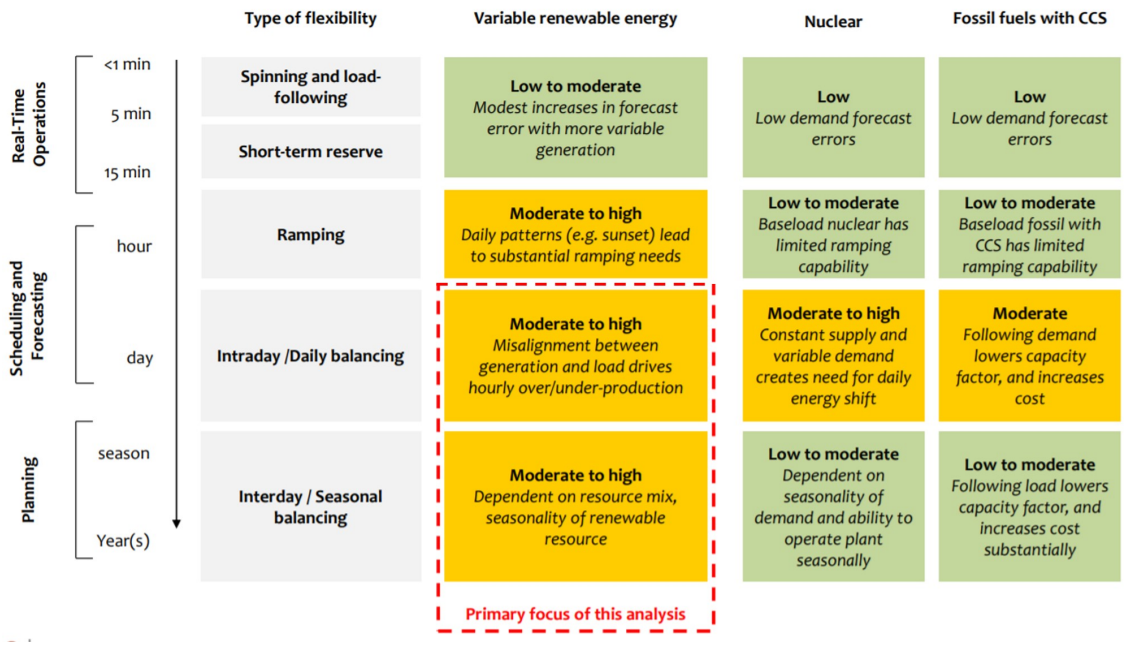

Figure 1.17: The increase in network flexibility required by low-carbon power source [41]

At low levels of VRE penetration (the definition of which used in this thesis found in Equation 3.1) i.e. less than 5% networks (depending on location) are able to balance the additional variations between supply and demand without the implementation of any additional flexibility. However, as VRE penetration increases so does the magnitude and frequency of variations that need to be managed. This is compounded by the fact that the inherent network flexibility also decreases as there is also proportionally less dispatchable capacity. Multiple investigations concluding that with higher penetration comes the necessity to dramatically lower the system minimum load points below their current annual minimums [42, 43, 1]. As shown in Figure 1.18, the increase in VRE penetration requires additional network flexibility in order to maintain stability. This however is highly dependent on the location specific problem regardless of the VRE penetration. For example, Ireland and Denmark were considered by the IEA to have similar "Phase 4" flexibility requirements in 2017 despite having $\sim$24% and $\sim$49% VRE penetration respectively. The reasons for this sensitivity of flexibility requirements include any or all of the following: the proportion of the VRE penetration accountable to wind (or conversely solar photovoltaic) sources, the shape of the solar PV energy profile, the shape of the wind

energy profile, the capacity factor of the solar PV source, the capacity factor of the wind source and the shape of energy demand profile. Figure 1.18 and the multitude of variables that a network's flexibility is dependent upon (specified above) demonstrate the importance of achieving research objective 2 (Chapter 1) to identify the impact that location and other key variables have on the flexibility requirements to balance a power network with VRE integration.

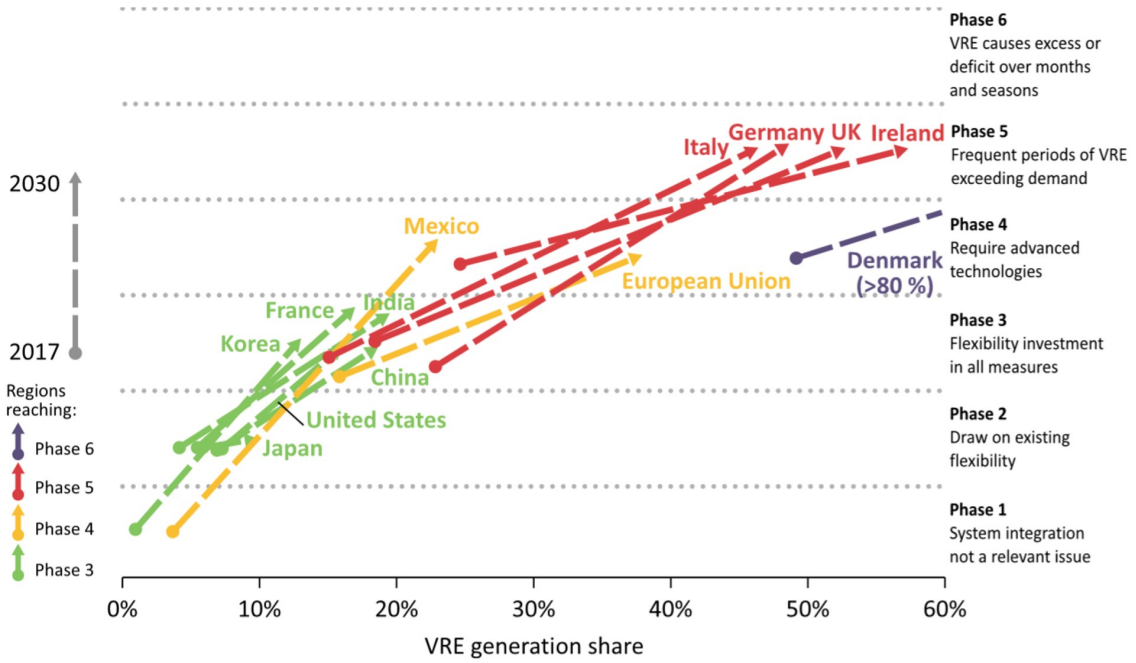

Figure 1.18: The IEA's prediction (in their New Policies Scenario) of future network flexibility requirements by country and variable renewable energy (VRE) penetration [44]

The importance of effective and efficient investment decisions to enable the transition to higher VRE penetration cannot be overstated. The problem that must be managed is substantial: *"The Committee on Climate Change estimates that intermittency will add 1 p/kWh to the cost of renewables when their share of total electricity rises to 24% in 2020. For comparison, the direct cost of generating a unit of electricity from offshore wind is currently 7.5-11.5 p/kWh and the average household uses 3,300kWh each year. The Nuclear Energy Agency (NEA) estimates that the cost of managing intermittency if wind generates 10% or 30% of UK electricity to be 0.9p/kWh or 1.6p/kWh respectively, or between 8-21% of the direct cost of onshore wind. For solar, the NEA estimates costs of 2.6p/kWh or 3.5p/kWh"* [45].

However, these are estimated integration costs because they are for current systems without added flexibility. They have varying methodologies which may not provide accurate results. Inefficient decision / policy making with regards to VRE implementation and the flexibility methods used could result in these additional costs for network operators and consumers without careful planning due to stranded costs. Katzenstein and Apt noticed (in the USA) that cost of load following back-up (between 15-60 minutes in duration) to support wind intermittency dropped by as much as 40% (from 7.5 to 4.5$/MWh) with increased capacity factor and that marginal benefits of interconnection to other geographically located wind farms diminished rapidly [46].

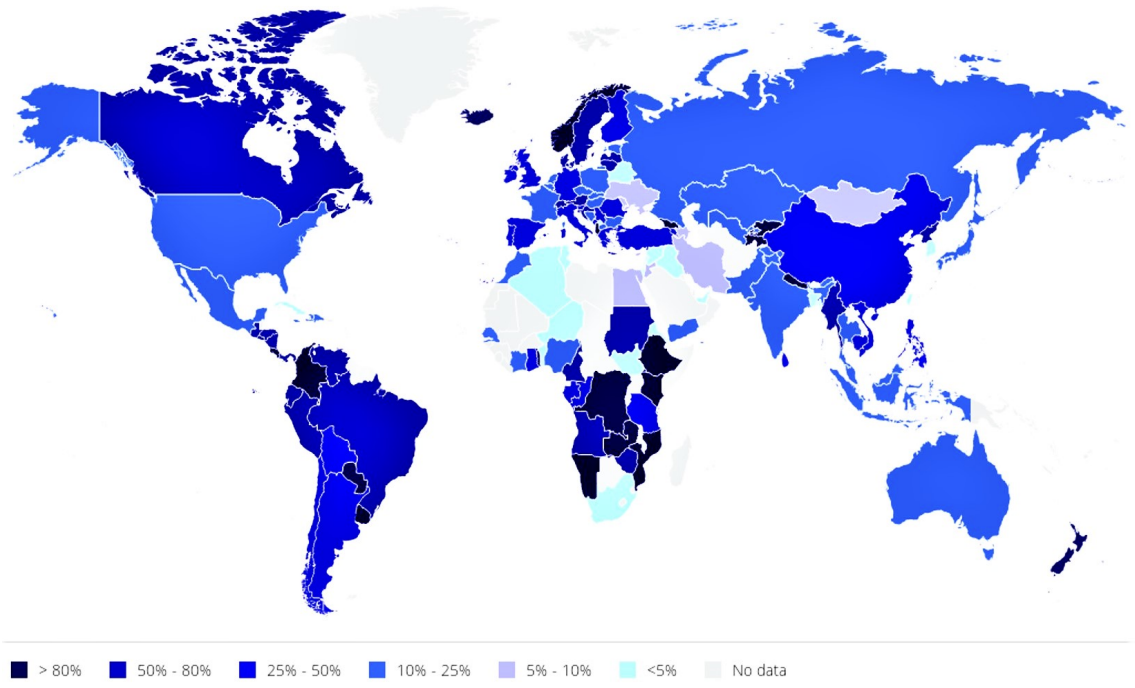

Figure 1.19: Share of renewable in electricity production 2017 [47]

As shown in Figure 1.19 at present a significant number of countries have low VRE penetration. With VRE being targeted as the dominant form of energy supply in many countries capacity, transmission and network planning is required so that its integration is seamless and cost efficient. This requires techno-economic analysis of the network. The demand and supply that are specific to the location need to be considered, the balancing requirement for a given VRE penetration identified and

the optimal supply and balancing implementation pathways enacted. Islanded or semi-islanded electrification of other sectors using VRE (as proposed by the IRENA [32]) will have the same problems due to the inherent intermittency of VRE. In these sectors these same flexibility methods may be more expensive (e.g. demand side management (DSM) consisting of the ramping of industry production) but also present opportunities (e.g. sector coupling).

1.3.2 Available Solutions i.e. Options for Additional Network Flexibility

The mitigation methods that can be employed to provide additional network flexibility (listed in Figure 1.20) are limited by different factors. They can be organised by those that mitigate the problems of VRE integration, DSM and Interconnection, and others that provide external capacity to manage the problems such as reserve capacity, curtailment and electrical energy storage. Figure 1.20 highlights the different options currently available for increasing a network's flexibility. In this section (1.3.2) I have provided a brief description of each of these available technologies.

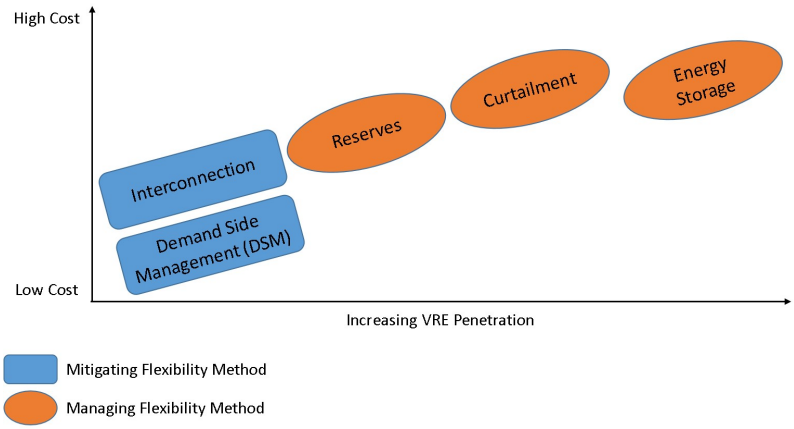

Figure 1.20: Flexibility methods by cost and VRE penetration. Adapted from [48]

Demand Side Management (DSM)

This method of mitigating the flexibility required, shifts (or reduces) demand to improve the alignment of the supply and demand profiles (as shown in Figure 1.21). The most common reasons for doing this are to either reduce the daily peak demand

(Figure 1.21) and / or to increase demand at the local profile minima in the middle of the day (i.e. mitigation of the duck curve, Figure 1.22). Despite the apparent benefit of simply mitigating the problem, DSM has two notable challenges. The flexibility of demand as a function of magnitude and time is highly significant in quantifying the amount of available DSM resource available to the network operator [49, 50]. DSM is limited to at most weekly balanding and how it can be leveraged in practice is still unclear. While using real-time pricing has been suggested, particularly in combination with IoT, there are concerns that poor implementation of this not correctly taking into account fuel poverty could have significant adverse effects. The application of DSM with significant consumers (such as industry) has been and currently is the practice for many networks. However, such implementation is often very costly.

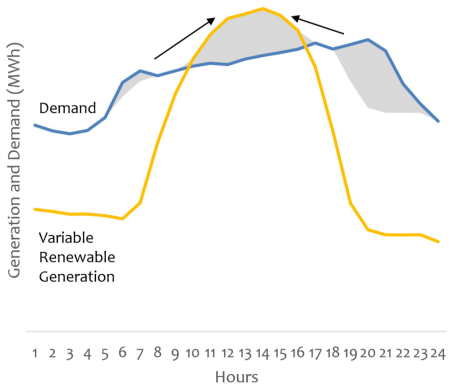

Figure 1.21: Example of the flexibility that demand side management (DSM) can provide [41]

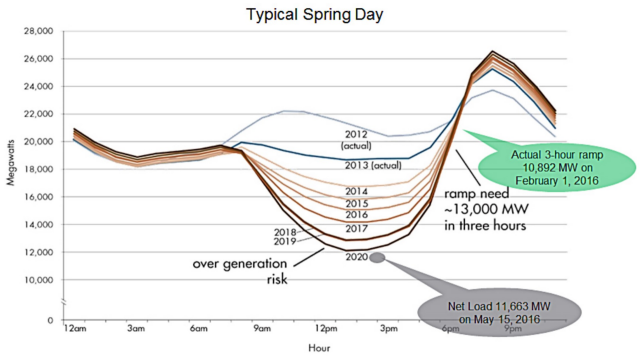

Figure 1.22: California Independent System Operator 'duck curve': large scale deployment of solar PV causing network demand to drop [51]

Interconnection

Similar to DSM, interconnection mitigates the flexibility required by shifting energy. However, with interconnection this is both supply and demand and the shift is geographically rather than temporally. As shown in Figure 1.23, interconnection can provide a substantial amount of flexibility by capitalising on the distribution of both renewable resource and demand. It does also have its limitations. The amount of power that can be transferred is entirely dependent on the capacity of

the connection, the available anti-correlation is determined by the mix of supply chosen at the other end of the connector (e.g. the UK's High Voltage Direct Current (HVDC) Cross-Channel interconnection to France with substantial nuclear capacity) [37].

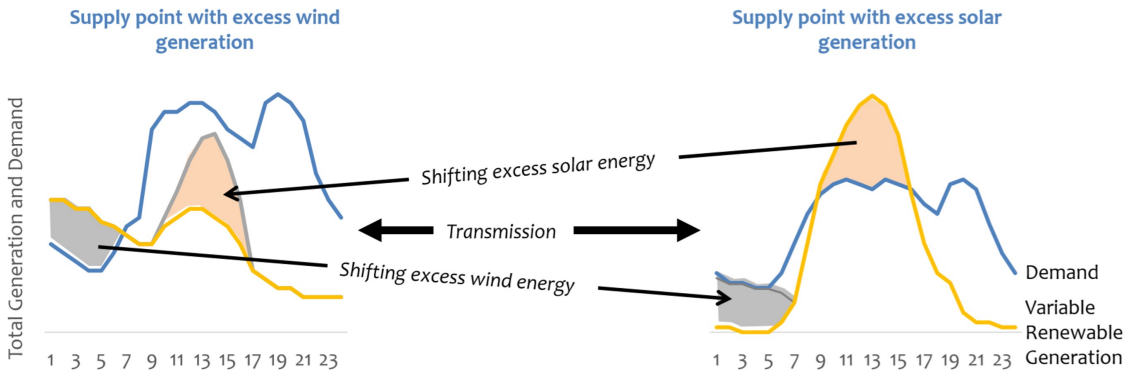

Figure 1.23: Example of the flexibility that interconnection can provide [41]

Reserve Capacity / Peaker Plants

The first of the management flexibility methods, flexible generation / reserve capacity / peaker plants are power sources that provide additional supply when required (e.g. periods of high demand). Commonly fossil-fuel (such as natural gas and diesel oil) based this is a dispatchable power source similar to the conventional plants that maintain baseload, but operate significantly fewer full load hours (FLH). These are not to be confused with the operating reserves such as enhanced-fast / fast frequency services or spinning and non-spinning reserves which respond to a network failure much faster, for a different duration and provide a lower power. Despite their excellent ability to meet flexibility demands, they are highly capital intensive and likely to be an unsustainable method of providing a significant amount of flexibility due to their dependence on fossil-fuels.

Curtailment

Curtailment of VRE is a consequence of over-sizing the capacity of renewable sources to reduce the number of deficits and thereby eliminate the need for other flexibility methods (Equation 3.7). However, this waste of energy past a certain magnitude

is not an economically efficient method (i.e. when Equation 1.3 holds true). At lower VRE penetration levels this is a highly effective method of flexibility as the amount of energy curtailed is likely to be low (depending on the flexibility of the operational dispatchable sources). However, if curtailment as a flexibility method is used independently, as VRE penetration increases the proportion of deficits met per unit of curtailed energy substantially decreases.

$$\text{LCOE} \times \int_{1}^{\text{T}} \text{Curtailed Energy(t)}\,\text{dt} > \text{Cost of Alternative Flexibility} \tag{1.3}$$

Electrical Energy Storage

Energy storage however, unlike any other flexibility method, acts as an energy sink when required and can re-introduce this energy (excluding losses) as a dispatchable energy source. This functionality, in addition to the ability to shift energy for larger periods of time than DSM [52], does come with downsides. The functionality of storage is dependent on the technology chosen and (until recent reductions for some technologies i.e. batteries) at greater cost than other methods of flexibility [53, 54, 55]. Particularly in longer storage methods where one cannot 'sweat the

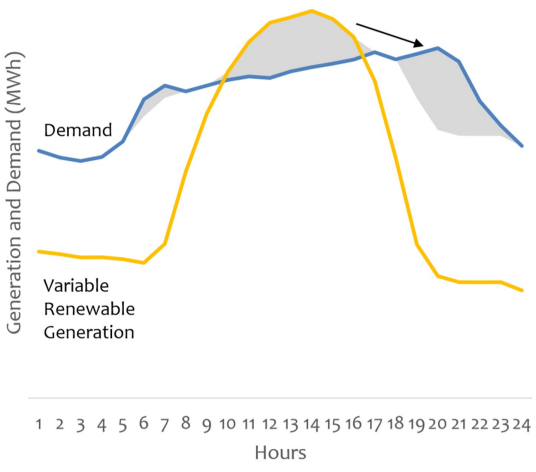

Figure 1.24: Example of the flexibility that short-term electrical energy storage can provide [41]

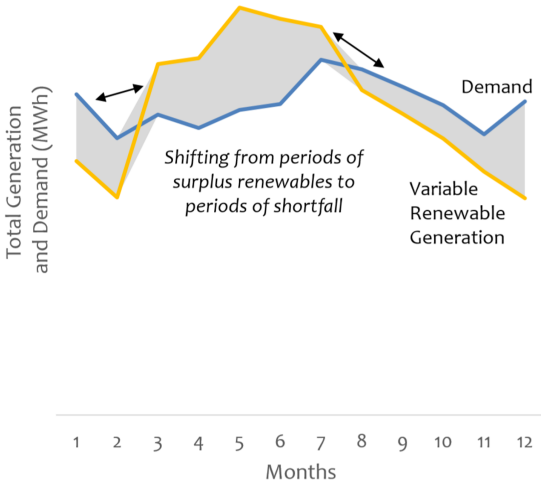

Figure 1.25: Example of the flexibility that long-term electrical energy storage can provide [41]

capital' (i.e. use numerous times to recoup the value of the asset), alternative

options such as peaker plants can be notably cheaper. For additional details on individual storage technologies and their applications see Palizban and Kauhaniemi or Denholm [53, 48].

1.3.3 Selecting Solutions: Techno-Economic Models and Modelling Tools

The move from fossil-fuelled dispatchable energy sources to renewable ones is a "once in a history transition" [56] with predicted global CAPEX likely to exceed total current assets (£70-80Tn) in 10-15 years. However, conventional planning methods based on dispatchable capacity management are not applicable. The variability of VRE sources is unlike what the system has seen before and due to the emissions targets conventional planning methods and solutions are not applicable. Instead new methods have to be constructed. This section provides a brief overview of the techno-economic modelling tools available and the subsequent results from their use.

Connolly [57] provides an excellent review of 37 of the best known tools in 2010 across a range of applications (from single building to national systems). H2RES [58], HOMER [59] and TRNSYS16 [60] are the tools of particular interest given their characteristics, their micro-grid focus and scenario time-frame of multiple years. Pietzcker [61] provides an alternative review of such tools specifically focussing on mitigation-process integrated access models (MP-IAMs) that analyse and identify long-term transformation pathways (e.g. the VRE sources and flexibility required to most efficiently achieve net-zero emissions).

While the tools described in these reviews are extremely useful for designing and operating networks with VRE integration from the micro-grid to national scale "it is evident... that there is no energy tool that addresses all issues related to integrating renewable energy, but instead the 'ideal' energy tool is highly dependent on the specific objectives that must be fulfilled" [57]. Even so, "properly capturing the flexibility [requirements] in energy system models requires increasing levels of details

which, given the limitation in modelling techniques and computing power, implies finding a proper balance between details and scope" [62]. Improving the efficiency of these tools would therefore enable the incorporation of additional model complexity, thereby improving their accuracy. For example many of these tools (including MP-IAMs), due to the significant complications that it entails, neglect that an "electricity supply system dominated by renewable energy cannot be viewed in isolation from wider energy supply and demand issues" [63].

The use of these models can be classified (as shown by Kondziella and Bruckner's overview [64]) depending on whether they consider technical, economic or market optimisation. As to which flexibility methods that should be deployed, their magnitude and when the results of these models varies, predominantly due to different assumptions, locations considered and scope of analysis (e.g. power sector or entire energy system). One general result that can be gleamed is that it is likely that the solution to the implementation of high levels of VRE often requires notable network flexibility most efficiently made up of a number of methods. As noted by Brandon when considering energy storage requirements for the UK: "it is... clear that there is no one 'winning' energy storage technology, but rather that a portfolio of technologies needs to be developed to deliver cost effective, durable and safe energy storage solutions, supporting UK grid decarbonisation." [65].

Historically electricity consumers have been treated as customers whose demand must be met by supply regardless of power and duration (excluding specific industrial demand contracts). To this end the status-quo for balancing supply and demand has been oversimplified and entirely focussed on the supply side. The inertia of how the balance is managed is hard to work against. To that end many believe that combination of flexibility solutions implemented will be a combination of methods [66, 67, 65], but biased towards supply-side options [45, 68]. Energy storage is seen as the preferable option by many academics and commercial entities given that historically grid balancing has been achieved through stored energy by fossil-fuel generators (e.g. coal hill or a barrel of diesel next to a power station) [69].

Quantifying a network's flexibility requirements in terms of energy storage (research objective one (Chapter 1) provides a temporal aspect of the balancing requirements and therein identification of how difficult it is to use available power that would be otherwise curtailed.

1.3.4 Which Energy Storage Method?

Electricity storage has been seen by some as the silver bullet to matching supply with demand. Even more specifically, batteries, perhaps due to their large scale development and the alignment of their technical characteristics to current problem management, are to the general population as well as many more informed industry stakeholders the solution. Despite characteristically stating that it is "spurious to attempt to pick winners" (i.e. the solutions) Helm [70] makes the following analogy to holistically explain energy storage: "car batteries might become to the electricity industry what petrol tanks in cars and trucks are to oil storage". While making the explanation accessible he also reaffirms the readers belief that batteries are and could be the dominant energy storage method. De-constructing the analogy, the parallels that can be drawn are quite apt. The majority of the supply and demand balancing for transport fuel is done 'behind-the-curtain', (out of sight of the consumer). If the same is true for the future of energy storage then significant capacity will be required beyond-batteries.

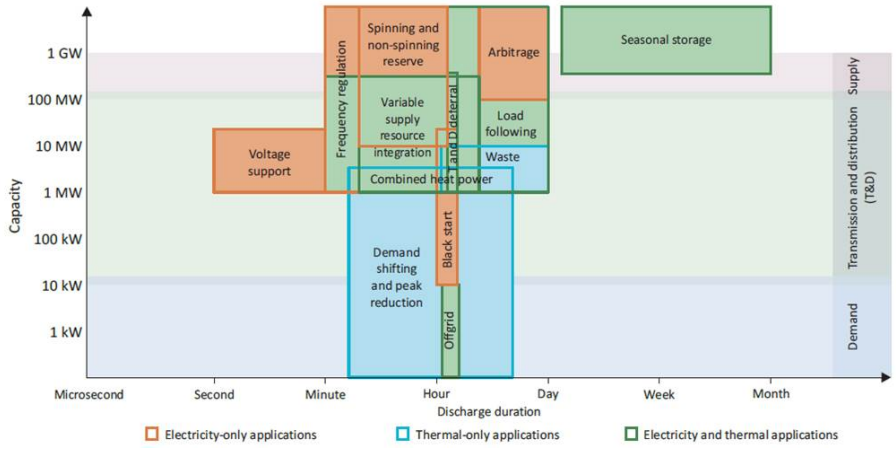

Figure 1.26: Network applications' capacity and discharge time [71]

In many countries (Figure 1.18) the VRE penetration has already required investment in flexibility (e.g. the enhanced frequency response tender [72]), and energy storage for $\tau \ll 1hour$ (i.e. Li-ion batteries) has proven the most cost competitive of all flexibility methods to meet the requirements. With the VRE penetration continuing to increase, flexibility requirements will increase. As highlighted by the Climate Policy Initiative [41], while the majority of the flexibility methods can be used to manage up to diurnal variations, beyond this very few options are viable. In their analysis, to manage the "interday/seasonal shifting" only hydrogen production (Figure 1.26), operation of existing fossil fuel plants more flexibly and delayed plant retirement have a "high" degree of technical fit. Chemical electrical energy storage despite its lower round-trip efficiency and greater CAPEX than shorter-term energy storage method [73] provides a non-location specific method of seasonal energy storage and a decoupling of rated power and energy.

1.3.5 Why Ammonia is a Favourable Energy Vector

To meet the likely future seasonal electrical energy storage requirements sustainably, power-to-X (P2X) currently appears the most promising solution, despite hydrogen's high specific energy consumption (kWh/kg of hydrogen produced). However, which chemical should be prioritised? Currently there is substantial work in this field with particular focus on hydrogen, synthetic methane, methanol, ammonia and Methylcyclohexane (MCH):

- Hydrogen: requires less flexibility in the production system
- Synthetic Methane: requires minimal adaptation of the current energy networks. It can utilise the existing capital assets, specifically gas networks, CCGT power plants, domestic heating, and industry.
- Methanol: Extremely versatile fuel that could have additional use in transport
- Ammonia: Significant existing demand and therefore infrastructure due to global dependence on it for nitrogen based fertilisers

- MCH: Thermodynamically favourable release of energy

The main difficulty of using hydrogen is its storage. It has an extremely low boiling temperature and requires careful storage due to hydrogen embrittlement. As shown by Bartels [74] (Figure 1.27), for long-term electrical energy storage the cost of the hydrogen storage in its diatomic form compared with storage of another compound such as ammonia is prohibitive.

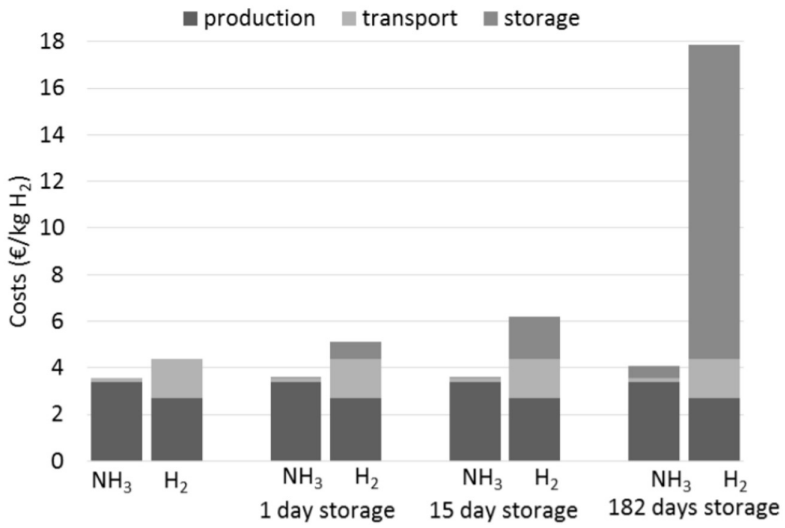

Figure 1.27: Cost of Hydrogen Production and Storage: Hydrogen vs. Ammonia as a hydrogen vector [74]

Of the remaining contenders the production of methanol and methane requires a carbon feedstock and would continue to have CO_2 emissions. Consideration of the control volume around methanol production in particular, shows that if subsequently burnt methanol is at best a hydrogen carrier [75]. No carbon is sequestered from the original feedstock. A similar argument can be made against methane. Decarbonised ammonia on the other hand, requires only water and air for feedstock and has no carbon content. Beyond its sustainability ammonia is considered by many as a "perfect carrier" because of its high hydrogen density, mature synthesis process, existing worldwide distribution infrastructure and easy catalytic decomposition [76, 77].

Chemical Characteristics of Ammonia

The concept of using ammonia for energy storage, as a hydrogen carrier or direct gasoline substitute has been appealing for some time given its chemical properties [78, 79, 80] that compare very favourably against hydrogen:

- Lower Heating Value (LHV) = 14.1GJ/m^3 (vs. H_2=8.4GJ/m^3 & Unleaded Gasoline (ULG) 29.8GJ/m^3)
- Boiling point = -33.3°C at 1bar or 20°C at 10bar
- Stable chemical with high hydrogen volumetric and gravimetric density (×1.3 greater than liquid hydrogen, see Figure 1.28)
- Relatively safe: non-explosive, narrow flammability range and easy to detect
- Substantial existing infrastructure (shipping, pipelines and storage)
- Considerable existing production, transport and safety know-how

In particular, its high volumetric (0.107kg-H_2/l) and gravimetric hydrogen density (Figure 1.28) in combination with a high boiling point facilitates a low cost storage of a large quantity of energy. A common concern that people initially have with the concept of using ammonia as an for energy storage is its safety; Highlighted by Valera-Medina [81] as one of the four key barriers. However, as pointed out by Gupta [82] it represents less of an issue from an explosion safety standpoint (30m to 1.5kW/m^2) than all other fuels benchmarked (e.g. diesel, 200m to 1.5kW/m^2). For use in large scale energy storage (not distributed) the more challenging risks, such as the steady-state release, can be readily managed as they are at existing production plants.

Technical Characteristics of Ammonia

Current Ammonia production amounts to 180Mt per year at a price of \$165-720t^{-1} (January 2010-April 2019) [84] with over 80% being used for nitrogen based fertiliser production [85]. By 2050, its production is predicted to increase to 270Mt per year.

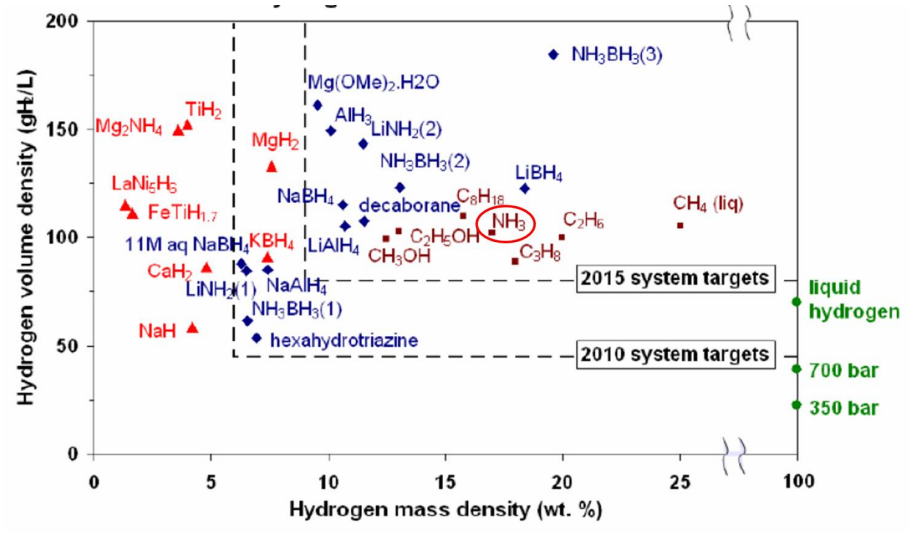

Figure 1.28: Hydrogen densities of compounds against American transport storage targets [83]

The magnitude of production not only means that there is significant existing infrastructure that could be used but also invaluable know-how of ammonia production and handling.

Beyond its use as an energy vector, decarbonising ammonia production is an environmental imperative in its own right given society's dependence on synthetic ammonia, with 48% of the global population currently supported by synthetic nitrogen fertiliser [86]. Dependent on fossil-fuels (particularly liquified natural gas (LNG) and coal) for both energy and hydrogen feedstock, ammonia production currently accounts for 1.8% of global fossil fuel consumption [87], 420Mt per year CO_2 emissions ($\sim$1.3% of global emissions). If by 2050 we are still dependent on fossil-fuel based production methods, CO_2 emissions due to ammonia production will exceed 630Mt per year.

Use of Ammonia as an Energy Vector

In 1935 Ammonia Casale Ltd. received a patent to burn a mixture of ammonia and hydrogen in an internal combustion engine. Interest in ammonia specifically as an energy vector has been renewed slowly since the 1970s [88]. This interest has grown and adapted into numerous ideas for implementation such as Ahlgren's duel-fuel

concept with methanol [89].

Once you want to convert the energy back to electricity there are a variety of options: decomposition for a hydrogen fuel cell, ammonia fuel cells [90, 91] or combustion in gas turbines [92]. While the hydrogen fuel cell is a mature technology, the energy consumption required for decomposition and the poisoning nature of ammonia to many fuel cells makes this route difficult. Gas turbines are similarly mature, but the use of ammonia in them less so. Despite the difficulties of reducing the NO_x down to acceptable levels while maintaining performance, but recent results [92, 81] have shown that run rich and humidified it is achievable (29.8% efficiency (similar to natural gas) [93] or even 31.47% with a concentration of 80% [81]. Solid Oxide fuel cells have been primarily considered for small scale production (i.e. transport) but have achieved ∼50% [93]. In this thesis the technical process used for converting ammonia-to-power has been assumed to be gas turbines. This is primarily due to its technology readiness level (TRL) and the pre-existing use of gas turbines with natural gas in the power sector.

1.3.6 Methods of Ammonia Production

Existing Ammonia Synthesis Methods

The reversible dissociation of ammonia can be seen in Equation 1.4 and the impact of temperature and pressure on yield in Table 1.1 (a more comprehensive table can be found in Appl [94]).

$$N_2(g) + 3\,H_2(g) \longrightarrow 2\,NH_3(g) \qquad \Delta H_f^\circ = -92.5\,kJ \tag{1.4}$$

The two main types of production currently in commercial operation both use HB (Equation 1.4) and differ in their source of hydrogen: steam reforming of natural gas or other light hydrocarbons and partial oxidation of heavy fuel oil or vacuum residue. The process of coal gasification has been phased out by many countries, but China

Temperature (C)	Absolute pressure (atm)						
	1	**10**	**50**	**100**	**300**	**600**	**1000**
200	15.3	50.7	74.4	81.5	89.9	95.4	98.3
300	2.2	14.7	39.4	52.0	71.0	84.2	92.6
400	0.4	3.9	15.3	25.1	47.0	65.2	79.8
500	-	1.2	5.6	10.6	26.4	42.2	57.5
600	-	0.5	2.3	4.5	13.8	23.1	31.4
700	-	-	1.1	2.2	7.3	11.5	12.9

Table 1.1: Equilibrium percent concentrations of ammonia at various temperatures and pressures [95]

is still using this method and India currently aims to in the near future [96]. At present, the clearly dominant method of production globally is steam reforming. A single-train modern steam reforming plant produces 1,000-1,500 t/day of ammonia [97].

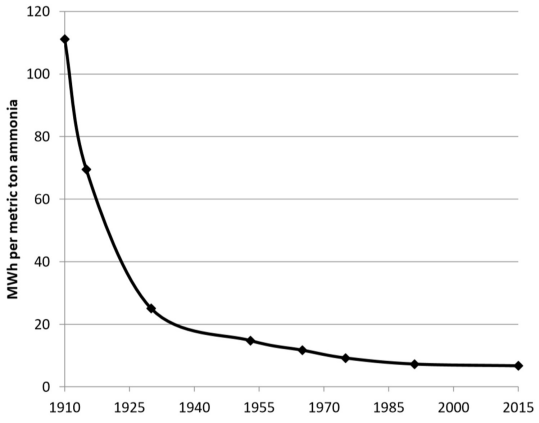

Figure 1.29: Specific energy consumption per ton of ammonia 1910-2015 [98]

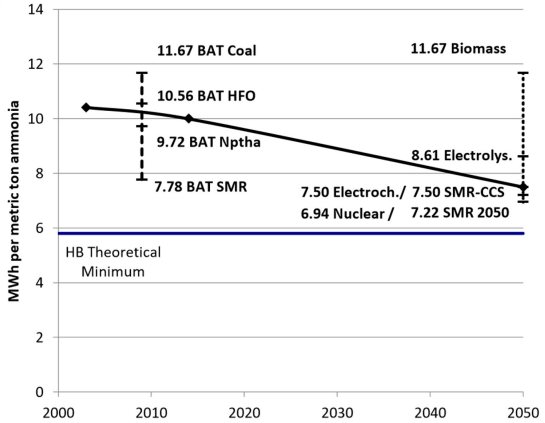

Figure 1.30: Specific energy consumption per ton of ammonia 2000-2050 [98]

Expressed by the lower heating value (LHV) of methane, the thermodynamic minimum feed to the process is 4.98 GCal/tonne NH_3. Of this 0.53 Gcal/tonne NH_3 is lost as heat rejection and 4.44 GCal/tonne NH_3 recovered as chemical energy in the ammonia product. In reality however plants are at most c. 75% efficient and are commercially operated at 20-30% conversion per pass. As shown in Figures 1.29 and 1.30 the efficiency has improved significantly and is now close to the HB theoretical minimum. Even with 25% improvement, the energy efficiency by 2050 are not in-line with the required emission reductions [98]. For a more detailed explanation of ammonia synthesis including basic catalysts and kinetics see Appl [94] or Morgan [99]. As shown in Figures 1.31 and 1.32, the sourcing of hydrogen from

water instead of fossil fuel significant reduces the process size as there is no need for pre-treatment. Importantly, the purity of the syngas enables the use of catalysts with higher activity that could not be used previously because of their susceptibility to poisoning.

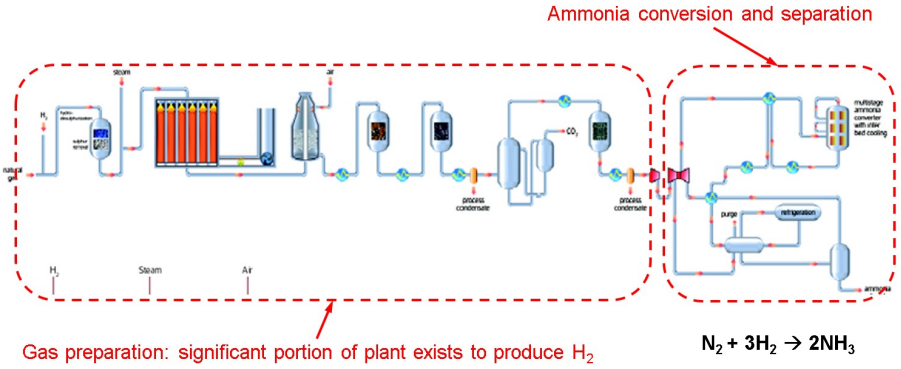

Figure 1.31: Ammonia production process: conventional SMR [100]

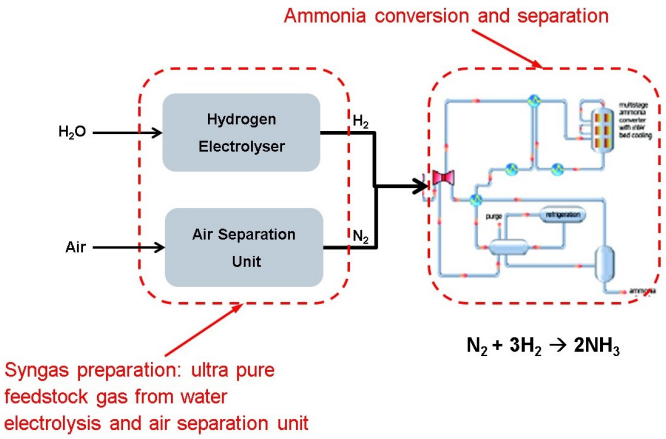

Figure 1.32: Ammonia production process: proposed method with water electrolysis [100]

In recent years, while incremental development of the existing HB (particularly low pressure Haber-Bosch) has still been undertaken (Figure 1.30), the majority of research has been on electrolytic and electrochemical production. Electrolytic production (Figure 1.32) using HB synthesis, but getting hydrogen feedstock from the electrolysis of water using VRE significantly reduces the size of the plant and eliminated CO_2 emissions. Electrochemical production, unlike improvement of conventional HB, can potentially reduce the required energy input by more than 20% [101].

Considering the production based on lower CO_2 emitting production methods, Bicer [102] determined that HB synthesis based on hydro-power, nuclear power, biomass and municipal waste could achieve 0.38, 0.84, 0.85 and 0.34kg_{CO_2} equivalent per kg of ammonia respectively. A significant reduction on the global average from conventional production methods 2.867kg_{CO_2} equivalent per kg of ammonia [103].

Developing Ammonia Synthesis Methods

The significant development improvements to achieve the reduction in specific energy consumption shown in Figures 1.29 and 1.30 has been due to catalyst development. Examination of Equation 1.4 with knowledge of Le Chatelier's principle or simply looking at Table 1.1 makes clear the importance of high pressure to the reactor single-pass yield. It is therefore understandable that the development of catalysts and reactor modifications to date have focussed primarily on enabling the reduction of operating pressure without compromising yield (to avoid the difficulties of working at high pressures) [80]. These developments have reduced the pressure to 80-120atm [104] as the catalysts has developed to be more active from Fe_3O_4-based (1913), $Fe_{1-x}O$-based (1986), Ru-based (1992) to Co-Mo-nitride (2000) [80, 105].

Recently however, two methods have been focussed on (as shown in Figure 1.33) differentiated by the type of technology being implemented. In line with current development, Siemens' view is to use existing technology (i.e. alkaline / PEM electrolyser with HB for synthesis and gas turbine for $NH_3$2P) for the synthesis and gas turbines for the extraction of energy from ammonia in the short-term. In the medium to long-term they aim to capitalise on the development of electrochemical methods to achieve a more efficient and perfectly flexible process.

Electrochemical processes enable the production of ammonia on request. However, current methods while perfectly flexible have only been demonstrated at lab scale and are at best $\times$10 smaller production capacity per unit area than required. Many different electrolytic systems are currently under development and they are classified by type: liquid electrolyte (room temperature), molten salt (300-500°C), composite

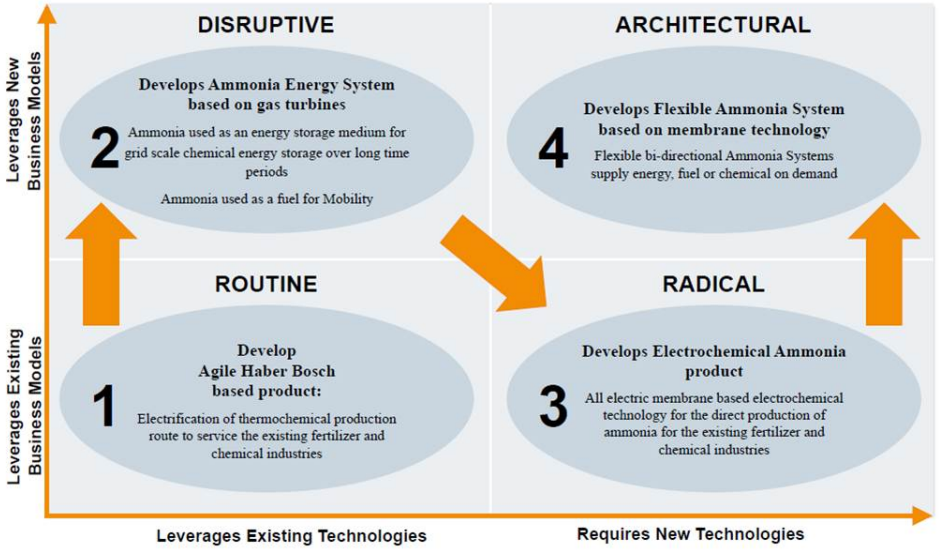

Figure 1.33: Siemens' view of the ammonia innovation landscape [87]

membrane (300-700°C) and solid electrolyte (25-800°C) [80, 101]. An explanation of each type electrochemical method can be found in Morgan [99] and Giddey [101].

Chapter 2

Literature Review

In this chapter a concise and critical review of the existing literature is presented to demonstrate understanding of the existing body of knowledge, to identify gaps in it and justify that said gaps warrant investigation. It is the contention of this chapter that two gaps exist. Considering the impact of VRE integration on the flexibility requirements of electricity networks, an improved understanding of the fundamental supply-demand balancing problem is required. This can be quantified in terms of the magnitude and as a function of the duration of energy storage required. Thereby enabling identification of the requirement for seasonal storage at certain VRE penetrations and mix of VRE sources, and the impact on this of using other flexibility methods in combination. Secondly, the electrolytic production of ammonia using VRE. For islanded production the combined optimisation of the VRE source selection, plant design and operation is required. With this functionality the range of currently achievable LCOA, its components, its potential for future reduction and the cost of plant flexibility required can be identified. These results can be used to find the best locations for current and future islanded 'green' ammonia production and by calculating its LCOS, whether it has potential to be economical to meet seasonal energy storage requirements.

2.1 Network Flexibility Required for Renewable Energy Integration

In this section existing literature has been reviewed on the impact that VRE integration has on the network flexibility requirement. To aptly demonstrate the identified gaps in the existing knowledge base, given the substantial quantity of relevant published work and fast moving nature of this topic, this section has been divided (in alignment with Figure 1.20) to consider two different approaches: investigations that quantify the flexibility requirement of power networks using mitigating methods (i.e. interconnection and demand side management (DSM)) and those using managing methods (i.e. operating reserves, curtailment and electrical energy storage). This review has focussed specifically on quantification of the network flexibility required as energy storage requirements given the identified gap in the existing knowledge. However before considering these methods to quantify the flexibility required, this section first considers literature investigating how the balancing problem is set up. A good overview of the importance of network flexibility can be found in [106].

Sinden states that "the successful integration of wind power into electricity networks will be assisted by understanding the characteristics of the resource, and how these characteristics relate to key issues regarding the wind power and energy security" [107]. While applicable for the consideration of all VRE integration (i.e. solar PV as well), understanding the temporal alignment of supply and demand is only an initial starting point to determine the network flexibility required for VRE integration. Intelligent selection of VRE sources and their mix can mitigate balancing problems, but further investigation is required to understand the network flexibility required for successful integration of significant VRE capacity.

This type of analysis, while able to provide some initial insight into the applicability of using specific VRE sources for a given network, is not able to quantify or differentiate the network flexibility requirement at the level of detail required. This is particularly the case at higher levels of VRE penetration. There is however notable

precedence for such investigations due to the useful, if limited, insights that they can provide.

With a considerable amount of literature to choose from demonstrating such studies, I have selected a few considering similar locations to demonstrate how the question posed and the subsequent results can be useful. Considering the integration of wind power into the UK power network, Sinden showed that wind power (independently) has a weak positive correlation with electricity demand. Wind resource in the UK aligns well with demand both diurnally (showing a "clear pattern of higher wind power output in the daylight hours"), seasonally and with peak and non-peak electricity demand [107]. In contrast, Grubb's analysis [108] of the top 1% of demand found negative correlation with the wind. Huber developed on this analysis by assessing the alignment of wind and solar photovoltaic profiles in combination with demand for 23 European countries [109]. They focussed significantly more on the impact that ramping limitations had on the flexibility requirement (significantly only diurnal i.e. 1-12 hours). They concluded that flexibility requirements, even with VRE mix optimisation, increased significantly when RE penetration (Equation 3.1) passed 30% and especially if the fraction of the VRE met by solar passed 20-30%.

The main focus of this type of investigation is to manage the variability of VRE sources. To date, the quantification of the network flexibility required to enable VRE integration has been achieved by assessing the need for any one method / free-variable (such as reserve, VRE curtailment, DSM or energy storage) and holding the others constant (barring).

2.1.1 Mitigating Methods of Flexibility

Interconnection

There have been relatively few studies that have focussed specifically on quantifying the requirement for network flexibility in terms of interconnection capacity. The main reason for this is that, while it is widely accepted that interconnection will

increase a network's flexibility [110], it is entirely dependent on the net demand of the two networks that are being connected as to its effectiveness. Terrier is a good example of considering interconnection for network flexibility [111]. He shows that with greater interconnection, reliability levels within the North European power system (Sweden, Finland, Norway, Denmark, Estonia, Latvia and Lithuania) are greatly increased.

Demand Side Management (DSM)

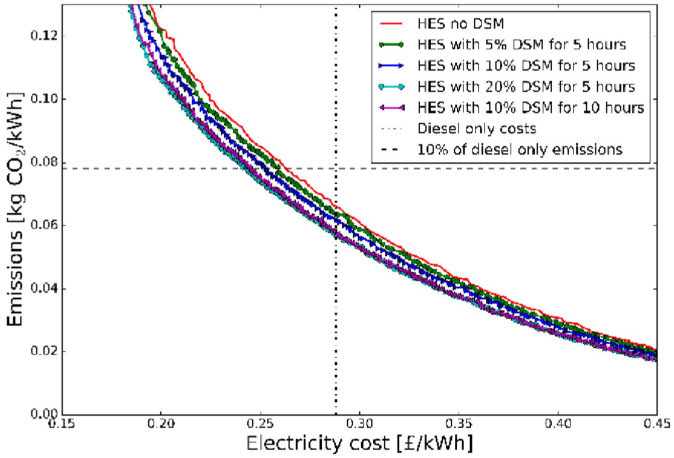

Figure 2.1: Pareto front for the hybrid energy system in Westray with and without DSM [112]

A flexibility method that can mitigate the need for alternative flexibility methods is demand side management (DSM). As Friedrich [112] showed, by investigating the potential for DSM in the islanded hybrid energy system in Astypalaia and Westray (see Figure 2.1), the use of even "low levels" of DSM (i.e. 10% shiftable demand for 10 hours) has the potential to significantly reduce the need for alternative flexibility methods (reserve requirement such as the flexible diesel generators considered in this case) and therefore reduce emissions and LCOE. Figure 2.1 shows that the application of DSM in this power network can reduce electricity cost. Moreover, the DSM's effectiveness at doing this is highly dependent on the fraction of demand and the maximum time of any shift in demand. The potential for DSM, however, both magnitude and magnitude of time shifting, is still a topic of investigation. Such investigations are key to identifying the magnitude of the role that DSM will be

able to play in VRE integration [50, 113]. Electrification of high energy demanding sectors (i.e. transport, heat and industry) will lead to notable changes in demand and its overall flexibility. This has the potential of significantly increasing the amount of flexibility that DSM can provide.

2.1.2 Managing Methods of Flexibility

Operating Reserves

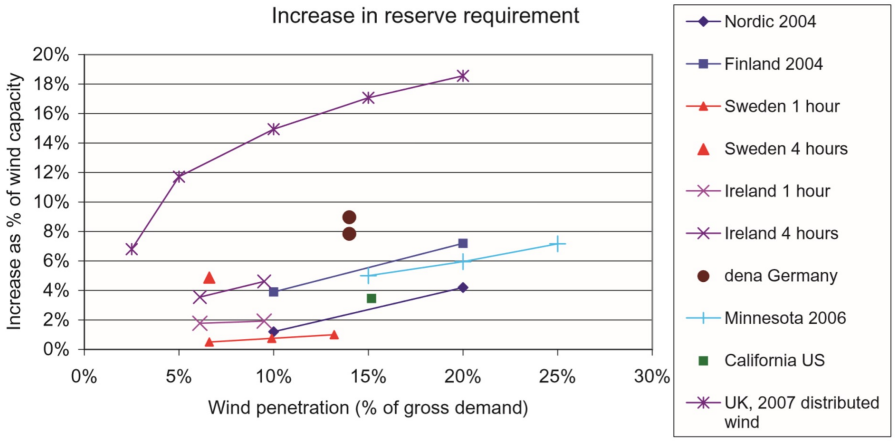

Figure 2.2: Results for the increase in reserve requirement (as a percentage of the rated wind capacity) due to wind power penetration [114]

An excellent overview of many significant papers in this field have been reviewed by Holttinen [114]. They succinctly summarise many detailed studies that have looked at different geographies on the impact of VRE penetration on reserve requirement (i.e. flexible generation required to meet deficits). It should be noted that while many of the cited analyses are investigating the impact of VRE variability on the need for reserves, all of them are using an VRE profile that is wind power only (i.e. no solar PV). As shown in Figure 2.2, the reserve requirements vary significantly with geography. However, due to the detail of these models there are few data points and the impact at higher levels of VRE has not been quantified. *"Wind integration has mainly been studied up to wind penetration levels of 10–20% of gross demand (up to 50% of peak load), with some first efforts to study higher penetration levels of 40–50% of gross demand [115, 116]. What happens at larger penetration levels, where wind becomes a more dominant part of the power system, is still not completely*

clear. Studies will have to cover larger interconnected areas to take the cross border transmission into account properly [117]" [114]. An overview by Heard, B.P. et al. of the studies that have attempted to fill this gap in understanding at high VRE penetration, showed that most have at best partial "coverage" of the problem [118].

Quantifying network flexibility as reserve requirement has evolved quickly since the publication of [114] in 2011. This is particularly true of the VRE penetration levels that have been investigated. Recent studies have considered up to 40% VRE penetration by capacity [110]. However, it is still true that the operating reserve requirements for VRE penetration greater than that is still unclear.

Curtailment

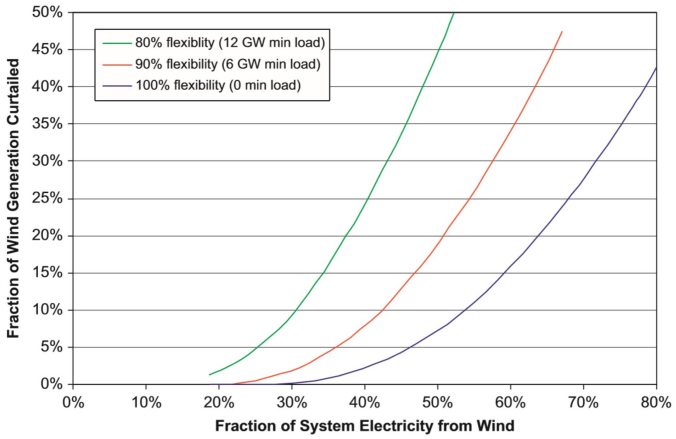

Figure 2.3: Results for the total curtailment as a function of usable wind energy penetration for different flexibilities of the Texas, USA (ERCOT) grid [1].

Integration of excess capacity, i.e. a larger rated power than required to meet VRE penetration targets (Equation 3.1), and curtailing the excess energy when there is a surplus has been a method favoured by many studies, arguably because it is the most utilised method in practice at the moment. In practice, curtailment is often a tell-tale sign of a network's lack of flexibility: often paying for but not using available energy.

Denholm [1] used curtailment as one flexibility variable they investigated for wind and solar integration. They found, among many conclusions, that the required curtailment of VRE varies significantly with network minimum load (see Figure

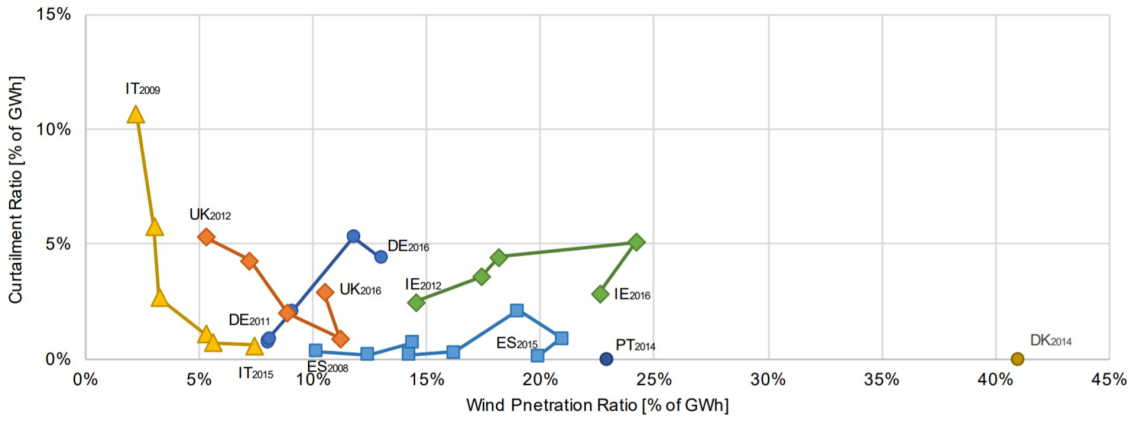

Figure 2.4: Wind energy curtailment in Europe [110, 119, 120].

2.3). Denholm's analysis was developed by Tuohy and O'Malley [121] to include the impact of wind predictability. They noted that relaxing the perfect foresight assumption (i.e. prediction of VRE) exacerbated the need for curtailment and that energy storage would aptly reduce this requirement.

Electrical Energy Storage

The investigations that have looked into the requirement for electrical energy storage to facilitate VRE integration have largely looked at the impact that VRE penetration and mix of VRE sources have on the magnitude of storage required. While for the majority this impact is considered as part of a techno-economic analysis (Section 1.3.3), a few consider the fundamental technical requirement. The techno-economic models are not considered here but their results show that energy storage is likely to play a considerable role in providing the required flexibility [122, 123, 124]. An excellent overview of these studies, with a particular focus on long term chemical storage (hydrogen and power-to-gas), was conducted by Blanco [125].

Heide's analysis investigates the magnitude of storage required. They note that the optimal mix of VRE supply is key to minimising the storage need as VRE penetration increases (see Figure 2.5) [126]. Heide then developed upon this work by assessing the optimal VRE mix and storage requirement for a "simplified European power system" [127] concluding that the VRE mix and storage required is dependent on the objective function employed. Rasmussen developed on this ([127]) to show

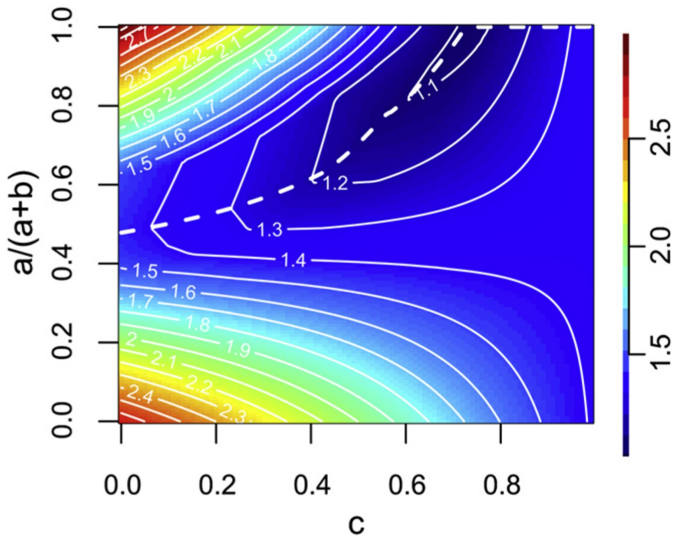

Figure 2.5: Maximum stored energy required for all of Europe as a function of the fraction of wind and solar VRE energy supplied by wind ($a/(a+b)$) and VRE penetration (c). "The dashed curve represents the seasonal optimal mix between wind and solar power generation as a function of the remaining fossil-nuclear power generation. The unit of the contours is given in average monthly load over Europe" [126].

that a fully renewable European power system is viable with "low efficiency hydrogen storage and a level of balancing equal to what is today provided by storage lakes." [128]. Whereas Mitra's proposed method of quantifying the requirement for storage is based on the required reliability (similar to the confidence level method presented previously) of the supply to meet demand [129]. However, all of these investigations have not quantified the required storage as a function of storage duration (τ) (even if some such as [41] have considered the requirement for a single duration of storage such as "seasonal"). A similar analysis by the Climate Policy Initiative also considered the impact that the proportion of wind had on the magnitude of interday / seasonal storage required for Germany and California (Figure 2.6) but this was for a single VRE penetration and grouped a large period of storage duration.

Another approach by Denholm and Hand [1] considered the impact of the minimum demand, VRE penetration, VRE mix on the amount of energy that had to be curtailed for network stability. The results showing that the flexibility of the system affects the potential curtailment of energy from variable sources without storage are interesting, the second key result is of relevance here: The ability of storage (4, 8,

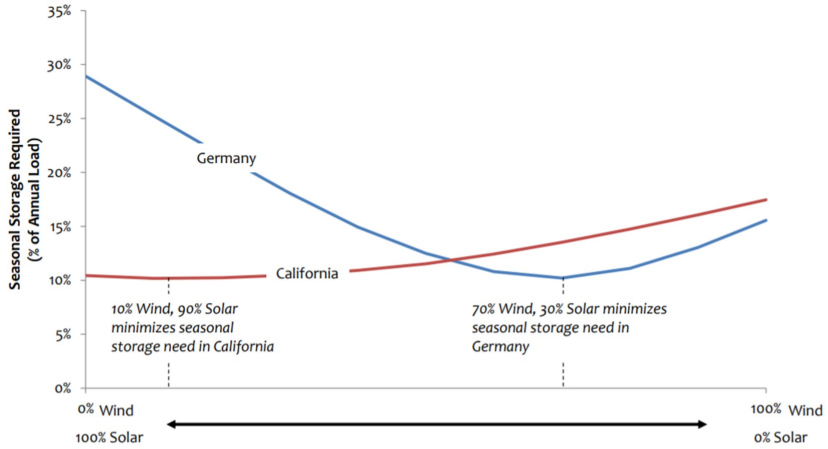

Figure 2.6: Cumulative interday / seasonal storage required as a function of the proportion of VRE met by wind for Germany and California [41]

12 and 24 hour duration storage) to mitigate the curtailment required was shown to be significant at high VRE penetration (up to 80%). Denholm concluded that when solving the mismatch of VRE supply and demand, one should consider the "many alternative technologies that can increase grid flexibility" [48]).

These results provide a manifold of feasible flexibility requirements. However, all of the analyses presented here are weakened by their use of a single method to quantify flexibility requirement (i.e. only providing a two dimensional slice through the manifold). There is, therefore, a gap in the existing knowledge for considering the impact of simultaneously using multiple methods of flexibility and identification of the flexibility requirement in terms of energy storage as a function of τ.

2.1.3 Gap in Flexibility Requirement Knowledge Base

There is a gap in our understanding of the fundamental flexibility requirement with increased VRE penetration. Existing literature on the impact that VRE integration has on the network flexibility requirement has only ever investigated individual locations, a few hypothetical networks and (barring Denholm and Hand [1]) only used one flexibility method i.e. reserves of VRE curtailment (see Figures 2.2 and 2.3). Quantification of not only the use and also size of energy storage by duration will provide a better understanding of the problem that needs to be mitigated or

managed. How this changes with VRE penetration and the mix of VRE deployed will provide 3D surfaces thereby improving on the 2D slices investigated to date. Identifying how other flexibility methods mitigate this requirement (both magnitude and type of storage) will provide valuable insights.

2.2 'Green' Ammonia Production and Use

In this section, existing literature has been reviewed on the production of decarbonised ('green') ammonia production. The small amount of existing literature on the topic (and particularly their results) is difficult to compare because of (as shown in Table 2.1) notable differences in VRE resources considered, the grid connectivity and the purpose of production (i.e. commodity vs. P2NH_3). Despite this, the results to date suggest that electrolytic production using HB synthesis (Figure 1.32) has significant potential to substitute conventional production (dependent on fossil-fuels for both energy and feedstock) and additional use as for energy storage.

2.2.1 Production of 'Green' Ammonia

The production of decarbonised 'green' ammonia can be split into two developing methods (as described in Section 1.3.6 and shown in Figure 2.7): electrolytic with Haber-Bosch and electrochemical. This review focusses on the first of these methods and ignores the latter. The rationale behind this is that, despite electrochemical methods having significant potential, due to their comparably high flexibility and greater energy efficiency, as noted in Section 1.3.6, their technology readiness means that they are unlikely to be implemented at large scale in the short to medium-term. Despite this, there has been quite significant interest particularly in direct solar-driven thermochemical production. This has been primarily due to the exergy efficiency possible by not converting to intermediary electricity (and thereby incurring additional efficiency losses). Lovegrove in particular has over the past two decades [130, 131] reviewed this from first principle exergy analysis [132] through to

plant design [133].

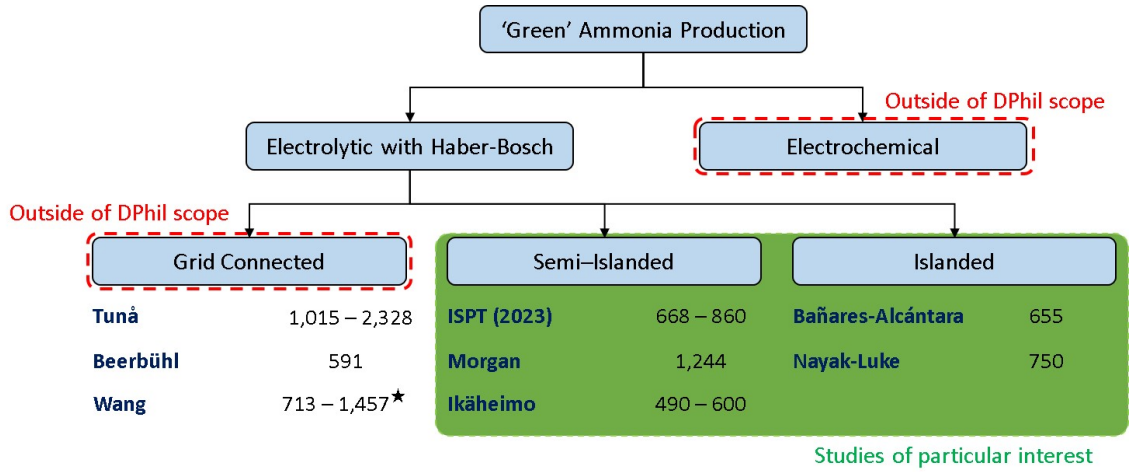

Figure 2.7: Overview of the achievable levelised cost of ammonia (LCOA) estimates in USD/t from previous investigations into 'green' ammonia production. ★: Back calculated from LCOE and $\eta = 60\%$ of LHV

Comparison of research into electrolytic production (and particularly the results) is difficult and should be done with considerable care. As shown in Figure 2.7, the models constructed can be separated by the type / lack of grid connection. 'Grid connected' is defined here as being entirely dependent on the power network for the electricity provided to the production process. 'Semi-islanded' as being dependent on VRE sources while also being able to source power from the grid. 'Islanded' production is when VRE sources are the only available power. This separation is essential to ensure a fair comparison of the models and their results. Given that this process flexibility comes at additional cost, it not only impacts the achievable LCOA but the design of the plant and its operation. While production based on power supply from the grid avoids these costs, if the ammonia produced is used as a commodity (rather than in a closed loop for energy storage) then if the grid is not VRE dependent, it risks being an expensive and inefficient method. For example, if the grid is CCGT dependent (as many are becoming) then, instead of using natural gas for production directly (by SMR), efficiency losses are accumulated through power production and electrolysis.

Despite grid connected electrolytic production having significant differences to semi-

and fully-islanded production, there are some interesting findings that can be taken from these studies. Beerbühl's analysis for example, despite being grid connected (and therefore having a dependable power source) took into account the variation in the price of grid electricity (specifically the hourly day-ahead market price for the PHELIX market in 2013)[134]. Capitalising on lower electricity prices / avoiding higher prices led to the notable use of a 'hydrogen buffer'. The use of such a buffer to provide the necessary / advantageous flexibility to the production process has been used extensively in subsequent analyses. This is achieved through hydrogen storage and the over-sizing of the hydrogen production process relative to the HB synthesis and air separation (ASU) processes. Despite the high CAPEX of the hydrogen production process (be it the battrolyser [135], solid oxide fuel cell (SOFC), alkaline or proton exchange membrane (PEM) electrolyser) its ability to ramp quickly has resulted in its use to mitigate adverse variability in electricity price and renewable power sources.

Wang's analysis optimised (by mixed integer non-linear programming) the production process, focussing on the production of ammonia to manage diurnal power variations [136]. They show that, despite the unfavourable operating schedule of 10 hours ammonia production then 10 hours ammonia-to-power re-integration, ammonia at 240$/MWh of delivered energy "can compete with pumped hydro and compressed air energy storage systems".

Focussing on those investigations close to my topic of research in the islanded production of 'green' ammonia (Figure 2.7) it is noticeable that the range of estimated achievable LCOA is quite large and not yet competitive with conventional production in the context of the average spot price for the NOLA, Black Sea, Middle East, Western Europe and US Tampa markets 2010-April 2019: maximum 720$/t, mean 426$/t and minimum 165$/t. Morgan's analysis, despite resulting in the least competitive LCOA estimate, was a comprehensive analysis of ammonia production in the Gulf of Maine predominately using offshore wind power [99]. The investigation considered the sizing of the process and through sensitivity analysis showed

that, even in semi-islanded operation, the minimum power of synthesis had significant impact on the LCOA. Ikäheimo's analysis, using Balmorel, considering the mutual benefits of semi-islanded production, showed that renewable ammonia could be produced competitively and be used for conventional consumption (i.e. fertiliser and industrial use) as well as for energy storage and distribution [137]. The ISPT analysis, aside from considering a different geography, had particular novelty for considering alternative methods of hydrogen production.

Authors & reference	Inputs / Constraints						Results	
	Location considered	**VRE sources considered**	**Electrolyser specific energy consumption**	**Grid connection / Plant purpose**	**Plant size [t/day]**	**Discount rate [%]**	**LCOA [$/t]**	**Electrolyser size [MW_e]**
Tunå, P. et al. [138]	Not specified	General (specifies cost)	Constant (4.25kWh/Nm^3)	Grid dependent / Commodity	18.5 5.6	5-12%	1,015-2,328 1,078-2,392	10* 3*
Beerbühl, S. et al. [134]	Germany	N.A.	Non-linear (3.54-4.40kWh/Nm^3)	Grid dependent / Commodity	Not specified	Not specified	588	34.0-34.76
Bañares-Alcántara, R. et al. [139]	Victoria, Australia	Wind	Constant (47-64.5kWh/kg)	Islanded / Commodity or ES	48	8%	655	33.31
ISPT (Goeree-Overflakkee: Case 2) [140]	Middelharnis, Netherlands	Wind	Constant (53kWh/kg)	Semi-islanded / Commodity	109.6 (40MW_e)	7%	524–857 (2023) 429–926 (2030)	20*
Wang, G. et al. [136]	Germany	N.A.	RSOFC: Not specified	Grid dependent / Diurnal ES	100MW_e	7.49%	709-1,450 ★	10*
Morgan, E. et al. [99]	Gulf of Maine, USA	Wind (370MW_e)	Constant (4.8kWh/Nm^3)	Semi-islanded / Commodity	300 (145MW_e)	7%	1,224 (580 minimum)	Not specified
Ikäheimo, J. et al. [137]	Northern Europe	Wind, Solar PV and Hydro	Piecewise (41-47kWh/kg)	Semi-islanded / Commodity	Not specified	7%	488-597	Not specified
Nayak-Luke, R. et al. [141]	Lerwick, Scotland	Wind and Solar PV	Constant (53.4kWh/kg)	Islanded / Commodity	228 (202MW_e	0%	736	196

Table 2.1: Comparison of previous investigations into 'green' ammonia production, their inputs / constraints and results. Arranged by date of publication. Abbreviation: ES – Energy Storage; *: Defined variable; ★: Back calculated from LCOE and $\eta = 60\%$ of LHV [142]. LCOA has been converted from Euros when appropriate: \$1 = 0.8793EUR [143]

The battolyser [135], SOFC and even solid state ammonia synthesis (SSAS i.e. electrochemical production) were compared with LCOA estimations using an electrolyser. The SOFC and battolyser proving more economical in the 2023 scenario (463-588$/t and 573-757$/t), only SOFC in 2030 (438-598$/t). The low LCOA in these and the electrolyser estimates is achieved due to the high load factor of the hydrogen production (90%) and 8500 operating hours with a cost of electricity at 35EUR/MWh.

Only two studies have considered islanded 'green' ammonia production prior to this thesis. ISPT's rationale for not completing a full analysis aptly highlights the reason for this. Islanded operation requires that, even in periods of insufficient power from the variable renewable sources, the production plant still needs to be kept in operation at its minimum power level (25%) [140]. However, while the resources in Goeree-Overflakkee were not suitable to manage this economically Bañares-Alcántara's analysis showed that at a good location (such as Victoria, Australia) with favourable VRE resources and operation of a buffer, it is not only technically viable but promising. However, Bañares-Alcántara's analysis operated an ammonia buffer rather than hydrogen. This, despite having the advantages of easier storage, is a less efficient method of providing the flexibility required than a hydrogen buffer. The other novelty in Bañares-Alcántara's analysis was to consider the catalyst used, comparing the industry standard iron with ruthenium and CoMoN. This analysis found that PEM electrolysis with a cryogenic ASU and iron catalyst was the best combination considered and could achieve 655$/t equivalent to approximately 251$/MWh. The low LCOA achieved is, in part, due to the $\$50.4\text{MWh}^{-1}$ LCOE used with no cost for curtailment.

2.2.2 Gap in 'Green' Ammonia Knowledge Base

The principle gaps in the existing knowledge base (in alignment with research objectives three and four) identified were:

- Functionality to design the optimal islanded 'green' ammonia production process (VRE source selection and sizing in addition to plant design and operation).
- Identification of the current lowest achievable LCOA and, therein, the best locations globally for deployment.
- Quantification of the components of levelised cost of ammonia (LCOA) and prediction of the achievable reduction.
- Identification of the magnitude of cost attributable to the required flexibility of the process due to the VRE sources' variability.

Filling these gaps in knowledge would enable the benchmarking of decarbonised islanded production against conventional methods but also build on Ikäheimo's work to assess its economic viability for seasonal electrical energy storage. The consideration of islanded production provides the most conservative estimates of the achievable LCOA given that the production process must manage all of the renewable power sources' variability. Due to its technology readiness level, current research on the use of ammonia as an energy vector is still largely focussed on the technical development of gas turbine combustion and electrochemical methods (Section 1.3.5). Better understanding the current and future potential LCOA for decarbonised production would enable the levelised cost of storage (LCOS) for P2NH_3 to be calculated.

2.3 Importance of Achieving the Research Objectives

Decarbonisation of the power sector is an imperative if we are to achieve the reductions in CO_2 emissions required to achieve net-zero by 2050. This is not only because of the cut in reductions required from that sector (Section 1.2.3) but also because it is key to enabling the decarbonisation of the other key sectors by elec-

trification using VRE. However, to accurately determine and implement in a timely fashion the most efficient long-term transformation pathways, improved quantitative understanding of the problem is required to frame the policy discussions as well as facilitate additional complexity / accuracy of techno-economic models. This understanding would enable us to understand what VRE penetration and mix of VRE seasonal variations will be problematic and require management with (likely) seasonal electrical energy storage. At present, as demonstrated in this section, this is a gap in our understanding.

Having identified that seasonal electrical energy storage will be required and when (depending on the VRE penetration and mix of VRE sources), an economical decarbonised method needs to be developed. Ammonia, given its technical and chemical characteristics, is a promising option. However, at present there is little understanding of the currently achievable levelised cost of 'green' ammonia (and therefore LCOS), its key components and therefore if / how it can decrease. Moreover, the best locations for production, plant design and operation are also not understood given the variability of the VRE sources.

2.3.1 Decarbonising the Electrical Sector

Current academic research is biased towards short-term energy storage methods given their focus on 20-80% VRE penetration. The rationale behind this is simple: with low VRE penetration the services that are required are predominately short-term (i.e. frequency response or fast response) and, therefore, these are the time periods of operation that are highly valued economically. This could be a short sighted view. Meeting demand at high levels of VRE penetration with only short-term storage owing to seasonal variations would require a lot of energy to be curtailed [144]. Improving the understanding of the impact that the VRE mix and penetration have, for a given location, on a network's flexibility requirements will inform decision makers on the most efficient path of implementation to meet sustainability / VRE penetration targets. Moreover, by providing a viable domain

of technical solutions it will facilitate the implementation of additional complexity to techno-economic models (such as those outlined by Connolly [57] and Pietzcker [61]), thereby improving their accuracy and ability to inform these decisions.

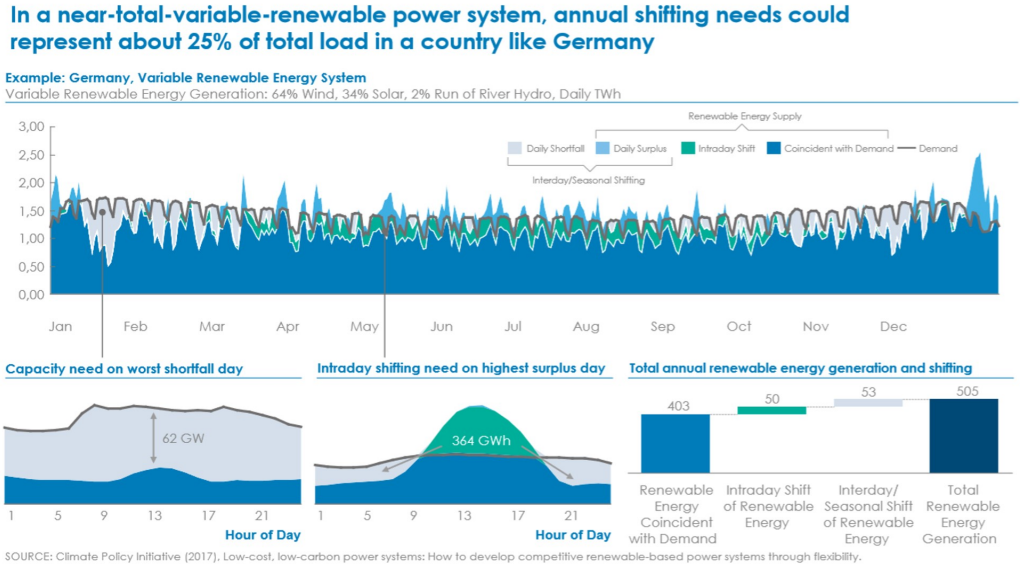

Figure 2.8: Germany's electrical energy storage requirements in 2017 with 36% of gross electricity consumption from renewable energy sources [41]

The VRE penetration of some networks (specifically those not supported by significant dispatchable hydroelectric power capacity) with increasing VRE penetration, such as the UK and Germany (Figure 2.8), have already prompted economists to discuss the beginnings of this problem. Helm for example describing, without quantification, a "threshold" of VRE penetration that when crossed, due to its additional variability, needs to be managed by network flexibility, means that "system average cost become important" [4]. This threshold, or 'tipping-point' as referred to in this thesis, is quantitatively identifiable with a fundamental understanding of the network's balancing problem (to identify the load factor of the dispatchable sources) and economic assumptions (e.g. costs). As the VRE penetration increases, as has been seen in many networks, additional tipping-points occur such as the first need for energy storage (usually batteries meeting the need for services such as enhanced frequency response). With further increases in VRE penetration, other tipping-points specific to location (e.g. energy storage requirements beyond a week in duration) may occur. Having a better understanding of when these may occur,

as well as the magnitude and type of solution/s that would be required as the VRE penetration increases beyond that level, would inform not only current decisions and R&D but future decisions, each of which would reduce the overall cost of meeting sustainability targets.

There is strong consensus amongst economists about the magnitude of the changes required in the power sector. Stern, describing this as a "one in a history transition" [56]. Helm, as challenges "on a scale and magnitude not witnessed since the reconstruction of the electricity industry immediately after the Second World War" [145]. The magnitude of the predicted investment required in electricity networks ($80-90T in the next 15 years i.e. comparable to all existing capital [56]) means that it is of paramount importance to invest effectively and efficiently. We must get this right the first time. We do not have the time (i.e. carbon emissions as noted in Section 1.2.1) or the resources (i.e. capital to waste on underutilised or stranded assets [146]) to do otherwise and the opportunity cost of acting otherwise, is potentially the largest in history. Commercially, it is a significant opportunity, with the value of flexibility predicted to be frequently higher than the value of energy [147].

In order to have an informed discussion on how to decarbonise the electrical sector, to identify the topics and technologies of significant importance to investigate and improve, we need to have a better understanding of the fundamental balancing problem that is trying to be resolved. More specifically, at the most fundamental level, we need to quantify the impact that variable renewable energy integration and new loads such as electrification of transport have on network flexibility. This provides a foundation, founded on the physical limits, for future investigation (e.g. network analysis and economic optimisation of flexibility methods). The importance of such a foundation when discussing variable renewable energy is most aptly described by the late Prof. MacKay, "it's about the physical limits to sustainable energy, not current economic feasibility. While economics is always changing, the fundamental limits won't ever go away. We need to understand these limits" [3]. I believe that current planning and implementation to achieve the sustainability

targets in many countries is marred by existing market design and current discussion having a limited understanding of the fundamental balancing problem posed by VRE integration considered. As a consequence, understandably taken aback in the complexity of managing the trilemma, many decision makers have opted to "pick winners" [4] when commissioning new power capacity and the subsequent additional services required. In the light of such decisions, Helm notes that in recent years techno-economic analysis of power networks has often become simply "a tool to support predetermined technology choices" [4]. Reform to facilitate achieving sustainability targets efficiently requires a sound understanding of the fundamentals of the problem, how these will change with any given decision / implementation and therefore the changing merit of any given option (in the short, medium and long-term) to meeting this objective. Failure to enact such reform of the existing market and improvement of the current validity of the discussion will at best lead to sustainability targets being met inefficiently (with regards to time and cost) and at worst impede their attainment.

2.3.2 Decarbonising the Chemical Sector

Industry is currently seen as the most challenging of the dominant CO_2 emitting sectors to decarbonise (Section 1.2.3). Therefore, despite its substantial emissions, it has received significantly less investigation. To determine which industrial process should be prioritised, they should be ranked using four key variables: fossil fuel dependence for energy (tCO_2/t), fossil fuel dependence for feedstock (t fossil fuel/t), current and predicted quantity of production (t/y) and potential for substitution. Arguably, the most significant chemical from such an analysis (depending on the weighting applied to each variable) is ammonia. Its current dependence on fossil fuels for energy and feedstock and society's dependence on it to support 48% of the population with limited potential for substitution, make it an ideal candidate. Electrolytic production is the most promising technology in the short to medium-term, but there is limited understanding of the achievable LCOA with this process. Func-

tionality to optimise the selection of VRE sources, design the production process and its operation, would achieve this and facilitate faster scale up and implementation of this technology. Further examination of the results could identify the key costs to reduce and technological developments that would be most impactful. Use of this model to compare the best locations for production would identify when this process would be commercially competitive.

2.3.3 Obtainable Synergies

The combination of these analyses will determine when seasonal electrical energy storage will be required and if 'green' ammonia production (in addition to production for conventional use i.e. fertilisers) could economically meet this requirement. This analysis is, therefore, of notable importance to further improve understanding ([137]) of where and when there is potential for a bi-directional synergy: the power network provided with an intraday to seasonal method of energy storage and flexible demand, the ammonia plant provided with a dispatchable source of power to minimise the process flexibility required (and therefore LCOA).

Improved understanding of the potential for this would facilitate revenue stacking [148] for the 'green' production of ammonia, thereby reducing investment risk and the achievable LCOA. This would increase the speed of implementation and scale up, facilitating the supply of sustainable ammonia to meet the growing demand. This is essential if certain targets such as the import of 3Mt p.a. by 2030 in Japan's ammonia strategy roadmap are to be achieved sustainably [98]. A comparative scenario can be seen developing in the electrification of transport. The electrification enables the decarbonisation of the transport sector and reduction of the operating costs for the user, while through the implementation of vehicle-to-grid (V2G) providing substantial short-term balancing services to the electricity network. This has been shown to have substantial potential in Germany (with the higher VRE penetration requiring frequency response) where vehicles have been used as a virtual storage device by numerous companies. P2NH_3 could be an equivalent but for longer

electrical energy storage requirements.

This chapter has shown that greater understanding is required of the network flexibility necessary to enable greater penetration of variable renewable energy sources. It is predicted that for many networks the most cost effective solution to meet this increased flexibility is the implementation of a range of methods. One such method proposed and currently being implemented to provide this increased flexibility is electrical energy storage. As noted by Strbac [122], large scale seasonal storage is predicted to play a significant role as part of this mix but out of no current need, this has largely not been implemented or planned for. Provision of such storage is primarily focussed on storage of the electrical energy chemically due to it capacity for large scale energy and power provision with considerable economies of scale. Of the chemicals available, ammonia is well suited to meeting this need due to its chemical and technical characteristics. However, the design of the optimal 'green' ammonia plant and its operation is not well understood. Achieving these objectives could not only inform decarbonisation of each of these independent sectors but also identify the viability of decarbonised ammonia to achieve a significant synergy between these two sectors.

Chapter 3

Methodology

The research to fill the gaps in the knowledge base identified in Sections 2.1.3 and 2.2.2 is based on the development and use of two models written in MATLAB: The energy storage requirement modelling tool (ESRMT) and the islanded ammonia production modelling tool (IAPMT).

3.1 Energy Storage Requirement Modelling Tool (ESRMT)

The research to improve the understanding of the flexibility requirement of any given electrical network, is founded upon the development of one methodology. This methodology has been developed into a modelling tool (the energy storage requirement modelling tool ESRMT), in MATLAB so that the impact that VRE integration, VRE mix and location have on the flexibility requirements of a network can be quantitatively identified in terms of its magnitude and as a function of energy storage duration.

This methodology was not developed as a techno-economic modelling tool (as shown in Figure 1.2). Instead it has been developed to enable users to improve their understanding of a network's flexibility requirements due to its environmental components

(i.e. demand and VRE profiles). Despite the notable differences in objectives, this work has (when applicable) been conducted in-line with the "recommended practices for wind integration studies" [149] so that the ESRMT, the definition of storage magnitude index (SMI) / storage duration index (SDI) and any subsequent results reliably meet research objectives one and two (and therein the first recommendation of future work by Holttinen [149]).

3.1.1 Overview

The objective for developing the ESRMT is to develop a tool that can quantify the fundamental technical problem of balancing electrical supply and demand as a function of the energy storage required. The requirement itself is expressed as both its magnitude (the fraction of demand that has to be met by stored energy) and as a function of the duration of storage (τ) required (its short / long-term bias). The ESRMT requires the input of the temporally aligned supply and demand energy vectors to consider selection of the decision variables and definition of the assumptions. The output from the ESRMT is primarily based on the calculated storage profile required. This is the amount of energy that has to be stored to meet demand as a function of storage duration (an example can be see in Figure 3.4). As explained later, to quantitatively identify the impact of any given independent (or combination of) decision variable(s) on the storage requirements, two non-dimensional normalised indices are calculated: the storage magnitude index (SMI) and the storage duration index (SDI). The other output from the ESRMT is the sizing (as a percentage of average energy demand) of the storage required for user defined ranges of storage duration (e.g. 1 hour $\leqslant \tau \leqslant$ 24 hours, 24 hours $< \tau \leqslant$ 168 hours and 168 hours $< \tau \leqslant$ 8760 hours).

The tool itself has been written in MATLAB. While the rest of this section provides a detailed description of the ESMRT's methodology, the following paragraph in combination with Figure 3.1 provides a simplistic overview of the calculation to provide additional clarity.

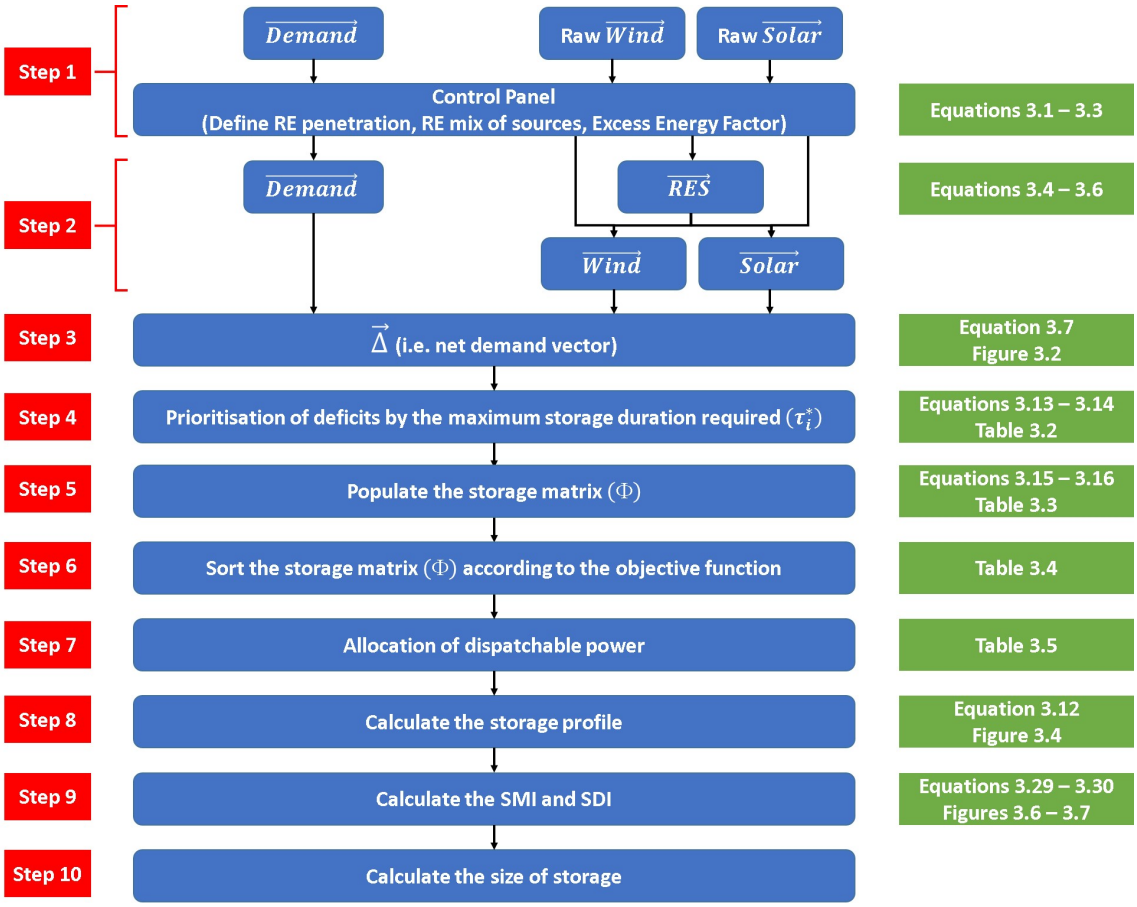

Figure 3.1: Overview of the energy storage requirement modelling tool's (ESRMT) methodology

1. The user provides the time synchronous supply and demand energy vectors to consider and using the control panel defines the decision variables to simulate and required assumptions.

2. The wind and solar PV energy profiles are scaled according to the control panel inputs (i.e. the defined simulation to run) and summed to provide the profile of the energy supplied by renewable sources.

3. Subtraction of the demand vector from the RES vector results in the delta vector

4. A calculation of the maximum storage duration for each time interval with a deficit enables the deficits to be ranked. This determines the order in which the intervals are considered so that shorter-term storage is preferred over longer-term alternatives.

5. By considering these time intervals sequentially the storage matrix is populated. This consists of columns for the surplus index, the duration of storage, the amount of energy shifted and the deficit index.

6. The storage matrix is sorted in accordance with the technical objective function selected (e.g. if the minimisation of the maximum storage duration is set then the matrix is sorted by the storage duration).

7. Available dispatchable energy is calculated and allocated using the sorted storage matrix until either there is no more available energy to allocate or there are no more deficits to fill (i.e. storage matrix is empty).

8. The remaining storage matrix is sorted by the storage duration. The cumulative sum of the energy stored provides the storage profile for that simulation.

9. The storage magnitude index (SMI) is taken directly from the storage profile and the storage duration index (SDI) is calculated from the shape of the profile relative to uniform duration storage.

10. To quantify the size of storage required (for a user specified range of storage duration) the amount of energy stored for those time periods is calculated for the entire time period. Determining the maximum of this determines the size of the storage required.

This analysis has distinct similarities to the well established pinch-analysis methodology commonly used in chemical engineering to minimise energy consumption. However, the differences are that all surplus is of equal value (unlike the magnitude of temperature in conventional pinch-analysis) and that the key consideration is minimising the duration of storage (whereas conventional pinch-analysis was irrespective of time). Precedence for such adaptation is well established [150, 151].

3.1.2 Assumptions and Inputs

The assumptions in the ESRMT are: either fundamental to the modelling tool and cannot be changed or those that user must define in the control panel.

The ESRMT assumes perfect foresight of all future energy provided and demanded and that that the energy storage is lossless (i.e. perfect round-trip efficiency and no hourly losses). This means that the results achieved through use of the ESRMT underestimate the amount of energy stored. For example, if this assumption was relaxed (as noted in Section 7.3) and preventative control implemented to manage the risk of failure / requirement for load-shedding, then additional energy would be stored. The dispatchable energy to be allocated is assumed to be perfectly flexible (i.e. no ramping limitations) and without an upper limit (i.e. rated power is not specified).

The control panel of the ESRMT allows the user to provide the details of the simulation that they want to conduct. The user must first specify the decision variables to consider: VRE penetration (λ as defined in Equation 3.1), VRE mix (θ as defined in Equation 3.2), excess energy factor (μ as defined in Equation 3.3). These, as shown, dictate the amount of energy provided by: wind, dispatchable sources, and the summation of wind and solar ($\int_1^T Wind_t dt$, $\int_1^T Dispatch_t dt$ and $\int_1^T RES_t dt$ respectively). Secondly the user specifies whether the storage is perfect or imperfect (i.e. has a round trip efficiency lower than 100% and hourly losses), the objective function (either minimising the maximum storage duration or the maximum amount of energy stored in any given time period) for the allocation of dispatchable energy (when VRE penetration is not 100%). Finally the assumptions made are entered. This includes the specification of all those variables previously mentioned that have not been selected as decision variables, the period of time to consider from the datasets and other key variables such as imperfect storage variables (that were outlined above).

$$\lambda = \frac{\int_1^T RES_t dt}{\int_1^T RES_t + Dispatch_t dt} \tag{3.1}$$

$$\theta = \frac{\int_1^T Wind_t dt}{\int_1^T RES_t dt} \tag{3.2}$$

$$\mu = \frac{\int_1^T RES_t + Dispatch_t dt}{\int_1^T Demand_t dt} \tag{3.3}$$

3.1.3 Detailed Description of the Fundamental Calculation

Subsequent to the provision of the required energy profiles that are to be considered and the inputs (both the selection of the decision variables and definition of assumption variables) required from the user described above, the first stage of each simulation is to scale the variable renewable energy profiles in alignment with these inputs. Initially, this requires calculation of the total amount of energy that is to be supplied by the RES (Equation 3.4) in alignment with the definition for VRE penetration.

$$\int_1^T RES_t dt = \int_1^T Demand_t dt \times \lambda \times \mu = \int_1^T Wind_t + Solar_t dt \tag{3.4}$$

Using the calculated value of $\int_1^T RES_t dt$, the energy profiles for wind and solar PV and the specified variables to consider (VRE penetration, VRE mix and excess energy), the wind and solar PV energy profiles ($\overrightarrow{Wind}$ and $\overrightarrow{Solar}$ respectively) can be determined (Equations 3.4 to 3.6). These are summed to provide the supply energy profile provided by the RES ($\overrightarrow{RES}$). This, with the subtraction of the demand vector ($\overrightarrow{Demand}$) results in the important delta vector ($\overrightarrow{\Delta}$) (Equation 3.7) about which the entire simulation revolves. If Δ_t is positive there is a surplus of energy and conversely if negative there is a deficit.

$$\int_1^T Wind_t dt = \int_1^T RES_t dt \times \theta \tag{3.5}$$

$$\int_1^T Solar_t dt = \int_1^T RES_t dt \times (1 - \theta) \tag{3.6}$$

$$\overrightarrow{\Delta} = \overrightarrow{RES} - \overrightarrow{Demand} \tag{3.7}$$

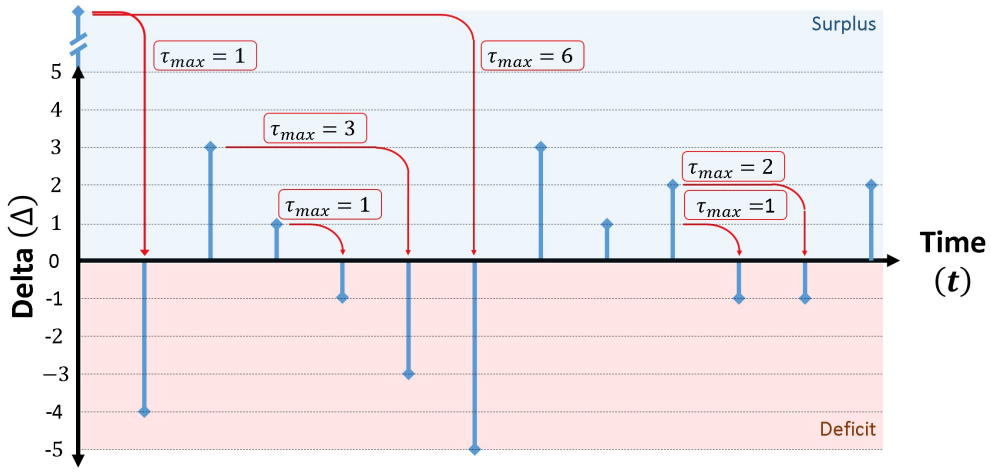

Figure 3.2: Example's delta profile (Δ). Energy deficits are provided with energy from surpluses (red lines). τ_{max} is the maximum storage duration for each deficit.

Figure 3.2 demonstrates the methodology. Each deficit is considered chronologically and an infinite 'virtual' surplus is defined at $t = 0$ as $\Delta_{t=0} = +\infty$. A cumulative summation of Δ is made backwards in time from the index of that deficit (t_i) ignoring any later Δ (i.e. when $t > t_i$). $t_{i\bullet}$ is the first index where the cumulative summation turns positive. $t_{i\bullet}$ determines the maximum storage duration required $\tau_{max} = t_i - t_{i\bullet}$. The deficits are then ranked by the maximum required storage duration (τ_{max}). The shortest required maximum storage durations (τ_{max}) are considered first because this mitigates the practical inefficiencies of storing energy for longer periods of time. This analysis enables the dispatchable power to be allocated optimally, as shown in Table 3.5 using the storage matrix. Deficits mitigated by the 'virtual' surplus are either allocated dispatchable power (see later) or are deficits that cannot be mitigated by storage. Dispatachable power is introduced later in this example.

Table 3.1 shows energy deficits' initial storage requirement, ranked by deficit index and Table 3.2 shows the same data ranked by τ_{max} so deficits with the smallest maximum storage duration are considered first. Table 3.3 shows a storage matrix for the ranked deficit indicies from Table 3.2, maximising short term storage use

to reflect actual practice. In practice short-term energy storage is prioritised to 'sweat the capital' e.g. hourly storage can store energy up to 4380 times a year vs. weekly storage 52 times a year. A consequence of meeting the shortest energy storage duration requirements is that surplus energy is always stored for the next available deficit.

Deficit Index ($t_{i\bullet}$)	τ_{max}
1	1
4	1
5	3
6	6
10	1
11	2

Table 3.1: Energy deficits' storage requirement, ranked by deficit index.

Deficit Index ($t_{i\bullet}$)	τ_{max}
1	1
4	1
10	1
11	2
5	3
6	6

Table 3.2: Energy deficits' storage requirement, ranked by the maximum storage duration τ_{max}.

Deficit Index ($t_{i\bullet}$)	**Storage Duration** (τ)	**Energy Stored** (E)	**Surplus Index**
1	1	4	0
4	1	1	3
10	1	1	9
11	2	1	9
5	3	3	2
6	6	5	0

Table 3.3: Storage matrix, showing each deficit's storage requirement (E and τ) and the earlier surplus index that is stored to mitigate the later deficit (surplus index vs. $t_{i\bullet}$)

Having identified the storage requirement (Table 3.3), a new variable can be introduced: dispatchable power. Whether dispatchable power is available depends on the users' defined VRE penetration (Equation 3.8). How the power is allocated depends on the user's specified objective function, either minimising the maximum required storage duration τ, or minimising the maximum amount of energy stored at any given time E. Regardless of the user's specified objective function, dispatchable power is first allocated to deficits and associated storage requirements currently met by the 'virtual' energy surplus (defined at $t = 0$ as $(\Delta_{t=0} = +\infty)$). In Table 3.3 these deficits have a surplus index of 0. The remaining storage requirements (where

surplus index is greater than zero) are ranked according to the user's specified objective function. This example assumes that the objective function is to minimise the maximum storage duration.

$$\int_1^{\mathrm{T}} \mathrm{Dispatch}_t \, \mathrm{dt} = \int_1^{\mathrm{T}} \mathrm{Demand}_t \, \mathrm{dt} \times (1 - \lambda) \times \mu \tag{3.8}$$

$$\rho = \frac{\int_1^{\mathrm{T}} \mathrm{Wind}_t + \mathrm{Solar}_t + \mathrm{Dispatch}_t - \mathrm{Demand}_t \, \mathrm{dt}}{\int_1^{\mathrm{T}} \mathrm{Wind}_t + \mathrm{Solar}_t \, \mathrm{dt}} \tag{3.9}$$

Deficit Index $(t_{i\bullet})$	**Storage Duration** (τ)	**Energy Stored** (E)	**Surplus Index**
1	1	4	0
6	6	5	0
5	3	3	2
11	2	1	9
4	1	1	3
10	1	1	9

Table 3.4: Storage matrix for power allocation. The storage requirements are ranked first by whether the surplus index is zero, second by the storage duration (τ), thirdly by the amount of energy stored (E) and finally by the deficit index.

Deficit Index $(t_{i\bullet})$	**Storage Duration** (τ)	**Energy Stored** (E)	**Surplus Index**
~~1~~	~~1~~	~~4~~	~~0~~
6	6	~~5~~ 4	0
5	3	3	2
11	2	1	9
4	1	1	3
10	1	1	9

Table 3.5: Final storage matrix

$$\overrightarrow{\tau} = [1, 2, 3, 4, 5, 6, 7 ... 8757, 8758, 8759, 8760] \tag{3.10}$$

$$\overrightarrow{E} = [2, 1, 3, 0, 0, 4, 0 ... 0, 0, 0, 0] \tag{3.11}$$

$$\sum_{\tau=1}^{t} E_t = [2, 3, 6, 6, 6, 10, 10 ... 10, 10, 10, 10] \tag{3.12}$$

This example assumes that there are five units of dispatchable power that can be

allocated to the deficits in Table 3.3. To allocate the dispatachable power efficiently, the storage requirements in the Storage Matrix (Table 3.4 are ranked first by whether the surplus index is zero, second by the storage duration (τ), thirdly by the amount of energy stored (E) and finally by the deficit index. This is shown in Table 3.4. Dispatchable power is allocated according to the ranking, starting with the first storage requirement in the matrix, until all power is allocated. The results are shown in Table 3.5. Allocating dispatachable power in this way identifies the deficits that cannot be met (e.g. four units of demand cannot be met at $t = 6$), surpluses that are curtailed (at $t = 7, 8$ and 12), and importantly the final storage matrix that defines the electrical storage requirements of the system. The amount of curtailed VRE depends not only on the demand, wind and solar power profiles provided, but also on how the dispatchable power has been allocated. The magnitude of the VRE curtailment as a fraction of the total VRE supplied is calculated using Equation 3.9.

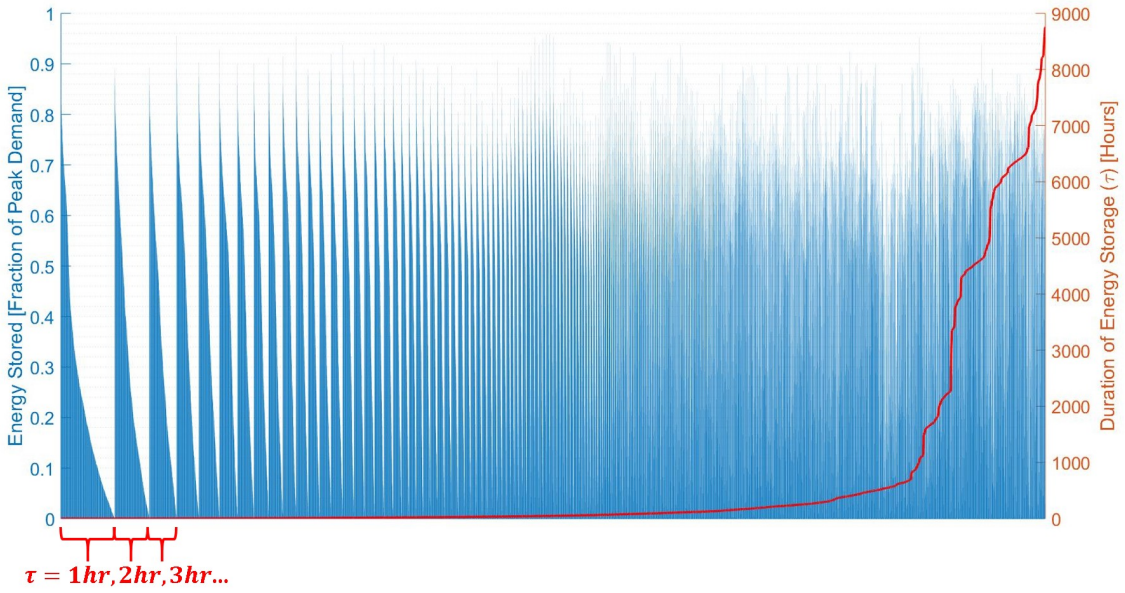

Figure 3.3: The calculated system storage requirement arranged by the duration of storage (τ) then the magnitude of energy moved (E) for Norman Wells, Canada with 100% RES penetration, 100% Wind:0% Solar PV power supply, no VRE curtailment, no DSM and no interconnection. The left vertical axis (blue bars) is the amount of energy stored E and the right vertical axis (red line) is the corresponding duration of storage τ.

To better visualise the magnitude and type of energy storage required three vec-

tors are defined / calculated: the storage duration vector (Equation 3.10), energy storage vector (Equation 3.11), and the cumulative energy storage vector (Equation 3.12). Plotting ever single time that energy stored however, (even sorted by the storage duration τ) has limited use. Little insight can be gleaned from Figure 3.3. However, when the cumulative energy storage vector is plotted against τ (as shown in Figure 3.4), this results in the 'storage profile' for that system. The amount of energy that has to be stored up to a given value of τ to balance the network can be readily determined. One strength of this is that the storage profile determines the requirement at the granularity of the input data (i.e. 1 hour). Subsequent grouping of the storage requirement enables the user to determine the relative importance of each storage type.

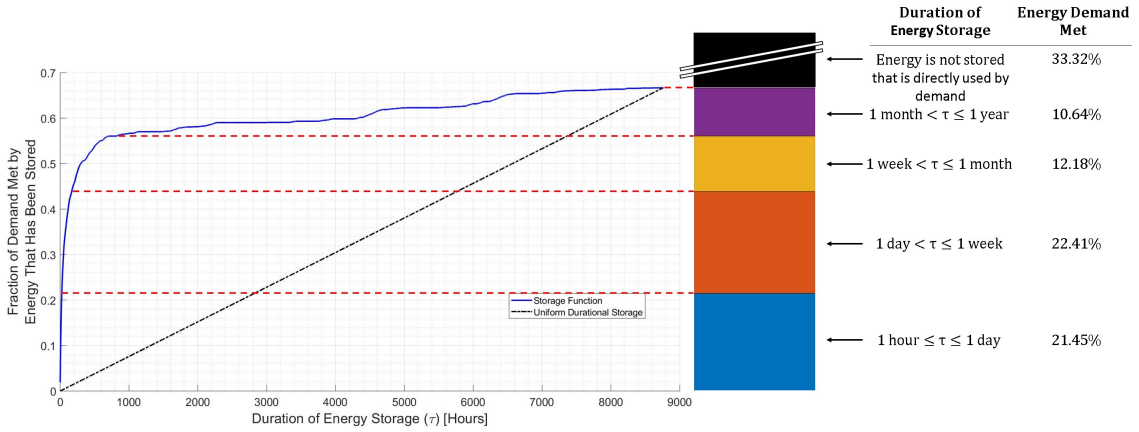

Figure 3.4: The 'storage profile' for Norman Wells, Canada with 100% RES penetration, 100% Wind:0% Solar PV power supply, no VRE curtailment, no DSM and no interconnection. The arbitrary grouping of the storage durations (presented as the stacked bar chart) show their relative importance / use.

To calculate the size of energy storage required the user specified maximum and minimum storage duration (τ) to be considered is used. Considering the storage matrix entries with a storage duration in this range a vector is constructed of the amount of energy in this storage for each time interval. The maximum value in this vector is the size of the storage required.

Algebraically, the process can be described by Equations 3.13 - 3.16. Equations 3.13 and 3.14 show the cumulative summation of the delta vector $\overrightarrow{\Delta}$, backwards in time, from a deficit index at t_i. The maximum storage duration (τ_{max}) is determined

using Equation 3.14 and the result of the cumulative summation in Equation 3.13; an example is shown in Table 3.1. Equations 3.15 and 3.16 populate the storage matrix Φ depending on whether the virtual surplus is required to fill the deficit considered; an example of this result is Table 3.3.

$$\overrightarrow{\Gamma_t} = \sum_{t=T}^{t=t_1} \Delta_t \tag{3.13}$$

$$t_{i\bullet} = \begin{cases} 0 & \text{If } \max(\overrightarrow{\Gamma}) \leqslant 0 \\ \text{t when } \overrightarrow{\Gamma} \text{ first goes positive} & \text{Otherwise} \end{cases} \tag{3.14}$$

$$\mathbf{\Phi} = [t_i \quad \overrightarrow{t_{t_i:T} - t_i} \quad \overrightarrow{\Delta_{t_i:T}} \quad \overrightarrow{t_{t_i:T}}] \tag{3.15}$$

If the virtual surplus is required then Φ is adapted as follows:

- Set $\Phi_{1,3} = \sum_{x=1}^{end} \Phi_{x,3}$ (The amount of energy shifted from the synthetic surplus at t = 0 once any other surplus/es have been used to meet the deficit).
- Set $\Phi_{1,2} = t_{i\bullet} - t_i$ (The storage duration of the energy shifted from the synthetic surplus to this deficit)
- Set $\Phi_{1,4} = 0$ (The time interval of the surplus i.e. the synthetic surplus at t = 0)

$$\mathbf{\Phi} = [t_i \quad \overrightarrow{t_{t_i:t_{i\bullet}} - t_i} \quad \overrightarrow{\Delta_{t_i:t_{i\bullet}}} \quad \overrightarrow{t_{t_i:t_{i\bullet}}}] \tag{3.16}$$

Only shifting energy from surpluses in $\overrightarrow{\Delta}$ (i.e. none from the virtual surplus at t = 0) then Φ is adapted as follows:

- Set $\Phi_{end,3} = \sum_{x=1}^{end-1} \Phi_{x,3}$ (Calculating the amount of energy shifted from the final surplus once any other surplus/es have been used to meet the deficit).

3.1.4 Output from the ESRMT

The storage profile when considered in isolation is a useful tool to identify the importance of different storage durations. However, comparison of tens (Figure 3.5), let alone thousands, of these to identify the sensitivity of a network's flexibility requirement (i.e. storage profile) to a given decision variable such as VRE penetration, is virtually impossible. Therefore, the information in the storage profile needs to be condensed down to two non-dimensional indices: the storage magnitude index (SMI) and the storage duration index (SDI). The SMI is a measure of the magnitude of storage required, specifically the fraction of total demand that is met by energy that requires storage for a year or less (Equation 3.17, where E_τ is the fraction of demand that is met by energy from storage with a duration of τ or less). As shown in Figure 3.6, It can be taken directly from the storage profile. It can range in value from 0, when there is no requirement for storage, to 1, when the demand is entirely dependent on energy that has been stored.

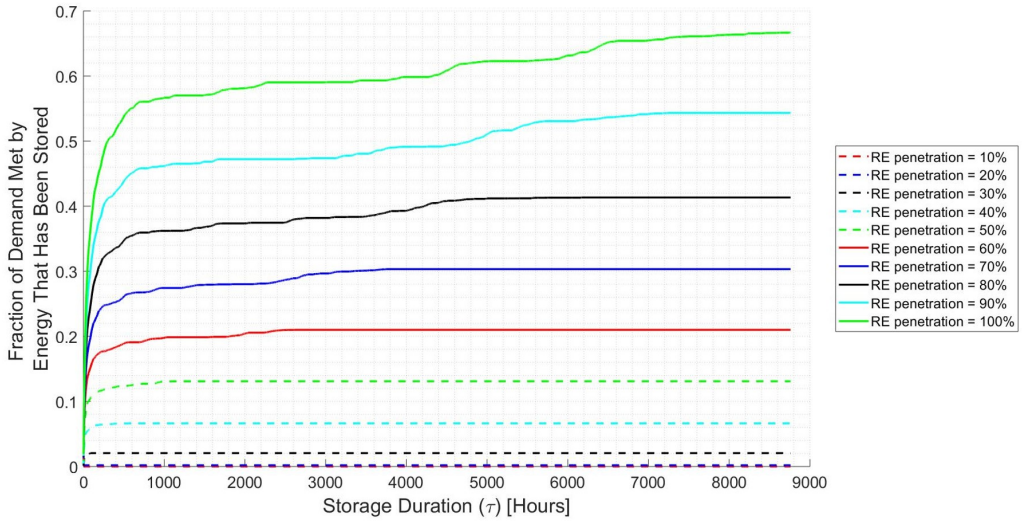

Figure 3.5: The difficulty in comparing storage profiles: Norman Wells, Canada with 100% Wind: 0% Solar PV power supply, no VRE curtailment, no DSM and no interconnection.

$$SMI = E_{\tau=8760} \tag{3.17}$$

$$SDI = \frac{\int_0^T |E_\tau - (\frac{\tau}{T} \times E_{\tau=8760})| d\tau}{\frac{T \times E_{\tau=T}}{2}} \tag{3.18}$$

The SDI is a measure of the mean storage duration required, specifically quantifying its short- / long-term bias by comparing against a theoretical dependence on all durations of storage equally (the uniform storage duration requirement in Figure 3.7). The calculation of SDI (Equation 3.17) requires finding the difference between the actual storage profile and a uniform storage duration requirement, then normalising this by the worst that it could be. It can range in value from -1, when the storage requirement is entirely dependent on yearly storage ($\tau = 8760$), to +1 when the demand is entirely dependent on hourly storage ($\tau = 1$). Therefore, if the SDI is positive the network's storage requirements are short-term biased, negative and the requirements are long-term biased. If the SDI is equal to zero, then despite storage still being required it is neither short- nor long-term biased: it is equally dependent on short- and long-term storage. In practice, as one would expect, the SDI is commonly positive and greater than 0.5 showing that the requirements are short-term biased.

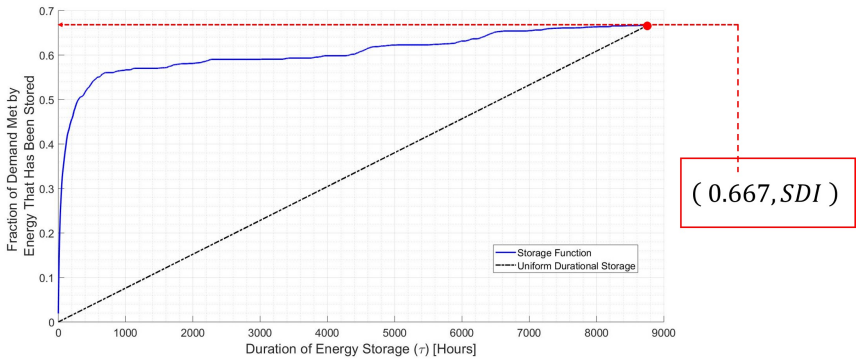

Figure 3.6: Definition of the Storage Magnitude Index (SMI): Fraction of demand met by energy that has been stored (Equation 3.17).

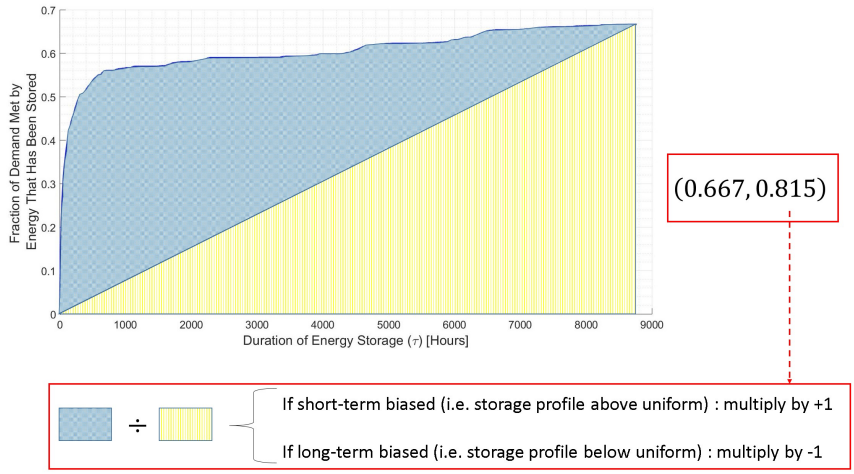

Figure 3.7: Definition of the Storage Duration Index (SDI): Normalised variance from uniform duration storage (Equation 3.18).

The two indices quickly provide a quantitative understanding of the magnitude and type of storage needed to meet a network's flexibility requirements. Use of these indices enables identification of the impact key variables have on the flexibility requirement. Despite the benefits of having the x- and y-axes being the two indices, such as being able to identify the impact of a variable on storage magnitude and duration from one graph (Figures 3.8 and 3.9), it was decided that this method of presentation was unclear and therefore untenable. Plotting one index with respect to the variables of interest has therefore been favoured (e.g. Figures 5.1 and 5.2).

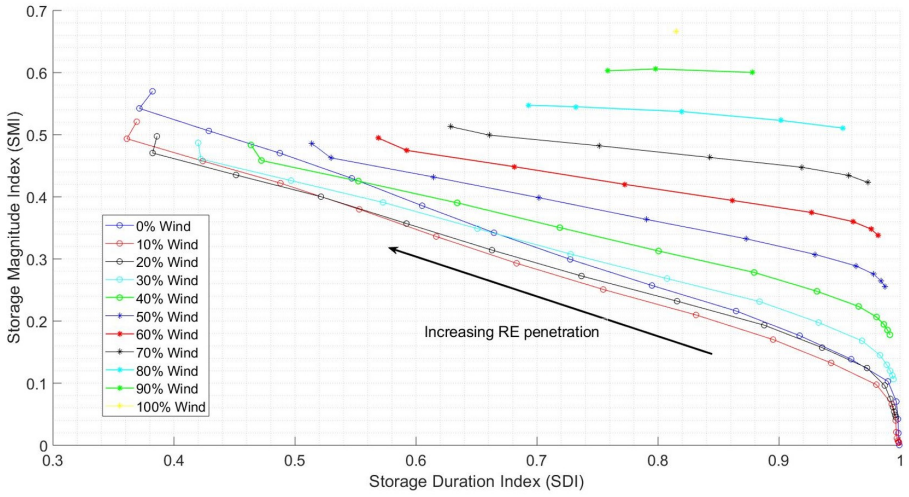

Figure 3.8: Impact of the VRE penetration on the storage magnitude and storage duration indices (SMI / SDI) for Norman Wells, Canada.

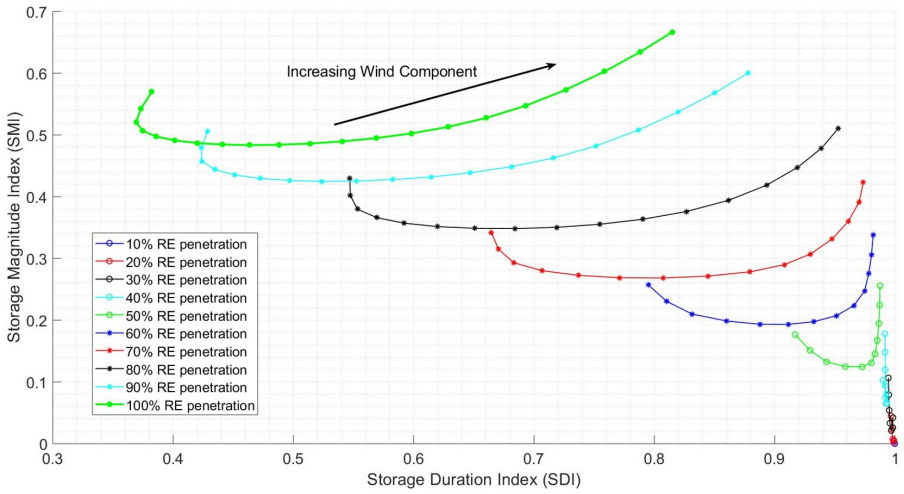

Figure 3.9: Impact of the mix of VRE sources on the storage duration index (SMI / SDI) for Norman Wells, Canada.

An alternative way of looking at this solution is to instead flip the storage profile (Figure 3.4) and therefore show the amount of energy curtailment that will be avoided due to implementation of storage depending on its maximum storage duration (Figure 3.10). The reasons that the results have not been presented in this way are two-found:

- It is not obvious that in addition to the curtailment that is mitigated (Figure 3.10) the requirement for additional energy reserves is also mitigated. Considering one flexibility method (energy storage) provides a temporal understanding of the balancing problem that is otherwise unclear.
- As with the storage profile, the identified amount of curtailment (and reserve capacity) mitigated from the result (Figure 3.10) is only correct if all shorter duration storage has been implemented. Otherwise, due to the short duration storage being preferred in the methodology (Section 3.1), it is only a lower estimate of the impact.

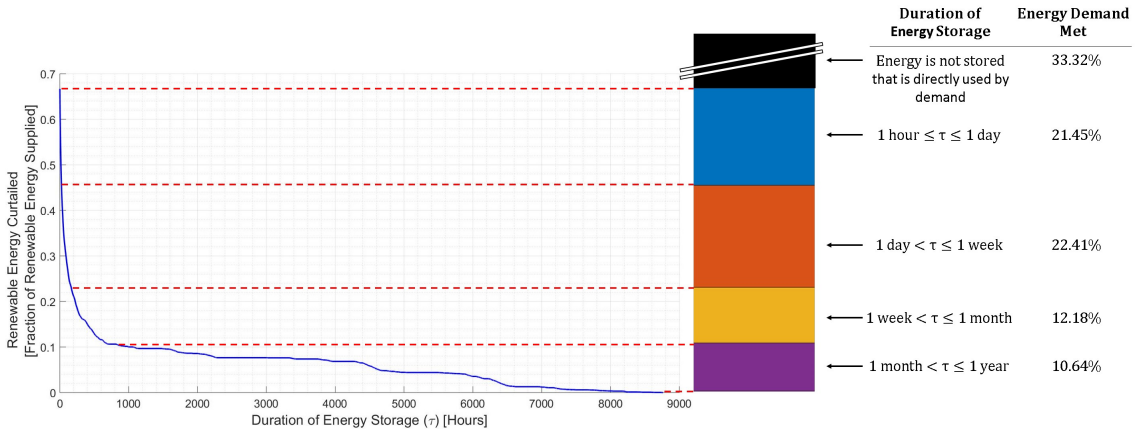

Figure 3.10: Norman Wells, Canada at 100% VRE penetration and 100% Wind: 0% Solar PV power supply, no DSM and no interconnection. The sensitivity of the amount of VRE curtailment mitigated to the energy storage duration.

3.2 Islanded Ammonia Production Modelling Tool (IAPMT)

The work on the electrolytic production of ammonia is based on the development of islanded ammonia production modelling tool (IAPMT), whose development has spanned for the duration of this project. As the name suggests it was developed to optimise the islanded electrolytic production of ammonia using renewable energy. The model when provided with VRE profiles optimises the mix of VRE sources selected, the design and operation of the production plant to minimise the levelised cost of ammonia (LCOA). A preliminary version, while having notable functionality and providing many useful insights (as described in Section 4.2.1), was developed upon to improve its accuracy and calculation speed. In this section, the methodology of the final model will be described and developments from the preliminary model highlighted [141].

3.2.1 Overview

The model constructed for this investigation was written in MATLAB to enable the high-level analysis required. It is based on use of a genetic algorithm to optimise, with the objective function of minimising the achieved LCOA, three decision

variables: the fraction of energy from wind (θ, i.e. the mix of VRE sources as defined in Equation 3.2), the rated power of the electrolyser (P^*_{Elec}) and the combined rated power of the HB synthesis and ASU ($P^*_{HB/ASU}$). In practice this is achieved (as shown in Figure 3.11) by setting up a generation of chromosomes (i.e. defining decision variables to consider) and for each chromosome calculating if the process design is technically viable; if so determine the best operation schedule and then calculate the LCOA. Having completed this for the entire generation, a new generation of chromosomes is populated using the best values (allowing for mutation). This continues until the defined number of populations has been completed. The best solution from the final population is output as the solution.

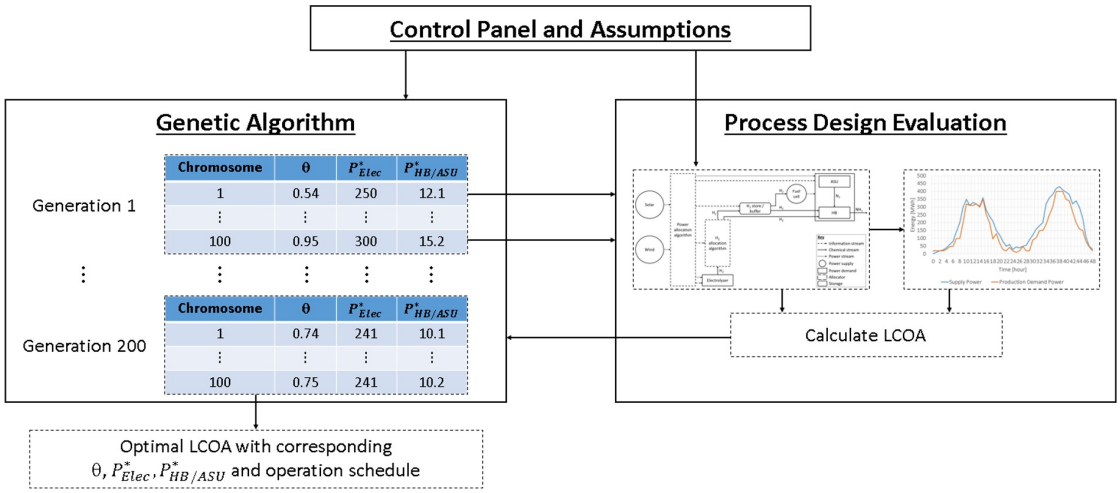

Figure 3.11: Overview of the islanded ammonia production modelling tool (IAPMT)

3.2.2 Assumptions

The assumptions made in the model can be separated into those relevant to the methodology and others to the calculations.

Methodological Assumptions

The model has been designed to operate using wind and solar energy data with thirty minute or hourly resolution. It is assumed that the electrolyser, the HB synthesis and the ASU are able to ramp instantaneously and to operate in steady state with constant specific energy consumption (as defined in Table 3.7) for the duration of

the time interval. This assumption is justifiable due to the hourly resolution of the power profiles (of both supply and process demand) used and that Siemens' SILYZER 300 has the ability to ramp at 10% rated power per second [152]. In the mechanism for the allocation of available energy within the process assessment(Step 6, Section 3.2.3) perfect forecasting of available energy is assumed.

The main variable about which the plant design is optimised is the average energy supplied to the plant. It has been defined as 100MW. The total rated power of the plant, total rated power of the VRE sources used or the average mass flow rate of ammonia produced could have been use but were opted against. Setting the rated power of the plant is similar to the method chosen. Using the total rated power of the VRE sources makes it more difficult to see the impact of the VRE profiles on the VRE selection and plant design. The average mass produced, instead of scaling the plant size, scales the rated power capacity of the VRE sources without regard for the availability of the VRE resource at that magnitude.

For the optimisation the rated power of the ASU and HB processes are lumped together (ASU/HB) as one of the decision variables that is optimised by the genetic algorithm. This is replicated during the power allocation (within the process assessment) by allocating power to the combination of the components. This is acceptable at present due to the small demand for power and capital expenditure (CAPEX) of the ASU relative to the HB process, and particularly in relation to the electrolyser. The control parameters that govern the operation of the genetic algorithm were defined after review of literature [153, 154, 155], initial trial and then subsequent discussion with Dr Manojkumar Ramteke (Indian Institute of Technology, New Delhi). Convergence was checked by comparing the results for over 20 locations with a brute force approach. In practice, the optimal solution was commonly converged upon within 80 generations. The use of a genetic algorithm was favoured over other derivative-free global optimisation algorithms primarily due to the nature of the problem. The genetic algorithm could handle the noisy environment well, was robust with respect to local minima, and could handle multiple objective functions

and in-viable solution spaces quickly. In addition to these reasons, practically the ease of parallelising the genetic algorithm substantially sped-up computational time when considering multiple locations.

Variable	**Value**
Number of generations	200
Number of population	100
Number of crossover	20
Probability of crossover	80%
Number of mutation	20
Probability of mutation	10%
θ initial population lower limit	0
θ initial population upper limit	1
P^*_{Elec} initial population lower limit	0
P^*_{Elec} initial population upper limit	$\overline{RES} \times 10$
$P^*_{HB/ASU}$ initial population lower limit	0
$P^*_{HB/ASU}$ initial population upper limit	$\overline{RES} \div 3$

Table 3.6: Genetic algorithm's control parameters [142]

Calculation Assumptions

The assumptions made for operation of the calculation can be divided in two: technical and economic. While all the technical assumptions are independent of location, a small proportion of the economic assumptions are dependent.

Location independent technical assumptions made in the model can be seen in Table 3.7. It should be particularly noted that the specific energy consumption of the three main processes (electrolysis, synthesis and air separation) are all constant. The functionality of non-constant specific energy consumption for electrolysis (using the piece-wise and non-linear functions [134, 137] respectively) was integrated into the model. However, prioritising the use of the power allocation mechanism has meant that this functionality has been currently not used. The reason for this is that introducing this additional snon-linearity significantly complicates the complexity of the power allocation mechanism. This has been identified in Chapter 7 as an important piece of future work. While this is a limitation in the current methodology (Section 7.2), and part of the proposed future work (Section 7.3), prioritisation of the power

allocation mechanism was made due to its greater impact on the achievable LCOA. By using constant specific energy consumption for the electrolyser the estimated LCOA will be more conservative than other estimates given that their functions of efficiency increases at lower loads (i.e. "the energy required per kilogram of hydrogen produced decreases from 4.40kWh/m^3 towards the thermodynamic minimum of 3.54kWh/m^3" [141]). The assumption used here over-scales the size of the electrolyser required in practice. While the minimum operating power of the synthesis process has been identified (by Morgan [99]) to have notable impact on the achievable LCOA, to date the 20% minimum power stated by Ostuni and Zardi [156] is technically unproven. The assumptions made for the global analysis (Section 4.2.2) can be seen in Table 3.8 of the location independent cost assumptions.

Variable	**Value**	**Reference**
Electrolyser lifetime	30 years	[157, 158, 159, 152, 160]
Wind lifetime	30 years	
Solar lifetime	30 years	
Hydrogen fuel cell lifetime	5 years	[160]
Synthesis and ASU lifetime	5 years	[161]
Maintenance downtime	20 days per year	[161]
Electrolyser specific energy consumption calculated from $\eta_{LHV} = 70\%$	47.571kWh/kg	[158, 152]
Synthesis specific energy consumption	0.532kWh/kg	[99]
ASU specific energy consumption	0.110kWh/kg	[162]
Energy losses in the compression of Hydrogen for storage	6.6% of LHV	[137, 163]
Hydrogen fuel cell efficiency	50% of LHV	[164]
Minimum operating power of Electrolyser	0% of P_{Rated}	[158, 152]
Minimum operating power of Synthesis & ASU	20% of P_{Rated}	[156, 165]

Table 3.7: Location independent technical assumptions for the production of ammonia in the IAPMT

3.2.3 Detailed Description

To adequately explain the IAPMT methodology, in alignment with Figure 3.11, it is separated into two parts, explanation of: the genetic algorithm and the process design evaluation.

Variable	Value	Reference
Electrolyser CAPEX (2019 scenario)	\$700kW^{-1} of P_{rated}	[158]
Electrolyser CAPEX (2030 scenario)	\$341kW^{-1} of P_{rated}	[158, 159, 166, 167]
Synthesis CAPEX	\$6,467kW^{-1} of P_{rated}	[137, 140]
ASU CAPEX	\$13,182kW^{-1} of P_{rated}	[137]
Hydrogen storage CAPEX	\$500kg^{-1}	[168]
Hydrogen fuel cell CAPEX	\$900kW^{-1} of P_{rated}	[161]
Operation and maintenance of all components	2% CAPEX per year	[137]
Cost of water feedstock	\$2t^{-1}	[138]
Discount factor for renewable energy (multinational production)	7.14%	[169]
Discount factor for production process (multinational production)	3.33% CAPEX p.a.	[169]

Table 3.8: Location independent economic assumptions for the production of ammonia in the IAPMT [142]

Genetic Algorithm

The genetic algorithm used was the multi-objective non-dominated sorting genetic algorithm (NSGA-II) developed by Deb [170], improving on the NSGA [171]. The source code written by Aravind Seshadri in MATLAB was provided by Dr Ramteke at IIT Delhi. I adapted it for use with the process design evaluation. While a detailed description and evaluation of the NSGA-II methodology can be found in [172], here I will explain its interconnection with the process design evaluation.

The interaction between the process design evaluation and the genetic algorithm is straightforward. The genetic algorithm provides the process design evaluation with the decision variables (θ, P^*_{Elec} and $P^*_{HB/ASU}$). The process design evaluation determines if the system specified is technically viable. If it is, then an optimal operation schedule is calculated, and the LCOA achieved is outputted to the genetic algorithm. If the system is not technically viable then the LCOA provided is defined as a null value. In this instance, this is interpreted by the genetic algorithm and the LCOA is changed to an excessively large number (i.e. a fixed penalty is applied). This penalty ensures that non-viable systems are avoided. Within the genetic algorithm this exchange of chromosome (i.e. decision variables) and the LCOA result occurs

after the population of chromosomes to consider for that generation has been compiled. For the preliminary model, the genetic algorithm had not been implemented and the provision of the decision variables was achieved through brute force.

Process Design Evaluation

The process design evaluation requires the input of wind and solar power profiles, technical and economic assumptions and the decision variables (i.e. θ, P^*_{Elec} and $P^*_{HB/ASU}$) to consider. The output from the assessment used by the genetic algorithm is the LCOA. However, once the optimal decisions variables have been determined the process design evaluation also provides all mass and energy flows within the process over the time period, the sizing of the other components required (i.e. hydrogen fuel cell and hydrogen storage) and all components of cost. The following description provides additional details of the steps shown in the Figure 3.12 overview.

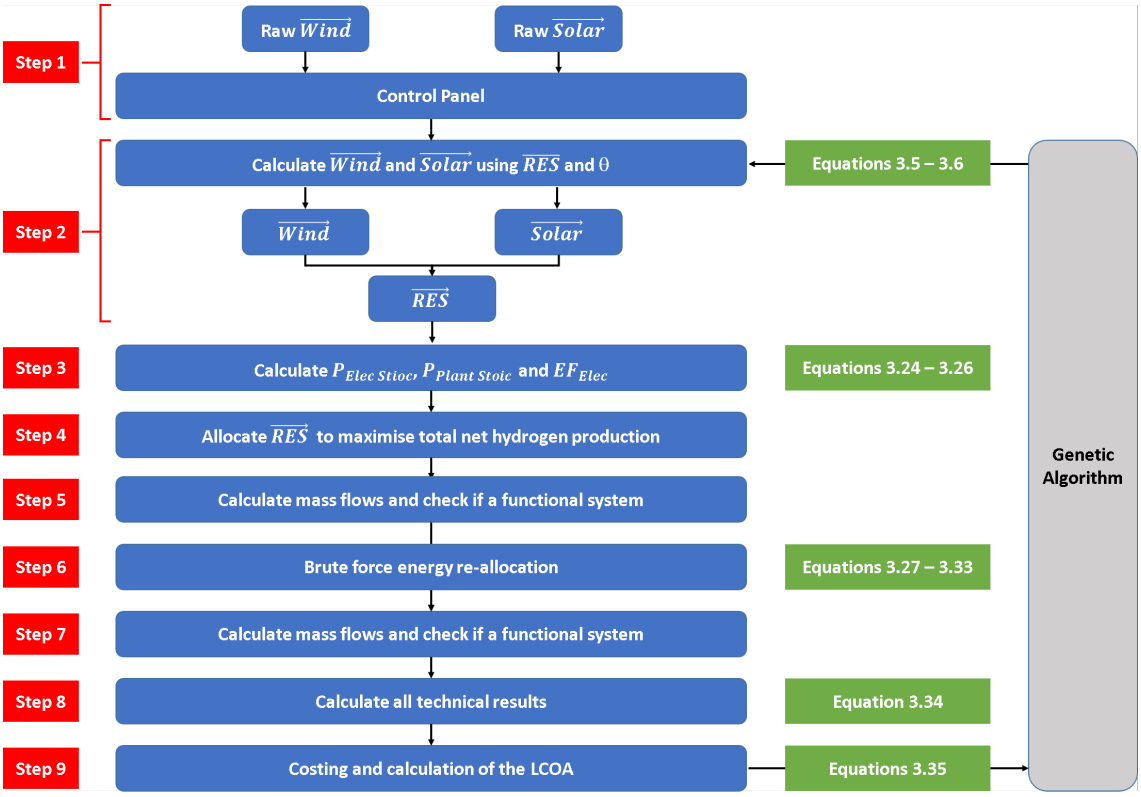

Figure 3.12: Overview of the islanded ammonia production modelling tool's (IAPMT) methodology

After the user has provided the temporally aligned wind and solar PV energy profiles

for the location being considered, they need to define the technical and economic assumptions (Tables 3.7, 3.8 and 4.1) and the control parameters for the genetic algorithm (Table 3.6). With the input of the decision variables, θ, P^*_{Elec} and $P^*_{HB/ASU}$), from the genetic algorithm (i.e. a chromosome) the wind and solar PV energy profiles ($\overrightarrow{Wind}$ and $\overrightarrow{Solar}$) can be scaled accordingly using Equations 3.5 and 3.6. The summation of these scaled profiles provides the supply energy profile ($\overrightarrow{RES}$) for the simulation.

Step 3, involves the calculation of the production plant's key power ratings. Specifically the stoichiometric power requirement for the electrolyser (i.e. power required to produce enough hydrogen feedstock for the HB to operate at rated power) and therefore the production plant as a whole ($P_{ElecStoic}$ and $P_{PlantStoic}$). This is achieved using the provided values for P^*_{Elec} and $P^*_{HB/ASU}$) with the user defined assumptions for the minimum operating power of the synthesis process and the specific energy consumption of the electrolyser ($SpecC_{Elec}$), HB ($SpecC_{HB}$) and ASU ($SpecC_{ASU}$) (Equations 3.19 and 3.20 where MM is the molecular mass). This enables the determination of how much the electrolyser has been oversized (i.e. the electrolyser excess factor EF_{Elec}) to provide flexibility to the production process (Equation 3.21).

$$P_{ElecStoic} = P^*_{HB/ASU} \left(\frac{SpecC_{Elec}}{SpecC_{HB}}\right) \left(\frac{MM_{H2}}{MM_{NH3}}\right) \left(\frac{3}{2}\right) \tag{3.19}$$

$$P_{PlantStoic} = P_{ElecStoic} + P^*_{HB/ASU} \tag{3.20}$$

$$EF_{Elec} = \left(\frac{P^*_{Elec}}{P_{ElecStoic}}\right) - 1 \tag{3.21}$$

In order to sift out those process designs that are technically infeasible, and thereby improve computational time, the supply energy profile ($\overrightarrow{RES}$) is allocated to the three processes (electrolyser, HB and ASU) to maximise the amount of hydrogen produced. This involves setting the HB and ASU to operate at its minimum operating power (as defined in Table 3.7) and enabling the electrolyser to be allocated any remaining energy, barring that required for the compression and storage of excess

hydrogen (excluding the maintenance period when all processes are allocated no energy). If the summation of the net hydrogen (i.e. hydrogen produced minus the hydrogen consumed) produced across the time period is not positive (i.e. there is excess hydrogen produced) then there is no operation schedule (without additional shut-down periods) that would make this a feasible process. This being the case the process design evaluation stops and outputs that the LCOA is null (i.e the process defined by the decision variables provided is not viable).

However, if the process is viable and there is excess hydrogen produced, this needs to be remedied as it is more beneficial (in terms of the achievable LCOA) to reduce the total amount of excess hydrogen and increase the amount of ammonia produced. This is achieved in Step 6: a brute force re-allocation of energy to the three processes (and hydrogen storage as required).

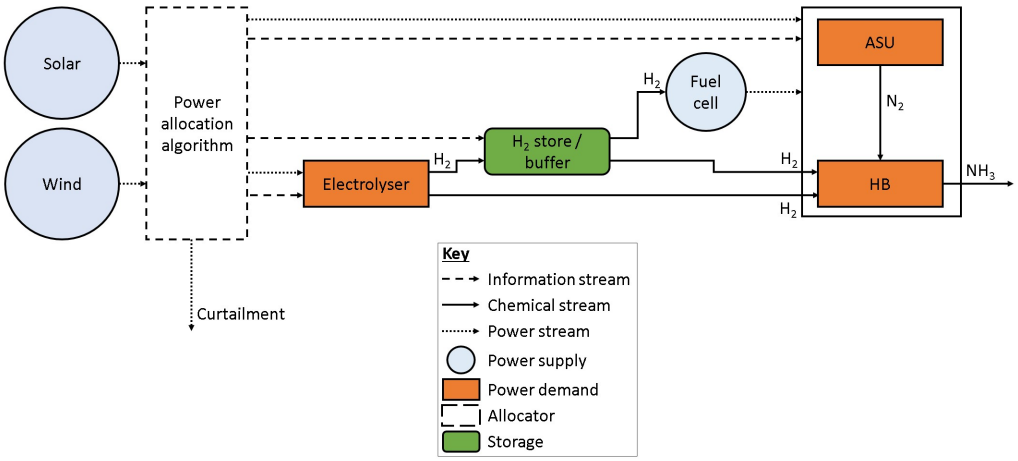

Figure 3.13: Process block diagram including power, chemical and information flows.

The brute force allocation method was preferred over other methods (such as use NSGA-II with and without a spline) as it is robust and provided insights during simulation of the problems faced by the process with an intermittent power source. The method itself is based on calculating the amount of energy that can be re-allocated, identifying the time indices that should be considered for re-allocation, calculating their individual potential for each method of re-allocation then by considering the indicies sequentially re-allocating the excess energy available.

The amount of energy that is available to be re-allocated is determined by considering the amount of excess hydrogen that is currently produced (when the energy profiles have been defined to maximise the amount of hydrogen produced) using Equation 3.22. This is determining the amount of energy that is currently allocated to the production of hydrogen (and its storage) that is not used for ammonia production.

$$\text{Energy to re-allocate} = \text{Total net mass of hydrogen produced} \times (SpecC_{Elec} + SpecC_{H2Store}) \quad (3.22)$$

Next the time indices that need to be considered are identified. The first and last indices of the time period to consider are identified by considering the current cumulative net hydrogen production vector. The first index to consider for re-allocation of energy is the index with the minimum value of this vector (Equation 3.23). The final value to consider is the index of the maximum of this vector between the minimum index and the end of the vector (Equation 3.24). These are defined so that, if possible, the storage size of the hydrogen storage required is minimised.

$$t_{First} = \text{Index of } min\left(\overrightarrow{\text{Cumulative sum of net hydrogen mass produced}}\right) \quad (3.23)$$

$$t_{Last} = \text{Index of } max\left(\overrightarrow{\text{Cumulative sum of net hydrogen mass produced}}_{t=t_{First}:T)}\right) \quad (3.24)$$

Over the identified time period the potential impact on the net-hydrogen produced of the energy re-allocated at each individual time interval is then identified. Using Equations 3.29, 3.30, 3.31, 3.32 and 3.33, the impact of the energy re-allocation is determined, in order or priority, by each method of energy re-allocation, shifting energy from:

1. Curtailment and Hydrogen Storage to Synthesis & ASU ($E_{Method1}$)
2. Electrolyser and Hydrogen Storage to Synthesis & ASU (hydrogen production

currently requiring storage) ($E_{Method2}$)

3. Electrolyser to Synthesis & ASU (hydrogen production currently not requiring storage) ($E_{Method3}$)
4. Electrolyser and Hydrogen Storage to Curtailment (hydrogen production currently requiring storage) ($E_{Method4}$)
5. Electrolyser to Curtailment ($E_{Method5}$)

$$\alpha = \frac{SpecC_{Elec} + SpecC_{H2Store}}{SpecC_{Elec}} = 1.0462... \tag{3.25}$$

$$\gamma = \frac{SpecC_{HB}}{SpecC_{HB} + \left(SpecC_{ASU} \times \frac{MM_{N2}}{MM_{NH3}} \times \frac{1}{2}\right)} = 0.8569... \tag{3.26}$$

$$\omega = \gamma \times \frac{MM_{N2}}{MM_{NH3}} \times \frac{3}{2} \times \frac{SpecC_{Elec}}{SpecC_{HB}} = 13.6049... \tag{3.27}$$

$$\phi = \frac{\omega \times SpecC_{H2Store}}{SpecC_{Elec}} = 0.6285... \tag{3.28}$$

$$E_{t,Method1} = max\Bigg(min\Bigg(\left(P_{t,Curtail} + P_{t,H2Store}\right), \frac{P_{t,Curtail}}{1-\phi}, \left(P^{*}_{HB/ASU} - P_{t,HB/ASU}\right)\Bigg), 0\Bigg) \tag{3.29}$$

$$E_{t,Method2} = max\Bigg(min\Bigg(\left(\frac{P^{\bullet}_{t,ElecExcess} + P^{\bullet}_{t,H2Store}}{\omega + 1}\right), \left(P^{*}_{HB/ASU} - P^{\bullet}_{t,HB/ASU}\right)\Bigg), 0\Bigg) \tag{3.30}$$

$$E_{t,Method3} = max\left(min\left(\left(P^{\bullet}_{t,Elec} - P^{\bullet}_{t,ElecExcess}\right), \left(P^{*}_{HB/ASU} - P^{\bullet}_{t,HB/ASU}\right)\right), 0\right) \tag{3.31}$$

$$E_{t,Method4} = P^{\bullet}_{t,ElecExcess} + P^{\bullet}_{t,H2Store} \tag{3.32}$$

$$E_{t,Method5} = P^{\bullet}_{t,Elec} - P^{\bullet}_{t,ElecExcess} \tag{3.33}$$

To re-allocate energy the methods are used sequentially until no further energy can be. For each method, the time intervals in the time series between t_{First} and t_{Last} are considered sequentially (Equations 3.34 and 3.35). The amount of energy that is re-allocated to / from the HB and electrolyser processes is calculated using Equation and the knowledge of the re-allocation method that is being used (i.e. discounting power re-allocation to / from these processes if necessary i.e. $\Delta P_{t,HB} = 0$ for Methods 4 and 5). The excess energy available to be re-allocated is reduced accordingly depending on energy required for hydrogen storage. Whether all methods were used and how significant each of them were was therefore highly dependent on the plant design that is being considered and the power supply profile. Method 1 increases the stoichiometric demand for hydrogen which in turn reduces the power required for storage of excess hydrogen produced (a converging infinite geometric series). Method 2 also increases the stoichiometric demand for hydrogen but also reduces the amount of hydrogen that is being produced. Method 3 is very similar to Method 2, but does not have to consider the power required for excess hydrogen production as there is none. Method 4 and 5 are the simplest and re-allocate power from hydrogen production to curtailment (excess and stoichiometric hydrogen production respectively). These final two methods are rarely, if ever, used in a well designed production plant.

$$\Delta E^{\bullet}_{t,Re-allocate} = \begin{cases} E_{t,Method1} \times \alpha \times \omega \\ E_{t,Method2} \times (\omega + 1) \\ E_{t,Method3} \times \alpha \times (\omega + 1) \\ E_{t,Method4} \\ E_{t,Method5} \times \alpha \end{cases} \tag{3.34}$$

$$\Delta E_{t,Re-allocate} = max\left(min\left(\Delta E^{\bullet}_{t,Re-allocate}, \int_{t=1}^{T} E_{Re-allocate}dt, \left(\left(\sum_{t=1}^{T} E_{Re-allocate}\right)_{t:t_{Last}}\right)\right), 0\right) \quad (3.35)$$

$$\Delta E_{t,Re-allocate} = \left(\left(\Delta P_{t,HB} \times \frac{\omega}{\gamma}\right) - P_{t,Elec}\right) \times \alpha \quad (3.36)$$

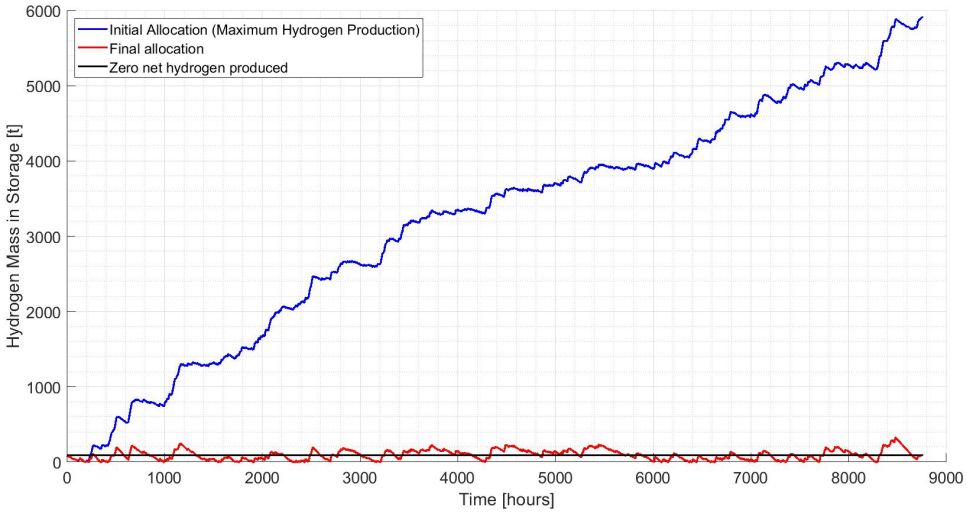

Figure 3.14: Cumulative net hydrogen produced with time. Illustration of before and after brute force energy re-allocation. Abashiri, Japan. $\theta = 0.7513$, $P^{*}_{Elec} = 409.6874MW$ and $P^{*}_{HB/ASU} = 5.5953MW$. Reduction of the hydrogen storage size required from 5910t to 327t.

With new energy profiles for the electrolyser, HB and ASU defined the total net amount of hydrogen produced (the mass of excess hydrogen produced over the entire time period) is checked to ensure that it is greater than or equal to zero (if it isn't then the re-allocation has performed incorrectly). The technical results from the process can now be collated. The size of the hydrogen storage required is the maximum absolute value of the cumulative net hydrogen production vector (the 'shifted' version of this vector is the red line in Figure 3.14). The rated power of the hydrogen fuel cell required is determined using Equation 3.37. The technical results include for all processes (electrolyser, HB, ASU, hydrogen storage and the hydrogen fuel cell): rated power / size, load factors, fraction of total supplied energy, the vector of the energy allocated for each time interval, mass flow vectors and the time

spent in different modes of operation.

$$P^*_{H2FC} = (max\,(\overrightarrow{m_{H2ConsumedEnergy}})) \times HHV_{H2} \times \eta_{H2FC} \tag{3.37}$$

Using the technical information and the assumptions for CAPEX and OPEX provided by the user in Step 1 (Tables 3.8 and 4.1), the process can now be costed, discount factors and capital replacement applied and the LCOA (Equation 3.38) calculated for output the genetic algorithm. One key component of this is the calculation of the LCOE for wind and solar PV. This is a location specific calculation achieved through use of defined installed cost per kW (Table 4.1) for that location, and the calculated energy vector being substituted into Equation 1.2. The cost of electricity is then attributed as part of each component's OPEX and the unused energy costed as curtailment.

$$LCOA = \frac{\sum_{t=1}^{T} \frac{CAPEX_t + OPEX_t}{(1+r)^t}}{\sum_{t=1}^{T} \frac{Mass_t}{(1+r)^t}} \tag{3.38}$$

A key difference between the final and the preliminary models is that the power allocation previously [141] was prescriptive. This means that the mode of operation and how the power was allocated was entirely defined by the supplied power ($\overrightarrow{RES}$). As shown in Figures 3.15 and 3.16, five modes of operation were defined based on the plant's four key power levels: plant rated power, plant stoichiometric power (when net hydrogen produced is zero), rated power of the HB and ASU and the minimum power of the plant. In the first mode of operation (when $RES_t \geqslant P^*_{Plant}$) all three processes (electrolyser, HB and ASU) operate at rated power. In the second mode, the electrolyser ramps down but the HB and ASU remain at rated power. In the third mode the electrolyser is operating at part load and with HB and ASU at rated power the net hydrogen produced is negative. Hydrogen is being drawn from storge for production of ammonia. In mode four the electrolyser is turned off and

the HB and ASU have been ramped down. Hydrogen is still drawn from storage for feedstock. In mode five there is not enough energy supplied to operate the plant. Hydrogen is therefore 'cannibalised' from storage for energy via the hydrogen fuel cell as well as the feedstock requirement.

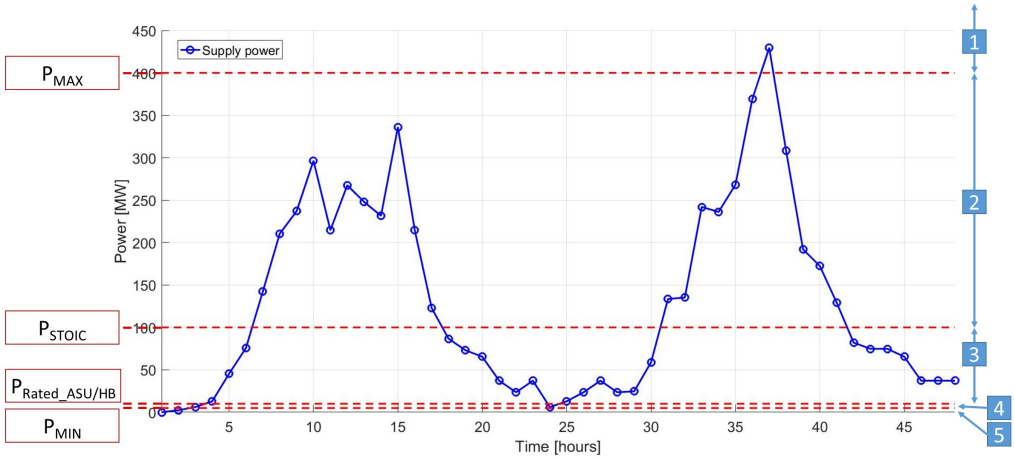

Figure 3.15: Power allocation to electrolyser and ASU/HB processes [141]

	Operating region	Operation	Allocated power: Electrolyser (Elec)	Allocated power: ASU/HB	Graphically
1	$P > P_{MAX}$	Curtail excess supply & store excess H_2	Rated power (P_{Rated_Elec})	Rated power $(P_{Rated_ASU/HB})$	Elec / ASU/HB
2	$P_{MAX} > P > P_{STOIC}$	Store excess H_2	$P_{Rated_Elec} - (P_{MAX} - P)$	$P_{Rated_ASU/HB}$	Elec / ASU/HB
3	$P_{STOIC} > P > P_{Rated_ASU/HB}$	H_2 from storage for feedstock	$P_{Rated_Elec} - (P_{MAX} - P)$	$P_{Rated_ASU/HB}$	Elec / ASU/HB
4	$P_{Rated_ASU/HB} > P > P_{MIN}$	H_2 from storage for feedstock and energy*	0	$P_{Rated_ASU/HB} - (P_{ASU/HB} - P)$	Elec / ASU/HB
5	$P_{MIN} > P$	H_2 from storage for feedstock and energy	0	P_{MIN}	Elec / ASU/HB

Figure 3.16: Power allocation to electrolyser and ASU/HB [141]

Whereas now, while $\overrightarrow{RES}$ still has considerable impact on how the plant operates, the brute force power allocation takes into account previous and forthcoming supplied power RES_t and the amount of hydrogen that is and will be in storage.

3.2.4 Cost of Flexibility Calculation

The cost of flexibility compares the LCOA achievable from the actual weather data against an 'ideal' power profile (Figure 3.17). Thereby enabling the comparison of the actually achievable LCOA, plant design and operation with an idealised scenario where the plant requires no flexibility.

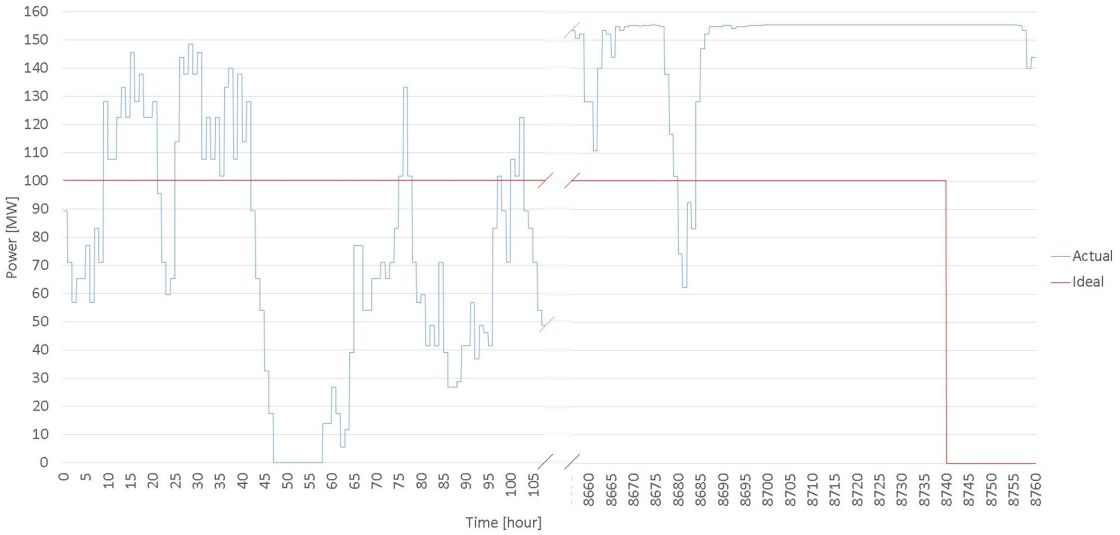

Figure 3.17: Actual and 'ideal' power profiles [142]

Attributing of the difference in the achievable LCOA to the components is difficult, particularly as both the numerator (cost) and denominator (mass of ammonia) in the LCOA calculation (Equation 3.38) change. Firstly the percentage increase of the two components and LCOA was determined (Equations 3.39, 3.40 and 3.41). Here, defined as x, y and z for the percentage change in total discounted cost, total discounted mass of ammonia produced and LCOA respectively.

$$Cost_{Actual} = Cost_{Ideal} \times (1 + x) \tag{3.39}$$

$$Mass_{Actual} = Mass_{Ideal} \times (1 + y) \tag{3.40}$$

$$LCOA_{Actual} = LCOA_{Ideal} \times (1 + z) \tag{3.41}$$

This enabled the calculation of the impact that the permutation of the percentage change in the numerator and the denominator independently had on the percentage change of LCOA ($\Delta_x z$ and $\Delta_y z$ respectively as defined in Equations 3.42 and 3.43).

$$\Delta_x z = \frac{x + \Delta x - y}{1 + y} - \frac{x - y}{1 + y} \tag{3.42}$$

$$\Delta_y z = \frac{x - (y + \Delta y)}{1 + (y + \Delta y)} - \frac{x - y}{1 + y} \tag{3.43}$$

$$\Delta z = \frac{x + \Delta x - (y + \Delta y)}{1 + (y + \Delta y)} - \frac{x - y}{1 + y} \tag{3.44}$$

Assuming the original percentage change of each component is zero (i.e. set $x = y = 0$) it can be determined that the addition of these individual impacts does not equal the permutation in the percentage change in LCOA (Equations 3.44 and 3.45). The difference ($\frac{\Delta x \Delta y}{1+\Delta y}$) needs to be 'fairly' removed from the change in cost and the change in mass produced. It has been removed proportionally relative to the independent impact of each component, through the calculation of a scale factor (Equation 3.46), thereby enabling the calculation of the impact of the numerator and denominator on the percentage change in LCOA (Equations 3.47 and 3.48).

$$\text{If} x = y = 0 \qquad \Delta_x z = \Delta x, \quad \Delta_y z = \frac{-\Delta y}{1 + \Delta y}, \quad \Delta z = \frac{\Delta x - \Delta y}{1 + \Delta y} \tag{3.45}$$

$$\text{Scale Factor} = \frac{\frac{x-y}{(1+y)}}{x - \frac{y}{(1+y)}} \tag{3.46}$$

$$\text{z attributable to change in cost} = x \times (\text{Scale Factor}) \tag{3.47}$$

$$\text{z attributable to change in mass} = \frac{-y}{1 + y} \times (\text{Scale Factor}) \tag{3.48}$$

Chapter 4

Calculations

The construction of the ESRMT and the IAPMT achieved the first and third research objectives respectively (Section 1.1.2). This Chapter, formed of one Section per model, subsequently outlines how the models were used and specifically the calculations that were performed to complete the two remaining research objectives:

1. Identify the impact that location, power supply and curtailment have (both independently and in combination for a given demand) on the energy storage requirement, with particular focus on seasonal requirements.

2. Identify the range of achievable LCOA for islanded 'green' production, the dominant cost components, the scope and likelihood of future reduction and benchmark this against conventional production.

4.1 Energy Storage Requirement Modelling Tool (ESRMT)

The simulations performed using the ESRMT can be best separated into three parts, with each one building on the previous work to increase complexity. The initial analysis, looking at a single location, identify the impact that power supply, specifically the VRE penetration and the mix of VRE sources (as defined in Equation 3.2)

both independently and in combination, have on the energy storage requirements of an electrical network (Section 4.1.1). The second analysis builds on this work by quantifying how the magnitude and the duration of storage required can be reduced through the introduction and increased dependence on another method of flexibility, specifically excess energy capacity / VRE curtailment (Section 4.1.2). Finally both of these analyses are performed for multiple places in Japan to identify the impact of location (i.e. available VRE resources and the location specific demand profile) (Section 4.1.3). This analysis is then expanded to include multiple locations across the UK, Canada and Australia.

The wind and solar power profiles have been calculated from weather data, specifically wind speed (at a specified height) and solar global horizontal irradiation, with hourly resolution. The wind speed (U) data provided is converted to power ($Wind_t$) using the Vestas V90 3.0MW (60Hz 109.4dB(A)) turbine's power profile (Figure 4.1) assuming an air density of 1.225 kg/m^3 using the fitted function in Equation 4.2) with cut-in and cut-out speeds set as 4m/s and 25m/s respectively. To achieve this the wind speed data (U_2) is used, with the provided height of measurement (H_2), to calculate the wind speed (U_1) at the hub height of the turbine ($H_1 = 80m$) using Equation 4.1. The location of the onshore wind installation is assumed to be on open flat terrain and therefore the roughness length $z = 0.03$.

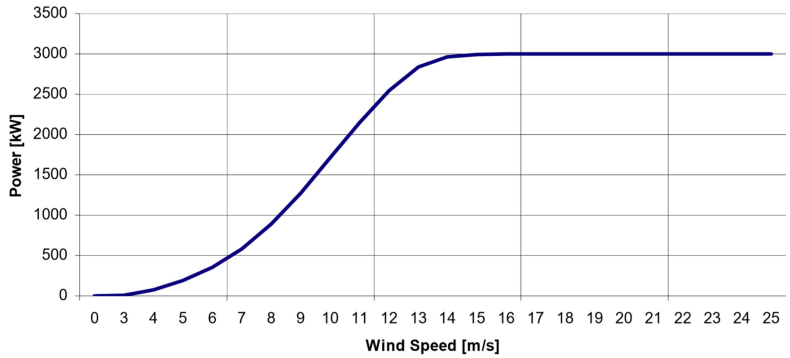

Figure 4.1: Power curve for the Vestas V90: 3.0MW, 60Hz 109.4dB(A) [173]

$$U_1 = U_2 \left(\frac{ln\frac{H_1}{z}}{ln\frac{H_2}{z}} \right) \tag{4.1}$$

$$Wind_t[\text{kW}] = 2731e^{-\left(\frac{U_t-27.29}{8.752}\right)^2} + 117.8e^{-\left(\frac{U_t-13}{1.779}\right)^2} - 5460e^{-\left(\frac{U_t-16.83}{6.677}\right)^2} + 1542e^{-\left(\frac{U_t-12.2}{4.773}\right)^2} + 7299e^{-\left(\frac{U_t-17.09}{6.626}\right)^2} \quad 4m/s \leqslant U \leqslant 24m/s \quad (4.2)$$

4.1.1 Impact of Power Supply (VRE penetration and VRE mix)

To determine the impact that VRE penetration and mix have on the energy storage requirements (to ensure that a network is balanced) the location of Shimizu/Ashizuri, Japan (Figure 4.2) was considered. The wind speed and solar global irradiation data was taken from the Meteonorm dataset [174] and converted to energy profiles using Equations 4.1 and 4.2. The demand energy profile was assumed to match the demand observed by the regional network (Shikoku) [175].

Using the ESRMT the storage requirement is quantified through the calculation and analysis of the SMI and SDI. This is achieved by considering VRE penetration from 5% to 100% in 5% increments and the fraction of total energy (provided by both VRE and dispatchable power sources) supplied by wind in 5% increments. To provide additional detail and explanation of how to interpret the SMI and SDI results, further analysis is conducted to quantify the storage use (i.e. total amount of energy stored) and size (i.e. size of the storage method) for four specified ranges of storage duration (τ):

1. $\tau < 24hours$
2. 24 hours $\leqslant \tau <$ 1 week
3. 1 week $\leqslant \tau <$ 1 month
4. 1 month $\leqslant \tau <$ 1 year

4.1.2 Impact of Curtailment / Capacity Margin

The calculations for this section consider mitigating the requirement for storage by incorporating an additional method of flexibility (see Section 1.3). Curtailment / excess energy was chosen because it is commonly used, and unlike other methods its potential is not dispatchable (i.e. it has technical limits dependent on the demand and the renewable power sources employed) and is not already being considered by one of the decision variables (i.e. the consideration of VRE penetration being similar to provision of additional reserve).

In practice, as explained in Section 3.1, enabling this feature activates another free variable the excess energy factor (μ, Equation 3.3). This means that the total amount of energy supplied over the time period considered is greater than the demand. With the total amount of excess energy provided by the VRE sources and dispatchable energy respectively is determined by the VRE penetration (λ, Equation 3.1). Due to the ESRMT's methodology, specifically Steps 3-5 in Section 3.1, the use of available VRE is prioritised over dispatchable power. This means that while the amount the amount of excess energy can be defined (using μ), VRE curtailment has to be calculated. In the calculations conducted the 'curtailment' of energy has been quantified as the amount of energy provided by the renewable sources that is not used to meet demand (either directly or via storage) as a fraction of the total renewable energy supplied.

Using the ESRMT the impact of increased excess energy on the storage requirements is quantified through the calculation and analysis of the SMI and SDI. The first calculations performed use the results from the first analysis where $\mu = 0$ and VRE penetration ranges from 50% to 100% (in 5% increments) with a fixed proportion (50%) of supplied energy from wind sources. The impact of the excess considered by increasing μ from 0% to 100% in 5% increments and comparing the SMI and SDI results.

The second set of calculations investigates how the impact of the excess factor is

impacted by the VRE penetration and mix of VRE sources. To determine this, the amount of excess is fixed by defining μ and performing the analysis described in Section 4.1.1. Comparison of the SMI manifolds for the three excess factors considered, $\mu = 0, 0.25$ and 0.50, shows how the effectiveness of providing excess energy to mitigate the amount of energy stored changes depending on the VRE penetration and mix of VRE sources. Similar comparison of the SDI manifolds shows its effectiveness of mitigating longer-term (i.e. interday and seasonal) storage requirements.

4.1.3 Impact of Location

Up to this stage the calculations have only considered one location (Shimizu/Ashizuri, Japan). While useful, the amount of insights that can be gleaned increases significantly when duplicating this analysis for other locations, both within the Japan and in other countries. For example, any similarities that can be drawn from multiple locations would highlight a common network flexibility problem that will require management regardless of location.

To identify the impact of location, the same analysis was conducted at each location considered. The demand was taken from historical data or a profile (UK) and the supply was scaled accordingly. This analysis largely consisted of the analyses described in Section 4.1.1 and 4.1.2 but with a small adaptation to the first set of calculations in Section 4.1.2. Instead of considering VRE penetration from 50% to 100% with a fixed proportion of supplied energy from wind sources, VRE penetration from 5% to 100% is considered for a fixed proportion of the VRE supplied energy (0%, 50% and 100%). For clarity of explanation, in Section 5.1.3 an overview of the results for each country is presented (to compare the impact of intra-country location), followed by the consideration of the most and least challenging locations in depth.

Locations in four countries (shown in Figures 4.2, 4.3, 4.4 and 4.5) were selected

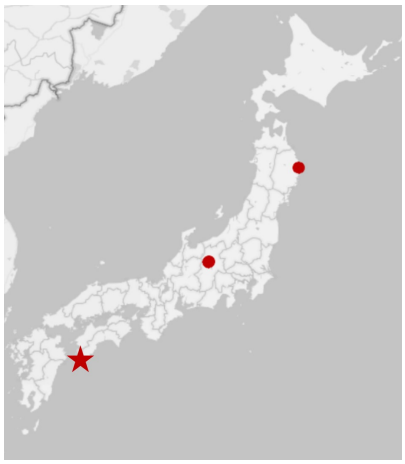

Figure 4.2: Japan: Locations assessed using the ESRMT. See Table 7.1 for specific locations. ⋆: Shimizu/Ashizuri.



Figure 4.3: UK: Locations assessed using the ESRMT. See Table 7.2 for specific locations.

for simulations due to their notable differences in demand profiles, renewable energy resources and the availability of reliable and detailed demand data: Japan, UK, Canada and Australia. The wind and solar data was for all locations, barring the UK, was taken from Meteonorm [174] for a 'representative' year. These were predominantly based on readings, but interpolated for others. Further details of the methodology and accuracy of these can be found in [176, 177]. For the UK, ground readings from the Met Office Integrated Data Archive System [178] was preferred (despite being the basis for the Meteonorm data for these locations) given the 2000-2016 dataset available. Availability of reliable demand data, with the required hourly resolution and time period of at least five years, impeded more locations being simulated using the ESRMT. For the locations in Japan and Australia demand was

assumed to be same as that seen by the regional network (as outlined in Section 7.3.3). In the UK, the demand was taken to be the ELEXON defined load profile for "domestic unrestricted customers" (Profile Class 1), with weekday / Saturday / Sunday and (five) seasonal variations applied to a common 24 hour energy demand profile [179, 180]. For Canada the demand for Ontario was used for all locations.

Fewer locations were considered in Japan, the UK and Canada due to limited



Figure 4.4: Canada: Locations assessed using the ESRMT. See Table 7.3 for specific locations. △: Most challenging location (Norman Wells), ★: Least challenging location (Winnipeg).



Figure 4.5: Australia: Locations assessed using the ESRMT. See Table 7.4 for specific locations. △: Most challenging location (Wagga Wagga Airport), ★: Least challenging location (Cape Grim).

data availability. In Japan for example the demand data from the regional network operators only provided one year of data. Having run simulations at many of these locations and compared the results for 1-year of data against those using a dataset containing over 5-years, it was observed that the differences were often considerable, particularly when calculating the storage requirements for τ beyond a week storage. The decision to not consider these locations further (given the data available) was

because the magnitude of impact on the SMI and SDI was significant enough to make comparison with these locations obsolete.

4.2 Islanded Ammonia Production Modelling Tool (IAPMT)

The simulations conducted using the IAPMT can be separated into two parts:

1. Use of the preliminary IAPMT (noted in Section 3.2 and explained in detail in [141]) to identify the key decision variables that should be considered and initial results for the LCOA's sensitivity to them.
2. Use of the final IAPMT model at 534 locations in 70 countries to determine the viability of islanded ammonia production.

Due to the preliminary nature of the model used and the purpose of the simulations, the focus of this thesis will be on the latter simulations. The calculations performed and the key insights from the initial analysis will be explained in Section 4.2.1. Further details of this preliminary work can be found in [141].

4.2.1 Identifying Key Decision Variables

Using the preliminary version of the IAPMT with a brute force approach rather than formal optimisation, such as the genetic algorithm explained in Section 3.2.3, the islanded production of 'green' ammonia at Lerwick (UK) was simulated. Met Office 2000-2016 wind and solar MIDAS data with hourly resolution was used to calculate (using Equations 4.1 and 4.2) the wind and solar PV power profiles [178]. The LCOE for each sources, 67 and 80GBP/MWh respectively, was taken from historic data [181, 182]. Similar to the global analysis calculations process design was based on the assumption that the average power supply was fixed at 100MW regardless of the mix of VRE sources. After trial of decision variables the mix of VRE sources (Equation 3.2), stoichiometric power demand (the amount of power required for the

HB and ASU to run at rated power and the electrolyser to produce a stoichiometric quantity of hydrogen feedstock) and the electrolyser excess factor (Equation 3.21) were used as decision variables. The importance of the first and second of these variables can be seen in the achievable LCOA (Figure 4.6). Given the IAPMT's dependence on the hydrogen buffer for the process flexibility required to manage the intermittent VRE sources, the electrolyser excess factor was shown to be an enabling variable. For example, consider the 60% wind, 40% solar PV line in Figure 4.6. As the stoichiometric power demand increases the LCOA initially falls. To achieve this increase in hydrogen demand (as there is no ramping of the synthesis or ASU) in the production of ammonia the electrolyser rated power needs to increase. However due to the intermittent nature of the VRE resources, the electrolyser's load factor decreases thereby requiring its rated power to be further increased to compensate (i.e. increased electrolyser over-sizing). The magnitude of over-sizing required to balance the process worsens as the stoichiometric power demand increases due to the diminishing amount of energy supplied at higher power levels. The impact of this phenomenon can be seen on the curve. As the stoichiometric demand increases past 87MW the LCOA begins to increase. In order to support the increase of the HB & ASU constant power demand, the over-sizing of the electrolyser needs go increase substantially. Considering Equation 3.38, this substantial additional cost to ensure the plant is technically functional is no longer smaller than the increase in ammonia produced, therefore LCOA increases (As shown in Figure 4.6). Another important take-away from this is that the range of technically feasible plant size (here shown as stoichiometric power) is highly specific to the percentage of energy supplied by wind.

Besides the decision variables, five parameters were identified that had significant impact on the achievable LCOA. Two production cost variables: the LCOE and electrolyser CAPEX per kW; and two production process variables: the minimum operating power of the HB & ASU and the ramping rate of the HB & ASU. Of the cost variables the impact from the LCOE was the most significant and aligned with

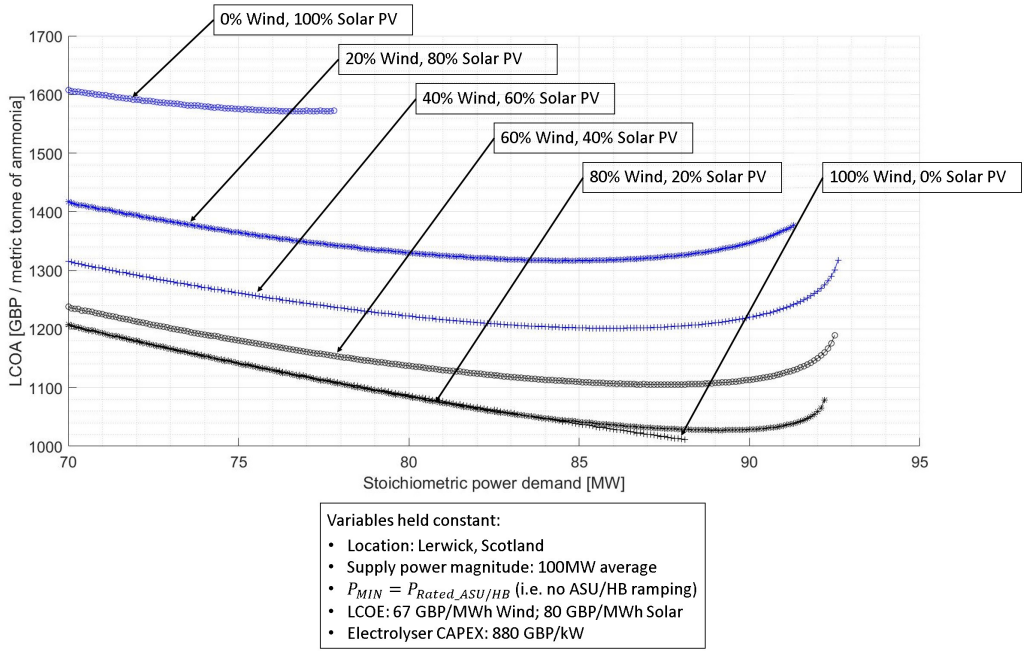

Figure 4.6: LCOA sensitivity to the mix of VRE sources and the corresponding plant sizing to minimise the LCOA for a 100MW average power supply [141]

Beerbuhl, S. et al.'s result that a ±0.97GBP/MWh variation results in ±10GBP/t ammonia (Figure 4.7) [183]. The sensitivity of the LCOA to the flexibility of the HB & ASU was significant. This showed the notable importance of the minimum operating power assumption on the LCOA if the HB & ASU can ramp moderately quickly.

These findings shaped the development of the IAPMT methodology (particularly use of the genetic algorithm and improvement of the power allocation), but also the global analysis calculations. With a high flexibility in the HB & ASU processes it was seen that for Lerwick the use of a representative year compared well with the results for the actual 17 year energy profile dataset. The energy profile of the representative year being less variable than the actual data had little effect due to the large power requirement of the perfectly flexible electrolyser. The small discrepancies were due to the representative year not having the same frequency of time intervals with no power for the wind profile. In addition to changing the decision variables, it was clear by the sensitivity of the LCOA to these key variables that considering a future scenario with lower predicted LCOE and electrolyser CAPEX and assuming

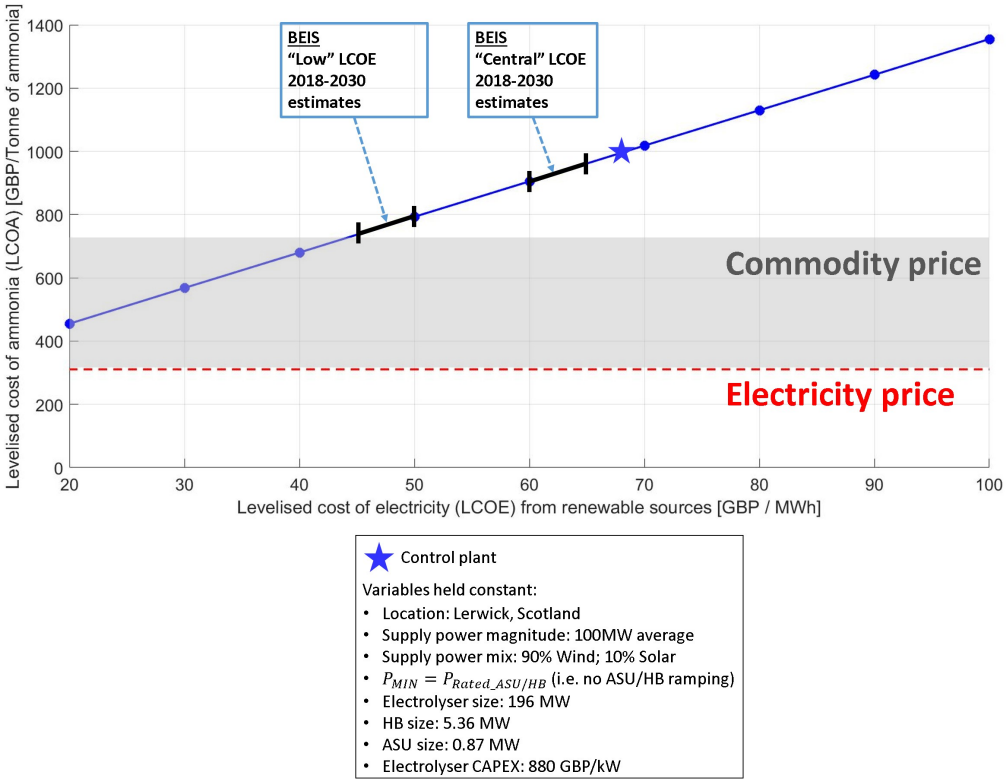

Figure 4.7: LCOA sensitivity to the VRE sources' LCOE, benchmarked against the 2007-2018 global range of ammonia spot prices and the LCOA required to compete with baseload power generation [141]. BEIS: UK Government Department for Business, Energy and Industrial Strategy.

a minimum operating power (i.e. 20%, in line with Ostuni and Zardi [156] were important.

4.2.2 Global Analysis

Having updated the IAPMT to improve accuracy and computational time, changed the key decision variables (Electrolyser rated power ($P_{ElecRated}$), HB & ASU rated power ($P_{HB/ASURated}$) and identified important key variables, a more detailed analysis could be performed. The objectives of the global analysis were to:

1. Identify the range of LCOA achievable, currently and by 2030.
2. Quantify the impact of VRE intermittency on the LCOA as well as the design and operation of the plant.
3. Identify scope for future cost reductions.

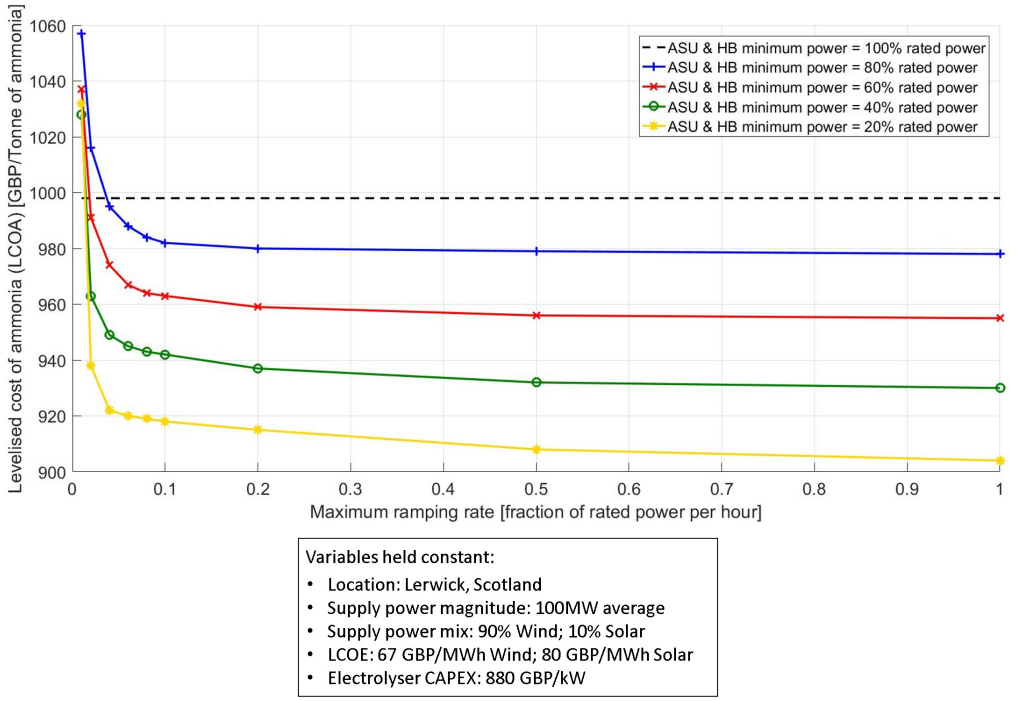

Figure 4.8: LCOA sensitivity to the minimum operating power and the ramping capability of the synthesis process [141]

4. Identify the best locations for implementation, the site-specific optimal plant design and when it will be commercially viable.

5. Consider if there are financial barriers to implementation as at any of these locations.

To achieve this the IAPMT was used to calculate the optimal mix of VRE sources, plant design and its operation for 534 locations in 70 countries (Figure 4.9). The VRE data supplied to the model was from Meteonorm [174] and the wind speed and global solar irradiation data was converted to energy profiles as described at the beginning of this chapter. To achieve the first of these objectives each location was simulated in a present-day and a 2030 scenario. While the technical assumptions (Table 3.7) and the majority of the economic assumptions remained unchanged (Table 3.8), due to the maturity of the production process, the LCOE (for both wind and solar PV) and the electrolyser CAPEX change. The reduction in electrolyser CAPEX (from \$700kW^{-1} to \$341kW^{-1}) is based on predictions in literature [158, 159, 166, 167]. However, to estimate the achievable LCOE for the 2030 scenario I

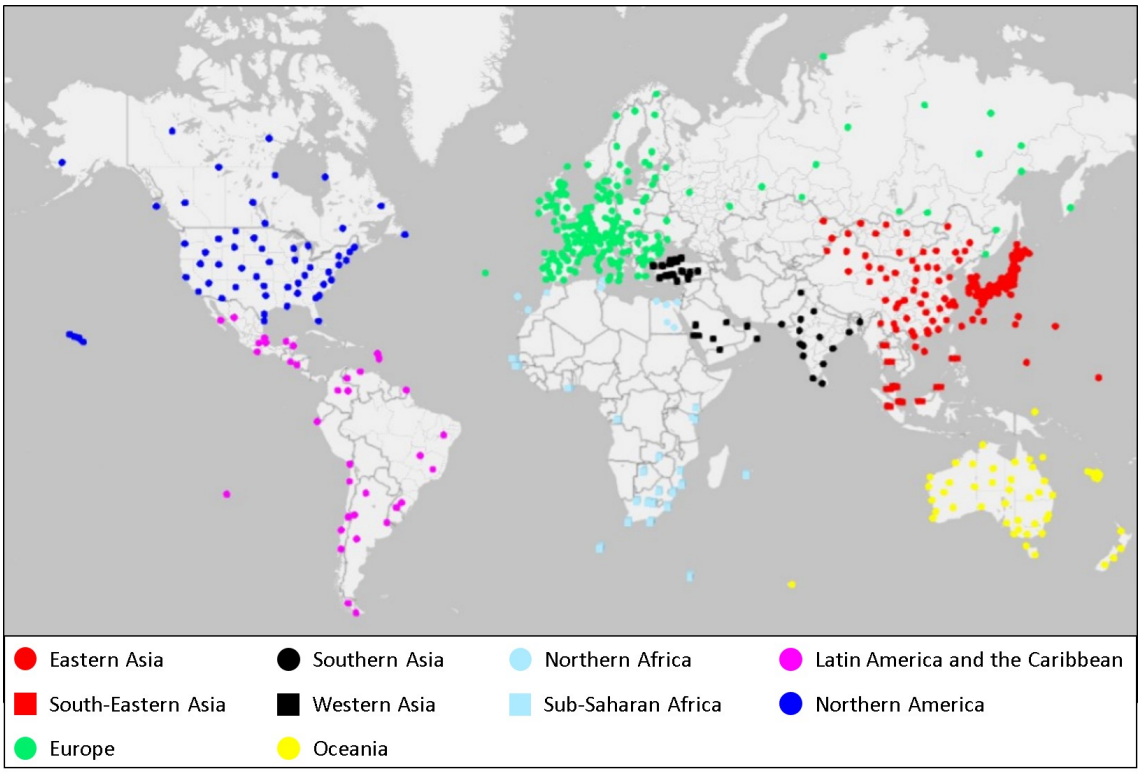

Figure 4.9: The 534 locations in 70 countries considered using the IAPMT grouped by geographic region [142].

fitted two functions (Equation 4.3 and 4.4) to the global average LCOE for onshore wind and solar PV (Figure 4.10) [184]. Estimating a 42.7% and 67.1% reduction of the current LCOE to onshore wind and solar PV (equivalent to -4.5% and -8.9% CAGR), this same scale factor was applied to the LCOE calculated for each location.

$$\text{Wind LCOE}_{2008+t} = 121.8e^{-0.4682t} + 65.7e^{-0.0451t} \qquad 1 \leqslant t \leqslant 22 \qquad (4.3)$$

$$\text{Solar LCOE}_{2008+t} = 460.6e^{-0.5478t} + 102.9e^{-0.09022t} \qquad 1 \leqslant t \leqslant 22 \qquad (4.4)$$

To achieve the fifth objective for the global analysis, each location was simulated (for both the present-day and 2030 scenarios) under two financing constraints: one for a multi-national corporation who could therefore obtain favourable discount rate (i.e. global minimum) and domestic production dependent on the discount rate achievable in country. The discount rates (obtained from [169]) therefore can vary significantly depending on the country. For example, production in India by a domestic corporation is simulated using the discount factors in Table 4.1. The

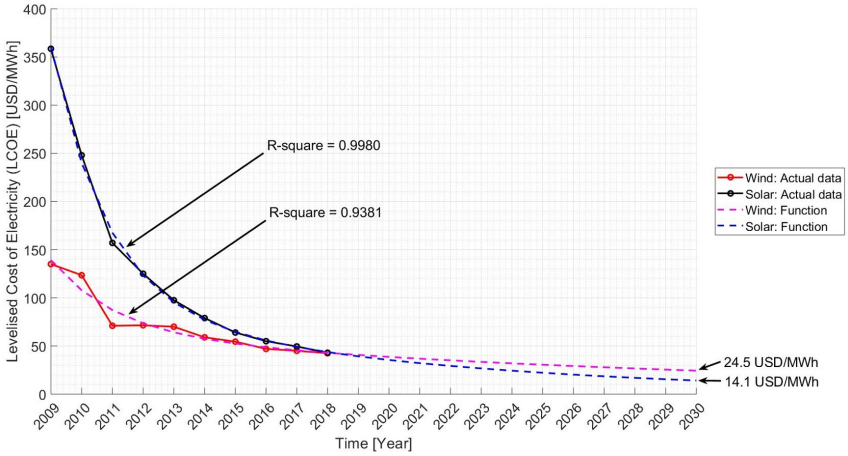

Figure 4.10: Second-order exponential functions fitted to global weighted average LCOE for wind and solar PV to predict the reduction by 2030 [184, 142].

Variable	**Value**	**Reference**
Installed cost of onshore wind	$\$1{,}097\text{kW}^{-1}$	[184]
Installed cost of solar PV	$\$661\text{kW}^{-1}$	[184]
Discount factor for renewable energy (domestic production)	5.50%	[169]
Discount factor for production process (domestic production)	9.65%	[169]

Table 4.1: Location dependent economic assumptions for the production of ammonia in the IAPMT. The values given as an example are those used for locations in India [142].

inputs to the IAPMT by country can be found in Appendix C. Whereas production by a multi-national corporation is modelled using a discount factor of 3.33% and 7.14% for the VRE and production components of the process respectively (Table 3.8).

Chapter 5

Results

This chapter is formed of two parts, each presenting and analysing the results obtained from the use of the ESRMT and IAPMT respectively. This structure replicates that of Calculations (in Chapter 4).

5.1 Energy Storage Requirements Due to VRE Integration

5.1.1 Impact of Power Supply (VRE penetration and VRE mix)

This section (5.1.1) has two aims:

1. To demonstrate how to quantify the storage requirements and identify the impact of the decision variable/s using the results from the ESRMT, particularly the SMI and SDI.
2. To identify the impact of VRE penetration and the mix of VRE sources on the magnitude and duration of electrical energy storage required.

First, the magnitude of the energy storage required. The 0% constant fraction of energy provided by wind in Figure 5.1 shows that as the VRE penetration increases

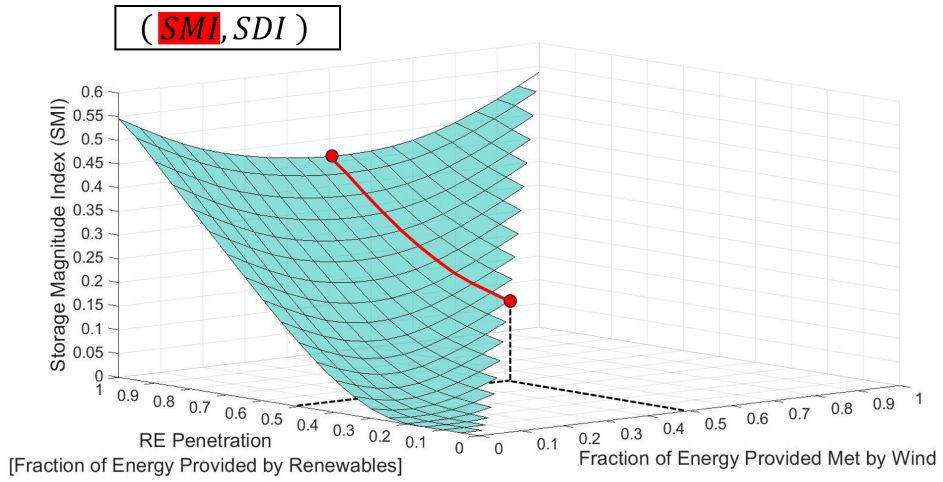

Figure 5.1: Impact of VRE penetration and the mix of VRE sources on the fraction of demand met by storage for Shimizu, Japan. No other flexibility methods employed.

so does the SMI (i.e. the magnitude of demand that must be met by energy that has been stored). This applies from no requirement at low VRE penetration to up to ∼55%. While this relationship between the magnitude of storage required and VRE penetration is expected, the assumption that no other flexibility method (e.g. Section 1.3.2) is currently available causes the notable increase in SMI as λ tends to 1. The excess energy factor is zero which increases the energy storage requirement magnitude (i.e. $\mu = 0$ in Equation 3.3). At 100% VRE penetration the impact of VRE mix (θ, Equation 3.2) on the storage magnitude is clearest. For both $\theta = 0$ or $\theta = 1$ the SMI is similar (∼55% of demand is met by energy that has been stored). A mix of VRE reduces this requirement to 41.23% at 55% Wind : 45% Solar.

As shown (Figure 5.2) at very low VRE penetration there is no requirement for storage ($SMI = 0$). How quickly the storage requirement changes with VRE penetration depends on θ. With a solar dominated VRE supply (i.e. $\theta = 0$) at 25% VRE penetration only 0.6% demand requires stored energy. However, in a wind dominated supply (i.e. $\theta = 1$ and the fraction of energy provided met by wind is 25%) 3.1% of demand requires stored energy. If there is no storage requirement the SDI does not have a value and therefore is not plotted as part of the manifold. As explained in Section 3.1.4, the SDI is a measure of the average storage duration required, specifically quantifying its short- / long-term bias. Let us first consider

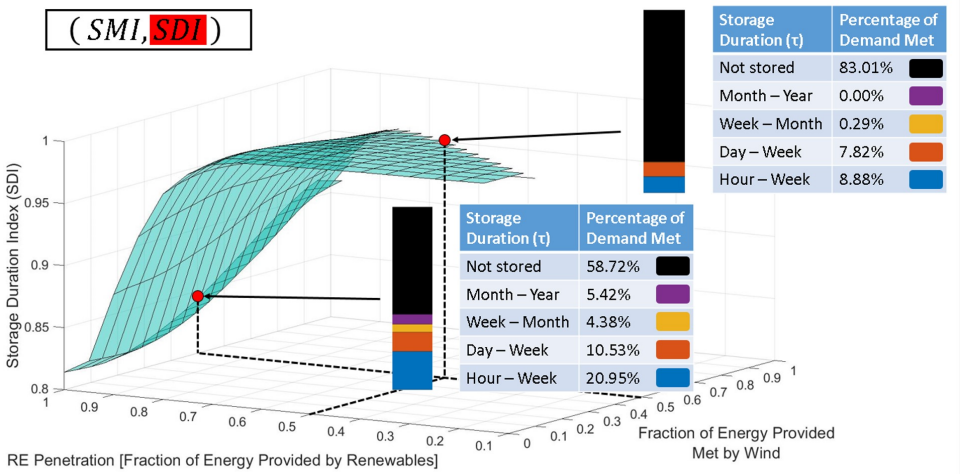

Figure 5.2: Impact of VRE penetration and the mix of VRE sources on the variance of storage for Shimizu, Japan. No other flexibility methods employed.

two points on the manifold:

- Point 1, SDI = 0.844: $\lambda = 1, \theta = 0.50$ (100% VRE penetration with 50% Wind: 50% Solar (by energy))
- Point 2, SDI = 0.991: $\lambda = 0.5, \theta = 1$ (50% VRE penetration with 100% Wind: 0% Solar)

The SDI of Point 1 shows that it is short-term biased (as it is positive), but does require longer-duration storage (as it is not greater than ~ 0.98). Whereas, Point 2's SDI shows it is short-term biased and is likely to be entirely dependent on short-term storage (as it is very close to 1). This interpretation of the SDI to identify the storage dependence (in terms of how long energy is required to be stored for) is very useful to identify trends in the results. This is clear in Figure 5.2 where the duration of energy storage required is in five groups. At Point 1, as expected, there is a high short-term storage requirement but also longer term storage. Point 2 is very short-term biased. In the bar chart of Point 1, the energy storage requirement sum equals the SMI. The SDI value indicates how short- / long-term the storage requirement is. Figure 5.2 shows an important result: it identifies quantitatively the 'tipping-point', after which the storage requirement is substantially less short-term biased. With a lower wind penetration the tipping point is at a higher VRE penetration and sharper. For example, at $\theta = 0$ (i.e. 100% solar) the SDI is greater

than 0.990 until the VRE penetration passes 70% penetration. Whereas this same SDI milestone is passed when VRE penetration is 55% with $\theta = 1$. A solar based systems requires more long-term storage more quickly compared to a wind based system. By 80% VRE penetration the solar based system already has a lower SDI.

5.1.2 Impact of Curtailment / Excess Energy Factor

Other flexibility methods may be used to mitigate the requirement for storage. The provision of excess energy at Shimizu shows how effective excess energy is for mitigating the magnitude and long-duration storage requirements. Applying Excess energy to the scenarios on the red line in Figure 5.1 shows the impact of VRE penetration on the SMI, where wind is consistently 50% of the total energy supplied as the VRE penetration increases from 50% to 100% (i.e. introducing solar PV energy). The impact on the SMI, shown in Figure 5.3, is considerable. At 50% VRE penetration (all wind energy) allowing 21.6% VRE curtailment eliminates the energy storage requirement. However, as the VRE penetration increases this concave relationship between VRE curtailment and the magnitude of energy storage required quickly develops into a distinctly convex relationship. I.e. as the VRE penetration increases the ability of excess energy provision to mitigate the energy storage required diminishes substantially. This is expected because as VRE penetration increases the storage requirements depend more on the correlation between the VRE supply profile and VRE demand. The magnitude of the impact is significant. At 100% VRE penetration 20% excess energy mitigates 2.2% of the (41.2%) storage requirement; 5.0% at 80% and 7.5% at 50% VRE penetration. Figure 5.4 shows excess energy to be highly efficient at mitigating any dependence on long-term storage: the SDI is greater than 0.985 for all VRE penetrations, except VRE penetration over 90%, with only 5% excess energy provision. Plotting the impact of excess energy instead of the VRE penetration is more useful (Figure 5.5). Comparing the SMI when 0%, 25% and 50% excess energy is provided shows the low impact that excess energy provision has at high VRE penetration (as noted previously). Importantly

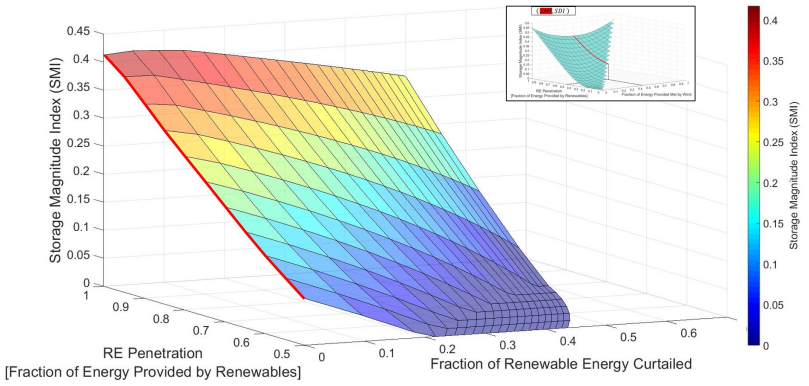

Figure 5.3: Impact of VRE penetration and VRE curtailment on the SMI for Shimizu, Japan.

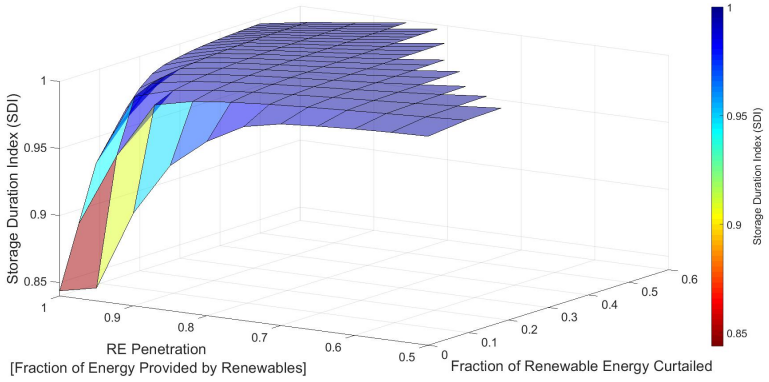

Figure 5.4: Impact of VRE penetration and VRE curtailment on the SDI for Shimizu, Japan.

it identifies two additional findings not in Figure 5.3:

1. Separation of the manifold from SMI = 0 (i.e. no storage required) is greatly affected by excess energy regardless of the mix of VRE sources

2. The effectiveness of excess energy to mitigate the magnitude of storage required depends highly on the mix of VRE sources.

Plotting the SDI by wind energy fraction shows long-term energy storage requirements are quickly eroded. The tipping-point moves independent of the θ. This is clear when comparing the storage size for 0% and 25% excess energy (Figures 5.7a and 5.7b). Energy storage is required after 60% VRE penetration. If the excess energy factor exceeds 25% the size of long-term energy storage decreases. In Shimizu (Japan) it can be seen that with excess energy the long-term storage requirements

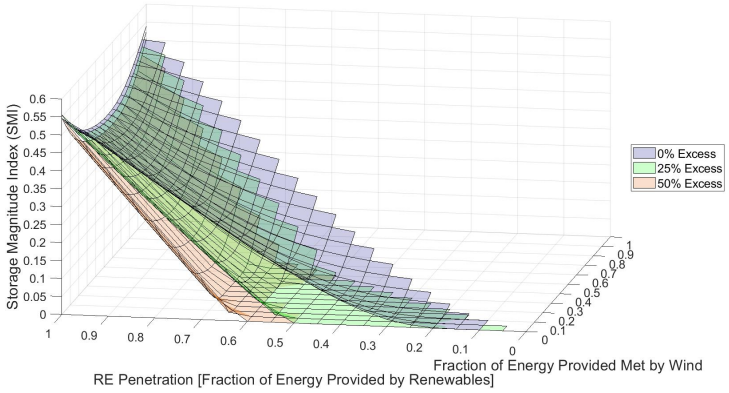

Figure 5.5: Shimizu, Japan: Impact of Curtailment, VRE penetration and the mix of VRE sources on the SMI.

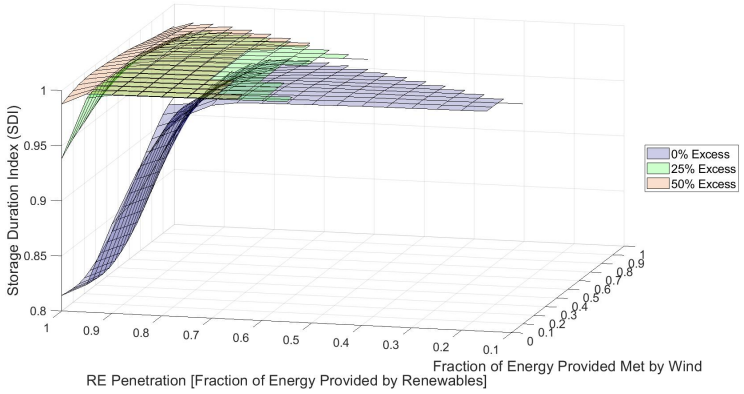

Figure 5.6: Shimizu, Japan: Impact of Curtailment, VRE penetration and the mix of VRE sources on the SDI.

can be mitigated by being more reliant on shorter-term energy storage (Figure 5.7c). For Figure 5.7 and all subsequent figures comparing the storage size required in Section 5.1.3 the objective function is technical not economic (to minimise the maximum storage duration, τ_{max}, as outlined in Section 3.1.3) .

5.1.3 Impact of Location

To achieve the second research objective (Section 1.1.2), to identify the impact that location has on the energy storage requirement, particularly seasonal requirements, and how this is mitigated by curtailment, the comparison of multiple locations was considered using the ESRMT. This section presents and analyses the results of the locations by country (Japan, UK, Canada and Australia). It compares results inter-

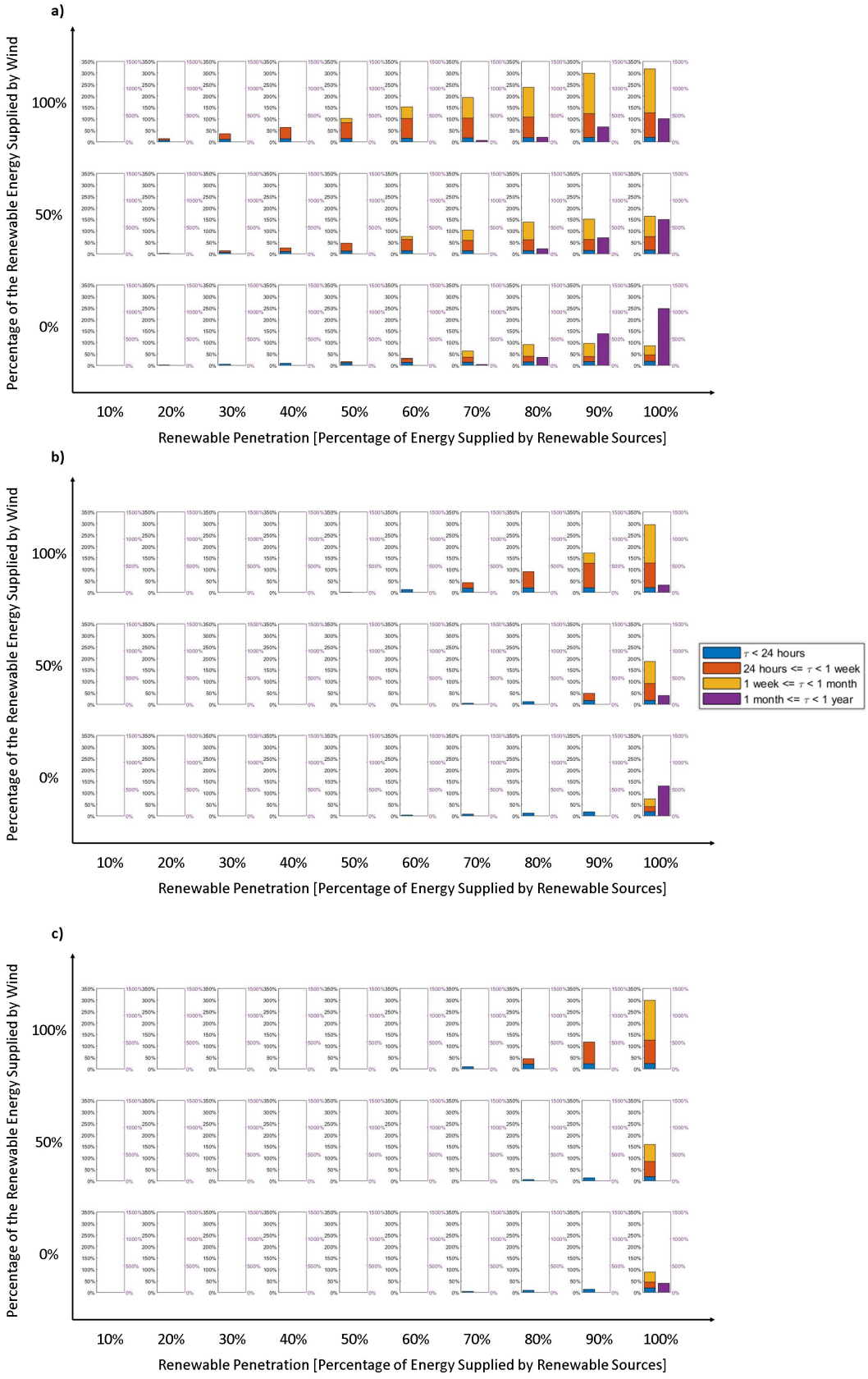

Figure 5.7: Shimizu, Japan: Storage size required for a) 0%, b) 25% and c) 50% excess energy.

country to identify the impact that location has on the storage requirements. It then focuses on the most and least challenging locations (in terms of the magnitude and long-duration storage requirements) in Canada and Australia shows how location impacts the magnitude, use and size of storage required as well as how effective the provision of excess energy is to mitigate those requirements.

Japan

The two other locations considered in Japan (Miyako and Matsumoto) have similar SMI manifolds (i.e. dependence on the amount of energy stored) that are smaller than Shimizu's. Figure 5.8 shows that despite this difference, the dependence on energy storage across the three locations is very similar when VRE penetration is below 50%. The exception is the separation between the 'maximum' and 'minimum' when wind dominates the VRE mix. The 'minimum' has a SMI less than 0.004 at 15% VRE penetration, whereas the maximum has a SMI of 0.031. This difference only grows with VRE penetration. At 100% VRE penetration the difference in SMI is considerable at over 0.17. The SDI shows a strong short-term bias in the

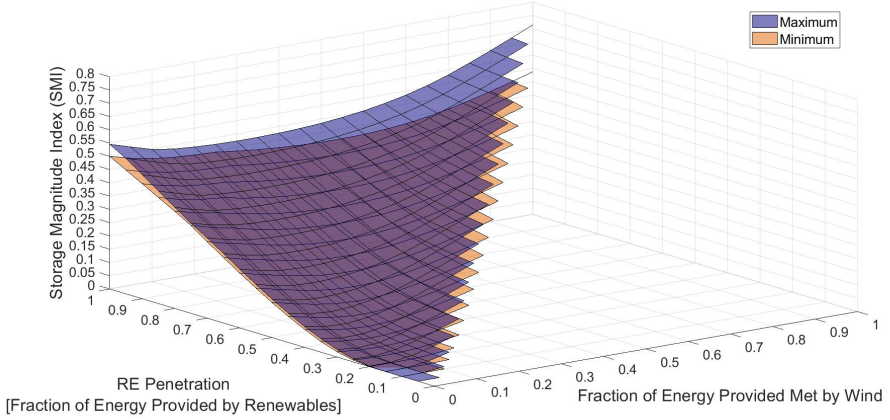

Figure 5.8: Japan: Impact of location, VRE penetration and the mix of VRE sources on the magnitude of storage required

storage requirement until high VRE penetration at all of these locations. When wind dominates the VRE supply this bias is particularly strong. The tipping-point for both manifolds is at 75% VRE penetration. The minimum SDI is 0.911 at 100%

penetration. There is minimal separation at 100% VRE penetration (the difference in SDI is 0.008). However, with solar dominating VRE supply (i.e. $\theta \to 0$) this short-term bias is eroded: the tipping point for the most challenging location ('minimum') moves to 65% VRE penetration; the SDI is 0.750 at 100% VRE penetration. The

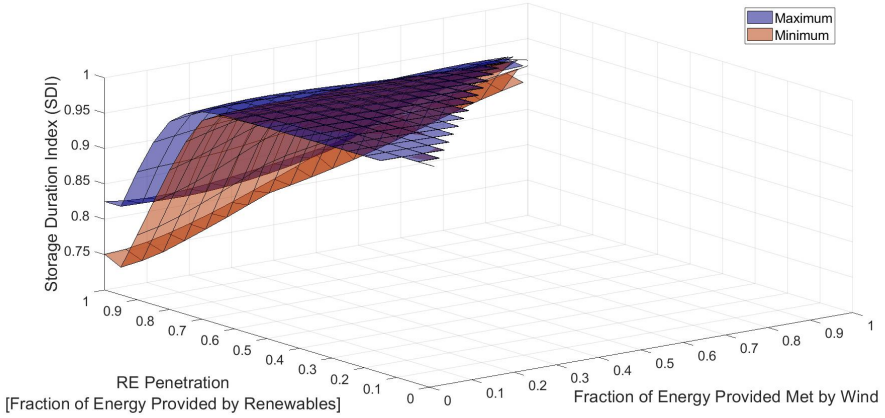

Figure 5.9: Japan: Impact of location, VRE penetration and the mix of VRE sources on the variance of storage required

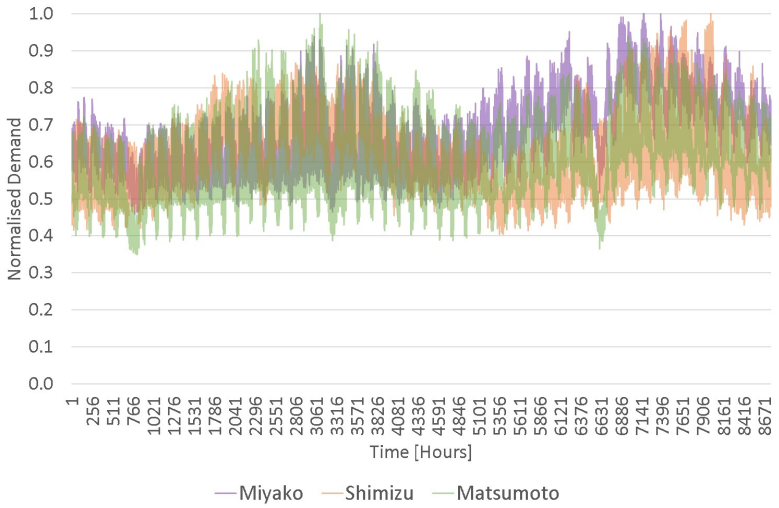

Figure 5.10: Differences in electricity demand for the three locations considered in Japan. These have been normalised against the peak demand in each demand profile.

demand profile is the main reason for the differences in the SMI and SDI for these locations. While the VRE resources differ by location, the magnitude of diurnal and seasonal variations in demand (as shown in Figure 5.10) is the key difference.

UK

Reviewing seven locations across the UK (Figure 4.3), energy storage requirements were expected to be very different due to different VRE profiles available. Inspecting the magnitude of the storage required, it can be seen in Figure 5.11 that the separation of the manifolds is similar to that seen for Japan. The SDI is 0.072 for solar and 0.136 for wind dominated supply at 100% VRE penetration. However, as wind resource is less intermittent in the UK (Figure 5.12), there are two notable differences:

- As $\theta \to 1$ the VRE penetration at which energy storage is first required increases substantially (up to 35% for $\theta = 0$ for the least challenging location)
- The SMI for all UK locations decreases (rather than increases) as $\theta \to 1$ at high VRE penetration.

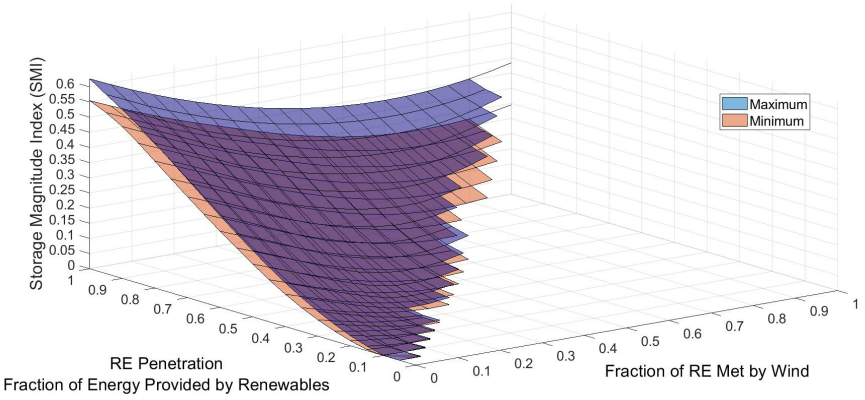

Figure 5.11: UK: Impact of location, VRE penetration and the mix of VRE sources on the magnitude of storage required

The most significant difference between the solutions for the locations in Japan and the UK is the SDI. The tipping-point locations and the SDI value at 100% VRE penetration are the biggest differences. The UK 'minimum' has a tipping point between 30% and 60% showing that implementing solar requires longer-term storage at relatively low VRE penetration. The UK 'maximum' has a lower tipping-point (c.50-75% VRE penetration depending on θ) than Japan's. After the tipping point the manifolds separate significantly. The UK minimum shows a larger long-term

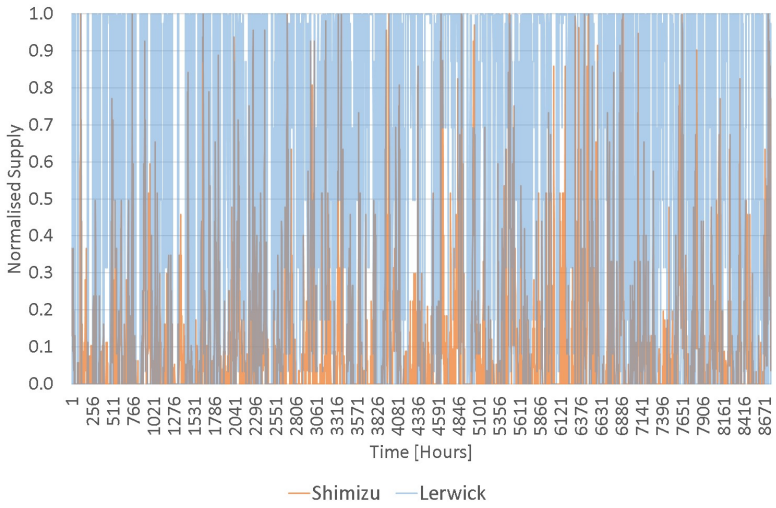

Figure 5.12: Comparison of the normalised electricity supply from wind for Lerwick (UK) and Shimizu (Japan)

storage requirement if more than 50% of the VRE energy supplied is solar.

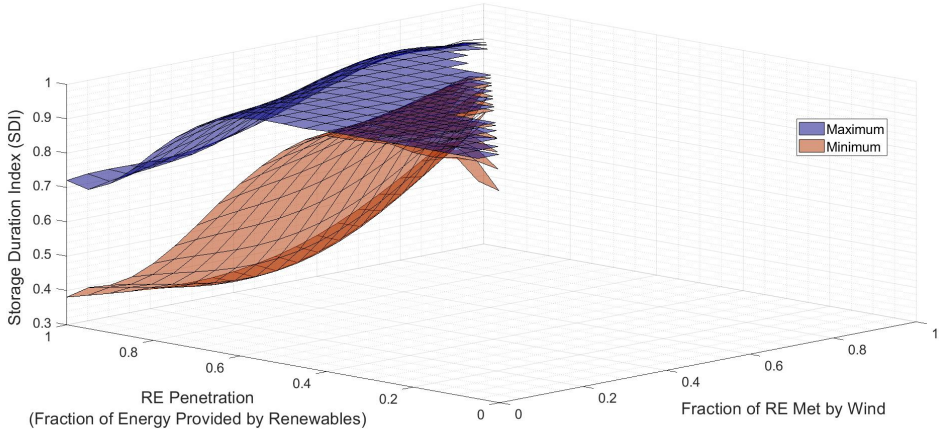

Figure 5.13: UK: Impact of location, VRE penetration and the mix of VRE sources on the variance of storage required

Canada

The magnitude of energy that needs to be stored (SMI) to manage balancing deviates by location, unlike locations in the UK and Japan (Figure 5.14). As θ tends to 1 the impact on the storage requirement varies by location, however when $\theta = 0$ there is less variation and the SMI is similar to previous results. The most challenging locations (i.e. maximum) have a SMI manifold similar to Japan, with higher energy storage dependence. The least challenging locations (i.e. minimum) have a lower

dependence (SMI = 0.415 at 100% VRE penetration, similar to the UK locations). The dependence on long-term storage also varies by location. The most significant

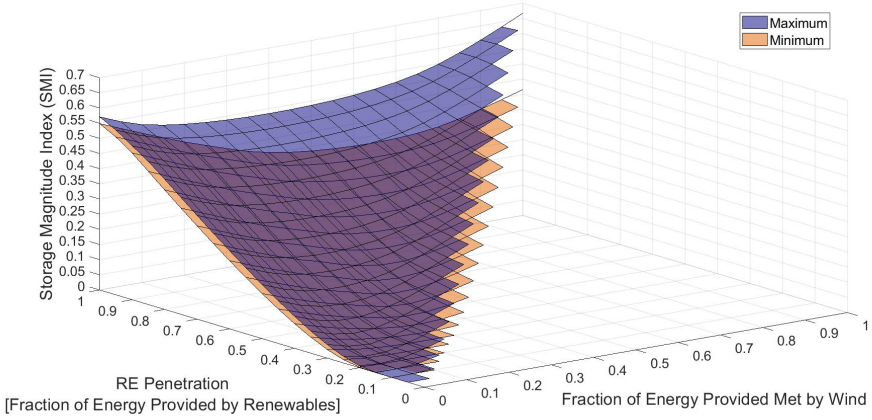

Figure 5.14: Canada: Impact of location, VRE penetration and the mix of VRE sources on the magnitude of storage required

points in Figure 5.15 are the difference in storage requirement at 100% VRE penetration, the difference between the best and worst locations' tipping-point and that θ has an impact on this same tipping point.

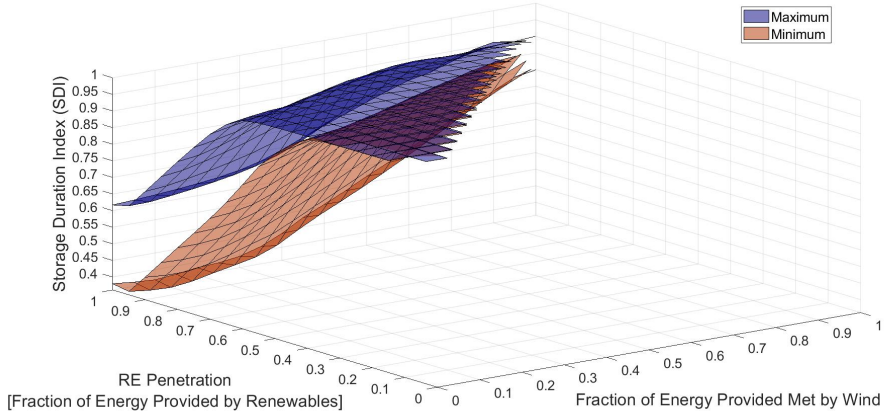

Figure 5.15: Canada: Impact of location, VRE penetration and the mix of VRE sources on the variance of storage required

Australia

Notable similarities can be drawn between the results (both SMI and SDI) for Canada and Australia. The SMI manifold for the most challenging location (i.e.

maximum in Figure 5.16) is similar to that of Canada. The exception is that a mix of VRE sources (i.e. $\theta = 0.4 - 0.6$) more substantially reduces the amount of energy storage required. However, the SMI for the least challenging location (i.e. minimum) when $\theta > 0.6$ is considerably different. Due to the excellent wind resource (with a capacity factor of 64.3%) minimal energy is required to be stored until VRE penetration exceeds 50%. The SMI is only 0.259 at 100% VRE penetration. The

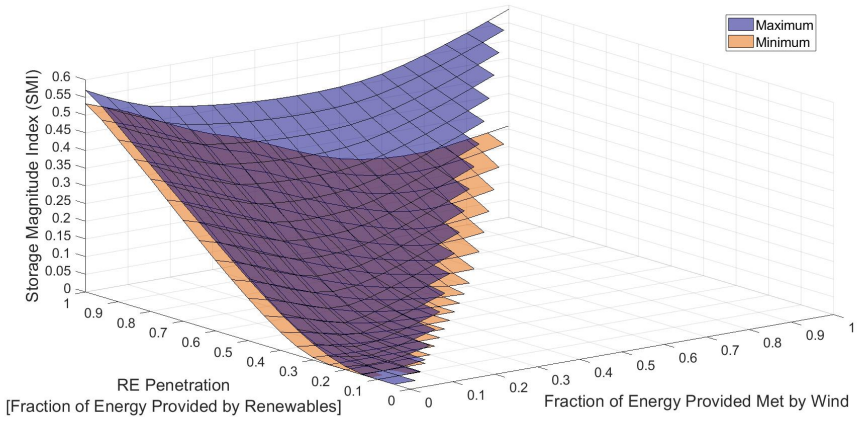

Figure 5.16: Australia: Impact of location, VRE penetration and the mix of VRE sources on the magnitude of storage required

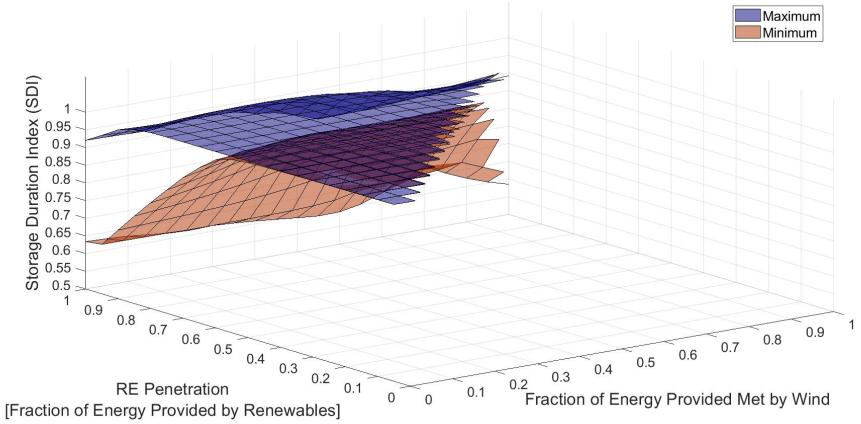

Figure 5.17: Australia: Impact of location, VRE penetration and the mix of VRE sources on the variance of storage required

SDI results show that the combination of excellent wind and solar resources for some locations in Australia (i.e. maximum in Figure 5.17) the storage requirements are very short-term biased even at high VRE penetration. Despite having considered

23 locations, the most challenging locations (despite having a tipping point at 60% VRE penetration) do not have the same dependence on long-term storage at high VRE penetration like the some locations in the UK or Canada: Even at 100% VRE penetration with $\theta = 0$, the SDI is equal to 0.634.

Canada: Most & Least Challenging Locations

Winnipeg was selected as the least challenging location considered in Canada because of its low maximum SMI and the high minimum SDI (i.e. small dependence on long-term energy storage). The most challenging, Norman Wells, being selected for the opposite (Figure 4.4).

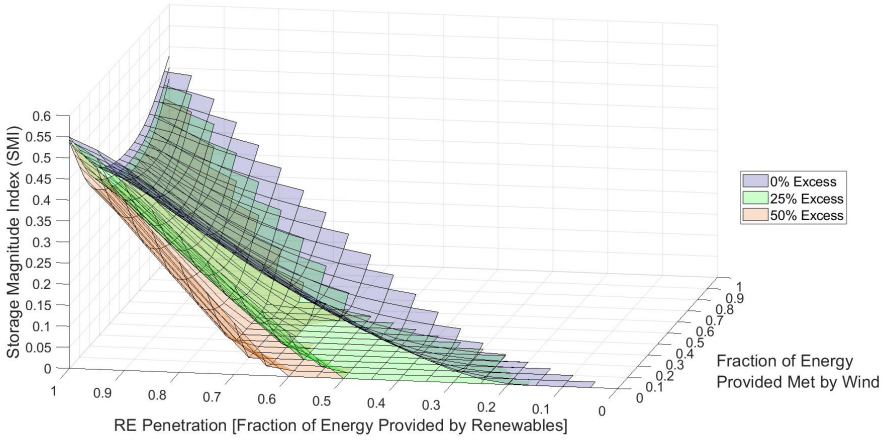

Figure 5.18: Winnipeg, Canada: SMI for 0%, 25% and 50% excess energy.

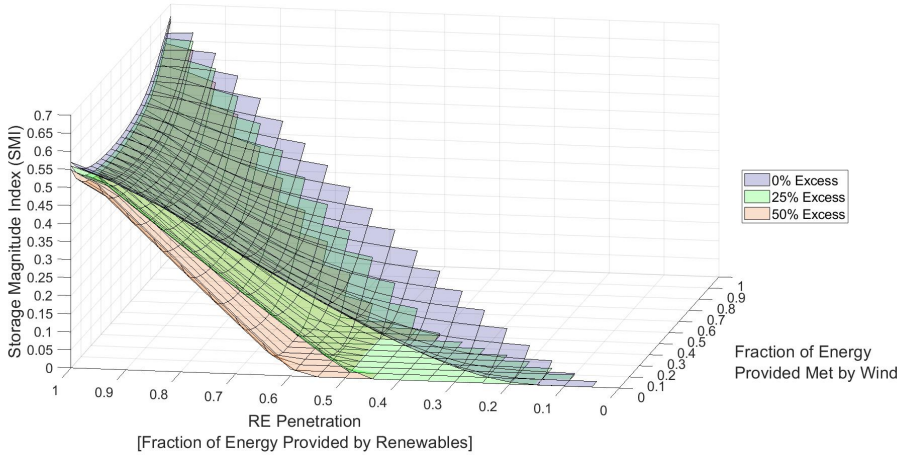

Figure 5.19: Norman Wells, Canada: SMI for 0%, 25% and 50% excess energy.

The application of excess energy, in agreement with the results considering Shimizu

(Section 5.1.2), has notable impact on when energy storage is first required. For Winnipeg, when 25% excess power is provided the first occurrence of energy storage requirements moves from 20% to 50% VRE penetration for $\theta = 0$, and from 20% to 60% for $\theta = 1$. For Norman Wells this shift is comparable, from 15% to 45% VRE penetration for $\theta = 0$ and from 10% to 40% for $\theta = 1$. The addition of more excess energy (up to 50% excess) has considerably less impact on the amount of energy that has to be stored (Figures 5.22 and 5.24) and the size of storage required (Figures 5.23 and 5.25) for both Winnipeg and Norman Wells. In agreement with the findings in Section 5.1.2, the impact of excess energy has little effect on the SMI at high VRE penetration dominated by solar. However, when dominated by wind the SMI can be seen in Figures 5.20 and 5.21 to be highly dependent on location: the SMI for Winnipeg at 100% VRE penetration and $\theta = 1$ shifts from 0.478 at 0% excess to 0.424 at 50% excess, whereas for Norman Wells it only changes from 0.667 to 0.652.

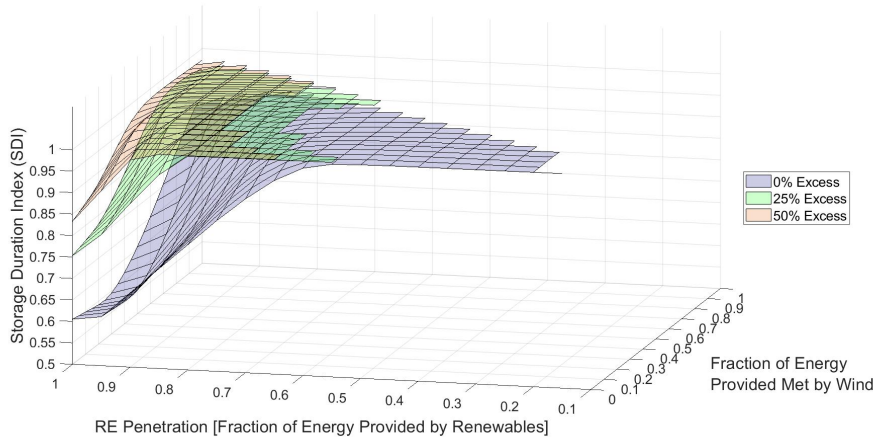

Figure 5.20: Winnipeg, Canada: SDI for 0%, 25% and 50% excess energy.

An interesting result, only identifiable through the comparison of more than one location, is the impact that the excess energy has on the short-term storage bias. Comparing Figures 5.20 and 5.21 it can be seen that the effectiveness of excess energy to mitigate long-term storage requirements is highly dependent on the location considered. This is most easily identifiable when considering how the tipping point and SDI values at 100% VRE penetration change with excess energy. Similar to the

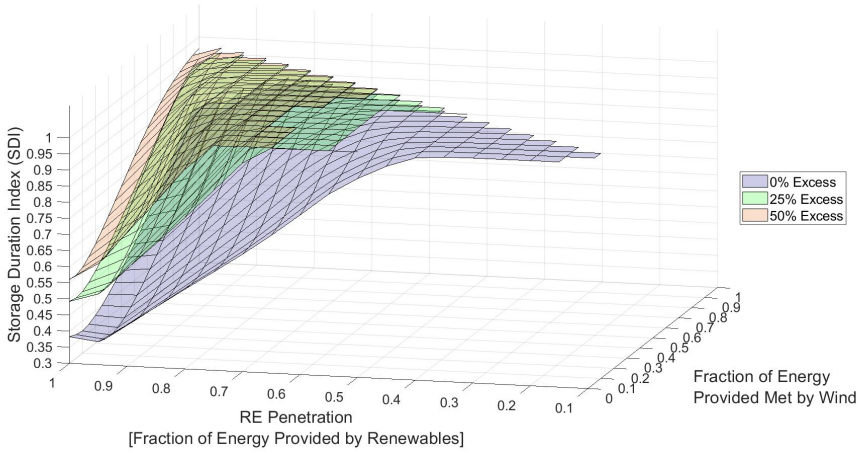

Figure 5.21: Norman Wells, Canada: SDI for 0%, 25% and 50% excess energy.

impact on SMI, the application of excess energy is most impactful when first applied and its capacity for mitigation diminishes.

Figures 5.22 and 5.24 demonstrate these findings in more depth specific to four hypothetical storage technologies (as outlined in Section 4.1.1) by showing the fraction of energy that meets demand by the duration of storage required. They show that for solar dominated supply the storage requirement is dominated by daily and seasonal storage. While the magnitude of energy stored is similar, the less challenging location (i.e. Winnipeg Figure 5.22) is more dependent on daily storage. Wind dominated supply on the other hand, is particularly reliant on storage between a day and a week (24 hours $\leqslant \tau <$ 1 week). The application of excess energy in such networks is shown to be particularly useful at mitigating the need for long-term storage (1 month $\leqslant \tau <$ 1 year).

Figures 5.23 and 5.25 show the size of energy storage required as a percentage of mean daily demand. These make it abundantly clear that storage size for $\tau <$ 24 hours is relatively small independent of θ and location. For both locations when supply is wind dominated, they are highly dependent on storage with 1 day $\leqslant \tau <$ 1 month. Whereas, when solar dominates, long-term storage is essential. Despite the similarity in the rate of storage size growth with VRE penetration, the magnitude of long-term storage, in particular, is considerably different: Winnipeg requiring the

storage with 1 month $\leqslant \tau <$ 1 year to be 2,076% of mean demand at 100% VRE penetration and θ=0; Norman Wells, instead, requiring 3,379% (over a month of average demand). The application of excess energy has very similar impact on the storage sizes required at both locations. It delays the first need for storage and the emergence of any longer-term storage requirement (i.e. the tipping-point) to higher VRE penetration levels. However, unlike the findings for Shimizu (Section 5.1.2), excess energy at high VRE penetration when $\theta \to 0$ has limited impact on the size of long-term storage required.

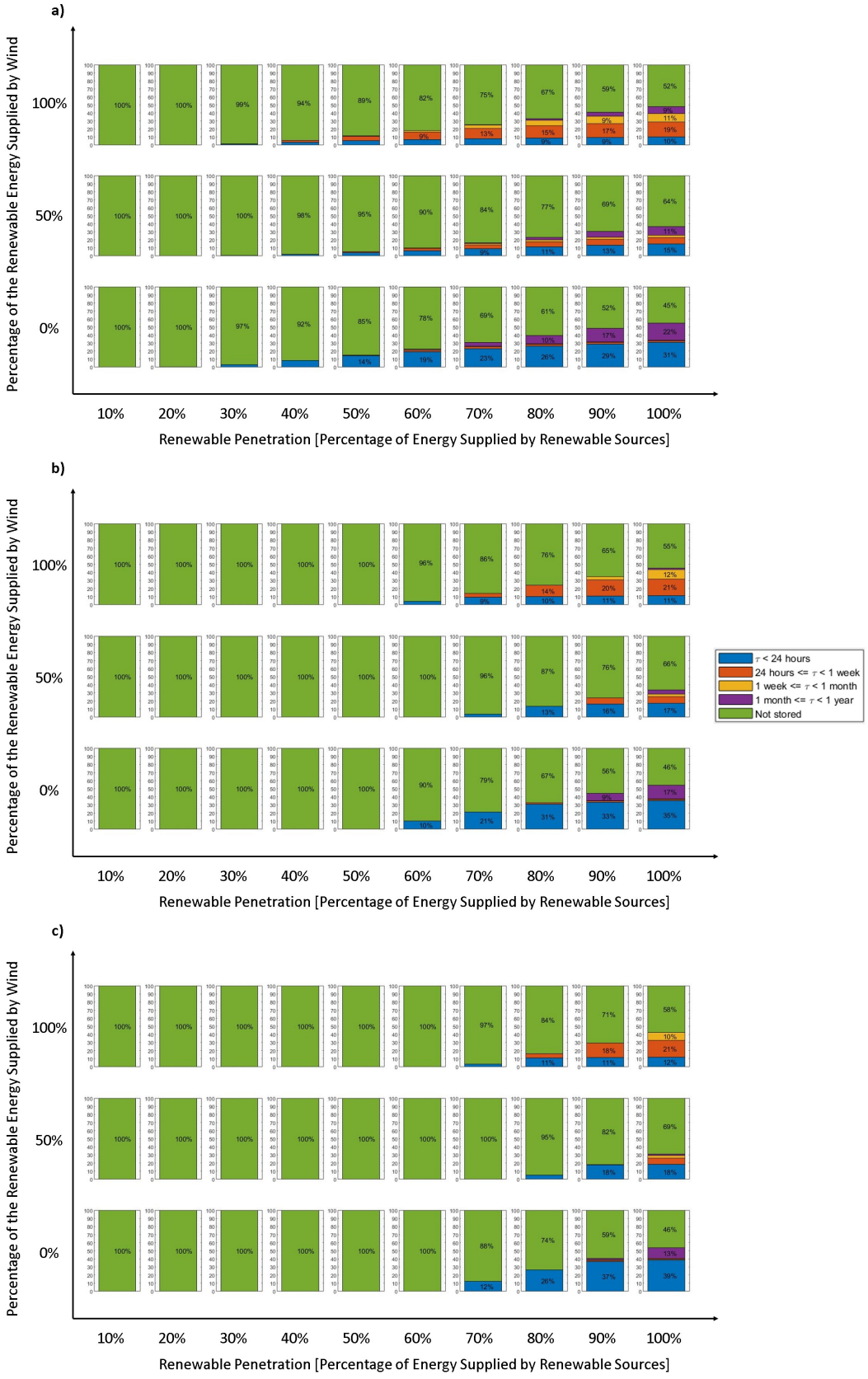

Figure 5.22: Winnipeg, Canada: Storage use required as a percentage of the total energy used to meet demand for a) 0%, b) 25% and c) 50% excess energy.

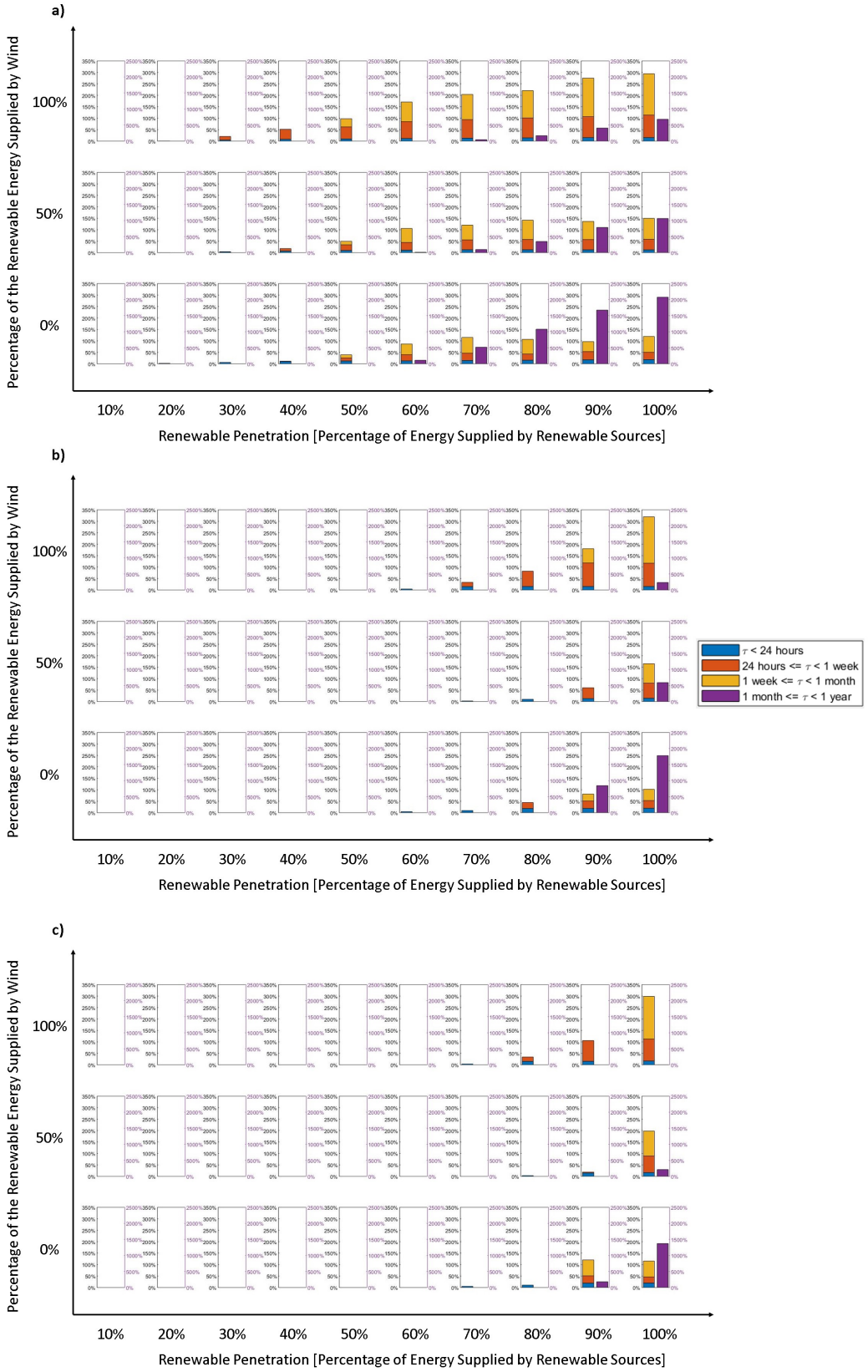

Figure 5.23: Winnipeg, Canada: Storage size required as a percentage of mean daily energy demand for a) 0%, b) 25% and c) 50% excess energy. Left axis: all $\tau < 1$ month; Right axis: 1 month $\leqslant \tau < 1$ year.

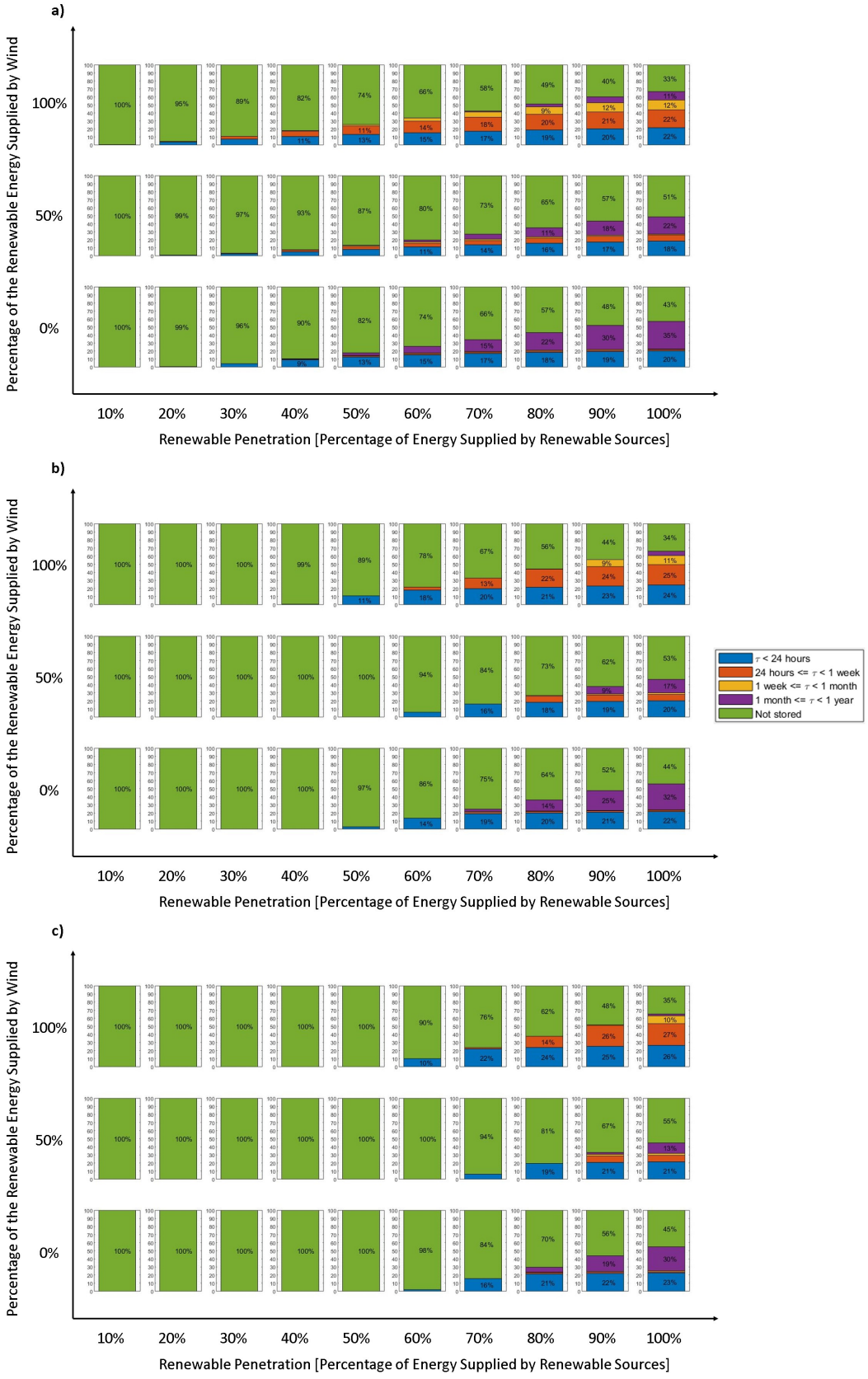

Figure 5.24: Norman Wells, Canada: Storage use required as a percentage of the total energy used to meet demand for a) 0%, b) 25% and c) 50% excess energy.

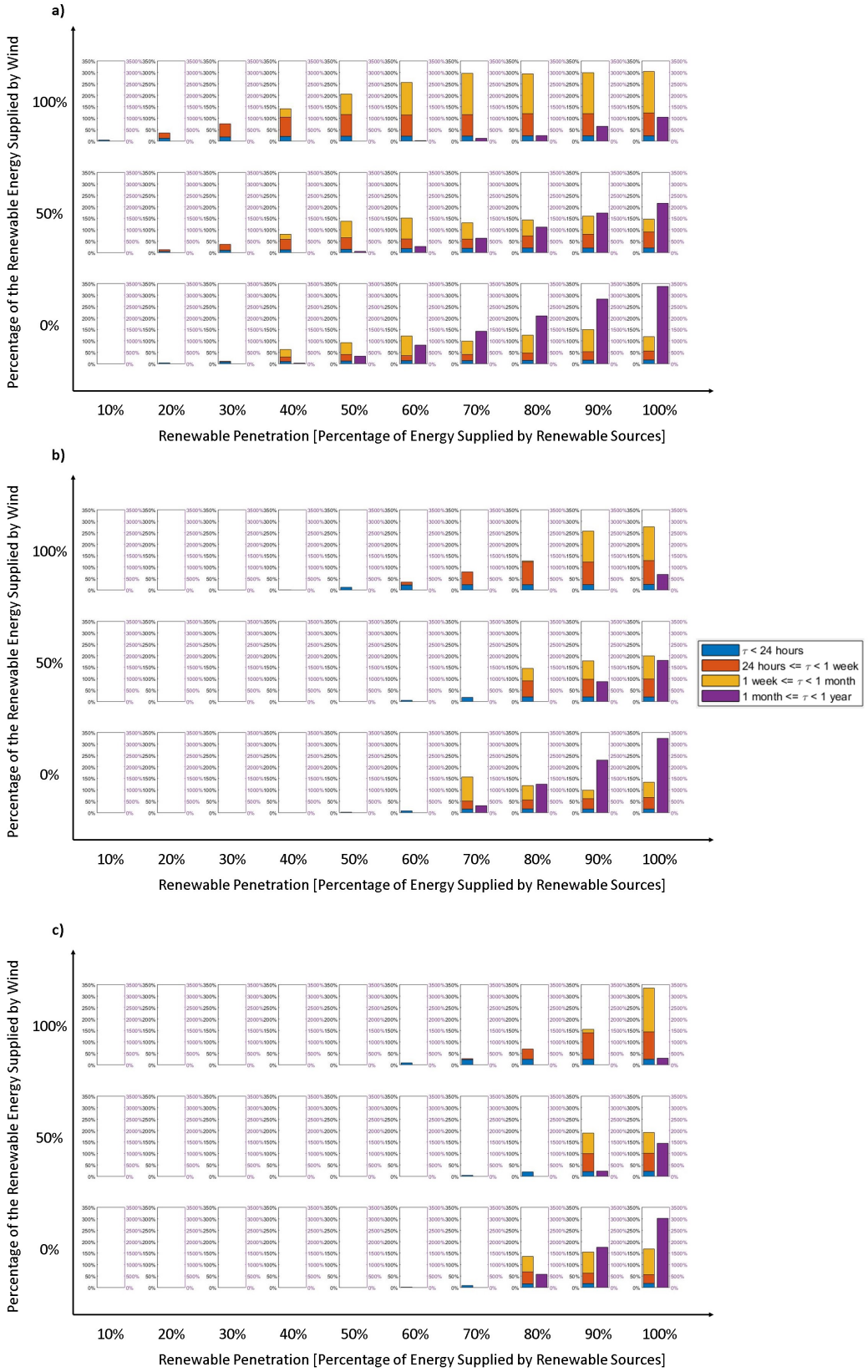

Figure 5.25: Norman Wells, Canada: Storage size required as a percentage of mean daily energy demand for a) 0%, b) 25% and c) 50% excess energy. Left axis: all τ < 1 month; Right axis: 1 month $\leqslant \tau <$ 1 year.

Australia: Most & Least Challenging Locations

For Australia, Cape Grim (Tasmania) was selected as the least challenging location considered and Wagga Wagga Airport the most challenging (Figure 4.5). Figure 5.26 shows that in terms of the minimum SMI achievable, Cape Grim is the least challenging location across the four countries considered. When $\theta \to 1$ the SMI dramatically decreases even at high VRE penetration (SMI = 0.265 at 100% VRE penetration). Figure 5.27 shows that Wagga Wagga has a remarkably similar requirement for storage (in terms of the SMI) to Shimizu (Figure 5.5). Comparison of Figure 5.26 and 5.5 shows that the impact of providing excess energy on the SMI is highly dependent on the location. In Cape Grim, excess energy has considerable impact on when storage is first required (i.e. when SMI is > 0) as $\theta \to 1$.

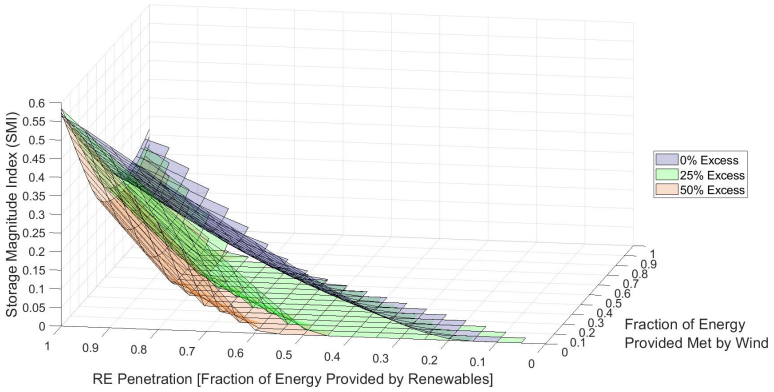

Figure 5.26: Cape Grim, Australia: SMI for 0%, 25% and 50% excess energy.

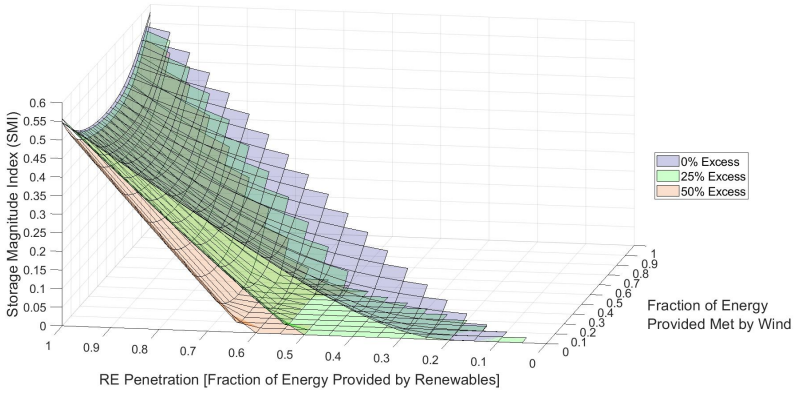

Figure 5.27: Wagga Wagga, Australia: SMI for 0%, 25% and 50% excess energy.

Figures 5.28 and 5.29 show the influence of the location in Australia on the duration of storage required. The impact of the excellent wind resource in Cape Grim can

be seen once again. The tipping-point when $\theta = 1$ at over 85% VRE penetration compared with 65% for Wagga Wagga. With little wind involvement (i.e. $\theta \to 0$) the shape of the manifold is similar to Wagga Wagga and other previously considered locations. Wagga Wagga's tipping point is very different to Cape Grim and is virtually independent of θ. The application of excess energy shifting the tipping point evenly for all θ unlike Cape Grim.

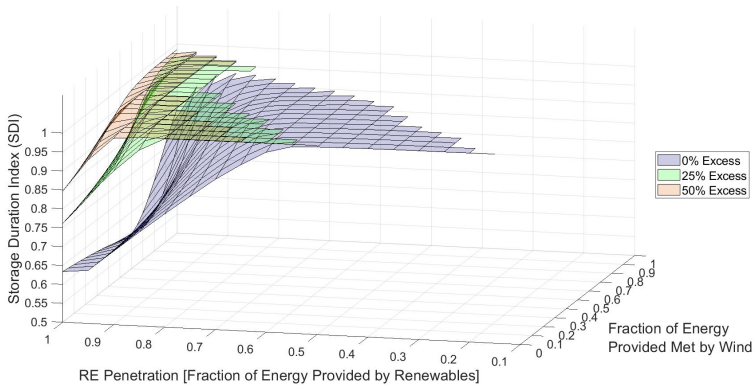

Figure 5.28: Cape Grim, Australia: SDI for 0%, 25% and 50% excess energy.

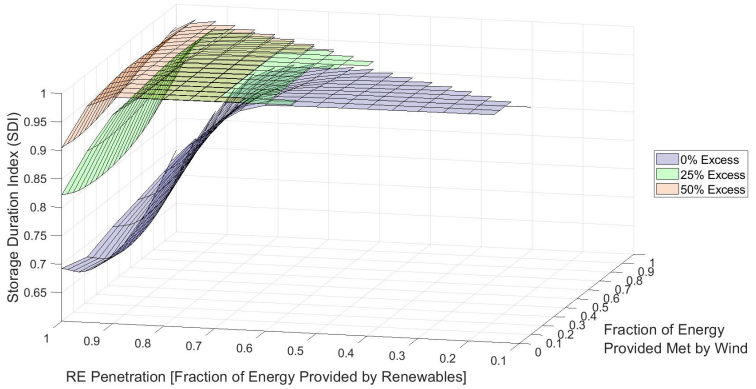

Figure 5.29: Wagga Wagga, Australia: SDI for 0%, 25% and 50% excess energy.

Figures 5.30 and 5.32 show that while the trends identified previously (when inspecting Winnipeg and Norman Wells, Canada) exist, their magnitude is significantly diminished due to the better VRE resource. At $\theta = 1$ medium-term storage is still dominant, but due to the wind resource the amount of energy that has to be stored is notably reduced. This is also the case when $\theta = 0$. While diurnal and seasonal storage are required, the proportions are different. Reduced seasonal variation at the two Australian locations means that the storage requirement can be met with a

greater dependence on diurnal storage. Moreover, the application of excess energy is more effective for all VRE penetrations to mitigate the remaining long-term storage.

The wind resource has significantly reduced the size of storage required at Cape Grim (Figure 5.31). So much so, that the common trend that storage is required at lower VRE penetration when wind dominates supply (as shown in Figure 5.33) is reversed. Comparison of the storage size required in Canada with Figures 5.31 and 5.33 shows that the better VRE resource and improved alignment with demand notably reduces the size of all storage duration.

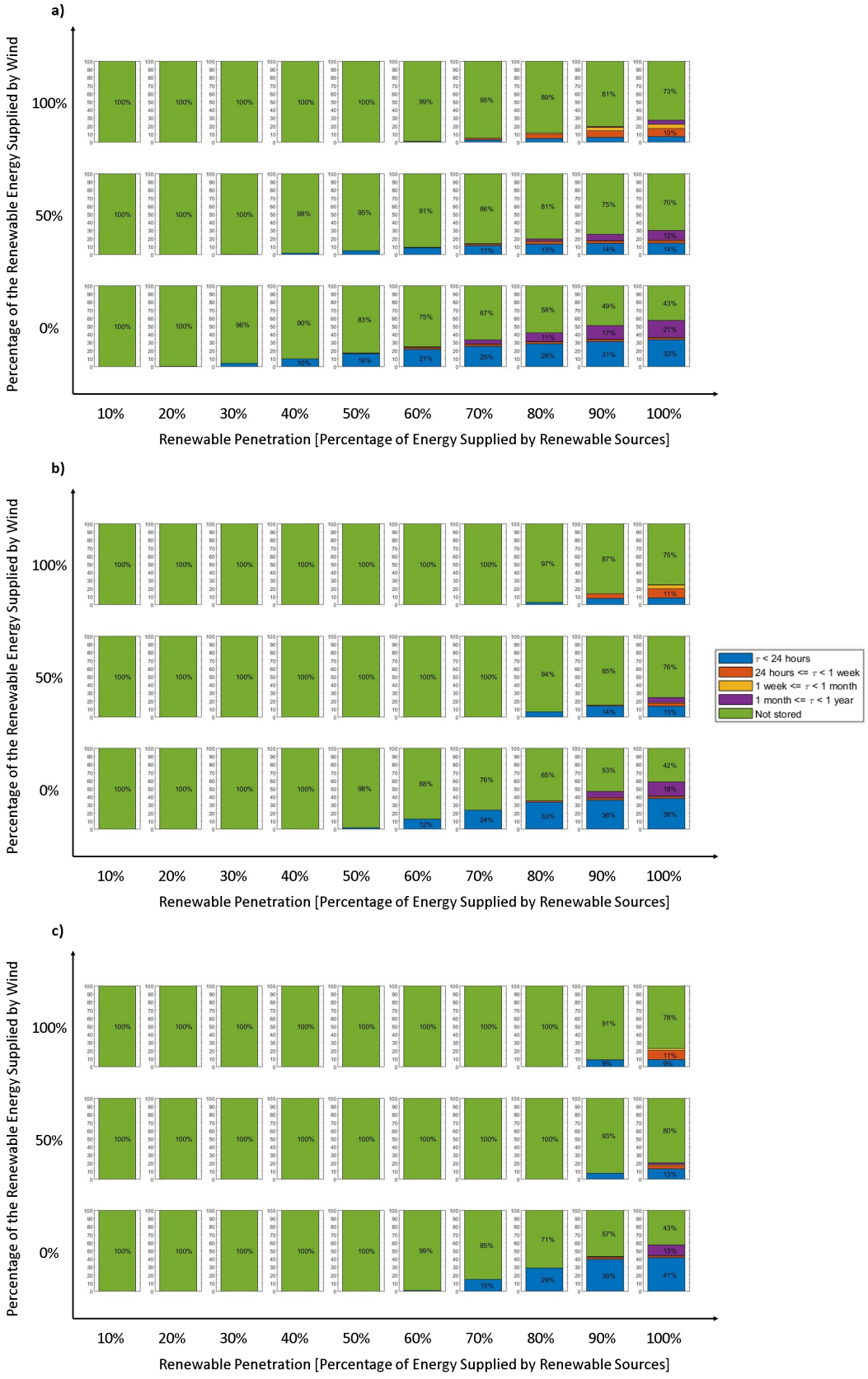

Figure 5.30: Cape Grim, Australia: Storage use required as a percentage of the total energy used to meet demand for a) 0%, b) 25% and c) 50% excess energy.

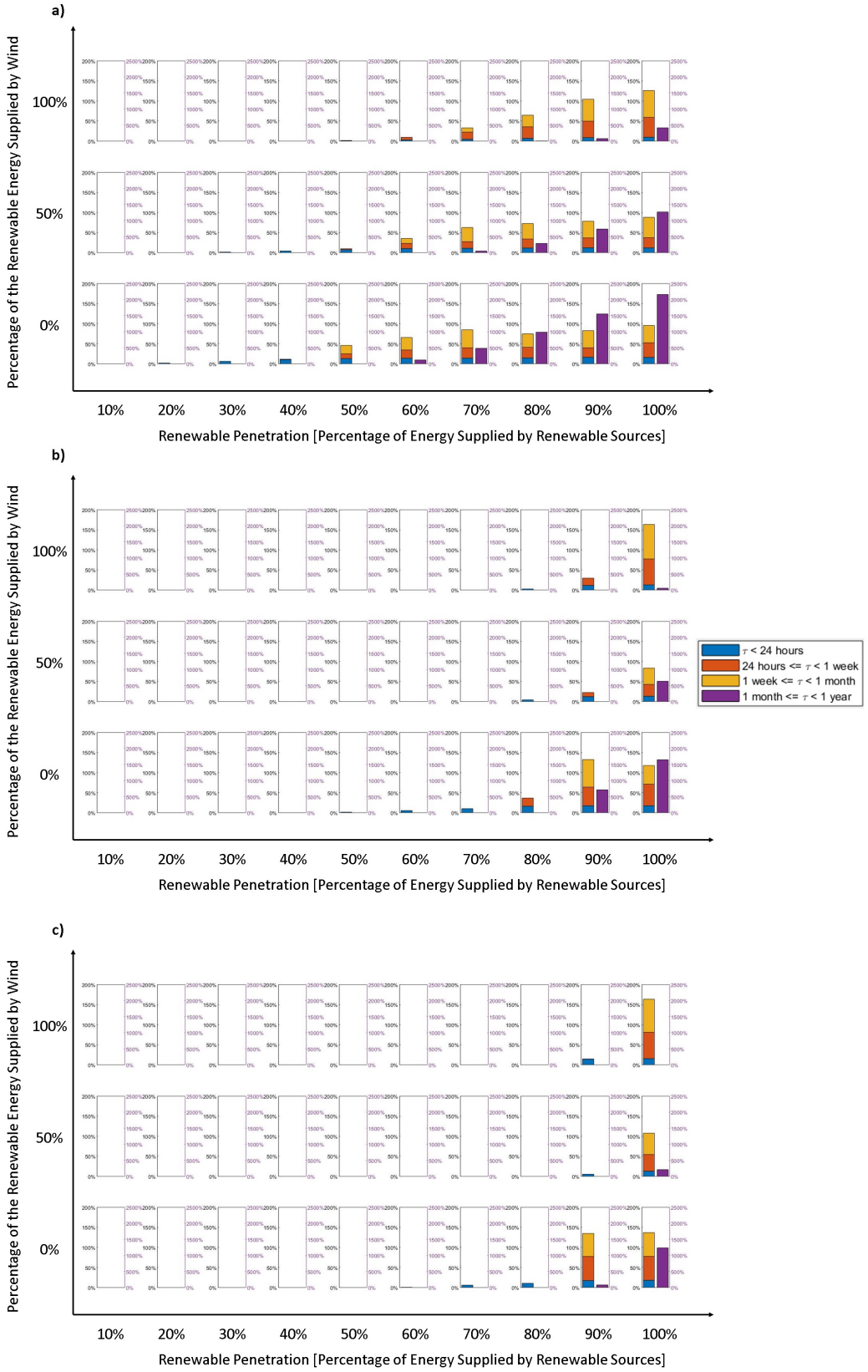

Figure 5.31: Cape Grim, Australia: Storage size required as a percentage of mean daily energy demand for a) 0%, b) 25% and c) 50% excess energy. Left axis: all τ < 1 month; Right axis: 1 month $\leqslant \tau <$ 1 year.

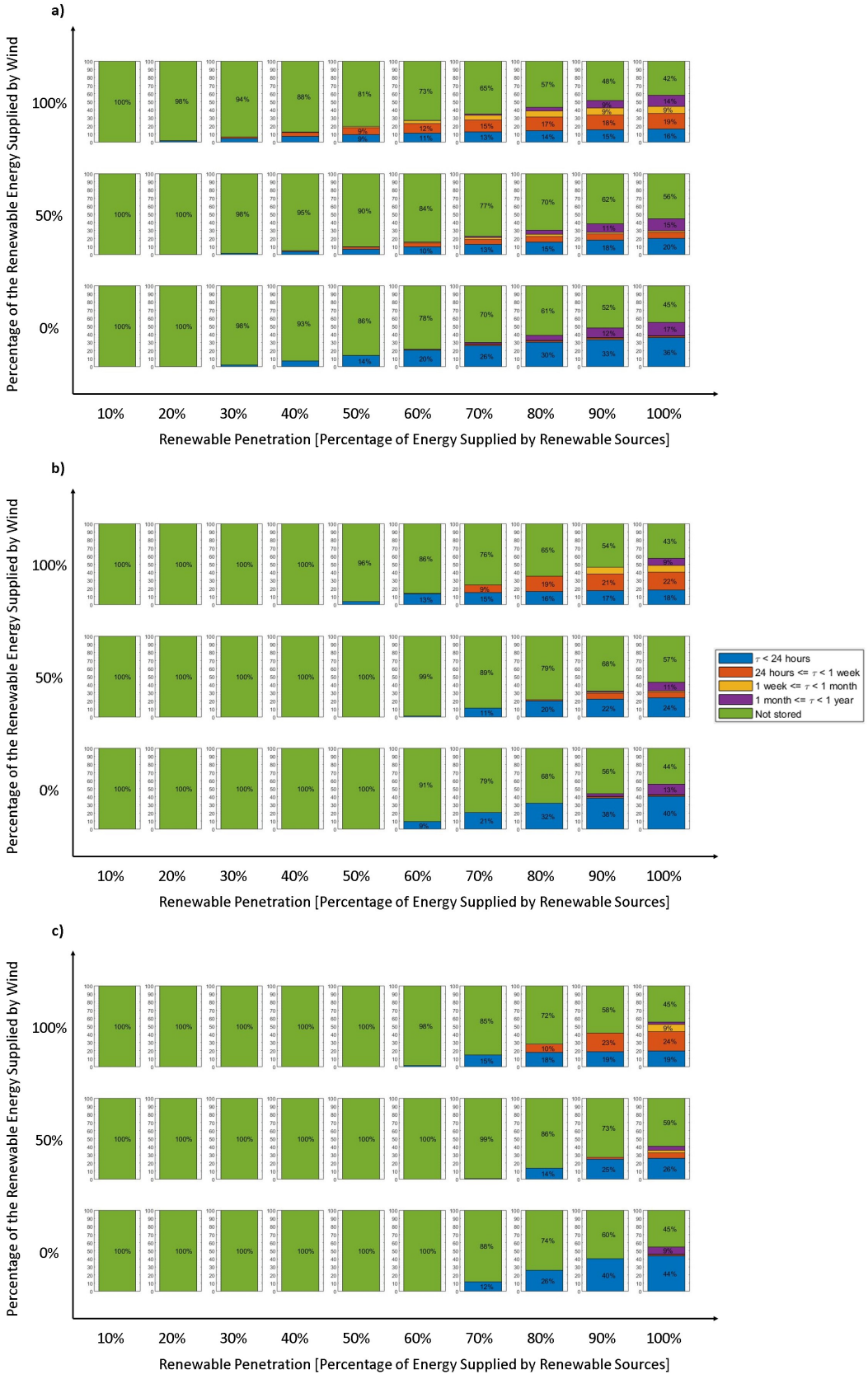

Figure 5.32: Wagga Wagga, Australia: Storage use required as a percentage of the total energy used to meet demand for a) 0%, b) 25% and c) 50% excess energy.

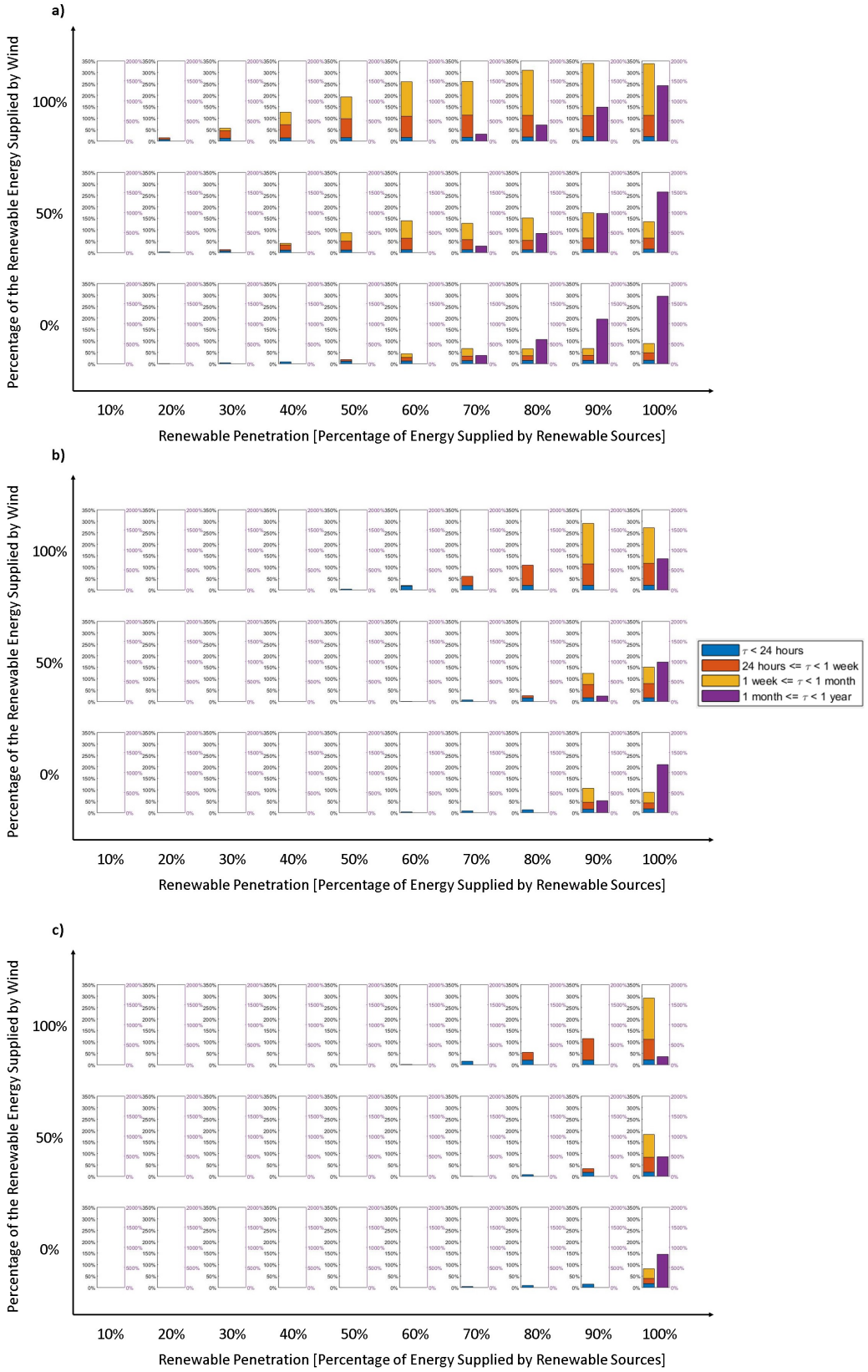

Figure 5.33: Wagga Wagga, Australia: Storage size required as a percentage of mean daily energy demand for a) 0%, b) 25% and c) 50% excess energy. Left axis: all τ < 1 month; Right axis: 1 month $\leqslant \tau <$ 1 year.

Comparison of Locations

There are clear similarities between many of the results that enable us to draw conclusions from the impact that VRE penetration and the mix of VRE sources have on the storage requirements and the effectiveness of excess power provision to mitigate them. The development of the SMI with VRE penetration is very predictable when the supply is solar dominated. The first requirement for storage is at ∼20% (as shown in Figures 5.5, 5.11, 5.14 and 5.16). The requirement then increases, in a convex relationship with VRE penetration, until a point of inflexion at ∼75% VRE penetration. At 100% VRE penetration the SMI is in the range of 0.50-0.55. The incorporation of wind as part of the mix of VRE sources (i.e. as θ increases from 0 towards 1) delays the tipping point to a greater VRE penetration. However, this delay is highly dependent on the location considered. In all locations, barring those with world class wind resource (e.g. Cape Grim), the size of energy storage required as VRE penetration increases is first noticeable when wind dominates supply. The short-term storage requirement ($\tau < 24$ hours) mentioned previously only requires very small energy capacity. The ability of excess energy to mitigate long-term storage is good at lower VRE penetration, but not high penetration. This is particularly problematic when the supply is solar dominated given that a mix of diurnal and seasonal storage is required. However, this is less of a problem for when wind dominates supply which is predominantly dependent on 1 day $\leqslant \tau <$ 1 month storage.

However, there are notable differences between locations that are equally important. The impact of θ on the SMI differs significantly by country and, in the case of Canada and Australia, location. For the UK and particularly for some locations (e.g. Cape Grim) in Australia as $\theta \to 1$ the SMI substantially decreases. However, in Japan, Canada and other Australian locations considered the impact was the opposite. The VRE penetration at which the tipping point occurs and the magnitude of the dependence on longer-term storage at high VRE penetration are both highly specific to location.

5.2 Global Potential for Islanded 'Green' Ammonia Production

This section presents the IAPMT simulation results [142]. To meet the global analysis objectives (Section 4.2.2), the results for the present-day and 2030 domestic and multi-national corporation production scenarios are compared. There are three sections to these results:

1. Identify the range of LCOA achievable, currently and by 2030, to choose best locations for implementation and when it will be commercially viable (objectives 1 and 4).

2. Quantify the impact of VRE intermittency on the LCOA by comparing results from an 'ideal' power profile against realistic renewable power profiles. Identify the key reasons for the difference and therefore how to manage the VRE intermittency through the production process design and operation (objective 2).

3. Identify the LCOA's key components at the most favourable locations and how reducing these components contributes to reducing LCOA to determine the minimum possible LCOA (objective 3). Quantify the impact that domestic financing has on the achievable LCOA, the plant design, and operation. From the most favourable locations identify those that may have financial barriers to implementation without multi-national corporation involvement or government support.

5.2.1 LCOA Achievable

Figure 5.34 shows the range of achievable LCOA in the 2019 scenario for production by a multi-national and domestic corporation. The LCOA range ($\$473t^{-1}$ to $\$2{,}464t^{-1}$) and median ($\$962t^{-1}$) for production by a multi-national corporation is in line with previous LCOA estimates for islanded and semi-islanded production

(Section 2.2.1). Every geographic region, barring South-Eastern Asia and Western Asia, has a location able to produce green ammonia below the maximum benchmark of $\$720t^{-1}$ (see Appendix D for results by country). While this is promising, only a lower LCOA would be competitive with convention (fossil-fuel dependent) production, even with favourable financing. Figure 5.35 shows that locations with excellent wind resource (i.e. with full load hours equivalent greater than 2,000) have the lowest LCOA currently. The significantly greater capacity factors enable higher electrolyser and synthesis load factors. The solar reliant locations (by necessity due to limited wind resource or high wind costs), are only able to support up to 3,200 electrolyser FLH with a fundamentally diurnal power source. This results in a higher LCOA, despite the often lower LCOE of solar PV compared with onshore wind. The installed cost of solar PV not the solar resource available (i.e. solar capacity factor) determines the achievable LCOA in these locations, Figure 5.35b.

Figures 5.34a and 5.34b show the impact of domestic financing. Many locations' LCOA increases due to the higher financing cost. Locations depending on solar PV (with electrolyser FLH of 2,500-3,200) are most adversely affected. While some of the lowest solar reliant LCOA estimates in Sub-Saharan Africa and Southern Asia increase by over $\$100t^{-1}$, others in North Africa increase considerably more (Figure 5.39).

Figure 5.36 shows the range of achievable LCOA changes by 2030. The LCOA range of $\$310t^{-1}$ to $\$1{,}762t^{-1}$ and median of $\$483t^{-1}$ for production by a multi-national corporation is significant when compared against the benchmarks. The best location in each geographic region is below $\$394t^{-1}$ (see Appendices for results by country). The lowest LCOA estimates (with high electrolyser FLH) have decreased $\sim\$150t^{-1}$, but the most significant development is the reduction in solar dependent production LCOA. The LCOA achievable at these locations (with electrolyser FLH from 2,500-3,200) 'catches-up' with the lower wind dependent LCOA (from the 2019 scenario). The LCOA falls by up to $\$300t^{-1}$ (Figure 5.36a). The installed cost of solar PV has less impact the LCOA achievable at these locations. The financial barriers

to domestic production still exist, but the range of LCOA achievable is \$319t^{-1} to \$2,014t^{-1} with a median of \$531t^{-1}. 5 locations can achieve an LCOA below \$350t^{-1}.

Comparing the plant design for three specific locations that have $\theta \approx 0$, 0.5 and 1 shows how the availability of VRE resources and the cost of using them have an impact on the LCOA and the plant design. Table 5.1 shows that in 2019 the solar dependent locations cannot achieve the low LCOA that the wind based production processes can. The synthesis load factor is lower due to seasonal variation. Diurnal variations result in additional electrolyser over-sizing. These both contribute to a higher LCOA despite a lower LCOE. The systems with a wind supply component minimise curtailment: the production process is smaller and the hydrogen buffer provides flexibility. Electrolyser over-sizing can be reduced to enable lower LCOA in wind powered processes where diurnal variation is lower.

	Solar Dominated		**Wind & Solar**		**Wind Dominated**	
	New Delhi India		**Minamitorishima Japan**		**Cape Grim Australia**	
	2019	**2030**	**2019**	**2030**	**2019**	**2030**
θ	0.00	0.00	0.60	0.35	1.00	0.99
P_{Elec} [MW]	232	193	174	156	145	143
$P_{HB/ASU}$ [MW]	12.6	10.8	12.0	8.2	10.0	9.9
Supply FLH	1,957	1,957	2,196	1,956	5,625	5,384
LCOE [\$ MWh^{-1}]	25	8	34	14	28	16
Electrolyser Excess Factor [%]	35	31	7	40	6	6
Hydrogen Storage [t]	16	12	20	18	44	40
VRE Curtailed [%]	16	25	8	19	0	1
Electrolyser Load Factor [%]	34	36	49	48	64	65
Synthesis Load Factor [%]	44	46	52	66	68	68
LCOA [\$/t]	635	339	608	336	473	310

Table 5.1: Impact of θ and the scenario on the LCOA, plant design and operation.

The reduction in LCOE and electrolyser CAPEX by 2030 has notable impact on the achievable LCOA and the design of the production process. The wind dependent processes LCOA reduction is entirely due to these reductions in cost. The design of the process and the selection of the mix of VRE sources is held relatively constant.

The reduction in the LCOA achievable in New Delhi and Minamitorishima is due to the LCOE / electrolyser CAPEX cost reduction and a new process design. Lower solar PV LCOE means that process flexibility from curtailment costs less. Moreover, curtailment is more competitive as a method of flexibility than the hydrogen buffer, compared with the 2019 scenario. In New Delhi, the electrolyser over-sizing and hydrogen storage size reduce and curtailment increases; θ is constant. This enables a lower achievable LCOA at solar dependent locations (it 'catches up' with wind). The achievable LCOA for a multi-national corporation in 2019 has a strong exponential relationship (Equations 5.1 and 5.2) with the supply capacity factor (SCF) (the actual energy output divided by the maximum possible energy output) as a percentage, with an R^2 of 0.7505. Lower solar PV LCOE and plant flexibility cost mean the same relationship is slightly weaker in 2030, with an R^2 of 0.7217). The SCF values used in all scenarios are secondary results of the VRE ratio (θ) determined in the LCOA optimisation. Therefore substituting a pre-determined SCF value, including those higher SCF values for some θ values (e.g. as $\theta \to 1$ for most wind resource locations), to the below equations is likely to produce an overly optimistic estimated achievable LCOA.

$$\text{LCOA}_{2019} = 9145e^{-0.2346\times SCF} + 917.4e^{-0.009553\times SCF} \qquad 5 \leqslant SCF \leqslant 65 \qquad (5.1)$$

$$\text{LCOA}_{2030} = 8764e^{-0.2746\times SCF} + 417.7e^{-0.004568\times SCF} \qquad 5 \leqslant SCF \leqslant 65 \qquad (5.2)$$

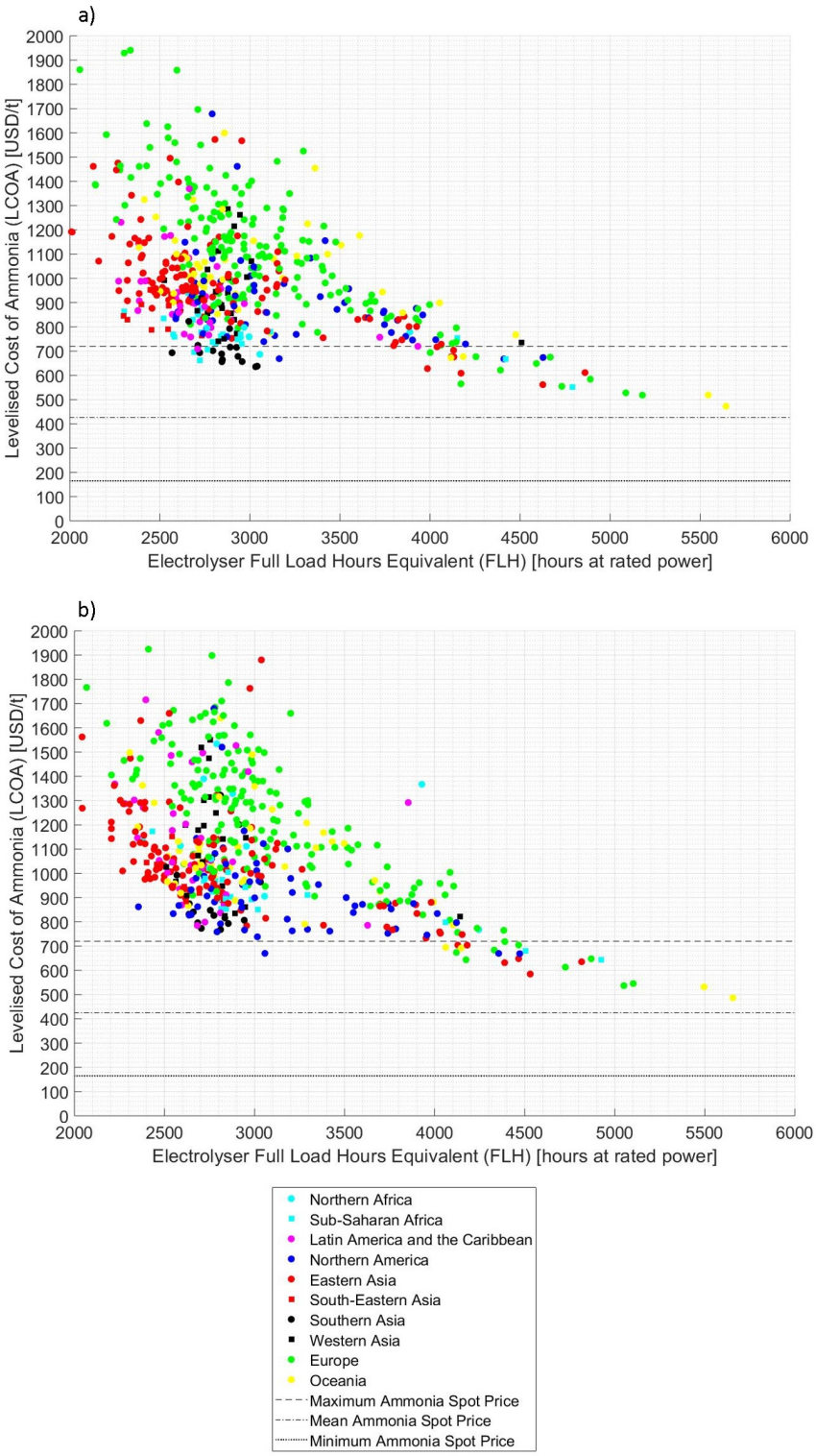

Figure 5.34: 2019 Scenario – Range of the optimal achievable LCOA and the respective electrolyser full load hours equivalent (FLH) grouped by geographic region for a a) multi-national and b) domestic corporation. Benchmarked against the maximum, mean and minimum of 2000-2019 NOLA, Black Sea, Middle East, Western Europe and US Tampa ammonia spot prices (720, 426 and $\$165t^{-1}$ respectively) [84]. Estimates above $\$2{,}000t^{-1}$ are not presented due to prioritisation of lower estimates.

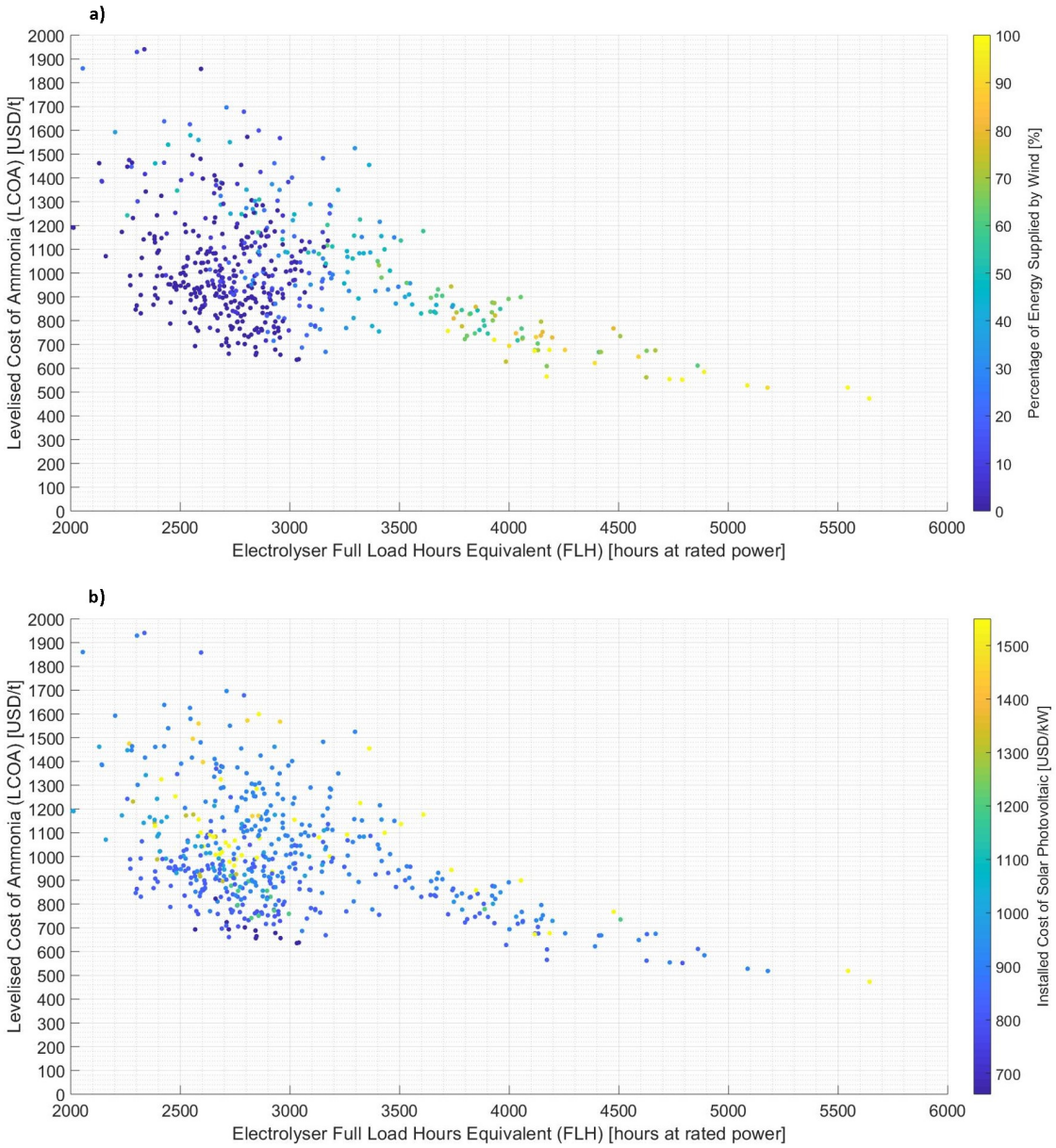

Figure 5.35: 2019 Scenario – Range of the optimal achievable LCOA and the respective electrolyser full load hours equivalent (FLH) for a multi-national corporation grouped by a) the VRE mix and b) installed CAPEX of solar PV.

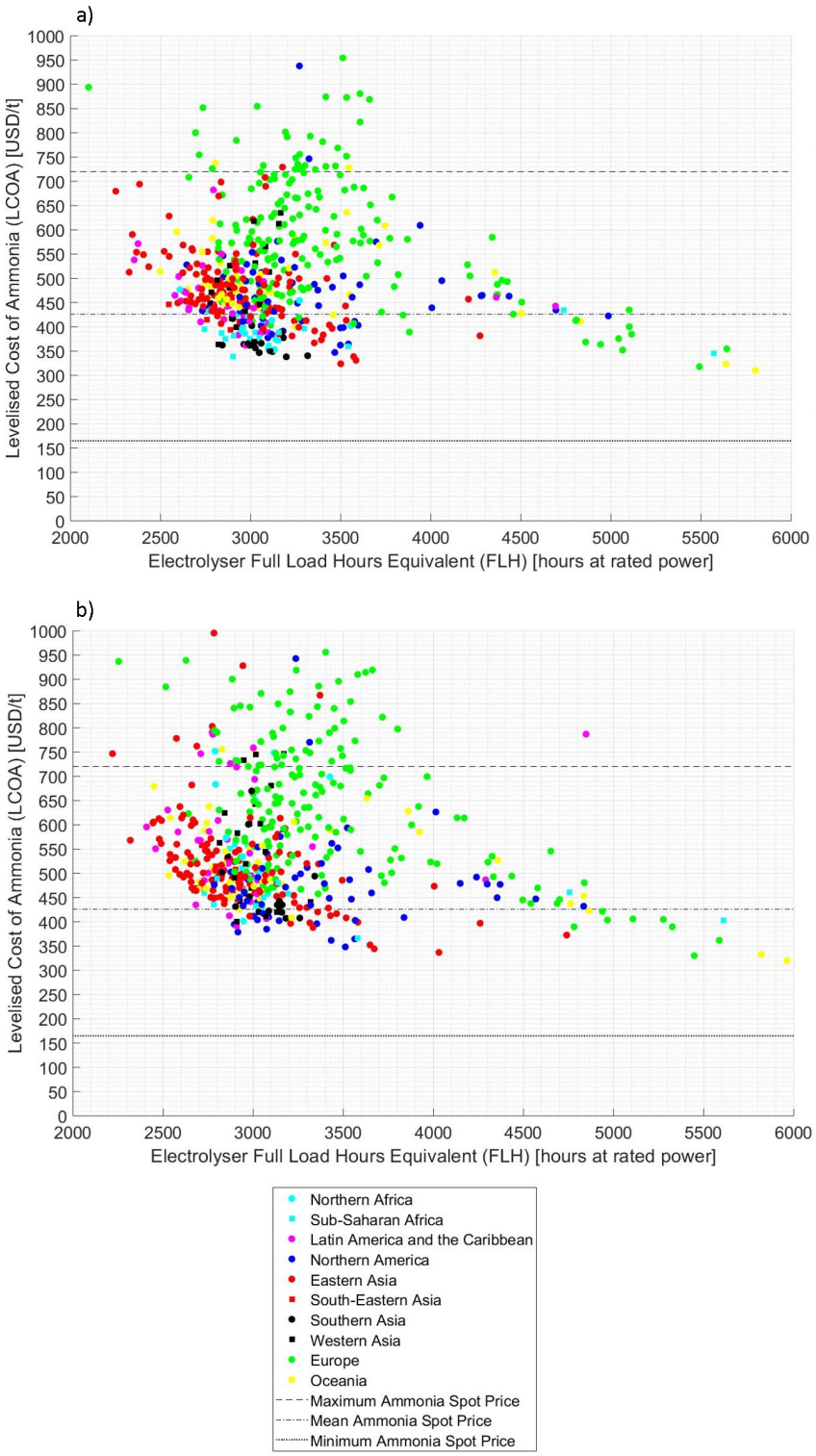

Figure 5.36: 2030 Scenario – Range of the optimal achievable LCOA and the respective electrolyser full load hours equivalent (FLH) grouped by geographic region for a a) multi-national and b) domestic corporation. Benchmarked against the maximum, mean and minimum of 2000-2019 NOLA, Black Sea, Middle East, Western Europe and US Tampa ammonia spot prices (720, 426 and $\$165t^{-1}$ respectively) [84]. Estimates above $\$1{,}000t^{-1}$ are not presented due to prioritisation of lower estimates.

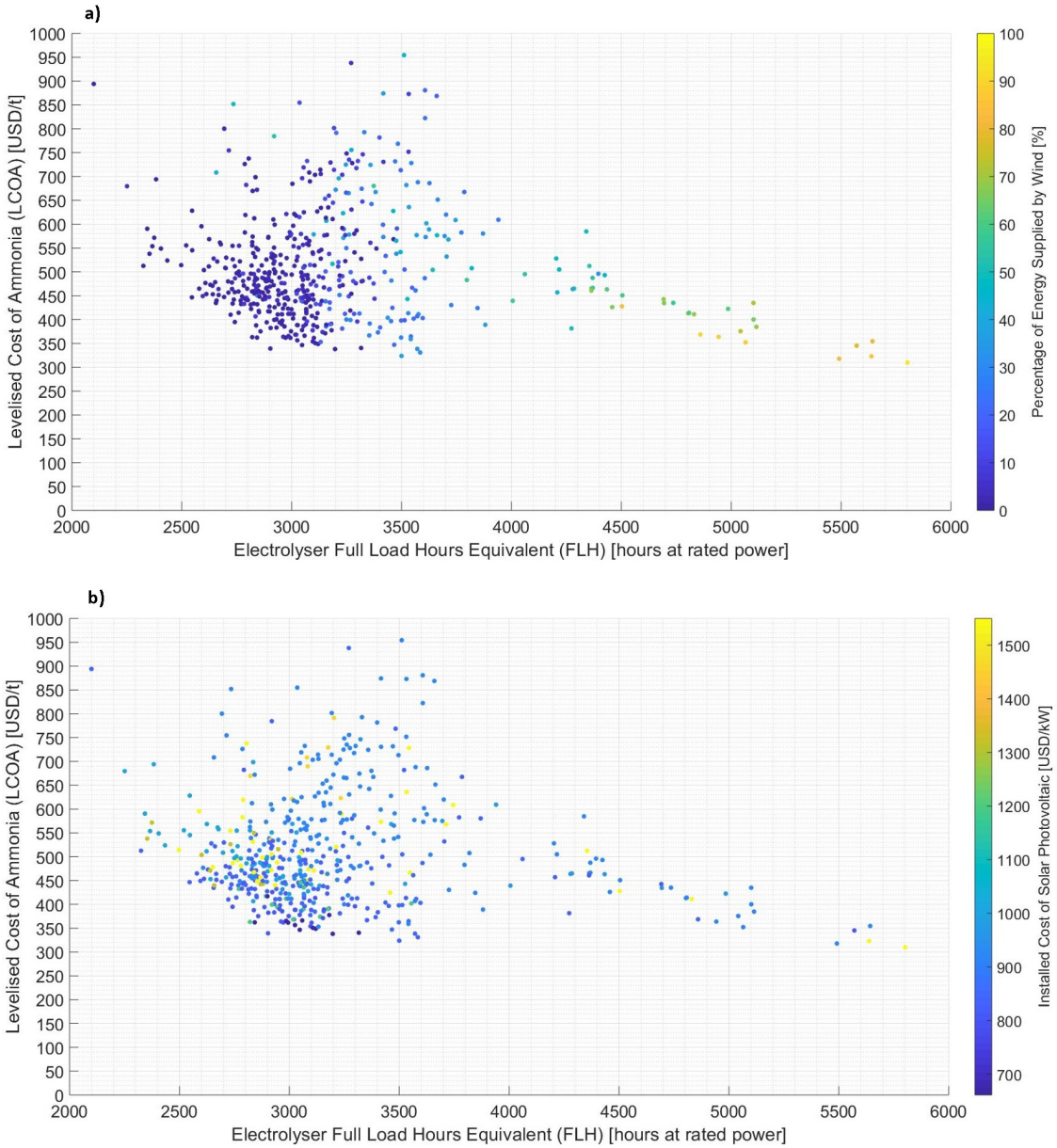

Figure 5.37: 2030 Scenario – Range of the optimal achievable LCOA and the respective electrolyser full load hours equivalent (FLH) for a multi-national corporation grouped by a) the VRE mix and b) installed CAPEX of solar PV.

5.2.2 Impact of VRE Intermittency

New Delhi, Minamitorishima and Cape Grim (as before) show how process flexibility can manage the VRE intermittency, depending on the VRE sources used and the date of implementation. There are two main production process flexibility methods: under-sizing the production plant relative to the VRE sources (i.e. curtailment of VRE), or a hydrogen buffer (i.e. over-sizing the electrolyser and using hydrogen

storage and a hydrogen fuel cell). In practice, the economically optimal solution is usually a combination of these methods depending on θ. Table 5.1 shows solar dependent production in 2019 relies on both methods; wind dependent production on the hydrogen buffer.

Comparing results from the VRE data calculations(Section 3.1.3) against an 'ideal' power profile results (Section 3.2.4) further highlights the impact of VRE intermittency on the LCOA. This is quantified and illustrated in Figure 5.38. The LCOA estimate using the 'ideal' profile (i.e. only using the VRE resource capacity factor) is overly optimistic. Present-day production simulations at the best locations have a 56% greater achievable LCOA than the ideal case, on average (Figure A). All locations, on average, have a 63% greater achievable LCOA (Figure B). Comparing results for 2030 demonstrates why this is important. The 2030 'ideal' power profile solutions are even less realistic. The best locations have a 76% higher LCOA (Figure C); all locations average LCOA is 91% higher (Figure D). Therefore, estimating the achievable LCOA is more complex than only using the supply capacity factor for VRE sources in a location. For reliable LCOA estimates, the cost of plant flexibility needs to be considered as well as VRE supply capacity factor and the LCOH.

Figure 5.38 shows that the plant's flexibility is a combination of curtailment (i.e. over-sizing the VRE supply sources relative to the plant) and the hydrogen buffer (i.e. hydrogen storage, hydrogen fuel cell and over-sizing the electrolyser). The dependence on one or both of these methods is very location specific. An all locations average shows that electrolyser over-sizing ('CAPEX Electrolysis'), hydrogen storage ('CAPEX Hydrogen Storage') and curtailment are high cost components of process flexibility to manage the VRE intermittency Figure 5.38. The amount of ammonia produced also affects LCOA: less ammonia is produced in the realistic scenario which increases the achievable LCOA. It accounts for 29.3% (best locations) / 36.7% (all locations) of the LCOA increase from 'ideal' to actual in 2019 (Table 7.5). This increases to 37.9% and 47.3% respectively in the 2030 scenario.

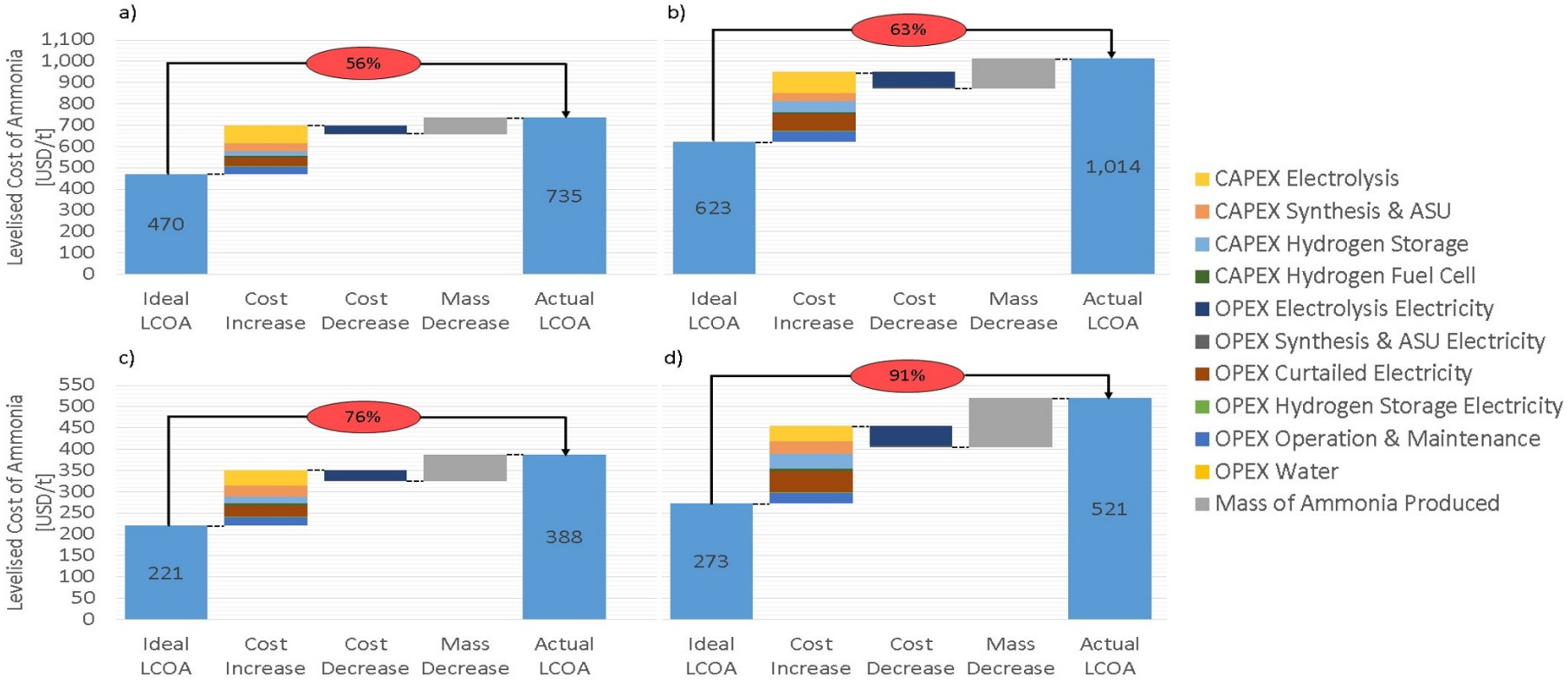

Figure 5.38: Cost of the required system flexibility for a Multi-national corporation: (a) mean of the lowest 100 LCOA estimates in the 2019 scenario, (b) mean of the all 534 locations in the 2019 scenario, (c) mean of the lowest 100 LCOA estimates in the 2030 scenario, (b) mean of the all 534 locations in the 2030 scenario.

5.2.3 Scope for Cost Reductions

Morgan [99] quantifies the key components of LCOA for semi-islanded operations, but not for islanded operations with a combination of solar and wind resource or for multiple locations. The lowest 10 LCOA estimates by geographic region (Figure 4.9) show the components of LCOA in the 2019 and 2030 scenarios respectively (Figures 5.39 and 5.40).

Hydrogen production, electrolyser CAPEX and OPEX, are the main costs in 2019, accounting for between 54.8-71.9% of the total in the best 10 locations by region. This is due to its high specific energy consumption, significant CAPEX per kW rated power and its over-sizing as part of the hydrogen buffer. Other key components of cost, such as hydrogen storage CAPEX and curtailment, also vary significantly by location: between 0.9-9.6% and 0.1-19.0% respectively. Figure 5.39a shows that at the extremes of these ranges these two variables have a strong anti-correlation: if hydrogen storage is a significant component of LCOA for a given location then curtailment isn't and visa versa. This is because at these locations one flexibility method is prioritised (i.e. curtailment or hydrogen buffer as discussed in Section 5.2.2). A complete breakdown of the components of cost by location can be found in Appendix G. The IAPMT findings and the estimated reduction of LCOA in 2030 show there is significant potential to reduce the LCOA if the electrolyser CAPEX and the VRE LCOE continue to fall. At solar dependent locations the impact of these cost reductions on LCOA is compounded by reducing key costs and the cost of plant flexibility. It is crucial to predict these variables' achievable decrease to determine how far the LCOA can fall. However, the magnitude and rate of this decrease is contentious [157].

Figure 5.40 shows that as electrolyser CAPEX and LCOE decrease, other costs increase. The synthesis CAPEX increases from 5.7-11.7% of LCOA in 2019 to 11.9-21.1% of LCOA by 2030. This cost, unlike electrolyser CAPEX and LCOE, is less likely to decrease. The technology is very mature and close to theoretical

maximum efficiency, therefore costs are only likely to fall from increased production (Figures 1.29 and 1.30). The scope for cost reduction for islanded production is tied to electrolyser CAPEX and VRE LCOE / or the management of the process' flexibility requirement. Connection to a dispatchable power supply would mitigate the costs attributable to the power source not being 'ideal' (Figure 5.38). Optimising the amount of energy from the dispatchable power supply would determine the achievable LCOA and how close this would be to the 'ideal' LCOA.

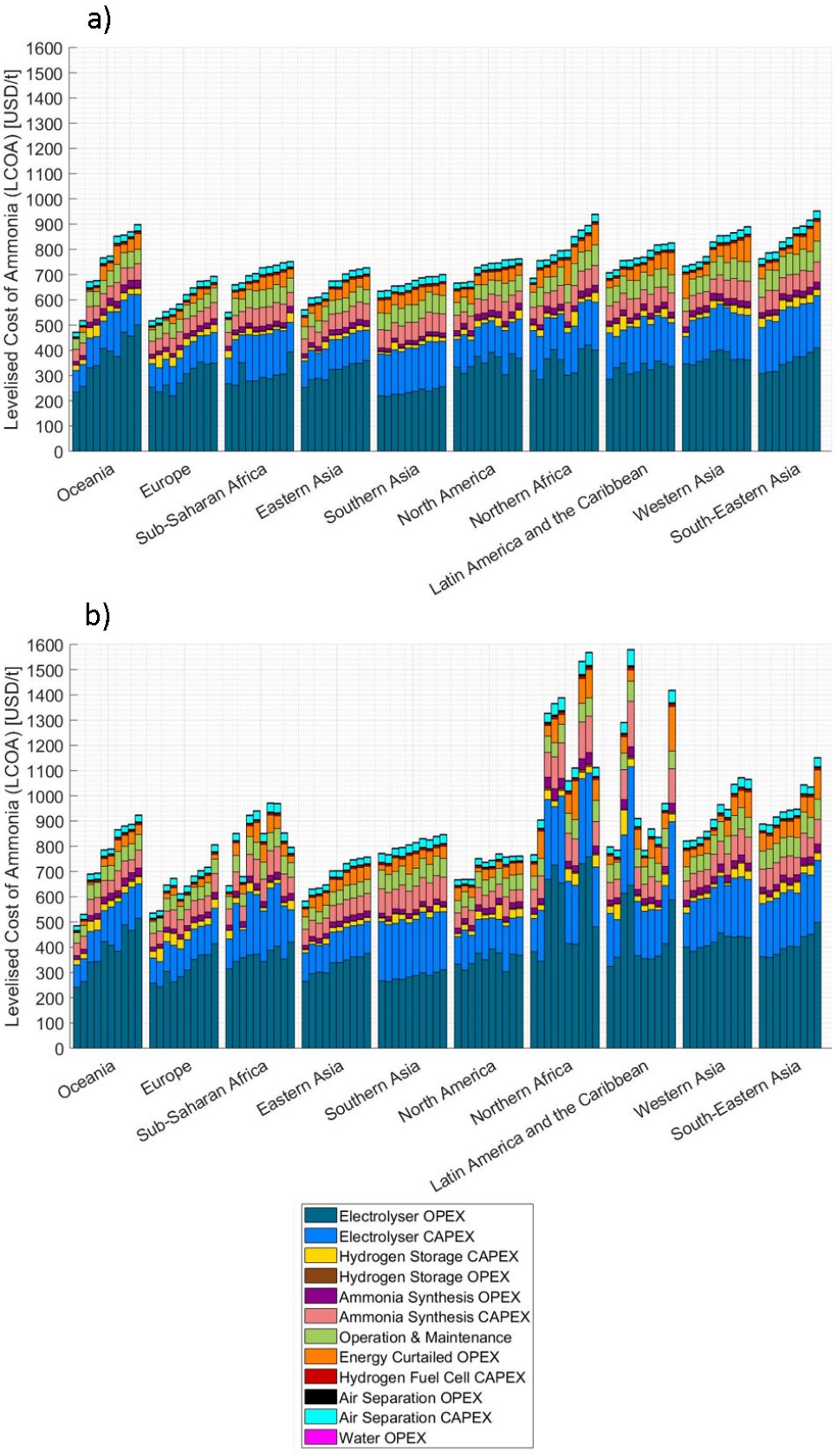

Figure 5.39: The components of the LCOA in 2019 for the 10 locations with the lowest LCOA estimates for a multi-national by region: (a) for multi-national corporation and (b) for domestic corporation.

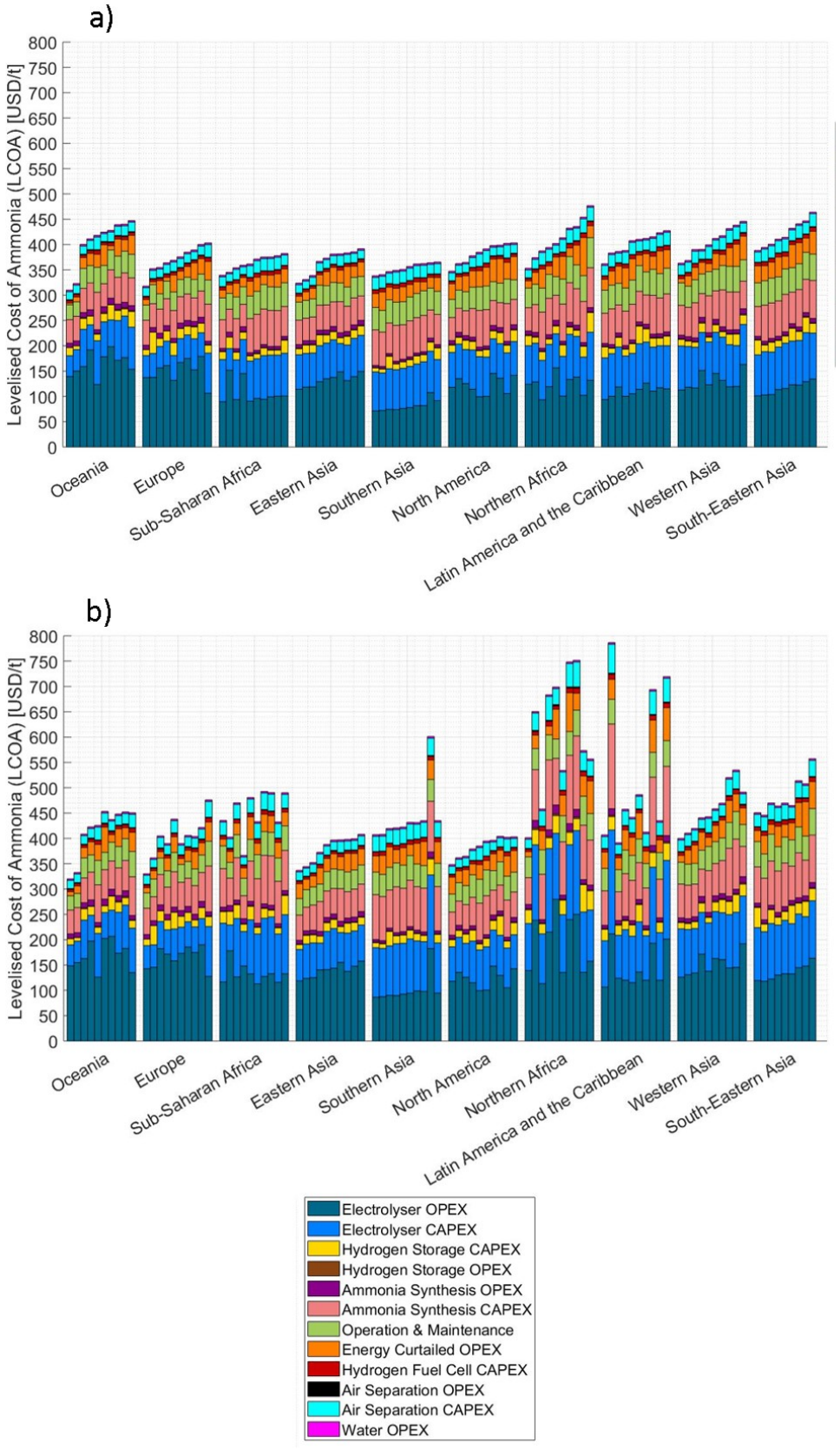

Figure 5.40: The components of the LCOA in 2030 for the 10 locations with the lowest LCOA estimates for a multi-national by region: (a) for multi-national corporation and (b) for domestic corporation.

Chapter 6

Discussion

This chapter shows that the research objectives have been met, highlights the contribution of this work and discusses the main findings in the context of decarbonising the power sector and ammonia production.

6.1 Overview of Environmental and Technical Context

To prevent the indefinite rise of global average temperature, and the significant impact that global warming has, the net-zero emission of greenhouse gases must be achieved. This must be attained by 2055 at the latest if the global average temperature is to remain below the 2°C target set in the Paris Agreement. Current policies and pledges are not consistent with the required pathway to achieve this target. The Kaya identity [18, 19] shows that the energy intensity of GDP and carbon intensity of energy need to improve. To achieve the latter of these, focus should be placed on decarbonising those sectors largely responsible for emissions and with potential for abatement. Using these criteria the power and industry sectors were selected for investigation using VRE integration.

Technically the use of variable renewable sources (e.g. wind or solar PV) beyond a

small proportion of total energy is difficult and requires network or process flexibility. In power networks there are many technical solutions to mitigate or manage the difficulties: DSM, interconnection, reserve capacity, curtailment or energy storage. Economic optimisation determine which is the best combination of these solutions for a specific VRE penetration or how to integrate best VRE. The latter is difficult. A mix of energy storage methods (i.e. short, medium and long-term duration) is a promising method. However, few technological options exist for long-term storage. Chemical electrical energy storage has potential but it is unclear currently which chemical/s will be used. Ammonia is one of the most promising, due to its highly favourable chemical and technical characteristics. Its production using VRE would not only provide long-term electrical energy storage, but also decarbonise an industry that global food production relies on (for use in nitrogen based fertilisers) and that represents a significant proportion of the industry sector's emissions.

6.2 Restatement of Research Objectives

In this context, the first research objective was to develop a tool to quantify an electrical network's flexibility requirement in terms of the amount and duration of energy storage required. Secondly, to use this tool to identify the impact that location, the renewables penetration and the mix of sources have on the energy storage requirement. The third objective was to develop a tool that using available VRE data could identify the optimal design and operation of an islanded 'green' ammonia production process. The fourth objective was to use this model to identify the range of achievable LCOA for islanded 'green' production, the dominant cost components, the scope and likelihood of future LCOA reduction and to benchmark this against conventional production. The final objective was to identify the economic viability of using 'green' ammonia to meet seasonal balancing requirements.

6.3 Contribution

6.3.1 Energy Storage Requirement Modelling Tool (ESRMT)

Modelling Tool

The Energy Storage Requirement Modelling Tool (ESRMT), developed in MATLAB, achieves the first objective. Using energy demand profiles and available VRE resource at a location, the ESRMT quantifies the required storage: the amount of energy stored, how long the energy is stored for and the storage size required for any given range of storage duration. Two non-dimension normalised indices, the storage magnitude index (SMI), and the storage duration index (SDI), identify the impact of the key variables, VRE penetration and the mix of VRE sources, on these requirements.

Results

The ESRMT shows how the energy storage requirements vary with VRE penetration and the mix of VRE sources at multiple locations in Japan, the UK, Canada and Australia. The results show that magnitude of storage required with a solar dominated VRE supply as VRE penetration increases is highly predictable, has notable dependence on diurnal and seasonal storage and varies little with location. However, as θ increases from 0 towards 1 (i.e. energy from wind sources becoming a larger proportion of the VRE provided) the magnitude of storage required varies considerably by location. At locations with high wind resource (i.e. a high capacity factor) the magnitude of storage required is largely mitigated as more wind is introduced (i.e. $\theta \to 1$). For those locations with poor wind resource, introducing wind exacerbates the storage problem. Regardless of the resource, the introduction of wind changes the duration of storage required by replacing the diurnal storage requirement with medium-term 1 day $\leqslant \tau <$ 1 month storage.

The ESRMT identified the effectiveness of supplying excess energy to mitigate these storage requirements (duration, use and size). The results showed that it was most

effective at lower VRE penetration for all locations. There was minimal seasonal storage requirement mitigation for a solar dominated supply, even with up to 50% excess energy. At other mixes of VRE supply the mitigation (for use and size of storage) was highly specific to location. At best it mitigated the storage requirement with $\tau > 1$ week. At others the long-term storage requirements could be mitigated but with increased shorter-term storage required. At worst, the excess energy had minimal impact. This therefore shows that for many locations the seasonal storage requirements cannot be easily mitigated.

6.3.2 Islanded Ammonia Production Modelling Tool (IAPMT)

Tool

The development of the islanded ammonia production modelling tool (IAPMT) in MATLAB achieves the third objective. Using the profiles for available VRE resource at specific locations the IAPMT optimises the mix of VRE sources, the sizing of the electrolyser, synthesis and ASU and their operation to minimise the LCOA. This shows the achievable LCOA and the plant design for any given location.

Results

The IAPMT models islanded ammonia production now and in a 2030 scenario for 534 locations in 70 countries provided the data to achieve the final objective. It also responds to the IEA challenge (as in [185]) to understand better which VRE sources to employ and the plant design for 'green' ammonia production. The range of LCOA achievable for these locations fell from $\$473t^{-1} - \$2,462t^{-1}$ in 2019 to $\$310t^{-1} - \$1,762^{-1}$ by 2030. Those locations dependent on solar resource fell the most, by up to $\$300t^{-1}$. It quantified the impact of the available VRE resource on the achievable LCOA and the plant design (to achieve the process flexibility required to manage the intermittent renewable energy supply). In 2019 solar dependent locations were more dependent on curtailed energy and required greater electrolyser over-sizing than wind dominated locations. Therefore solar dependent locations'

achievable LCOA were notably higher than wind dependent locations. However by 2030, the substantial fall in solar PV LCOE drove down the achievable LCOA substantially.

The components of the LCOA were identified and how they changed over time at the best locations was estimated. These results, production and 'ideal' energy profile analysis showed the scope for cost reduction. Decreasing electrolyser CAPEX and the VRE LCOE will be the main drivers of the lower LCOA for islanded electrolytic ammonia production. However, there is scope for grid connection (depending on its LCOE) to mitigate the costs of flexibility and drive the achievable LCOA towards the 'ideal' energy supply LCOA. Despite the additional operating cost that would be incurred using grid power, the reduction of the plant's flexibility requirements to manage the variability of VRE sources would lead to significant savings and therefore an even more competitive LCOA. This analysis showed, assuming fossil fuel feedstock (especially natural gas) prices remain relatively constant, decarbonised electrolytic production of ammonia will be competitive at the best locations by 2030. Further analysis of country specific financing showed the financial barriers to implementing green ammonia production at some of the best locations identified.

6.4 Discussion of Key Findings

6.4.1 Decarbonising the Power Sector

Decarbonisation of national power sectors is very important if the emission targets are to be met and and global warming key below the 2°C target. This is not only because it is commonly (with the exclusion of those countries with significant nuclear or hydroelectric capacity) a significant component of national GHG emissions, but also to enable the decarbonisation of the other key sectors through electrification. Effective policy design to meet VRE integration targets cost efficiently requires a good understanding of the problems that the incremental integration will bring. The ESRMT provides improved quantitative understanding of the problem. Using the

model to examine specific locations in detail provides stakeholders valuable insights to shape their key decisions. The ESRMT quantifies the how the requirement for energy storage changes with VRE penetration and the mix of VRE sources.

The potential future importance of the ESRMT's methodology, beyond providing stakeholders an improved understanding of the balancing problem, has been shown in the recent Helm Review for the UK Government [145]. The report advocates that "energy policy, regulation and market design are not fit for the purposes of the emerging low-carbon energy market, as it undergoes profound technical change", and that "the cost of energy is significantly higher than it needs to be to meet the government's objectives...,to be consistent with the Climate Change Act and to ensure security of supply". In other words, not only has the UK government in recent years managed the trilemma inefficiently with regards to cost, but the UK energy system is currently structured so that additional inefficiency in the face of more complex problems, due to decarbonisation, is all but guaranteed. It is therefore essential that any decision making process for selection and implementation of new renewable power capacity not only consider the tendered spot price but the short-, medium- and long-term implications on managing the trilemma. The system average cost (i.e. including management of the intermittency that those renewables bring to the current supply-demand balancing problem) in particular that would be passed through to the consumer needs to be considered as well as the network's ability to meet sustainability targets and maintain security of supply. Use of the ESRMT to consider any integration of new renewable power capacity would show the additional flexibility required. When costed this provides insight into the temporal aspect of the flexibility required not just its magnitude, as is the case with the commonly used capacity credit [186]. Not being informed of these requirements would effectively put decision makers in the "spurious" position of once again having to "pick winners" with imperfect information [70]. Potentially incurring singificant system costs in spite of the VREs having zero marginal cost.

The results from the ESRMT show that, despite the specific flexibility requirements

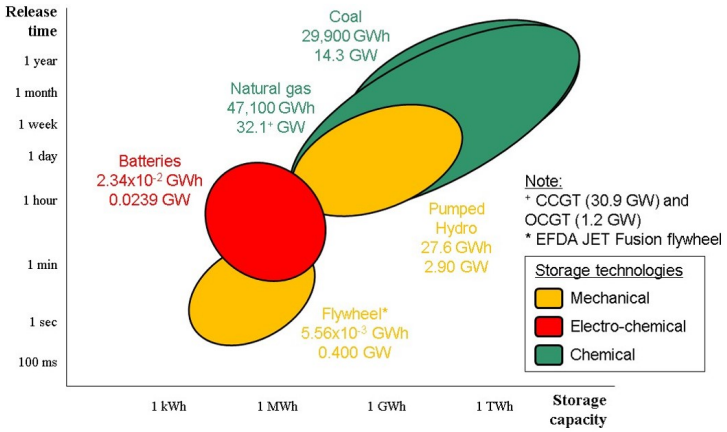

Figure 6.1: UK's current electrical energy storage capacity

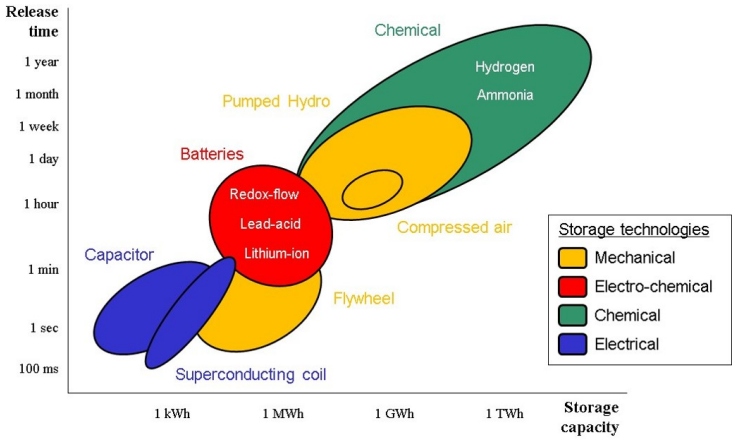

Figure 6.2: Current electrical energy storage technologies, where storage capacity is per installation

of each location being different, as VRE penetration increases there is a need for medium and long-term electrical energy storage. While this can be partially mitigated by the perfectly informed allocation of excess dispatchable energy, there is still significant requirement. At present the majority of energy storage is thought of as pumped hydroelectric (contributing to over 99% of global energy storage). However, as noted by Wilson, I.A.G. [66] this is somewhat of a fallacy. Taking the UK as an example, if instead of looking at the dominant methods used to store electricity all methods to store energy prior its use as electricity are considered (Figure 6.1), it is clear that the UK network's adequacy and diurnal balancing is met by fossil fuels (i.e. chemical energy storage). The only electrical energy storage methods that could replace this high energy capacity and long storage duration (Figure 6.2)

are also chemical (i.e. P2X: hydrogen, synthetic-methane, ammonia, etc.). Of the options available, ammonia is a favourable option due to its chemical and technical characteristics (Figure 6.3). The results from the IAPMT show that at the best locations islanded green ammonia production will be economically competitive with conventional production methods by 2030 without incentives. This therefore opens the possibility of additional production (at minimal additional cost due to the size of the production plant) to meet the seasonal electrical energy storage needs.

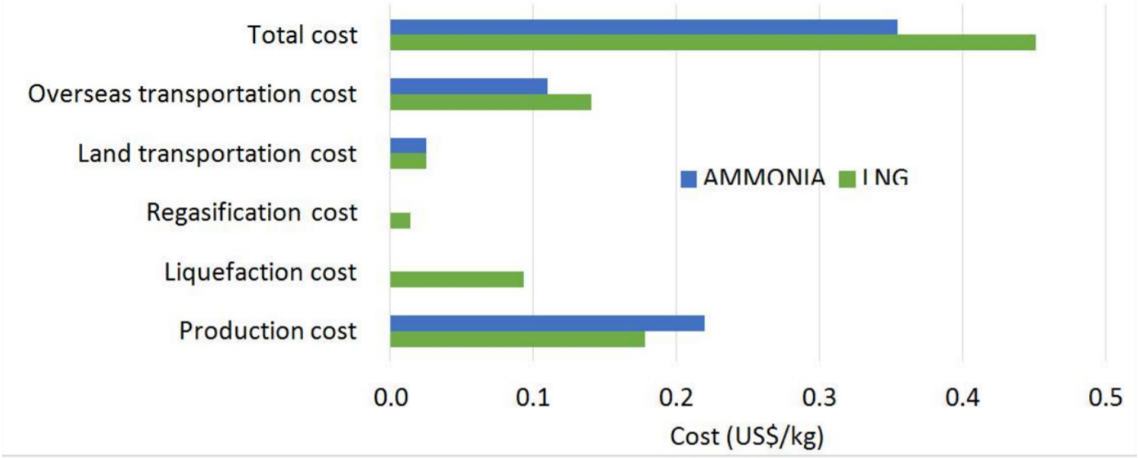

Figure 6.3: "Contribution of sub-processes to total cost of LNG and ammonia... in the US" [187]

Power-to-ammonia ($P2NH_3$) is a good prospect for meeting medium- to long-term energy storage requirements, but is it economically viable (research objective 4)? The results from the global analysis using the IAPMT (Section 5.2) show that islanded electrolytic production for many locations will drop below $\$350t^{-1}$ by 2030. Using the LCOA estimates from the global analysis, Equation 6.1 and assuming that the costs of power-to-ammonia are independent of location (Table 6.1) enables calculation of the LCOE for electrolytically produced ammonia. The capital components of this system would be the storage of ammonia and its combustion in a gas turbine. The operational components would be the cost of the ammonia fuel (taken as the LCOA calculated previously) and operation & maintenance costs. This analysis shows that current production at the best location, with LCOA of $\$453t^{-1}$ is currently able to achieve an LCOE of $\$357MWh^{-1}$. Uncompetitive against gas peaker plants at $\$152$-$206MWh^{-1}$ [188]. However by 2030, driven by the LCOA of

$\$310t^{-1}$, this will improve to $\$252MWh^{-1}$ before any technological improvements have been taken into account. This LCOE would therefore require a carbon tax of $\$90.01t^{-1}$ of CO_2 or the number of uses per year to increase to be competitive with gas peaker plants.

$$LCOE = \frac{\sum_{t=1}^{T} \frac{CAPEX_t + OPEX_t}{(1+r)^t}}{\sum_{t=1}^{T} \frac{Energy_t}{(1+r)^t}} \tag{6.1}$$

Variable	Value	Reference
Ammonia Storage CAPEX	$\$1{,}032t^{-1}$	[137, 158]
Gas turbine CAPEX	$\$565kW^{-1}$ of P_{rated}	[189, 190]
Operation and maintenance of all components	2% CAPEX per year	
Ammonia-to-power energy per kg	29.7% of LHV	[93]
Operations per year	4	
Years of operation	25	[189]
Discount factor	7.14%	[169]

Table 6.1: Location independent technical and economic ammonia-to-power assumptions in the IAPMT [142].

6.4.2 Decarbonising Ammonia Production

In addition to meeting the seasonal electrical energy storage requirement, electrolytic ammonia production (i.e. decarbonised ammonia production) is itself an environmental imperative. Current production accounts for 1.8% of global fossil fuel consumption [87], supports 48% of the world's population [86] and has no substitutes. If current production methods were still used in 2050, ammonia production emissions would likely exceed 630Mt per year CO_2.

The results from the IAPMT show that islanded electrolytic production in the most favourable locations will be competitive with conventional methods by 2030 (assuming the price of gas remains at current levels). These findings and its potential use for medium and long-term energy storage means that action by stakeholders

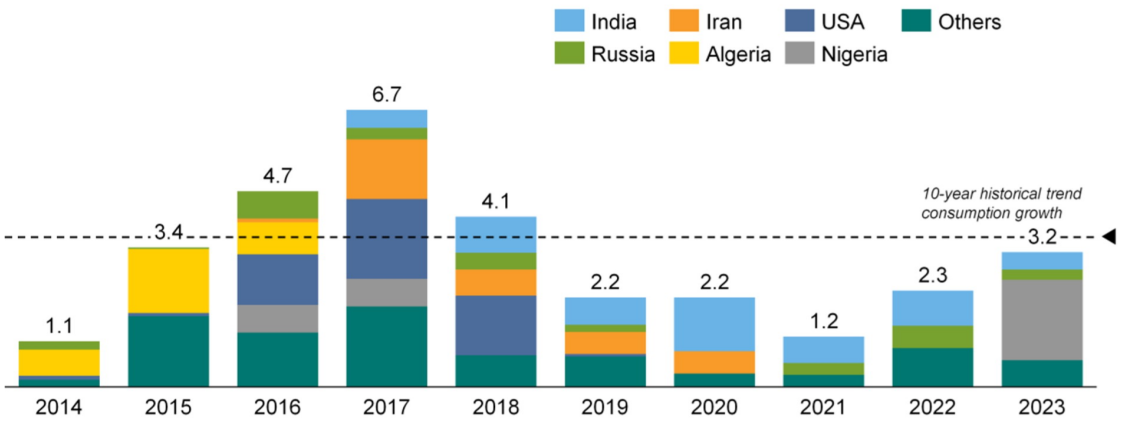

Figure 6.4: "Global urea capacity additions excluding China [million tonnes]" [85].

to incentivise its development, scale-up and large scale implementation are essential and prudent. The considerable additional capacity for nitrogen based fertiliser production that will be added before 2023 makes this even more significant (Figure 6.4). The size of these plants, their long lifetime and the magnitude of their GHG emissions means that the type of production plant chosen for each of these investments has considerable impact on CO_2 emissions from this sector for the foreseeable future.

Identified by Yara as one of the five key markets for fertilisers, a key example is India. It currently consumes 17.4Mt of nitrogen based fertilisers p.a., met by: importing 16% and 23% of India's total ammonia and urea stock; importing natural gas feedstock to support indigenous production; and setting the maximum retail price of urea (currently at INR5,360t^{-1} / \$74.49t^{-1} resulting in INR349.9B / \$4.87B and INR133.6B / \$1.86B budgeted in 2018-19 for indigenous production and imports respectively [191]). The improvement of security of supply by capitalising on the excellent solar resources using a green ammonia production process rather than focusing on coal gasification [96, 192] will not only be significantly more sustainable but also more economical (depending on date of implementation and coal subsidies).

The implementation of a carbon-tax to improve its cost competitiveness of electrolytic ammonia production would be highly impactful particularly against inefficient SMR, coal fed or naphtha fed production. Setting a tax of \$50t^{-1} CO_2 (reason-

able in the context of existing taxes / prices [193]), the production using SMR, coal and fuel oil would have to achieve LCOA of $\$210t^{-1}$, $\$140t^{-1}$ and $\$100t^{-1}$ respectively by 2030 to compete with the best decarbonised islanded production estimate [142]. How to implement and set a carbon price however is another problem entirely. Helm [4] illustrates the "general policy recommendation" to "fix the quantity when the slope of the damage function is steep relative to that of the cost function; fix the price when the cost function is steep relative to the damage function". With the target of 2°C warming it is likely that, as in the electricity sector [146], the "capital stock" for conventional fossil fuel based production has already been exceeded. The combination of these two concepts and assumption that the gradient of the damage function beyond 2°C warming exceeds the gradient of the cost function, then only decarbonised production can be newly installed.

6.4.3 Obtainable Synergies

Accelerating the implementation of decarbonised ammonia production to achieve the required rapid reduction in net-CO_2 emissions is important. Production for conventional consumption (e.g. fertilisers) will remain dominant. The additional revenue obtainable from its use to store electrical energy can increase the rate of return on such projects due to multiple revenue streams and reduced financing costs (due to a reduction in risk). The stacking of these revenues would facilitate implementation sooner.

There is significant potential for bi-directional synergies to be obtained. The power sector can gain medium to long-term energy storage capacity from the use of $P2NH_3$. The achievable LCOA for electrolytic production can be reduced by mitigating the costs attributed to plant flexibility with the use of a dispatchable power source (Section 5.2.2). With the "deployment of renewable solutions in energy consuming sectors, particularly buildings and industry, ...still well below the levels needed" [27], the dual use of 'green' ammonia production make it a highly promising option for further R&D and investment / subsidies. It is one of the most promising processes

to achieve the estimated payoff of $3 to $7 for every $1 spent in the energy transition [27].

In addition to substituting conventional production and meeting seasonal electrical energy storage needs, 'green' ammonia also has the potential for use in transport as an environmentally friendly substitute for gasoline [187]. This would be at an even greater price to being sold as a commodity and for seasonal energy storage. This revenue stacking would further increase the viability of the process. It has been a viable fuel since the outset of the combustion engine and one of the initial fuels considered. Due to the lower cost and availability of gasoline it did not win this competition, but in recent years has been used as a fuel additive (e.g. Ad-Blue [194]).

Chapter 7

Conclusion

This chapter highlights the key findings from this research, its limitations and future work.

7.1 Key Findings

In conclusion, this thesis shows that 'green' ammonia production in the best locations will be competitive against conventional methods by 2030 and a cost efficient method for medium to long-term electrical energy storage. This will facilitate the decarbonisation of ammonia production while also supporting the increased penetration of VRE sources to decarbonise the power sector.

Furthermore, the research presented here has demonstrated the validity of the three thesis hypotheses (Section 1.1.1):

1. The magnitude and duration of energy storage required when integrating VRE supply in an electrical network are quantifiable using the ESRMT. The storage profile determined by the ESRMT provides a detailed understanding of the balancing problem that requires management. Calculation of the SMI, SDI and storage sizes required enable the identification of the impact that VRE penetration and the mix of VRE sources have on the storage requirements, as

well as how effective other flexibility methods (such as excess energy) are in mitigating these. Consideration of locations in four countries showed that at high VRE penetration seasonal energy storage is required that is not easily mitigated. This requirement changes with the mix of VRE sources but even locations with world-class VRE resources still require network flexibility. This work improves the understanding of flexibility required for the integration of VRE sources and particularly the mix of energy storage technologies that will be required [65].

2. Decarbonising ammonia production is an environmental imperative as it supports 48% of the population's food supply and produces considerable emissions. The IAPMT enables the potential of any location to be considered for islanded ammonia production. The LCOA achievable determined along with the optimised mix of VRE sources, plant design and operation schedule. The use of the IAPMT to consider production at 534 locations in 70 countries has enabled the potential for 'green' ammonia and the impact of location to be determined. Currently the best location is able to achieve an LCOA of $\$473 t^{-1}$ but by 2030 this is predicted to fall to $\$310 t^{-1}$. At present, the best locations for production are those with excellent wind resource. However, the predicted fall in the LCOE of solar PV will result in locations with favourable solar resource becoming competitive by 2030. The principal cost at present is the production of hydrogen but with falling costs this is likely to diminish by 2030. The cost of the process flexibility required (i.e. the curtailment and the hydrogen buffer) to manage the intermittency of the VRE sources is, and will remain, a notable component of the LCOA for islanded production. Consideration of domestic financing has identified that even for some of the best locations, financial barriers exist that need to be overcome.

3. The predicted reduction in LCOA by 2030 will make 'green' ammonia an economically viable method for medium- and long-term electrical storage. This will be able to meet the requirements of the power sector as VRE penetration

increases. By 2030 ammonia is predicted to have an LCOE of \$257MWh^{-1} if it is used as a fuel in a gas turbine four times a year \$206MWh^{-1}. There are considerable bi-directional synergies that can be achieved through the production and use 'green' ammonia. The power sector is provided with a cost efficient method of long-term electrical energy storage to facilitate its required decarbonisation through increased VRE penetration. The LCOA of the ammonia production would decrease as the dispatchable energy from the grid would mitigate the costs of process flexibility.

7.2 Critical Review

This thesis has achieved the research objectives and thereby filled gaps identified in the knowledge base. However, it has limitations. These have been separated by the model they are specific to and whether they refer to the methodology or the calculations conducted.

7.2.1 Energy Storage Requirement Modelling Tool (ESRMT)

Methodology

The main areas for development of the ESRMT involve challenging its current assumptions. Specifically, that the ESRMT has perfect foresight of supply and demand, that the energy storage is perfect (i.e. lossless) and that the dispatchable energy can ramp instantaneously and doesn't have a capacity limit.

Relaxing the assumption of perfect foresight would require the application of either preventative or reactionary control to manage the uncertainty. Either of these would result in a larger amount of energy being stored and provide a more accurate result of the storage requirement. The results presented in this thesis are therefore an underestimate of the amount of storage required. The two other assumptions have been deliberately implemented to ensure that the calculation of the SMI and SDI has not been technology specific. Relaxing these assumptions would similarly require

greater storage but also prior definition of technical specifications such as the storage losses, rated power of the dispatchable source and its ramping capability.

The other limits of the ESRMT are its current scale of applicability and that only excess energy provision has been considered to mitigate the storage requirement. At present the ESRMT can be used to consider micro-grids or those power networks with close to perfect interconnection. Therefore, if a user is willing to assume perfect interconnection the ESRMT can be used to identify the energy storage requirements of large / national networks.

7.2.2 Islanded Ammonia Production Modelling Tool (IAPMT)

Methodology

The IAPMT currently also assumes perfect foresight. However, due to the current assumption that the electrolyser is perfectly responsive, relaxing this on its own would have little to no affect. Ramping limitations could be considered for the synthesis and ASU components but as the initial analysis showed (Section 4.2.1), this would likely have little impact on the LCOA unless it was particularly slow (less than 5% of rated power per hour). Even if it was significant, the problem could be avoided through re-circulation of the purge at times of low power as proposed by Rossi [195].

More significantly, the specific energy consumption of the processes are all constant in steady-state operation. Adaptation of this to use non-linear specific energy consumption and dynamic analysis would provide additional insights.

Calculations

Despite considering 534 locations in 70 countries it cannot be said that the best locations globally have been identified. These locations were considered because of their geographic spread but also due to the reliability of the available data. Additional data should be gathered and used with the IAPMT to provide an improved under-

standing of the best locations available. For example, when considering Morocco, a country with some of the lowest solar PV LCOE estimates, only one location could be considered.

7.3 Future Work

The future work proposed building on this thesis can be separated into three sections:

7.3.1 Development of the ESRMT

Incorporation of technical limits on the dispatchable energy and the predictability of supply and demand will further improve the reliability of the model. Their addition as decision variables would enable their impact on the storage requirement to be quantified. For example, the definition of the rated power of the dispatchable supply would limit the amount of energy that could be allocated in any given time interval to mitigate the storage required. This would be particularly useful in analysing the problems that networks with conventional power generators will face over the next 5/10 years as VRE penetration increases.

To date, the use of the ESRMT has only considered the use of excess energy provision to mitigate the storage requirements. The independent and combined impact of other flexibility methods such as DSM and interconnection should be incorporated. While the implementation of DSM would likely only mitigate the short-term storage currently identified, the functionality required to consider the impact of interconnection would enable the scale of the ESRMT's applicability to increase.

Finally, the impact of additional demand such as heat and / or transport electrification is of notable significance to investigate. This would not only show the additional difficulties that would have to be managed but also the applicability of flexibility methods to mitigate them.

7.3.2 Development and Use of the IAPMT

Development of the IAPMT to incorporate non-linearity into the specific energy consumption, formal optimisation of the power allocation while retaining its computational speed would be valuable. Its subsequent use would provide many useful insights. Consideration of production across the globe would identify the best locations available.

This work could be developed by incorporating semi-islanded operation and the introduction of other available VRE sources (i.e. tidal or hydroelectric). This would reduce the achievable LCOA and further refine the best locations for 'green' ammonia production. Having identified locations of specific interest, location specific analysis is required in the context of the water-energy nexus to ensure the applicability of the plant design and operation.

7.3.3 Use of Both Modelling Tools for More Applied Investigations

Understanding better the economic viability of using ammonia for long term energy storage requires detailed techno-economic optimisation of the power network. This research has identified the need for seasonal energy storage as VRE penetration increases and ammonia's ability to meet this need. Future analyses should consider both local ammonia production (with the bi-directional synergies obtainable) and the import of ammonia from locations with lower LCOA estimates.

An equivalent analysis that would also be of significant value would be the consideration of ammonia for zero-emission commercial shipping. The results of the more detailed global study of ammonia production (Section 7.3.2), combined with predicted shipping demand would enable the study of how to decarbonise this sector.

Bibliography

[1] P. Denholm and M. Hand. Grid flexibility and storage required to achieve very high penetration of variable renewable electricity. *Energy Policy*, 39(3):1817–1830, 2011.

[2] IRENA. Planning for the renewable future: Long-term modelling and tools to expand variable renewable power in emerging economies. Report, International Renewable Energy Agency (IRENA), 2017.

[3] D.J.C. MacKay. *Renewable energy - Without the hot air*. UIT Cambridge Ltd., 2008.

[4] D. Helm. *The Carbon Crunch*. Yale University Press, New Haven, revised and updated edition, 2015.

[5] IPCC. Climate change 2014: Mitigation of climate change. contribution of working group iii to the fifth assessment report of the intergovernmental panel on climate change. Report, Intergovernmental Panel on Climate Change (IPCC), 2014.

[6] IPCC. An ipcc special report on the impacts of global warming of 1.5c above pre-industrial levels and related global greenhouse gas emission pathways, in the context of strengthening the global response to the threat of climate change, sustainable development, and efforts to eradicate poverty. Report, Intergovernmental Panel on Climate Change (IPCC), 2018.

[7] J.H. Butler. *Carbon Dioxide at NOAA's Mauna Loa Observatory reaches new milestone: Tops 400 ppm*, 2019 (accessed September 25, 2019). `https://www.esrl.noaa.gov/gmd/news/7074.html`.

[8] D. Lüthi, M. Le Floch, B. Bereiter, T. Blunier, J. M. Barnola, U. Siegenthaler, D. Raynaud, J. Jouzel, H. Fischer, K. Kawamura, and T.F. Stocker. High-resolution carbon dioxide concentration record 650,000–800,000 •years before present. *Nature*, 453(7193):379–382, 2008.

[9] R. Lindsey. *Climate Change: Atmospheric Carbon Dioxide.*, 2019 (accessed September 25, 2019). `https://www.climate.gov/news-features/understanding-climate/climate-change-atmospheric-carbon-dioxide`.

[10] J. Rogelj, G. Luderer, R. C. Pietzcker, E. Kriegler, M. Schaeffer, V. Krey, and K. Riahi. Energy system transformations for limiting end-of-century warming to below 1.5 c. *Nature Climate Change*, 5(6):519–527, 2015.

[11] Richard J. Millar, Jan S. Fuglestvedt, Pierre Friedlingstein, Joeri Rogelj, Michael J. Grubb, H. Damon Matthews, Ragnhild B. Skeie, Piers M. Forster, David J. Frame, and Myles R. Allen. Emission budgets and pathways consistent with limiting warming to 1.5• c. *Nature Geoscience*, 10:741, 2017.

[12] V. Krey and K. Riahi. Implications of delayed participation and technology failure for the feasibility, costs, and likelihood of staying below temperature targets—greenhouse gas mitigation scenarios for the 21st century. *Energy Economics*, 31(Supp.):S94–S106, 2009.

[13] V. Bosetti, C. Carraro, and M. Tavoni. Climate change mitigation strategies in fast-growing countries: The benefits of early action. *Energy Economics*, 31:S144–S151, 2009.

[14] Climate Action Tracker. Cat september 2019 update, 6th October.

[15] N.H. Stern. *A Blueprint for a Safer Planet : How to Manage Climate Change and Create a New Era of Progress and Prosperity*. Bodley Head, London, 2009.

[16] C. Le Quéré, R. M. Andrew, P. Friedlingstein, S. Sitch, J. Hauck, J. Pongratz, P. A. Pickers, J. I. Korsbakken, G. P. Peters, J. G. Canadell, A. Arneth, V. K. Arora, L. Barbero, A. Bastos, L. Bopp, F. Chevallier, L. P. Chini, P. Ciais, S. C. Doney, T. Gkritzalis, D. S. Goll, I. Harris, V. Haverd, F. M. Hoffman, M. Hoppema, R. A. Houghton, G. Hurtt, T. Ilyina, A. K. Jain, T. Johannessen, C. D. Jones, E. Kato, R. F. Keeling, K. K. Goldewijk, P. Landschützer, N. Lefèvre, S. Lienert, Z. Liu, D. Lombardozzi, N. Metzl, D. R. Munro, J. E. M. S. Nabel, S. I. Nakaoka, C. Neill, A. Olsen, T. Ono, P. Patra, A. Peregon, W. Peters, P. Peylin, B. Pfeil, D. Pierrot, B. Poulter, G. Rehder, L. Resplandy, E. Robertson, M. Rocher, C. Rödenbeck, U. Schuster, J. Schwinger, R. Séférian, I. Skjelvan, T. Steinhoff, A. Sutton, P. P. Tans, H. Tian, B. Tilbrook, F. N. Tubiello, I. T. van der Laan-Luijkx, G. R. van der Werf, N. Viovy, A. P. Walker, A. J. Wiltshire, R. Wright, S. Zaehle, and B. Zheng. Global carbon budget 2018. *Earth Syst. Sci. Data*, 10(4):2141–2194, 2018.

[17] World Bank. *World DataBank*, 2016 (accessed September 20, 2019). `http://databank.worldbank.org/data/home.aspx`.

[18] Y. Kaya. Impact of carbon dioxide emission control on gnp growth: interpretation of proposed scenarios. *Intergovernmental Panel on Climate Change/Response Strategies Working Group, May*, 1989.

[19] M.R. Raupach, G. Marland, P. Ciais, C. Le Quéré, J.G. Canadell, G. Klepper, and C.B. Field. Global and regional drivers of accelerating co2 emissions. *Proceedings of the National Academy of Sciences*, 104(24):10288, 2007.

[20] M. Roser, H. Ritchie, and E. Ortiz-Ospina. *World Population Growth*, 2019 (accessed September 20, 2019). `https://ourworldindata.org/world-population-growth`.

[21] M. Roser. *Economic Growth*, 2019 (accessed September 20, 2019). `https://ourworldindata.org/economic-growth`.

[22] H. Ritchie and M. Roser. *Energy Production and Changing Energy Sources*, 2019 (accessed September 20, 2019). https://ourworldindata.org/energy-production-and-changing-energy-sources.

[23] H. Ritchie and M. Roser. *CO2 and Greenhouse Gas Emissions*, 2019 (accessed September 20, 2019). https://ourworldindata.org/co2-and-other-greenhouse-gas-emissions#cumulative-co2-emissions.

[24] International Energy Agency (IEA). *Global Energy and CO2 Status Report 2019*, 2019 (accessed September 20, 2019). https://www.iea.org/geco/.

[25] C. Goodall. *The Switch: How Solar, Storage and New Tech Means Cheap Power for All*. Profile Books, London, UK, 2016.

[26] IRENA. Global energy transformation: A roadmap to 2050 (2019 edition). Report, International Renewable Energy Agency, 2019.

[27] IRENA. Renewable power generation costs in 2018. Report, International Renewable Energy Agency, 2018.

[28] J. Ambrose. *New windfarms will not cost billpayers after subsidies hit record low*, 2019 (accessed September 20, 2019). https://www.theguardian.com/environment/2019/sep/20/new-windfarms-taxpayers-subsidies-record-low.

[29] T. Naucler and P-A. Enkvist. Pathways to a low-carbon economy: Version 2 of the global greenhouse gas abatement cost curve. *McKinsey and Company*, 192, 2009.

[30] B.W. Griscom, J. Adams, P.W. Ellis, R.A. Houghton, G. Lomax, D.A. Miteva, W.H. Schlesinger, D. Shoch, J.V. Siikamäki, P. Smith, P. Woodbury, C. Zganjar, A. Blackman, J. Campari, R.T. Conant, C. Delgado, P. Elias, T. Gopalakrishna, M.R. Hamsik, M. Herrero, J. Kiesecker, E. Landis, L. Laestadius, S.M. Leavitt, S. Minnemeyer, S. Polasky, P. Potapov, F.E. Putz, J. Sanderman,

M. Silvius, E. Wollenberg, and J. Fargione. Natural climate solutions. *Proceedings of the National Academy of Sciences*, 114(44):11645–11650, 2017.

[31] D. O'Driscoll. Carbon abatement potential of reforestation. Report, University of Manchester, 2018.

[32] IRENA. Hydrogen from renewable power: Technology outlook for the energy transition. Report 978-92-9260-077-8, IRENA, September 2018.

[33] ETC. Better energy, greater prosperity. Report, Energy Transitions Commission (ETC), 2017.

[34] I.A.G. Wilson, A.J.R. Rennie, and P.J. Hall. Great britain's energy vectors and transmission level energy storage. *Energy Procedia*, 62(Supplement C):619–628, 2014.

[35] I.A.G. Wilson. *Enery-charts dot org: Charting Great Britain's Energy Transition*, 2019 (accessed September 20, 2019). `http://energy-charts.org/`.

[36] T. Brown, A. Gambhir, N. Florin, and P. Fennell. Reducing co2 emissions from heavy industry: a review of technologies and considerations for policy makers. Report, Grantham Institute for Climate Change, Imperial College, 2012.

[37] M. Laughton. *Variable renewables and the Grid: An overview*, book section 1, pages 1–30. Earthscan Publications Ltd., London, UK, 2007.

[38] P. Massara. The energy future - disruption and data. In *Oxford Energy Colloquia*, 2015.

[39] D. Milborrow. *Wind power on the grid*, book section 2, pages 31–54. Earthscan Publications Ltd., London, UK, 2007.

[40] IEC. Grid integration of large-capacity renewable energy sources and use of large-capacity electrical energy storage. Report IEC WP RE-EES:2012-10(en), International Electrotechnical Commission, 2012.

[41] Climate Policy Initiative. Low-cost, low-carbon power systems: How to develop competitive renewablebased power systems through flexibility. Report, Climate Policy Initiative, 2017.

[42] R.A. Walling, V. Banunarayanan, A. Chahal, L. Freeman, Martinez. J., N. Miller, D. Van Zandt, and M. Walling. Analysis of wind generation impact on ercot ancilliary services requirements. Report, General Electric Energy, 28th March 2008.

[43] M.R. Milligan and B. Kirby. *Calculating wind integration costs: separating wind energy value from integration cost impacts.* National Renewable Energy Laboratory Golden, 2009.

[44] International Energy Agency (IEA). World energy outlook 2018. Report 9789264306776, IEA, 13 November 2018.

[45] POST. Intermittent electricity generation. Press release, The Parliamentary Office of Science and Technology, May 2014.

[46] W. Katzenstein and J. Apt. The cost of wind power variability. *Energy Policy*, 51:233–243, 2012.

[47] International Energy Agency (IEA). *Atlas of Energy*, 2019 (accessed September 20, 2019). `http://energyatlas.iea.org/#!/tellmap/-1118783123/3`.

[48] P. Denholm, E. Ela, B. Kirby, and M. Milligan. The role of energy storage with renewable energy generation. Report NREL/TP-6A2-47187, National Renewable Energy Laboratory (NREL), January 2010.

[49] J.L. Ramírez-Mendiola, P. Grünewald, and N. Eyre. The diversity of residential electricity demand – a comparative analysis of metered and simulated data. *Energy and Buildings*, 2017.

[50] P. Grunewald, M. Diakonova, D. Zilli, J. Bernard, and A. Matousek. What we do matters – a time-use app to capture energy relevant activities. *Energy and Buildings*, (161):63–71., 2017.

[51] CAISO. *What the duck curve tells us about managing a green grid*, 2019 (accessed September 20, 2019). https://www.caiso.com/Documents/FlexibleResourcesHelpRenewables_FastFacts.pdf.

[52] H.L. Ferreira, R. Garde, G. Fulli, W. Kling, and J.P. Lopes. Characterisation of electrical energy storage technologies. *Energy*, 53:288–298, 2013.

[53] O. Palizban and K. Kauhaniemi. Energy storage systems in modern grids—matrix of technologies and applications. *Journal of Energy Storage*, 6:248–259, 2016.

[54] M. Beaudin, H. Zareipour, A. Schellenberglabe, and W. Rosehart. Energy storage for mitigating the variability of renewable electricity sources: An updated review. *Energy for Sustainable Development*, 14(4):302–314, 2010.

[55] IEC. Electrical energy storage white paper. Report IEC WP EES:2011-12(en), International Electrotechnical Commission, 2011.

[56] N. Stern. Towards a low-carbon future. In *Resource Conference 2017*, 2017.

[57] D. Connolly, H. Lund, B.V. Mathiesen, and M. Leahy. A review of computer tools for analysing the integration of renewable energy into various energy systems. *Applied Energy*, 87(4):1059–1082, 2010.

[58] H2RES. *H2RES Model*, 2019 (accessed September 20, 2019). http://www.powerlab.fsb.hr/h2RES/.

[59] HOMER Energy LLC. *HOMER*, 2019 (accessed September 20, 2019). http://www.homerenergy.com/.

[60] University of Wisconsin-Madison. *A TRaNsient SYstem Simulation program*, 2019 (accessed September 20, 2019). http://www.trnsys.com/.

[61] R. C. Pietzcker, F. Ueckerdt, S. Carrara, H. S. de Boer, J. Després, S. Fujimori, N. Johnson, A. Kitous, Y. Scholz, P. Sullivan, and G. Luderer. System integra-

tion of wind and solar power in integrated assessment models: A cross-model evaluation of new approaches. *Energy Economics*, 64:583–599, 2017.

[62] I. Hidalgo Gonzalez, P. Ruiz Casello, A. Sgobbi, W. Nijs, S. Quoilin, A. Zucker, and C. Thiel. Addressing flexibility in energy system models. Report JRC95354, European Commission: Joint Research Centre – Institute for Energy and Transport, 2015.

[63] D.G. Infield and S. Watson. *Planning for variability in the longer term: The challenge of a truely sustainable energy system.* Earthscan Publications Ltd., London, UK, 2007.

[64] H. Kondziella and T. Bruckner. Flexibility requirements of renewable energy based electricity systems – a review of research results and methodologies. *Renewable and Sustainable Energy Reviews*, 53(Supplement C):10–22, 2016.

[65] N.P. Brandon, J.S. Edge, M. Aunedi, E.R. Barbour, P.G. Bruce, B.K. Chakrabarti, T. Esterle, J.W. Somerville, Ding Y.L., C. Fu, P.S. Grant, P.J. Hall, C. Huang, G.H. Leng, Y.L. Li, V.L. Martins, M.E. Navarro, J. Posada, O. Gil, A.J.R. Rennie, D.J. Rogers, G. Srbac, S. Pérez Villar, V. Yufit, J. Wang, and D.A. Worsley. Uk research needs in grid scale energy storage technologies. Report, Energy SuperStore, 2016.

[66] I.A.G. Wilson, P.G. McGregor, and P.J. Hall. Energy storage in the uk electrical network: Estimation of the scale and review of technology options. *Energy Policy*, 38(8):4099–4106, 2010.

[67] T.U. Daim, X. Li, J. Kim, and S. Simms. Evaluation of energy storage technologies for integration with renewable electricity: Quantifying expert opinions. *Environmental Innovation and Societal Transitions*, 3:29–49, 2012.

[68] S. Few, A. Gambhir, G. Offer, J. Nelson, and N. Brandon. Energy storage for balancing intermittent renewables: Outlook for a range of technologies up to

2030, informed by expert elicitation and historical data. In *UK Energy Storage Conference 2015*, 2015.

[69] D. Swift-Hook and A.G. Ter-Gazarian. The value of storage on power systems with intermittent energy sources. *Renewable Energy*, 5(5-8):1479–1482, 1994.

[70] D. Helm. *Burn Out : The Endgame for Fossil Fuels.* Yale University Press, New Haven, 2017.

[71] M.C. Lott, S-I. Kim, and C. Tam. Technology roadmap: Energy storage. Report, International Energy Agency (IEA), 2014.

[72] NGET. Enhanced frequency response tender, 20th August.

[73] M. De Koster. Energy storage – maturity and cost of storage technologies. Report, Laborelec, 2015.

[74] J.R. Bartels. *A feasibility study of implementing an ammonia economy.* Thesis, Iowa State University, 2008.

[75] I.S. Metcalfe. Chemical energy storage. In *Oxford Energy Symposium*, 2018.

[76] A. Klerke, C.H. Christensen, J.K. Norskov, and T. Vegge. Ammonia for hydrogen storage: challenges and opportunities. *Journal of Materials Chemistry*, 18(20):2304, 2008.

[77] C.H. Christensen, T. Johannessen, R.Z. Sørensen, and J.K. Nørskov. Towards an ammonia-mediated hydrogen economy? *Catalysis Today*, 111(1-2):140–144, 2006.

[78] T. Lipman and N. Shah. Ammonia as an alternative energy storage medium for hydrogen fuel cells. Report UCB-ITS-TSRC-RR-2007-5, UC Berkeley, 1st November 2007.

[79] M. Zander and W. Thomas. Some thermodynamic properties of liquid ammonia: Pvt data, vapor pressure, and critical temperature. *Journal of Chemical & Engineering Data*, 24(1):1–2, 1979.

[80] A. Basile, L. Di Paola, F.I. Hai, and V. Piemonte. *Membrane reactors for energy applications and basic chemical production*. Woodhead Publishing, Oxford, 2015.

[81] A. Valera-Medina, H. Xiao, M. Owen-Jones, W. I. F. David, and P. J. Bowen. Ammonia for power. *Progress in Energy and Combustion Science*, 69:63–102, 2018.

[82] N. Gupta. Ammonia as a renewable eenrgy carrier: Opportunities and challenges. In *Grand Renewable Energy 2018 International Conference and Exhibition*, 2018.

[83] Eucidare Ltd. Ammonia: New possibilities for hydrogen storage and transportation. Report, Eucidare Ltd., 2008.

[84] Bloomberg. *Commodities*, 2019 (accessed May 1, 2019). `https://www.bloomberg.com/markets/commodities`.

[85] Yara. *Yara Fertilizer Industry Handbook*, 2018 (accessed March 2, 2019). `https://www.yara.com/siteassets/investors/057-reports-and-presentations/other/2018/fertilizer-industry-handbook-2018-with-notes.pdf/`.

[86] J.W. Erisman, M.A. Sutton, J. Galloway, Z. Klimont, and W. Winiwarter. How a century of ammonia synthesis changed the world. *Nature Geoscience*, 1(10):636–639, 2008.

[87] T. Hughes. Green ammonia. *Oxford Energy Colloqia*, 2015.

[88] L. Green. An ammonia energy vector for the hydrogen economy. *International Journal of Hydrogen Energy*, 7(4):355–359, 1982.

[89] W.L. Ahlgren. The dual-fuel strategy: An energy transition plan. *Proceedings of the IEEE*, 100(11):3001–3052, 2012.

[90] C. Zamfirescu and I. Dincer. Using ammonia as a sustainable fuel. *Journal of Power Sources*, 185(1):459–465, 2008.

[91] R. Lan, J.T.S. Irvine, and S. Tao. Ammonia and related chemicals as potential indirect hydrogen storage materials. *International Journal of Hydrogen Energy*, 37(2):1482–1494, 2012.

[92] A. Valera-Medina, S. Morris, J. Runyon, D. G. Pugh, R. Marsh, P. Beasley, and T. Hughes. Ammonia, methane and hydrogen for gas turbines. *EGYPRO Energy Procedia*, 75:118–123, 2015.

[93] A. Valera-Medina. Ammonia based blends for stable combustion in gas turbines and engines. In *NH3 Event*, 2018.

[94] M. Appl. *Ammonia*, book section 2. Production Processes, pages 139–225. Wiley-VCH Verlag GmbH and Co. KGaA, Weinheim, 7th edition, 2012.

[95] M.B. Hocking. *Handbook of chemical technology and pollution control*. Elsevier Inc., third edition, 2005.

[96] Gorvernment of India. Annual report 2017-18. Report, Ministry of Chemicals and Fertilizers, Goverment of India, 2017.

[97] EFMA. Production of ammonia. Report, European Fertilizer Manufacturers' Association, 2000.

[98] T. Brown. The sustainable ammonia synthesis investment universe. In *NH3 Event*, 2018.

[99] E.R. Morgan. *Techno-economic feasibility study of ammonia plants powered by offshore wind*. Thesis, University of Massachusetts Amherst, 2013.

[100] I. Wilkinson. Green ammonia for energy storage and beyond. In *3YP Presentation*, 2017.

[101] S. Giddey, S.P.S. Badwal, and A. Kulkarni. Review of electrochemical ammonia production technologies and materials. *International Journal of Hydrogen Energy*, 38(34):14576–14594, 2013.

[102] Y. Bicer, I. Dincer, C. Zamfirescu, G. Vezina, and F. Raso. Comparative life cycle assessment of various ammonia production methods. *Journal of Cleaner Production*, 135:1379–1395, 2016.

[103] T. Brown. *Ammonia production causes 1 percent of total global GHG emissions*, 2016 (accessed September 20, 2019). `https://ammoniaindustry.com/ammonia-production-causes-1-percent-of-total-global-ghg-emissions/`.

[104] G.R. Maxwell. *Synthetic nitrogen products: A practical guide to the products and processes*. Klewer Academic Publishers, 2005.

[105] H. Liu. Ammonia synthesis catalyst 100 years: Practice, enlightenment and challenge. *Chinese Journal of Catalysis*, 35(10):1619–1640, 2014.

[106] J. Cochran, M. Miller, O. Zinaman, M. Milligan, D. Arent, B. Palmintier, M. O'Malley, S. Mueller, E. Lannoye, and A. Tuohy. Flexibility in 21st century power systems. Report, National Renewable Energy Lab.(NREL), Golden, CO (United States), 2014.

[107] G. Sinden. Characteristics of the uk wind resource: Long-term patterns and relationship to electricity demand. *Energy Policy*, 35(1):112–127, 2007.

[108] M.J. Grubb. On capacity credits and wind-load correlations in britain. *London, U.K., Mechanical Engineering Publications Ltd*, 1988.

[109] M. Huber, D. Dimkova, and T. Hamacher. Integration of wind and solar power in europe: Assessment of flexibility requirements. *Energy*, 69:236–246, 2014.

[110] H. Holttinen, L. Söder, and E. Ela. *Design and operation of power systems with large amounts of wind power: Final report, IEA WIND Task 25, Phase 4 2015-2017*. VTT Technical Research Centre of Finland, 2018.

[111] V. Terrier. *North European Power Systems Reliability.* Thesis, KTH, 2017.

[112] D. Friedrich. Evaluation of the effect of flexible demand on the design and operation of hybrid energy systems. In *Offshore Energy and Storage Symposium*, 2016.

[113] H. Yang, L. Lu, and W. Zhou. A novel optimization sizing model for hybrid solar-wind power generation system. *Solar Energy*, 81(1):76–84, 2007.

[114] H. Holttinen, P. Meibom, A. Orths, B. Lange, M. O'Malley, J.O. Tande, A. Estanqueiro, E. Gomez, L. Söder, G. Strbac, J.C. Smith, and F. van Hulle. Impacts of large amounts of wind power on design and operation of power systems, results of iea collaboration. *Wind Energy*, 14(2):179–192, 2011.

[115] P.B. Eriksen and A. Orths. The challenges and solutions of increasing from 20 to 50 percent of wind energy coverage in the danish power system until 2025. *Proceedings of the 7th International Workshop on Large Scale Integration of Wind Power and on Transmission Networks for Offshore Wind Farms*, 2008.

[116] P. Meibom, R. Barth, H. Brand, B. Hasche, H. Swider, D.and Ravn, and C. Weber. All island grid study. wind variability management studies, 28 September.

[117] F. Van Hulle, J.O. Tande, K. Uhlen, L. Warland, M. Korpås, P. Meibom, P.E. Sørensen, P.E Morthorst, N.A Cutululis, G. Giebel, H.V. Larsen, A. Woyte, G. Dooms, P.-A. Mali, A. Delwart, F. Verheij, C. Kleinschmidt, N. Moldovan, H. Holttinen, B. Lemström, S. Uski-Joutsenvuo, P. Gardner, G. van der Toorn, J. McLean, S. Cox, K. Purchala, S. Wagemans, A. Tiedemann, P. Kreutzkamp, C. Srikandam, and J. Völker. Integrating wind : Developing europe's power market for the large-scale integration of wind power. Report, European Wind Energy Association (EWEA), 2009.

[118] B.P. Heard, B.W. Brook, T.M.L. Wigley, and C.J.A. Bradshaw. Burden of proof: A comprehensive review of the feasibility of 100renewable-electricity

systems. *Renewable and Sustainable Energy Reviews*, 76(Supplement C):1122–1133, 2017.

[119] Y. Yasuda, L. Bird, E.M. Carlini, A. Estanqueiro, D. Flynn, A. Forcione, E. Gómez Lázaro, P. Higgins, H. Holttinen, D. Lew, S. Martin-Martinez, J. McCam, N. Menemenlis, and Smith J.C. International comparison of wind and solar curtailment ratio. Report WIW15-111, 15th Wind Integration Workshop, 2016.

[120] WindEurope. Wind power project database, 20th February.

[121] A. Tuohy and M. O'Malley. *Wind Power and Storage*, pages 465–487. John Wiley and Sons, 2012.

[122] G. Strbac, M. Aunedi, D. Pudjianto, P. Djapic, F. Teng, A. Sturt, D. Jackravut, R. Sansom, V. Yufit, and N. Brandon. Strategic assessment of the role and value of energy storage systems in the uk low carbon energy future. Report, Report for Carbon Trust, 2012.

[123] J. Eyer and G. Corey. Energy storage for the electricity grid: Benefits and market potential assessement guide. Report SAND2010-0815, Sandia National Laboratories, 2010.

[124] I.A. Arbon, A. Bissell, T. Fox, S. Garvey, W. Holt, N. Holmes, D. Kenning, A.R. Knox, C. Matson, T. Peters, D. Pearson, A. Price, C. Pulham, M. Reid, and G. Wilson. Energy storage the missing link in the uk's energy commitments. Report, Institute of Mechanical Engineers (IMechE), April 2014.

[125] H. Blanco and A. Faaij. A review at the role of storage in energy systems with a focus on power to gas and long-term storage. *Renewable and Sustainable Energy Reviews*, 81:1049–1086, 2018.

[126] D. Heide, L. von Bremen, M. Greiner, C. Hoffmann, M. Speckmann, and S. Bofinger. Seasonal optimal mix of wind and solar power in a future, highly renewable europe. *Renewable Energy*, 35(11):2483–2489, 2010.

[127] D. Heide, M. Greiner, L. von Bremen, and C. Hoffmann. Reduced storage and balancing needs in a fully renewable european power system with excess wind and solar power generation. *Renewable Energy*, 36(9):2515–2523, 2011.

[128] M.G. Rasmussen, G.B. Andresen, and M. Greiner. Storage and balancing synergies in a fully or highly renewable pan-european power system. *Energy Policy*, 51:642–651, 2012.

[129] J. Mitra. Reliability-based sizing of backup storage. *Power Systems, IEEE Transactions on*, 25(2):1198–1199, 2010.

[130] R. Dunn, K. Lovegrove, and G. Burgess. A review of ammonia-based thermochemical energy storage for concentrating solar power. *Proceedings of the IEEE*, 100:391–400, 2012.

[131] K. Lovegrove, A. Luzzi, and H. Kreetz. A solar-driven ammonia-based thermochemical energy storage system. *Solar Energy*, 67(4–6):309–316, 1999.

[132] K. Lovegrove, A. Luzzi, M. McCann, and O. Freitag. Exergy analysis of ammonia-based solar thermochemical power systems. *Solar Energy*, 66(2):103–115, 1999.

[133] H. Chen, P. Pei, and M. Song. Lifetime prediction and the economic lifetime of proton exchange membrane fuel cells. *Applied Energy*, 142:154–163, 2015.

[134] S. Beerbühl, M. Fröhling, and F. Schultmann. Combined scheduling and capacity planning of electricity-based ammonia production to integrate renewable energies. *European Journal of Operational Research*, 241(3):851–862, 2014.

[135] F.M. Mulder, B.M.H. Weninger, J. Middelkoop, F.G.B. Ooms, and H. Schreuders. Efficient electricity storage with a battolyser, an integrated ni–fe battery and electrolyser. *Energy and Environmental Science*, 10(3):756–764, 2017.

[136] G. Wang, A. Mitsos, and W. Marquardt. Conceptual design of ammonia-based energy storage system: System design and time-invariant performance. *AIChE*

Journal, pages 1620–1637, 2017.

[137] J. Ikäheimo, J. Kiviluoma, R. Weiss, and H. Holttinen. Power-to-ammonia in future north european 100 heat system. *International Journal of Hydrogen Energy*, 43(36):17295–17308, 2018.

[138] P. Tuna, C. Hulteberg, and S. Ahlgren. Techno-economic assessment of non-fossil ammonia production. *Environmental Progress and Sustainable Energy*, 33(4):1290–1297, 2014.

[139] Bañares-Alcántara, R, G. Dericks III, M. Fiaschetti, P. Grünewald, J.M. Lopez, A. Yang, L. Ye, and S. Zhao. Analysis of islanded ammonia-based energy storage systems. Report, University of Oxford, September 2015.

[140] ISPT. Power to ammonia: Feasibility study for the value chains and business cases to produce co2-free ammonia suitable for various market applications. Report TESI115001, Institute for Sustainable Process Technology (ISPT), 18th May 2017.

[141] R. Nayak-Luke, R. Bañares-Alcántara, and I. Wilkinson. "green" ammonia: Impact of renewable energy intermittency on plant sizing and levelized cost of ammonia. *Industrial and Engineering Chemistry Research*, 57(43):14607–14616, 2018.

[142] R.M. Nayak-Luke and R. Banares-Alacantara. Techno-economic viability of the islanded-production of ammonia from renewable power (under review). *Energy & Environmental Science*, 2019.

[143] XE.com. *International Exchange Rates*, 2019 (accessed March 2, 2019). `https://www.xe.com/currency/usd-us-dollar`.

[144] C. Budischak, D. Sewell, H. Thomson, L. Mach, D.E. Veron, and W. Kempton. Cost-minimized combinations of wind power, solar power and electrochemical storage, powering the grid up to 99.9 *Journal of Power Sources*, 225:60–74, 2013.

[145] D. Helm. Cost of energy review. Report, Department for Business, Energy and Industrial Strategy (BEIS), 25th October 2017.

[146] A. Pfeiffer, R. Millar, C. Hepburn, and E. Beinhocker. The '2c capital stock' for electricity generation: Committed cumulative carbon emissions from the electricity generation sector and the transition to a green economy. *Applied Energy*, 179:1395–1408, 2014.

[147] G. Strbac. Addressing flexibility in energy system models. In *Addressing flexibility in energy system models*, 2014.

[148] S. Wittrig. The ammonia economy: Global potential and possible pathways. In *NH3FUEL Conference*, 2014.

[149] H. Holttinen, M. O'Malley, M. Milligan, and J. C. Smith. Recommended practices for wind integration studies. In *IEEE Computer Society*, volume 2014-October. IEEE Computer Society, 2014.

[150] J.J. Klemes, P.S. Varbanov, T.G. Walmsley, and X. Jia. New directions in the implementation of pinch methodology (pm). *Renewable and Sustainable Energy Reviews*, 98:439–468, 2018.

[151] S. Bandyopadhyay. Design and optimization of isolated energy systems through pinch analysis. *Asia-Pacific Journal of Chemical Engineering*, 6(3):518–526, 2011.

[152] Siemens. Silyzer 300: The next paradigm of pem electrolysis. Report PDLD-T10120-00-74000, Siemens, 2018.

[153] R. Roeva, S. Fidanova, and M. Paprzycki. Influence of the population size on the genetic algorithm performance in case of cultivation process modelling. In *2013 Federated Conference on Computer Science and Information Systems*, page 371–376, 2013.

[154] Y.-A. Zhang, Q. Ma, M. Sakamoto, and H. Furutani. Effects of population size on the performance of genetic algorithms and the role of crossover. *Artificial*

Life and Robotics, 15(2):239–243, 2010.

[155] D. Simon. *Evolutionary optimization algorithms*. John Wiley & Sons, 2013.

[156] R. Ostuni and F. Zardi. *Method for load regulation of an ammonia plant (Patent: US9463983B2)*, 2011 (accessed September 24, 2019). http://www.ic.gc.ca/opic-cipo/cpd/eng/patent/2790545/summary.html?type=number_search&tabs1Index=tabs1_1.

[157] O. Schmidt, A. Gambhir, I. Staffell, A. Hawkes, J. Nelson, and S. Few. Future cost and performance of water electrolysis: An expert elicitation study. *International Journal of Hydrogen Energy*, 42(52):30470–30492, 2017.

[158] A. Buttler and H. Spliethoff. Current status of water electrolysis for energy storage, grid balancing and sector coupling via power-to-gas and power-to-liquids: A review. *Renewable and Sustainable Energy Reviews*, 82:2440–2454, 2018.

[159] J.A. Lokke. *Nel Group*, 2017 (accessed Decebmber 4, 2018). https://www.fch.europa.eu/sites/default/files/S2.3-J.A.L%C3%B6kke,Nel.pdf.

[160] M. Waidhas. *Electrolyzer technology – the Siemens view*, 2016 (accessed June 3, 2018). http://www.scandinavianhydrogen.org/hfc-nordic-2016/.

[161] BMI. Manufacturing cost analysis of 100 and 250 kw fuel cell systems for primary power and combined heat and power applications. Report, Battelle Memorial Institute, January 2016.

[162] E. Morgan, J. Manwell, and J. McGowan. Wind-powered ammonia fuel production for remote islands: A case study. *Renewable Energy*, 72:51–61, 2014.

[163] M. Gardiner. Energy requirements for hydrogen gas compression and liquefaction as related to vehicle storage needs. Report, United States of America, Department of Energy, 2009.

[164] United States Departmet of Energy (US-DOE). *Hydrogen fuel cells*, 2006 (accessed June 10, 2018). `https://www.hydrogen.energy.gov/pdfs/doe_fuelcell_factsheet.pdf`.

[165] I.I. Cheema and U. Krewer. Operating envelope of haber–bosch process design for power-to-ammonia. *RSC Advances*, 8(61):34926–34936, 2018.

[166] T. Smolinka, C. Voglstätter, and A. Fallisch. Cost break down and analysis of pem electrolysis systems for different industrial and power to gas applications. In *Poster presentation, Int. Conf. Renewables Energies, Düsseldorf, Germany*, 2015.

[167] C. Noack, F. Burggraf, S.S. Hosseiny, P. Lettenmeier, S. Kolb, S. Belz, J. Kallo, K.A. Friedrich, T. Pregger, K.-K. Cao, D. Heide, T. Naegler, F. Borggrefe, U. Bünger, J. Michalski, T. Raksha, C. Voglstätter, T. Smolinka, F. Crotogino, S. Donadei, P.-L. Horvath, and G.-S. Schneider. Studie über die planung einer demonstrationsanlage zur wasserstoff-kraftstoffgewinnung durch elektrolyse mit zwischenspeicherung in salzkavernen unter druck, 2015.

[168] S. Schoenung. Economic analysis of large-scale hydrogen storage for renewable utility applications. In *International Colloquium on Environmentally Preferred Advanced Power Generation*, 2011.

[169] Finance3.1. *WACC Expert*, 2018 (accessed December 20, 2018). `http://www.waccexpert.com/`.

[170] K. Deb, S. Agrawal, A. Pratap, and T. Meyarivan. A fast elitist non-dominated sorting genetic algorithm for multi-objective optimization: Nsga-ii. In *International conference on parallel problem solving from nature*, pages 849–858, 2000.

[171] N. Siinivas and K. Deb. Multiobjective optimization using nondominated sorting in genetic algorithms. *Evol. Comput.*, 2(3):221–248, 1994.

[172] A. Seshadri. A fast elitist multiobjective genetic algorithm: Nsga-ii. 2009.

[173] Vestas Wind Systems A/S. General specification v90 - 3.0mw 60hz variable speed turbine. Report, Vestas Wind Systems A/S, 2nd March 2004.

[174] Meteotest. Meteonorm, 2018.

[175] Shikoku Electric Power Company. *Shikoku Power Demand*, 2019 (accessed September 20, 2019). `http://www.yonden.co.jp/denkiyoho/index.html`.

[176] Meteotest. Handbook part i: Software (version 7.2). Report, Meteotest, March 2017.

[177] Meteotest. Handbook part ii: Theory (version 7.2). Report, Meteotest, March 2017.

[178] MetOffice. Uk mean wind data, part of the met office integrated data archive system (midas), 2006.

[179] ELEXON. *Load Profiles and their use in Electricity Settlement*, 2013 (accessed September 20, 2019). `https://www.elexon.co.uk/wp-content/uploads/2013/11/load_profiles_v2.0_cgi.pdf`.

[180] ELEXON. *Operations and Settlement: Profiling*, 2017 (accessed September 20, 2019). `https://www.elexon.co.uk/operations-settlement/profiling/`.

[181] BEIS. *BEIS Electricity Generation Costs (November 2016)*, 2016 (accessed September 25, 2019). `https://www.gov.uk/government/uploads/system/uploads/attachment_data/file/566567/BEIS_Electricity_Generation_Cost_Report.pdf`.

[182] J. McClatchey. Hydrogen - key to enabling the replacement of oil, gas and coal by renewables? In *Scotland's Hydrogen Future*, 2015.

[183] S. Beerbühl, B. Kolbe, C. Roosen, and F. Schultmann. Synthesis of ammonia from intermittently generated hydrogen. *Chemie-Ingenieur-Technik*, 86(5):649–657, 2014.

[184] IRENA. Renewable power generation costs in 2017. Report, International Renewable Energy Agency, 2017.

[185] C. Philibert. *Producing ammonia and fertilizers: new opportunities from renewables*, 2017 (accessed November 5, 2018). http://www.ee.co.za/wp-content/uploads/2017/06/Producing-ammonia-and-fertilizers-new-opportunities-from-renewables.pdf.

[186] K.R. Voorspools and W.D. D'Haeseleer. An analytical formula for the capacity credit of wind power. *Renewable Energy*, 31(1):45 – 54, 2006.

[187] Hydrofuel Inc. *Green Ammonia (NH3): Manufacturing and Utilization Technologies and Research*, 2017 (accessed September 20, 2019). https://arpa-e.energy.gov/sites/default/files/1%20Hydrofuel%20-%20UOIT%20Presentation%20for%20ARPA-E%20Aug.%2017-18%2C%202017%20FINAL.pdf.

[188] Lazard Ltd. Lazard's levelised cost of storage analysis - version 3.0. Report, Lazard Ltd., 2017.

[189] LeighFisher Ltd. Electricity generation costs and hurdle rates: Lot 3: Non-renewable technologies. Report, Department of Energy and Climate Change, August 2016 2016.

[190] Z. Cesaro. Green ammonia-to-power in developing countries: Case study on indian electricity sector to 2040, 2019.

[191] Ministry of Chemicals and Goverment of India Fertilizers. *Demands for Grants (2018-19)*, 2018 (accessed March 13, 2019). https://www.india.gov.in/my-government/documents/demand-grant.

[192] Y. Sharma. *Government keen to source coal gasification technology from US*, 2019 (accessed February 14, 2019). https://economictimes.indiatimes.com/industry/indl-goods/svs/metals-mining/

government-keen-to-source-coal-gasification-technology-from-us/articleshow/67985392.cms?from=mdr.

[193] World Bank. *State and Trends of Carbon Pricing 2019*, 2019 (accessed September 20, 2019). https://openknowledge.worldbank.org/handle/10986/31755.

[194] German Association of the Automotive Industry (VDA). *AdBlue*, 2019 (accessed September 20, 2019). http://vda.de/en/topics/innovation-and-technology/ad-blue/AdBlue-brand-list-and-licensees-list.html.

[195] U. Rossi. Ammonia from renewables: handling plant load variations. In *NH3 Event*, 2018.

[196] Tohoku Electric Power Company. *Tohoku Power Demand*, 2019 (accessed September 20, 2019). http://setsuden.tohoku-epco.co.jp/graph.html.

[197] Chubu Electric Power Company. *Chubu Power Demand*, 2019 (accessed September 20, 2019). http://denki-yoho.chuden.jp/index.html.

[198] IESO. *Ontario: Hourly Demand Report*, 2019 (accessed September 20, 2019). http://reports.ieso.ca/public/Demand/.

[199] AIMO. *National Electricity Market Data dashboard*, 2019 (accessed September 25, 2019). https://www.aemo.com.au/Electricity/National-Electricity-Market-NEM/Data-dashboard#aggregated-data.

Appendices

Appendix A

The locations considered and the demand profile used in ESRMT simulations arranged by country.

Japan

Location	Latitude	Longitude	Demand Profile Reference
Miyako	39.641239	141.950912	[196]
Shimizu / Ashizuri	32.78019	132.95325	[175]
Matsumoto	36.24044	137.970016	[197]

Table 7.1: Locations in Japan simulated with the ESRMT

UK

Location	Latitude	Longitude	Demand Profile Reference
Lerwick	60.153	-1.15004	[180]
Holbeach	52.80384	0.014707	[180]
Cambourne	50.2128	-5.2948	[180]
Hawarden Airport	53.1818	-2.9753	[180]
Herstmonceux	50.8893	0.3224	[180]
Prestwick	55.50581	-4.60567	[180]
Altnaharra	58.28022	-4.44085	[180]

Table 7.2: Locations in the UK simulated with the ESRMT

Canada

Location	Latitude	Longitude	Demand Profile Reference
Baker Lake	64.3	-95.927	[198]
Churchill	58.75	-94.067	[198]
Goose	53.3	-60.367	[198]
Inukjuak	58.45	-78.117	[198]
Norman Wells	65.283	-126.75	[198]
Normandin	48.85	-72.533	[198]
Prince George	53.883	-122.667	[198]
Sandspit	53.25	-131.817	[198]
St Johns	47.517	-52.783	[198]
The Pas	53.967	-101.1	[198]
Winnipeg	49.9	-97.233	[198]

Table 7.3: Locations in Canada simulated with the ESRMT

Australia

Location	Latitude	Longitude	Demand Profile Reference
Sydney	-33.867	151.2	[199]
Wagga Wagga Airport	-35.15	147.45	[199]
Williamtown Airport	-32.783	151.817	[199]
Birdsville	-25.9	139.35	[199]
Boulia	-22.92	139.9	[199]
Brisbane	-27.383	153.1	[199]
Cairns Airport	-16.883	145.75	[199]
Cunnamulla	-28.067	145.683	[199]
Normanton	-17.667	141.083	[199]
Rockhampton Airport	-23.383	150.467	[199]
Roma	-26.57	148.78	[199]
Townsville	-19.25	146.75	[199]
Willis Island	-16.3	149.983	[199]
Adelaide	-34.933	138.533	[199]
Cook	-30.62	130.4	[199]
Marree	-29.65	138.05	[199]
Mt Gambier	-37.733	140.783	[199]
Cape Grim	-40.66	144.68	[199]
Hobart Airport	-42.833	147.5	[199]
Longerenong	-36.66	142.3	[199]
Mallacoota	-37.6	149.73	[199]
Melbourne	-37.817	144.967	[199]
Mildura	-34.217	142.083	[199]

Table 7.4: Locations in Australia simulated with the ESRMT

Appendix B

	2019 Scenario		2030 Scenario	
	Mean of lowest 10 LCOA estimates for each geographic region	**Mean of all 534 locations**	**Mean of lowest 10 LCOA estimates for each geographic region**	**Mean of all 534 locations**
Ideal supply profile LCOA [$/t]	**470**	**623**	**221**	**273**
CAPEX Electrolyser [% increase in LCOA]	32.3%	25.2%	22.3%	14.8%
CAPEX Synthesis & ASU [% increase in LCOA]	13.6%	9.8%	15.0%	11.2%
CAPEX Hydrogen Storage [% increase in LCOA]	8.1%	13.5%	9.5%	14.0%
CAPEX Hydrogen Fuel Cell [% increase in LCOA]	2.4%	1.7%	3.5%	2.4%
OPEX Electrolyser Electricity [% increase in LCOA]	-14.3%	-18.8%	-14.3%	-18.6%
OPEX Synthesis & ASU Electricity [% increase in LCOA]	-1.2%	-1.6%	-1.2%	-1.5%
OPEX Curtailed Electricity [% increase in LCOA]	15.5%	20.2%	15.3%	20.0%
OPEX Hydrogen Storage Electricity [% increase in LCOA]	1.2%	1.3%	0.8%	0.7%
OPEX Operation & Maintenance [% increase in LCOA]	13.4%	12.0%	11.7%	10.0%
OPEX Water [% increase in LCOA]	-0.1%	-0.1%	-0.4%	-0.4%
Mass of Ammonia produced [% increase in LCOA]	29.3%	36.7%	37.9%	47.3%
Actual supply profile LCOA [$/t]	**735**	**1,014**	**388**	**521**

Table 7.5: The cost of process flexibility required due to the variability of renewable energy sources [142]. Note that the summation of percentage increase not summing to 100% is due to rounding of the individual components to one decimal place.

Appendix C

The following table presents the country specific inputs to the IAPMT for the production of islanded 'green' ammonia production [27, 169].

Country	Geographic region	Number of locations simulated	Renewable Energy fixed costs		Domestic Corporation variables	
			Solar installed cost [USD/kW]	Wind installed cost [USD/kW]	Utilities Discount Factor [%]	Ammonia Plant Discount Factor [%]
Argentina	Lat. America & Caribbean	5	823	1,829	10.24	14.69
Australia	Oceania	37	1,550	2,124	3.64	7.49
Austria	Europe	6	921	1,868	3.76	7.60
Belgium	Europe	4	921	1,868	3.87	7.72
Bosnia & Herzegovina	Europe	1	921	1,868	9.34	13.17
Botswana	Sub-Saharan Africa	1	805	2,040	4.92	8.88
Brazil	Lat. America & Caribbean	5	823	1,829	5.33	9.31
Bulgaria	Europe	4	921	1,868	5.44	9.25
Canada	Northern America	11	955	1,718	3.68	7.48
Chile	Lat. America & Caribbean	7	823	1,829	4.33	8.20
China	Eastern Asia	51	1,005	1,197	4.43	8.24
Colombia	Lat. America & Caribbean	2	823	1,829	5.12	8.94
Congo	Sub-Saharan Africa	1	805	2,040	6.71	10.76
Croatia	Europe	2	921	1,868	5.81	9.66
Czech Republic	Europe	5	921	1,868	4.43	8.29
Denmark	Europe	7	921	1,868	3.73	7.53
Egypt	Northern Africa	5	1,201	1,320	10.67	15.01
El Salvador	Lat. America & Caribbean	1	1,319	2,184	6.13	9.97
Estonia	Europe	1	921	1,868	4.43	8.34

Country	Geographic region	Number of locations simulated	Renewable Energy fixed costs		Domestic Corporation variables	
			Solar installed cost [USD/kW]	Wind installed cost [USD/kW]	Utilities Discount Factor [%]	Ammonia Plant Discount Factor [%]
Finland	Europe	5	921	1,868	3.88	7.71
France	Europe	39	921	1,868	3.57	7.37
Germany	Europe	9	921	1,868	3.62	7.43
Ghana	Sub-Saharan Africa	1	805	2,040	8.53	12.84
Greece	Europe	3	921	1,868	9.11	13.32
Hungary	Europe	2	921	1,868	5.59	9.53
India	Southern Asia	12	661	1,097	5.50	9.65
Indonesia	South-Eastern Asia	1	832	1,221	5.52	9.52
Ireland	Europe	5	921	1,868	5.14	8.98
Italy	Europe	16	921	1,868	4.60	8.52
Japan	Eastern Asia	62	832	1,221	3.80	7.62
Kazakhstan	Northern Asia	1	1,463	1,605	5.44	9.41
Kenya	Sub-Saharan Africa	3	805	2,040	6.79	10.84
Republic of Korea, (South Korea)	Eastern Asia	8	832	1,221	4.18	8.03
Latvia	Europe	1	921	1,868	5.18	8.94
Lithuania	Europe	1	921	1,868	5.23	9.03
Republic of Macedonia	Europe	2	921	1,868	6.90	10.80
Malaysia	South-Eastern Asia	4	832	1,221	4.85	8.67
Mexico	Lat. America & Caribbean	9	1,319	2,184	4.52	8.51

Country	Geographic region	Number of locations simulated	Renewable Energy fixed costs		Domestic Corporation variables	
			Solar installed cost [USD/kW]	Wind installed cost [USD/kW]	Utilities Discount Factor [%]	Ammonia Plant Discount Factor [%]
Mongolia	Eastern Asia	5	1,463	1,605	8.35	12.57
Morocco	Northern Africa	1	805	2,040	5.51	9.34
Mozambique	Sub-Saharan Africa	3	805	2,040	6.67	10.69
Netherlands	Europe	4	921	1,868	3.78	7.64
New Zealand	Oceania	4	1,550	2,124	3.65	7.46
Nicaragua	Lat. America & Caribbean	1	1,319	2,184	9.08	13.30
Norway	Europe	2	921	1,868	3.71	7.55
Oman	Western Asia	2	1,201	1,320	4.75	8.55
Pakistan	Southern Asia	2	832	1,221	10.02	14.35
Papua New Guinea	Oceania	1	1,550	2,124	6.75	10.76
Peru	Lat. America & Caribbean	1	823	1,829	4.76	8.59
Philippines	South-Eastern Asia	1	832	1,221	5.21	9.07
Poland	Europe	3	921	1,868	4.59	8.44
Portugal	Europe	6	921	1,868	5.36	9.26
Romania	Europe	7	921	1,868	5.64	9.56
Russian Federation	Europe	18	832	1,221	5.40	9.40
Saudi Arabia	Western Asia	6	1,201	1,320	4.58	8.44
Senegal	Sub-Saharan Africa	2	805	2,040	6.47	10.32
Singapore	South-Eastern Asia	1	832	1,221	4.13	7.94
South Africa	Sub-Saharan Africa	8	805	2,040	5.13	9.08

Country	Geographic region	Number of locations simulated	Renewable Energy fixed costs		Domestic Corporation variables	
			Solar installed cost [USD/kW]	Wind installed cost [USD/kW]	Utilities Discount Factor [%]	Ammonia Plant Discount Factor [%]
Spain	Europe	16	921	1,868	4.66	8.58
Sri Lanka	Southern Asia	1	832	1,221	6.94	11.03
Sweden	Europe	7	921	1,868	3.77	7.54
Switzerland	Europe	7	921	1,868	3.87	7.64
Thailand	South-Eastern Asia	2	832	1,221	5.16	9.00
Tunisia	Northern Africa	2	805	2,040	6.62	10.66
Turkey	Western Asia	14	921	1,868	5.50	9.64
Ukraine	Europe	2	1,463	1,605	11.14	15.07
UK	Europe	16	921	1,868	3.98	7.85
USA	Northern America	47	850	1,648	3.33	7.14
Venezuela	Lat. America & Caribbean	1	823	1,829	13.08	18.74
Zambia	Sub-Saharan Africa	1	805	2,040	6.70	10.80

Appendix D

The following table presents the results from the IAPMT for the production of islanded 'green' ammonia production in the 2019 scenario by a multinational corporation. The results are presented as a range of the solutions grouped by country.

Country	Number of locations simulated	Decision variables			Resulting variables								Objective
		Electrolyser rated power [MW]	HB & ASU rated power [MW]	Percentage of RE energy supplied by wind [%]	Percentage of RE rated power met by wind [%]	Supply energy profile Full Load Hours Equivalent	LCOE of energy supplied [$/MWh]	Percentage of RE energy curtailed [%]	Electrolyser load factor [%]	Haber-Bosch synthesis load factor [%]	Hydrogen storage size [t]	Electrolyser excess factor [%]	LCOA [$/t]
Argentina	5	198 – 273	11.1 – 14.5	0 – 98	0 – 93	1,516 – 3,136	38 – 41	7 – 28	30 – 42	39 – 49	28 – 111	16 – 38	757 – 896
Australia	37	137 – 307	8.8 – 16.1	0 – 100	0 – 100	1,363 – 5,637	28 – 91	0 – 19	28 – 64	37 – 69	20 – 93	3 – 105	473 – 1,325
Austria	6	152 – 241	9.9 – 12.9	0 – 92	0 – 75	1,116 – 3,995	30 – 70	3 – 30	30 – 59	40 – 63	43 – 334	6 – 61	518 – 1,411
Belgium	4	186 – 262	10 – 13.2	36 – 80	34 – 57	1,059 – 2,333	46 – 86	6 – 10	32 – 47	49 – 61	52 – 132	11 – 92	737 – 1,269
Bosnia & Herzegovina	1	211	11.6	0	0	1,263	53	29	31	40	123	34	1,193
Botswana	1	238	12.8	0	0	1,692	35	15	33	44	17	37	748
Brazil	5	246 – 294	10.7 – 14.6	0 – 1	0 – 2	1,209 – 1,711	36 – 50	13 – 17	28 – 32	39 – 53	36 – 61	37 – 77	766 – 989
Bulgaria	4	200 – 252	11.2 – 13.7	0 – 6	0 – 9	1,120 – 1,357	50 – 66	19 – 30	30 – 33	39 – 42	90 – 195	30 – 35	1,047 – 1,336
Canada	11	179 – 281	9 – 14.7	22 – 84	29 – 65	862 – 2,416	44 – 107	4 – 18	30 – 48	41 – 65	48 – 815	9 – 88	729 – 2,013
Chile	7	191 – 318	11.5 – 15.6	0 – 98	0 – 94	926 – 3,328	37 – 75	8 – 27	27 – 45	39 – 51	31 – 105	15 – 50	720 – 1,369
China	51	174 – 381	9.5 – 16.5	0 – 67	0 – 56	886 – 1,740	42 – 85	7 – 33	23 – 45	35 – 64	24 – 151	16 – 132	801 – 1,462
Colombia	2	299 – 311	11.6 – 12	0 – 0	0 – 0	1,234 – 1,383	44 – 49	13 – 14	26 – 27	48 – 50	76 – 78	89 – 90	907 – 989
Congo	1	333	15.6	0	0	1,459	40	7	26	39	44	57	864
Croatia	2	195 – 219	9.1 – 13.2	0 – 30	0 – 26	1,205 – 1,541	55 – 56	12 – 34	32 – 37	45 – 48	33 – 339	22 – 58	925 – 1,455
Czech Republic	5	190 – 258	9.5 – 14.5	24 – 70	23 – 46	1,069 – 1,758	56 – 81	8 – 17	32 – 45	41 – 65	46 – 173	6 – 94	874 – 1,273
Denmark	7	159 – 283	9.9 – 13.1	41 – 98	37 – 91	1,074 – 4,712	28 – 88	1 – 7	31 – 58	49 – 66	59 – 150	9 – 105	528 – 1,288
Egypt	5	188 – 279	10.2 – 14.7	0 – 53	0 – 49	1,834 – 2,132	41 – 48	6 – 12	31 – 44	41 – 60	22 – 32	7 – 78	759 – 896
El Salvador	1	322	12.1	1	3	1,707	57	5	27	52	74	96	988
Estonia	1	264	10.2	44	39	1,054	89	9	32	60	193	91	1,351
Finland	5	259 – 422	10.2 – 12.3	24 – 53	28 – 45	691 – 1,136	87 – 139	3 – 12	21 – 33	52 – 58	176 – 638	79 – 152	1,309 – 2,090
France	39	170 – 344	9.4 – 14.7	0 – 69	0 – 51	1,016 – 2,498	41 – 80	5 – 30	24 – 50	39 – 67	18 – 413	6 – 109	668 – 1,425
Germany	9	193 – 394	9.8 – 14.3	6 – 42	9 – 34	905 – 1,321	67 – 101	5 – 26	22 – 38	40 – 64	103 – 419	21 – 125	1,083 – 1,696
Ghana	1	281	11.2	1	1	1,668	36	11	29	53	56	84	770
Greece	3	187 – 228	10.6 – 12.7	0 – 3	0 – 5	1,472 – 1,639	41 – 48	22 – 31	32 – 35	41 – 43	67 – 97	28 – 31	938 – 1,051

Country	Number of locations simulated	Decision variables			Resulting variables								Objective
		Electrolyser rated power [MW]	HB & ASU rated power [MW]	Percentage of RE energy supplied by wind [%]	Percentage of RE rated power met by wind [%]	Supply energy profile Full Load Hours Equivalent	LCOE of energy supplied [$/MWh]	Percentage of RE energy curtailed [%]	Electrolyser load factor [%]	Haber-Bosch synthesis load factor [%]	Hydrogen storage size [t]	Electrolyser excess factor [%]	LCOA [$/t]
Hungary	2	267 – 322	10.7 – 11.5	6 – 13	12 – 19	1,094 – 1,129	67 – 73	8 – 18	26 – 29	51 – 53	264 – 362	83 – 105	1,301 – 1,391
India	12	218 – 294	10.7 – 14.7	0 – 0	0 – 0	1,356 – 1,957	25 – 36	8 – 19	29 – 35	41 – 52	14 – 53	33 – 67	636 – 823
Indonesia	1	285	13.9	0	0	1,310	47	15	28	40	42	51	953
Ireland	5	168 – 277	10.4 – 13.8	49 – 98	40 – 90	1,106 – 4,210	31 – 86	2 – 6	32 – 54	46 – 61	58 – 150	9 – 96	554 – 1,248
Italy	16	180 – 266	9.4 – 15.1	0 – 43	0 – 32	1,126 – 1,917	41 – 60	7 – 32	30 – 39	39 – 67	33 – 382	21 – 80	777 – 1,480
Japan	62	139 – 332	8.7 – 16.6	0 – 74	0 – 56	1,130 – 2,568	30 – 62	6 – 25	26 – 55	37 – 65	13 – 114	4 – 104	562 – 1,105
Kazakhstan	1	218	12.6	10	22	1,214	90	21	34	42	182	27	1,567
Kenya	3	250 – 281	11.8 – 13.4	0 – 1	0 – 2	1,802 – 1,885	32 – 33	7 – 14	31 – 32	45 – 53	25 – 48	46 – 75	697 – 732
Korea, Republic of (South Korea)	8	223 – 316	9.6 – 16	0 – 29	0 – 31	1,183 – 1,357	46 – 59	10 – 16	26 – 35	37 – 61	32 – 87	41 – 94	860 – 1,022
Latvia	1	302	11.5	13	24	868	97	15	26	49	676	93	1,929
Lithuania	1	213	9.5	41	36	1,037	89	16	37	60	119	66	1,350
Macedonia, Republic of	2	197 – 258	10.9 – 14	0 – 6	0 – 9	1,262 – 1,306	52 – 58	17 – 32	30 – 32	39 – 41	194 – 252	32 – 36	1,231 – 1,254
Malaysia	4	262 – 340	10.8 – 15.7	0 – 0	0 – 0	1,356 – 1,709	36 – 45	5 – 18	26 – 29	40 – 51	30 – 76	52 – 99	788 – 917
Mexico	9	270 – 321	10.1 – 15.6	0 – 13	0 – 13	1,345 – 1,962	49 – 72	5 – 16	26 – 31	38 – 62	24 – 61	40 – 99	896 – 1,231
Mongolia	5	223 – 325	11 – 14.3	0 – 4	0 – 7	1,225 – 1,519	71 – 88	9 – 24	26 – 32	40 – 55	37 – 312	27 – 117	1,171 – 1,573
Morocco	1	227	12.6	0	0	1,825	32	18	34	43	44	32	757
Mozambique	3	244 – 270	13.2 – 14.3	0 – 0	0 – 1	1,595 – 1,714	34 – 37	10 – 14	31 – 33	42 – 44	17 – 23	36 – 42	739 – 777
Netherlands	4	182 – 249	12.3 – 14.2	32 – 72	31 – 49	1,002 – 1,968	51 – 89	7 – 11	33 – 47	42 – 51	41 – 141	9 – 29	796 – 1,374
New Zealand	4	195 – 238	12.8 – 13.5	14 – 100	17 – 100	1,162 – 4,011	39 – 104	2 – 17	33 – 47	41 – 52	59 – 109	12 – 30	673 – 1,599
Nicaragua	1	317	12.3	0	0	1,491	65	7	27	50	74	89	1,087
Norway	2	188 – 314	11 – 12.8	48 – 88	41 – 63	895 – 2,471	45 – 107	5 – 5	28 – 47	51 – 58	58 – 219	8 – 111	731 – 1,540
Oman	2	144 – 270	10.3 – 14.1	0 – 69	0 – 59	1,929 – 2,291	41 – 46	9 – 20	32 – 51	43 – 52	22 – 27	3 – 41	735 – 856
Pakistan	2	233 – 246	10 – 12.7	0 – 6	0 – 9	1,706 – 1,778	36 – 36	12 – 18	33 – 33	43 – 58	33 – 35	35 – 80	716 – 793

Country	Number of locations simulated	Decision variables			Resulting variables								Objective
		Electrolyser rated power [MW]	HB & ASU rated power [MW]	Percentage of RE energy supplied by wind [%]	Percentage of RE rated power met by wind [%]	Supply energy profile Full Load Hours Equivalent	LCOE of energy supplied [$/MWh]	Percentage of RE energy curtailed [%]	Electrolyser load factor [%]	Haber-Bosch synthesis load factor [%]	Hydrogen storage size [t]	Electrolyser excess factor [%]	LCOA [$/t]
Papua New Guinea	1	317	12.2	0	0	1,625	70	7	27	50	54	91	1,129
Peru	1	276	11.5	0	0	1,845	33	8	31	53	47	76	709
Philippines	1	305	14.9	0	0	1,439	42	11	27	39	41	50	894
Poland	3	221 – 242	9.3 – 14.1	33 – 46	32 – 41	1,062 – 1,133	83 – 85	12 – 13	34 – 36	42 – 62	131 – 163	27 – 79	1,282 – 1,350
Portugal	6	180 – 260	11.9 – 13.5	0 – 60	0 – 45	1,482 – 2,104	37 – 55	6 – 25	30 – 46	41 – 51	29 – 222	12 – 41	767 – 1,108
Romania	7	178 – 235	10 – 13	0 – 9	0 – 14	1,222 – 1,424	48 – 62	20 – 33	31 – 36	40 – 52	45 – 338	22 – 73	1,043 – 1,357
Russian Federation	18	162 – 341	8.5 – 13.7	0 – 98	0 – 93	768 – 3,389	26 – 92	5 – 37	26 – 48	43 – 65	66 – 1579	12 – 124	565 – 2,464
Saudi Arabia	6	243 – 271	10 – 12.9	0 – 10	0 – 14	1,615 – 2,240	39 – 55	6 – 14	31 – 33	44 – 61	13 – 56	38 – 98	741 – 919
Senegal	2	275 – 289	11 – 11.4	0 – 2	0 – 2	1,677 – 2,000	30 – 35	8 – 9	29 – 31	53 – 56	34 – 62	84 – 86	661 – 758
Singapore	1	273	11.1	0	0	1,423	43	15	29	51	70	81	886
South Africa	8	170 – 262	8.8 – 13.6	0 – 99	0 – 96	1,470 – 4,626	32 – 43	0 – 18	31 – 55	42 – 65	20 – 74	8 – 85	552 – 830
Spain	16	191 – 278	8.9 – 15.4	0 – 41	0 – 35	1,189 – 2,046	38 – 62	8 – 30	30 – 40	39 – 70	38 – 169	19 – 102	687 – 1,207
Sri Lanka	1	260	9.7	25	22	1,682	40	6	33	65	36	98	715
Sweden	7	197 – 355	10.5 – 13.2	18 – 65	18 – 46	879 – 1,693	59 – 106	4 – 21	25 – 42	44 – 60	68 – 434	18 – 119	896 – 1,625
Switzerland	7	158 – 292	10.7 – 12.1	0 – 70	0 – 49	1,124 – 2,439	42 – 63	9 – 31	26 – 53	40 – 57	33 – 465	7 – 89	675 – 1,464
Thailand	2	261 – 293	10.9 – 14.1	0 – 0	0 – 0	1,695 – 1,727	35 – 36	9 – 13	29 – 31	43 – 53	46 – 66	53 – 76	764 – 790
Tunisia	2	212 – 252	12.1 – 13.8	0 – 1	0 – 1	1,676 – 1,726	35 – 35	17 – 23	31 – 34	40 – 42	32 – 98	28 – 34	798 – 852
Turkey	14	175 – 279	10.1 – 15.2	0 – 6	0 – 7	1,220 – 1,647	41 – 55	14 – 37	29 – 34	37 – 42	38 – 111	24 – 37	867 – 1,285
Ukraine	2	272 – 292	14.8 – 16.2	39 – 57	45 – 52	1,070 – 1,436	78 – 104	5 – 8	29 – 33	38 – 43	94 – 163	32 – 35	1,172 – 1,559
UK	16	151 – 326	9.7 – 14.1	21 – 98	22 – 91	843 – 4,102	32 – 99	3 – 18	27 – 56	45 – 63	43 – 329	7 – 119	584 – 1,638
USA	47	152 – 278	8.5 – 14.6	0 – 67	0 – 50	966 – 2,315	34 – 79	7 – 31	30 – 53	38 – 70	24 – 551	7 – 95	668 – 1,678
Venezuela	1	273	13.6	0	0	1,732	35	11	30	43	22	47	758
Zambia	1	296	12.6	0	0	1,463	40	9	29	48	68	72	836

Appendix E

The following table presents the results from the IAPMT for the production of islanded 'green' ammonia production in the 2030 scenario by a multinational corporation. The results are presented as a range of the solutions grouped by country.

Country	Number of locations simulated	Decision variables			Resulting variables								Objective
		Electrolyser rated power [MW]	HB & ASU rated power [MW]	Percentage of RE energy supplied by wind [%]	Percentage of RE rated power met by wind [%]	Supply energy profile Full Load Hours Equivalent	LCOE of energy supplied [$/MWh]	Percentage of RE energy curtailed [%]	Electrolyser load factor [%]	Haber-Bosch synthesis load factor [%]	Hydrogen storage size [t]	Electrolyser excess factor [%]	LCOA [$/t]
Argentina	5	168 – 236	10.5 – 13.1	0 – 68	0 – 39	1,517 – 1,881	13 – 22	10 – 32	32 – 50	40 – 55	30 – 89	10 – 35	415 – 461
Australia	37	136 – 291	7.9 – 15.2	0 – 95	0 – 82	1,357 – 4,848	16 – 38	2 – 21	30 – 66	38 – 71	15 – 56	2 – 100	310 – 636
Austria	6	121 – 210	8 – 11.7	0 – 83	0 – 56	1,116 – 3,320	16 – 27	7 – 52	32 – 63	40 – 65	23 – 228	4 – 55	318 – 728
Belgium	4	161 – 213	8.9 – 11.2	32 – 67	27 – 40	1,054 – 1,957	23 – 37	8 – 17	37 – 51	53 – 63	44 – 113	11 – 76	426 – 672
Bosnia & Herzegovina	1	185	10.4	0	0	1,263	18	35	33	41	76	30	573
Botswana	1	216	11.8	0	0	1,692	11	20	35	45	17	35	378
Brazil	5	193 – 269	10.2 – 14.2	0 – 0	0 – 1	1,209 – 1,730	11 – 16	14 – 28	30 – 35	40 – 53	20 – 61	32 – 77	388 – 480
Bulgaria	4	141 – 214	9.3 – 12	0 – 4	0 – 7	1,131 – 1,357	16 – 23	26 – 45	32 – 37	39 – 43	43 – 132	11 – 32	539 – 672
Canada	11	136 – 188	8.4 – 12.1	8 – 66	8 – 41	883 – 1,937	21 – 44	8 – 43	36 – 57	43 – 60	26 – 537	5 – 57	423 – 1,234
Chile	7	150 – 268	9.4 – 14	0 – 67	0 – 37	931 – 1,914	12 – 27	14 – 37	29 – 54	40 – 58	29 – 88	8 – 41	408 – 682
China	51	123 – 296	8.2 – 15.4	0 – 47	0 – 36	902 – 1,740	14 – 30	9 – 48	26 – 40	37 – 60	16 – 123	10 – 106	407 – 699
Colombia	2	220 – 235	10.1 – 11.3	0 – 0	0 – 0	1,234 – 1,383	14 – 16	24 – 25	30 – 32	44 – 50	23 – 47	44 – 72	444 – 473
Congo	1	203	9.4	0	0	1,459	13	27	33	52	42	60	426
Croatia	2	134 – 184	7.8 – 11.3	0 – 13	0 – 11	1,205 – 1,494	18 – 19	26 – 49	36 – 37	43 – 44	26 – 121	20 – 26	481 – 714
Czech Republic	5	157 – 189	10 – 11.4	12 – 53	12 – 29	1,066 – 1,469	26 – 31	16 – 33	36 – 50	43 – 51	26 – 59	4 – 22	487 – 653
Denmark	7	148 – 287	8.6 – 10.2	42 – 86	29 – 56	1,075 – 3,316	16 – 41	4 – 14	30 – 58	62 – 68	38 – 150	7 – 106	352 – 708
Egypt	5	185 – 265	8.4 – 14.4	0 – 23	0 – 20	1,840 – 2,132	14 – 18	11 – 21	32 – 41	41 – 65	19 – 26	32 – 65	374 – 436
El Salvador	1	272	11.2	0	0	1,729	18	12	30	52	64	78	471
Estonia	1	207	9.0	45	40	1,057	42	16	37	62	142	69	756
Finland	5	179 – 460	10.7 – 12.5	26 – 38	29 – 45	691 – 1,074	36 – 66	2 – 25	20 – 39	44 – 55	119 – 522	17 – 175	724 – 1,249
France	39	130 – 241	8.3 – 12.7	0 – 38	0 – 29	1,044 – 1,911	13 – 32	10 – 41	32 – 50	41 – 73	22 – 124	10 – 83	359 – 732
Germany	9	117 – 229	7.3 – 11.3	7 – 37	9 – 27	967 – 1,266	26 – 32	12 – 50	31 – 41	43 – 65	52 – 242	17 – 85	573 – 873
Ghana	1	228	9.9	0	1	1,670	12	21	32	53	40	69	388
Greece	3	135 – 196	8.9 – 11.1	0 – 1	0 – 1	1,497 – 1,623	14 – 15	28 – 46	34 – 38	40 – 43	33 – 71	11 – 30	484 – 541

Country	Number of locations simulated	Decision variables			Resulting variables								Objective
		Electrolyser rated power [MW]	HB & ASU rated power [MW]	Percentage of RE energy supplied by wind [%]	Percentage of RE rated power met by wind [%]	Supply energy profile Full Load Hours Equivalent	LCOE of energy supplied [$/MWh]	Percentage of RE energy curtailed [%]	Electrolyser load factor [%]	Haber-Bosch synthesis load factor [%]	Hydrogen storage size [t]	Electrolyser excess factor [%]	LCOA [$/t]
Hungary	2	130 – 172	8.7 – 10.4	2 – 9	4 – 13	1,116 – 1,177	21 – 26	33 – 48	36 – 37	40 – 43	66 – 115	10 – 22	660 – 748
India	12	168 – 240	9.4 – 12.3	0 – 2	0 – 7	1,356 – 1,957	8 – 12	17 – 35	32 – 38	45 – 54	11 – 39	30 – 62	338 – 417
Indonesia	1	229	11.8	0	0	1,310	15	24	31	43	30	43	464
Ireland	5	125 – 201	8.8 – 12.5	36 – 81	27 – 46	1,052 – 2,610	18 – 36	9 – 19	39 – 64	45 – 67	30 – 73	5 – 18	355 – 668
Italy	16	136 – 232	7.8 – 13.3	0 – 28	0 – 20	1,126 – 1,773	13 – 20	17 – 48	32 – 43	40 – 68	28 – 134	10 – 61	407 – 703
Japan	62	152 – 314	7.5 – 15.5	0 – 51	0 – 33	1,131 – 1,997	13 – 25	7 – 36	27 – 49	38 – 72	20 – 81	8 – 103	324 – 550
Kazakhstan	1	172	10.3	5	11	1,301	30	33	36	43	88	22	729
Kenya	3	203 – 242	9.8 – 12.2	0 – 1	0 – 2	1,802 – 1,886	10 – 11	16 – 23	33 – 35	46 – 54	16 – 26	40 – 56	354 – 375
Korea, Republic of (South Korea)	8	179 – 223	8.7 – 12.4	0 – 19	0 – 22	1,183 – 1,370	15 – 22	19 – 33	33 – 36	42 – 60	27 – 60	29 – 71	433 – 501
Latvia	1	104	6.4	8	16	911	34	55	40	46	120	19	1,087
Lithuania	1	208	12.8	35	31	1,027	39	17	37	43	91	19	725
Macedonia, Republic of	2	146 – 147	8.5 – 8.8	0 – 5	0 – 8	1,267 – 1,306	17 – 21	41 – 44	36 – 37	44 – 45	71 – 97	23 – 27	627 – 631
Malaysia	4	211 – 267	10.9 – 12.6	0 – 0	0 – 0	1,356 – 1,709	12 – 15	17 – 24	29 – 34	43 – 49	20 – 52	42 – 74	394 – 447
Mexico	9	214 – 311	9.9 – 15.1	0 – 4	0 – 4	1,345 – 1,962	16 – 24	6 – 26	27 – 34	38 – 56	22 – 76	37 – 90	440 – 572
Mongolia	5	177 – 228	10.3 – 13.2	0 – 1	0 – 1	1,225 – 1,526	23 – 29	19 – 34	32 – 35	41 – 43	24 – 89	25 – 33	536 – 708
Morocco	1	189	10.7	0	0	1,825	11	27	36	45	26	29	387
Mozambique	3	225 – 230	12.1 – 12.4	0 – 0	0 – 0	1,595 – 1,714	11 – 12	17 – 18	34 – 34	44 – 45	16 – 19	35 – 37	375 – 390
Netherlands	4	158 – 224	9.1 – 11.8	20 – 58	20 – 34	998 – 1,686	24 – 33	11 – 31	37 – 51	46 – 66	32 – 119	7 – 80	451 – 713
New Zealand	4	174 – 217	7.9 – 12	2 – 83	3 – 62	1,191 – 2,973	23 – 40	4 – 25	32 – 51	41 – 69	44 – 98	12 – 89	428 – 738
Nicaragua	1	276	11.4	0	0	1,491	21	12	30	51	60	78	504
Norway	2	137 – 270	9.5 – 10.3	49 – 71	36 – 42	898 – 1,758	24 – 51	9 – 14	31 – 58	59 – 62	37 – 185	6 – 93	435 – 852
Oman	2	223 – 246	8.6 – 13.1	0 – 22	0 – 15	1,849 – 1,929	15 – 18	12 – 13	33 – 36	44 – 68	19 – 33	38 – 90	390 – 417
Pakistan	2	210 – 232	9.8 – 11.7	0 – 5	0 – 7	1,706 – 1,786	12 – 13	15 – 23	34 – 34	44 – 58	27 – 32	32 – 74	364 – 402

Country	Number of locations simulated	Decision variables			Resulting variables								Objective
		Electrolyser rated power [MW]	HB & ASU rated power [MW]	Percentage of RE energy supplied by wind [%]	Percentage of RE rated power met by wind [%]	Supply energy profile Full Load Hours Equivalent	LCOE of energy supplied [$/MWh]	Percentage of RE energy curtailed [%]	Electrolyser load factor [%]	Haber-Bosch synthesis load factor [%]	Hydrogen storage size [t]	Electrolyser excess factor [%]	LCOA [$/t]
Papua New Guinea	1	293	11.7	0	0	1,625	23	10	29	51	49	84	514
Peru	1	226	10.2	0	0	1,845	11	18	34	54	37	64	362
Philippines	1	222	11.6	0	0	1,439	14	24	32	43	28	41	441
Poland	3	156 – 171	9.9 – 10.7	25 – 28	22 – 25	1,060 – 1,088	32 – 34	27 – 31	40 – 41	46 – 47	65 – 101	16 – 18	686 – 732
Portugal	6	152 – 270	7.2 – 13.9	0 – 27	0 – 16	1,449 – 1,835	12 – 22	12 – 37	30 – 44	41 – 67	24 – 108	26 – 77	403 – 557
Romania	7	123 – 221	8.3 – 12.9	0 – 8	0 – 15	1,198 – 1,422	16 – 26	21 – 49	33 – 39	41 – 43	19 – 167	9 – 30	538 – 719
Russian Federation	18	100 – 242	3.6 – 11.1	0 – 90	0 – 65	783 – 2,592	15 – 40	13 – 67	24 – 55	43 – 66	17 – 1069	6 – 148	369 – 1,687
Saudi Arabia	6	210 – 271	9 – 13.4	0 – 6	0 – 9	1,643 – 2,240	13 – 19	6 – 21	32 – 35	44 – 59	17 – 31	37 – 74	363 – 446
Senegal	2	224 – 241	9.8 – 10.1	0 – 2	0 – 2	1,677 – 2,000	10 – 12	14 – 20	33 – 33	54 – 57	28 – 42	69 – 75	339 – 382
Singapore	1	214	9.6	0	0	1,423	14	26	32	51	39	64	432
South Africa	8	133 – 268	8.3 – 14.3	0 – 77	0 – 44	1,468 – 2,712	11 – 18	9 – 27	31 – 64	41 – 71	16 – 43	12 – 63	345 – 413
Spain	16	147 – 233	8.7 – 12.4	0 – 22	0 – 14	1,201 – 2,045	12 – 22	10 – 40	32 – 38	37 – 70	19 – 138	9 – 97	353 – 597
Sri Lanka	1	239	9.4	18	16	1,665	15	11	34	64	31	88	368
Sweden	7	130 – 218	8.3 – 11.7	20 – 57	20 – 42	893 – 1,508	27 – 47	9 – 42	37 – 42	45 – 67	100 – 231	14 – 69	504 – 954
Switzerland	7	133 – 205	8.2 – 11.4	0 – 34	0 – 17	1,106 – 1,777	16 – 24	17 – 46	31 – 44	39 – 69	41 – 279	8 – 67	389 – 800
Thailand	2	206 – 218	9.3 – 11.3	0 – 0	0 – 0	1,695 – 1,727	12 – 12	22 – 24	33 – 35	46 – 54	31 – 46	42 – 62	388 – 401
Tunisia	2	148 – 185	9.8 – 10.7	0 – 1	0 – 1	1,676 – 1,726	12 – 12	29 – 41	36 – 37	40 – 44	26 – 33	11 – 27	413 – 454
Turkey	14	132 – 243	8.1 – 13.7	0 – 5	0 – 6	1,220 – 1,647	13 – 19	18 – 49	32 – 36	36 – 44	27 – 87	9 – 31	432 – 635
Ukraine	2	191 – 226	9.6 – 11.8	23 – 46	27 – 41	1,109 – 1,401	34 – 40	10 – 25	37 – 37	43 – 63	83 – 125	19 – 72	623 – 792
UK	16	138 – 235	8 – 11.7	13 – 88	14 – 56	848 – 2,818	19 – 39	4 – 32	35 – 58	44 – 66	28 – 190	5 – 83	364 – 855
USA	47	133 – 258	6.5 – 14.2	0 – 56	0 – 35	1,035 – 1,953	11 – 26	11 – 47	30 – 46	39 – 70	18 – 284	10 – 78	347 – 938
Venezuela	1	222	11.6	0	0	1,732	11	21	33	46	17	41	383
Zambia	1	204	9.5	0	0	1,463	13	25	34	52	50	58	423

Appendix F

The following table presents the results from the IAPMT for the production of islanded 'green' ammonia production in the 2019 scenario by a multinational corporation. The results are presented as a fraction of the LCOA.

Location	Country	Latitude	Longitude	Electrolyser OPEX [%]	Electrolyser CAPEX [%]	Hydrogen Storage CAPEX [%]	Hydrogen Storage OPEX [%]	Ammonia Synthesis OPEX [%]	Ammonia Synthesis CAPEX [%]	Operation & Maintenance [%]	Energy Curtailed OPEX [%]	Hydrogen Fuel Cell CAPEX [%]	Air Separation OPEX [%]	Air Separation CAPEX [%]	Water OPEX [%]
Arrecife Lanzarote	Spain	28.95	-13.6	46.5	23.1	3.1	0.7	2.9	6.7	8.7	4.4	0.7	0.5	2.3	0.5
Casablanca	Morocco	33.57	-7.67	37.5	22.5	3.4	0.5	2.3	9.9	9.7	9.0	1.0	0.4	3.4	0.4
Aswan	Egypt	23.97	32.78	48.3	21.5	2.2	0.7	3.0	7.1	8.2	5.0	0.7	0.5	2.4	0.4
Mersa Matruh	Egypt	31.33	27.22	51.7	16.1	1.5	0.3	3.2	8.7	7.3	6.3	0.9	0.5	3.0	0.4
El Kharga	Egypt	25.45	30.53	45.6	22.9	1.4	0.6	2.8	9.4	9.1	3.3	1.0	0.5	3.2	0.4
Tunis	Tunisia	36.83	10.23	37.8	21.1	2.5	0.5	2.3	9.6	9.0	12.2	1.0	0.4	3.3	0.4
Sidi Bouzid	Tunisia	35	9.48	36.4	21.8	6.7	0.5	2.2	9.5	10.2	7.8	1.0	0.4	3.2	0.4
El Arish	Egypt	31.12	33.75	46.3	21.0	1.7	0.6	2.8	9.0	8.6	5.2	0.9	0.5	3.1	0.4
El Natroon	Egypt	30.4	30.35	47.0	19.9	1.5	0.6	2.8	8.6	8.1	6.7	0.9	0.5	2.9	0.4
Funchal	Portugal	32.63	-16.9	42.6	20.2	4.0	0.6	2.6	8.3	8.7	8.6	0.9	0.4	2.8	0.4
Marion Island	South Africa	-46.88	37.87	48.5	18.4	5.3	0.2	3.0	9.9	9.1	0.1	1.0	0.5	3.4	0.6
Dakar	Senegal	14.73	-17.47	39.6	27.4	2.7	0.6	2.4	8.7	10.3	3.6	0.9	0.4	3.0	0.5
Gillot	France	-20.89	55.53	52.5	16.5	1.4	0.2	3.3	9.0	7.4	4.7	0.9	0.5	3.1	0.5
Garissa	Kenya	-0.47	39.63	39.9	26.4	3.6	0.5	2.5	8.8	10.3	3.3	0.9	0.4	3.0	0.5
Voi	Kenya	-3.4	38.57	39.5	25.5	1.9	0.5	2.4	10.1	10.1	4.6	1.1	0.4	3.5	0.5
Upington	South Africa	-28.43	21.27	40.2	23.4	1.5	0.5	2.4	10.2	9.5	6.9	1.1	0.4	3.5	0.5
Mombasa Airport	Kenya	-4.03	39.62	39.2	24.4	2.1	0.5	2.4	9.7	9.7	6.9	1.0	0.4	3.3	0.5
Beira	Mozambique	-19.83	34.85	40.9	24.4	1.5	0.5	2.5	10.0	9.7	5.3	1.0	0.4	3.4	0.4
Maun	Botswana	-19.98	23.42	40.9	22.9	1.3	0.5	2.5	9.8	9.2	7.7	1.0	0.4	3.3	0.4
Gough Island	UK	-40.35	9.88	52.3	15.5	5.0	0.2	3.3	7.3	7.5	4.7	0.8	0.5	2.5	0.4
Piura	Peru	-5.17	-80.6	40.2	26.0	3.5	0.6	2.5	8.6	10.1	3.9	0.9	0.4	2.9	0.5
Punta Arenas	Chile	-53	-70.85	46.0	17.2	7.1	0.2	2.9	8.7	8.9	4.2	0.9	0.5	3.0	0.4
Caracas Maiquetia	Venezuela	10.6	-66.98	40.3	24.8	1.6	0.5	2.4	9.8	9.8	5.5	1.0	0.4	3.3	0.4
Ushuaia Airport	Argentina	-54.8	-68.32	46.1	17.3	7.4	0.3	2.9	8.7	9.0	3.5	0.9	0.5	3.0	0.4
Petrolina	Brazil	-9.38	-40.5	40.8	23.3	3.9	0.6	2.5	7.8	9.3	7.4	0.8	0.4	2.7	0.4
Le Lamentin	France	14.6	-61	45.2	24.2	3.0	0.7	2.8	7.3	9.1	3.7	0.8	0.5	2.5	0.4

Location	Country	Latitude	Longitude	Electrolyser OPEX [%]	Electrolyser CAPEX [%]	Hydrogen Storage CAPEX [%]	Hydrogen Storage OPEX [%]	Ammonia Synthesis OPEX [%]	Ammonia Synthesis CAPEX [%]	Operation & Maintenance [%]	Energy Curtailed OPEX [%]	Hydrogen Fuel Cell CAPEX [%]	Air Separation OPEX [%]	Air Separation CAPEX [%]	Water OPEX [%]
Antofagasta	Chile	-23.43	-70.43	40.4	22.6	2.6	0.5	2.5	9.4	9.3	7.6	1.0	0.4	3.2	0.4
Raizet	France	16.27	-61.52	43.6	22.1	1.4	0.6	2.6	9.1	8.8	7.0	0.9	0.4	3.1	0.4
Brasilia	Brazil	-15.78	-47.93	42.2	22.3	4.2	0.6	2.6	7.4	9.0	7.6	0.8	0.4	2.5	0.4
Mendoza Airport	Argentina	-32.83	-68.78	40.6	21.0	2.1	0.5	2.5	9.2	8.7	10.5	1.0	0.4	3.1	0.4
Dodge City	USA	37.77	-99.97	49.9	16.5	1.9	0.2	3.1	9.0	7.5	6.8	0.9	0.5	3.1	0.5
Kahului	USA	20.9	-156.43	46.1	23.0	3.1	0.7	2.9	6.9	8.7	4.7	0.7	0.5	2.3	0.5
Lihue Kauai	USA	21.98	-159.35	49.8	15.6	2.3	0.2	3.1	8.4	7.2	8.6	0.9	0.5	2.9	0.5
Churchill	Canada	58.75	-94.07	51.5	15.9	3.5	0.2	3.2	8.4	7.6	4.8	0.9	0.5	2.9	0.4
Honolulu Oahu	USA	21.33	-157.92	47.3	21.4	1.8	0.6	2.9	7.1	8.1	6.7	0.7	0.5	2.4	0.4
New York	USA	40.65	-73.78	52.6	16.7	2.0	0.3	3.3	8.6	7.5	4.2	0.9	0.5	2.9	0.4
Inukjuak	Canada	58.45	-78.12	50.1	16.2	4.6	0.2	3.1	8.4	7.9	4.8	0.9	0.5	2.9	0.4
Tucson	USA	32.12	-110.93	39.9	23.1	1.8	0.5	2.4	10.2	9.5	7.1	1.1	0.4	3.5	0.4
Oklahoma City	USA	35.4	-97.6	50.7	16.6	1.8	0.3	3.2	8.7	7.4	6.5	0.9	0.5	3.0	0.4
Fort Worth	USA	32.83	-97.05	48.3	20.3	4.6	0.6	3.0	6.2	8.2	5.1	0.6	0.5	2.1	0.4
Kwajalein Island	Japan	8.73	167.73	45.0	18.7	2.0	0.2	2.8	10.5	8.6	6.4	1.1	0.5	3.6	0.6
Iwojima	Japan	24.78	141.31	46.6	19.2	1.8	0.2	2.9	10.5	8.7	4.5	1.1	0.5	3.6	0.5
Minamitorishima	Japan	24.3	153.97	47.3	16.4	1.2	0.2	3.0	9.2	7.4	10.4	1.0	0.5	3.1	0.5
Choshi	Japan	35.73	140.87	45.0	19.5	4.6	0.2	2.8	10.0	9.2	3.3	1.0	0.5	3.4	0.5
Nemuro	Japan	43.33	145.58	48.0	17.5	2.6	0.2	3.0	9.5	8.1	5.9	1.0	0.5	3.2	0.5
Naha	Japan	26.2	127.68	47.9	17.4	2.6	0.2	3.0	9.2	8.0	6.6	1.0	0.5	3.1	0.5
Ishigakijima	Japan	24.33	124.17	47.6	16.8	2.2	0.2	3.0	8.9	7.6	8.8	0.9	0.5	3.0	0.5
Omaezaki	Japan	34.6	138.22	48.4	16.8	2.6	0.2	3.0	9.1	7.8	7.0	0.9	0.5	3.1	0.4
Hachijojima	Japan	33.1	139.78	48.2	17.8	3.0	0.3	3.0	9.5	8.3	4.7	1.0	0.5	3.2	0.4
Tanegashima	Japan	30.73	131	49.4	16.5	2.0	0.2	3.1	9.1	7.6	7.2	0.9	0.5	3.1	0.4
Chiang Mai Airport	Thailand	18.78	98.98	40.3	23.9	4.7	0.6	2.5	7.9	9.6	6.3	0.8	0.4	2.7	0.4
Penang	Malaysia	5.3	100.27	39.9	26.1	2.0	0.6	2.4	10.0	10.2	3.6	1.0	0.4	3.4	0.4
Bangkok	Thailand	13.73	100.57	40.0	25.0	3.1	0.5	2.4	9.5	10.1	4.3	1.0	0.4	3.2	0.4
Kota Kinabalu	Malaysia	5.93	116.05	41.4	25.9	4.7	0.6	2.5	7.6	10.0	3.0	0.8	0.4	2.6	0.4
Kota Bahru	Malaysia	6.17	102.28	41.7	26.0	2.4	0.6	2.5	9.5	10.1	2.2	1.0	0.4	3.2	0.4

Location	Country	Latitude	Longitude	Electrolyser OPEX [%]	Electrolyser CAPEX [%]	Hydrogen Storage CAPEX [%]	Hydrogen Storage OPEX [%]	Ammonia Synthesis OPEX [%]	Ammonia Synthesis CAPEX [%]	Operation & Maintenance [%]	Energy Curtailed OPEX [%]	Hydrogen Fuel Cell CAPEX [%]	Air Separation OPEX [%]	Air Separation CAPEX [%]	Water OPEX [%]
Singapore Airport	Singapore	1.37	103.98	42.2	22.1	4.5	0.6	2.6	7.1	8.9	8.0	0.7	0.4	2.4	0.4
Science Garden	Philippines	14.63	121.01	41.8	23.6	2.5	0.6	2.5	9.1	9.5	5.6	0.9	0.4	3.1	0.4
Kuching	Malaysia	1.48	110.33	42.8	21.2	3.6	0.6	2.6	6.9	8.4	9.9	0.7	0.4	2.4	0.4
Bukit Kototabang	Indonesia	-0.2	100.32	43.0	21.6	2.5	0.6	2.6	8.3	8.7	8.2	0.9	0.4	2.8	0.3
New Delhi	India	28.58	77.2	34.0	25.9	1.4	0.4	2.1	11.3	10.5	8.5	1.2	0.3	3.8	0.5
Jodhpur	India	26.3	73.02	34.6	26.1	1.3	0.4	2.1	11.3	10.5	7.9	1.2	0.3	3.8	0.5
Vishakhapatnam	India	17.72	83.23	34.5	26.8	4.5	0.5	2.1	9.3	10.8	6.6	1.0	0.4	3.2	0.5
Ahmedabad	India	23.07	72.63	34.2	25.9	2.0	0.4	2.1	11.0	10.5	8.1	1.1	0.3	3.8	0.5
Thiruvananthapuram	India	8.48	76.95	34.9	26.5	2.1	0.4	2.1	10.7	10.6	7.0	1.1	0.4	3.6	0.5
Poona	India	18.53	73.85	34.9	25.2	2.0	0.4	2.1	10.7	10.3	8.8	1.1	0.4	3.6	0.5
Santacruz Bombay	India	19.12	72.85	34.3	28.3	3.1	0.5	2.1	11.2	11.5	3.2	1.2	0.3	3.8	0.5
Madras	India	13	80.18	35.8	26.6	3.1	0.5	2.2	10.5	10.8	4.8	1.1	0.4	3.6	0.5
Goa	India	15.48	73.82	35.7	25.6	2.1	0.5	2.2	10.4	10.3	7.7	1.1	0.4	3.5	0.5
Nagpur Sonegaon	India	21.1	79.05	36.4	25.7	2.0	0.5	2.2	10.8	10.4	6.4	1.1	0.4	3.7	0.5
Masira	Oman	20.67	58.9	47.1	14.7	2.1	0.2	2.9	8.3	6.9	13.0	0.9	0.5	2.8	0.4
Sharura	Saudi Arabia	17.47	47.12	46.2	23.8	1.7	0.7	2.8	8.0	8.9	3.4	0.8	0.5	2.7	0.4
Wadi Al Dawaser	Saudi Arabia	20.5	45.2	47.4	22.9	1.9	0.7	2.9	7.5	8.6	3.8	0.8	0.5	2.6	0.4
Jeddah	Saudi Arabia	21.68	39.15	47.1	21.7	2.2	0.7	2.9	7.2	8.3	5.8	0.7	0.5	2.4	0.4
Madinah	Saudi Arabia	24.55	39.7	47.7	20.4	3.6	0.7	2.9	6.8	8.1	5.9	0.7	0.5	2.3	0.4
Al Ahsa	Saudi Arabia	25.28	49.48	46.2	20.3	0.8	0.6	2.8	8.5	8.0	8.1	0.9	0.5	2.9	0.4
Silifke	Turkey	36.38	33.93	41.8	21.5	3.4	0.6	2.5	9.1	9.2	7.0	0.9	0.4	3.1	0.4
Buraimi	Oman	24.23	55.78	46.9	21.3	1.3	0.6	2.8	8.8	8.5	5.0	0.9	0.5	3.0	0.4
Mugla	Turkey	37.2	28.35	40.5	19.9	3.2	0.6	2.4	9.0	8.7	10.9	0.9	0.4	3.1	0.4
Taif	Saudi Arabia	21.48	40.55	51.5	19.6	2.8	0.8	3.2	5.7	7.4	5.5	0.6	0.5	2.0	0.4
Sonnblick	Austria	47.05	12.95	48.9	18.1	4.0	0.1	3.1	9.9	8.7	1.7	1.0	0.5	3.4	0.6
List	Denmark	55.02	8.42	44.5	18.1	9.6	0.2	2.8	9.3	9.9	0.3	1.0	0.5	3.2	0.6
Malin Head	Ireland	55.37	-7.33	47.2	18.5	5.4	0.2	3.0	9.9	9.2	1.1	1.0	0.5	3.4	0.6
Dickson Island	Russian Federation	73.5	80.23	38.8	20.6	6.5	0.2	2.4	10.7	10.2	4.8	1.1	0.4	3.6	0.6

Location	Country	Latitude	Longitude	Electrolyser OPEX [%]	Electrolyser CAPEX [%]	Hydrogen Storage CAPEX [%]	Hydrogen Storage OPEX [%]	Ammonia Synthesis OPEX [%]	Ammonia Synthesis CAPEX [%]	Operation & Maintenance [%]	Energy Curtailed OPEX [%]	Hydrogen Fuel Cell CAPEX [%]	Air Separation OPEX [%]	Air Separation CAPEX [%]	Water OPEX [%]
Lerwick	UK	60.13	-1.18	46.2	17.0	5.6	0.2	2.9	9.2	8.6	5.3	1.0	0.5	3.1	0.5
Skagen Fyr	Denmark	57.73	10.63	49.3	17.8	4.7	0.2	3.1	9.5	8.7	1.6	1.0	0.5	3.2	0.5
Aberporth	UK	52.13	-4.57	50.7	16.3	3.4	0.2	3.2	8.9	7.8	4.6	0.9	0.5	3.0	0.5
Guetsch	Switzerland	46.65	8.62	52.3	15.4	2.5	0.2	3.3	8.4	7.2	5.9	0.9	0.5	2.9	0.5
Valley	UK	53.25	-4.53	51.0	16.9	3.8	0.2	3.2	9.0	8.1	2.9	0.9	0.5	3.0	0.5
Belmullet	Ireland	54.23	-10	50.4	17.5	4.5	0.2	3.2	9.1	8.4	1.7	0.9	0.5	3.1	0.5
Cape Grim	Australia	-40.66	144.68	49.5	18.2	4.4	0.1	3.1	10.0	8.9	0.2	1.0	0.5	3.4	0.7
Willis Island	Australia	-16.3	149.98	49.4	16.8	3.7	0.1	3.1	9.5	8.2	3.8	1.0	0.5	3.2	0.6
Glenmore	Australia	-33.69	115.02	49.9	17.2	6.7	0.3	3.1	7.7	8.4	2.2	0.8	0.5	2.6	0.5
Wellington	New Zealand	-41.32	174.77	49.1	17.6	6.0	0.2	3.1	9.2	8.9	0.9	1.0	0.5	3.1	0.5
Carnarvon Airport	Australia	-24.88	113.67	53.0	14.2	2.9	0.2	3.3	7.8	6.8	7.4	0.8	0.6	2.6	0.4
Noumea	France	-22.28	166.45	51.2	20.1	3.1	0.6	3.2	6.2	7.8	4.0	0.6	0.5	2.1	0.4
Koumac	France	-20.57	164.28	44.0	20.9	1.5	0.6	2.7	8.7	8.4	8.5	0.9	0.4	3.0	0.4
Cook	Australia	-30.62	130.4	55.0	14.8	3.3	0.3	3.4	7.8	7.1	3.9	0.8	0.6	2.7	0.4
Ils Des Pins Moue	France	-22.6	167.45	52.3	19.1	2.4	0.7	3.3	5.8	7.2	5.8	0.6	0.5	2.0	0.4
Geraldton Airport	Australia	-28.78	114.7	55.7	13.4	2.6	0.3	3.5	7.2	6.3	6.9	0.7	0.6	2.4	0.4

Appendix G

The following table presents the results from the IAPMT for the production of islanded 'green' ammonia production in the 2030 scenario by a multinational corporation. The results are presented as a fraction of the LCOA.

Location	Country	Latitude	Longitude	Electrolyser OPEX [%]	Electrolyser CAPEX [%]	Hydrogen Storage CAPEX [%]	Hydrogen Storage OPEX [%]	Ammonia Synthesis OPEX [%]	Ammonia Synthesis CAPEX [%]	Operation & Maintenance [%]	Energy Curtailed OPEX [%]	Hydrogen Fuel Cell CAPEX [%]	Air Separation OPEX [%]	Air Separation CAPEX [%]	Water OPEX [%]
Arrecife Lanzarote	Spain	28.95	-13.6	35.1	21.6	5.5	0.5	2.2	13.0	11.0	4.0	1.3	0.4	4.4	0.9
Aswan	Egypt	23.97	32.78	34.4	20.5	3.1	0.5	2.1	14.7	10.7	6.2	1.5	0.4	5.0	0.9
Casablanca	Morocco	33.57	-7.67	24.1	20.2	4.4	0.3	1.5	18.5	12.2	9.7	1.9	0.2	6.3	0.9
El Kharga	Egypt	25.45	30.53	30.2	21.3	2.6	0.4	1.8	18.2	12.0	4.2	1.9	0.3	6.2	0.8
Mersa Matruh	Egypt	31.33	27.22	38.9	16.8	3.8	0.5	2.4	12.3	9.2	9.6	1.3	0.4	4.2	0.8
Tunis	Tunisia	36.83	10.23	24.3	19.0	5.4	0.3	1.5	17.7	11.9	10.9	1.8	0.2	6.0	0.8
El Arish	Egypt	31.12	33.75	30.8	20.7	3.2	0.4	1.9	18.1	11.9	3.9	1.9	0.3	6.2	0.8
El Natroon	Egypt	30.4	30.35	31.7	18.5	2.7	0.4	1.9	16.6	10.8	9.0	1.7	0.3	5.6	0.8
Sidi Bouzid	Tunisia	35	9.48	22.5	16.7	4.7	0.3	1.4	17.8	11.2	16.6	1.9	0.2	6.1	0.7
Funchal	Portugal	32.63	-16.9	27.7	19.9	8.1	0.4	1.7	16.6	12.4	4.9	1.7	0.3	5.6	0.7
Dakar	Senegal	14.73	-17.47	26.4	24.6	4.5	0.4	1.6	16.6	12.7	4.5	1.7	0.3	5.7	1.0
Marion Island	South Africa	-46.88	37.87	44.0	12.4	6.5	0.1	2.8	13.1	9.0	4.9	1.4	0.5	4.5	0.9
Garissa	Kenya	-0.47	39.63	26.5	22.2	4.2	0.3	1.6	16.8	12.1	7.6	1.7	0.3	5.7	0.9
Voi	Kenya	-3.4	38.57	25.0	22.0	2.8	0.3	1.5	18.6	12.3	8.1	1.9	0.3	6.3	0.9
Gillot	France	-20.89	55.53	40.4	18.7	4.0	0.5	2.5	12.3	9.7	5.1	1.3	0.4	4.2	0.9
Upington	South Africa	-28.43	21.27	25.9	21.1	2.6	0.3	1.6	19.1	12.2	7.5	2.0	0.3	6.5	0.9
Mombasa Airport	Kenya	-4.03	39.62	25.1	23.0	4.0	0.3	1.5	18.7	12.9	5.0	1.9	0.3	6.4	0.9
Beira	Mozambique	-19.83	34.85	26.4	21.9	2.6	0.3	1.6	19.0	12.4	6.2	2.0	0.3	6.5	0.9
Maun	Botswana	-19.98	23.42	26.6	21.4	2.6	0.3	1.6	18.8	12.2	7.0	1.9	0.3	6.4	0.9
Bloemfontein	South Africa	-29.1	26.3	25.8	22.9	3.7	0.3	1.6	19.6	13.1	3.2	2.0	0.3	6.7	0.8
Piura	Peru	-5.17	-80.6	25.9	22.8	5.9	0.4	1.6	16.5	12.6	5.9	1.7	0.3	5.6	0.9
Caracas Maiquetia	Venezuela	10.6	-66.98	26.2	21.9	2.8	0.3	1.6	18.4	12.2	7.3	1.9	0.3	6.3	0.9
Le Lamentin	France	14.6	-61	30.7	20.5	4.9	0.4	1.9	14.3	11.0	8.8	1.5	0.3	4.9	0.8
Petrolina	Brazil	-9.38	-40.5	25.8	20.5	3.4	0.3	1.6	17.5	11.7	10.2	1.8	0.3	6.0	0.8
Antofagasta	Chile	-23.43	-70.43	25.8	19.6	4.6	0.3	1.6	17.3	11.7	10.3	1.8	0.3	5.9	0.8
Raizet	France	16.27	-61.52	30.6	19.7	6.3	0.4	1.9	14.0	11.1	8.7	1.5	0.3	4.8	0.8
Mendoza Airport	Argentina	-32.83	-68.78	26.6	20.9	4.2	0.4	1.6	18.4	12.4	6.3	1.9	0.3	6.3	0.8
Brasilia	Brazil	-15.78	-47.93	27.8	22.0	8.4	0.4	1.7	14.7	12.4	5.0	1.5	0.3	5.0	0.8

Location	Country	Latitude	Longitude	Electrolyser OPEX [%]	Electrolyser CAPEX [%]	Hydrogen Storage CAPEX [%]	Hydrogen Storage OPEX [%]	Ammonia Synthesis OPEX [%]	Ammonia Synthesis CAPEX [%]	Operation & Maintenance [%]	Energy Curtailed OPEX [%]	Hydrogen Fuel Cell CAPEX [%]	Air Separation OPEX [%]	Air Separation CAPEX [%]	Water OPEX [%]
Cayenne-Rochea	France	4.83	-52.37	27.6	19.7	3.5	0.3	1.7	16.7	11.3	10.6	1.7	0.3	5.7	0.8
Arica-Chacalluta	Chile	-18.33	-70.33	26.7	21.5	5.0	0.4	1.6	18.0	12.6	5.1	1.9	0.3	6.1	0.8
Kahului	USA	20.9	-156.43	34.0	19.8	4.1	0.5	2.1	13.2	10.3	8.9	1.4	0.4	4.5	0.9
Lihue Kauai	USA	21.98	-159.35	37.3	18.8	3.7	0.4	2.3	13.1	9.9	7.4	1.4	0.4	4.5	0.9
Dodge City	USA	37.77	-99.97	34.4	18.5	4.9	0.4	2.2	13.5	10.3	8.7	1.4	0.4	4.6	0.9
Tucson	USA	32.12	-110.93	25.8	20.6	3.0	0.3	1.6	18.8	12.1	8.3	2.0	0.3	6.4	0.9
Honolulu Oahu	USA	21.33	-157.92	30.2	20.6	4.4	0.4	1.9	15.0	11.2	8.6	1.6	0.3	5.1	0.9
Las Vegas	USA	36.08	-115.17	25.6	19.8	3.7	0.3	1.6	18.3	11.9	9.5	1.9	0.3	6.2	0.8
Albuquerque	USA	35.05	-106.62	26.2	20.1	3.7	0.3	1.6	18.5	12.1	8.2	1.9	0.3	6.3	0.8
Fort Worth	USA	32.83	-97.05	34.1	17.1	5.4	0.4	2.1	12.3	9.7	12.2	1.3	0.4	4.2	0.8
Corpus Christi Airport	USA	27.77	-97.5	36.5	17.2	3.9	0.4	2.3	12.4	9.3	11.2	1.3	0.4	4.2	0.8
Hilo	USA	19.72	-155.07	28.3	20.2	5.7	0.4	1.7	14.7	11.3	10.2	1.5	0.3	5.0	0.8
Kwajalein Island	Japan	8.73	167.73	35.3	21.1	3.6	0.4	2.2	14.9	11.1	3.6	1.5	0.4	5.1	1.0
Minamitorishima	Japan	24.3	153.97	35.7	20.1	4.9	0.4	2.2	13.4	10.6	5.2	1.4	0.4	4.6	1.0
Iwojima	Japan	24.78	141.31	35.1	19.7	4.7	0.4	2.2	13.8	10.6	6.1	1.4	0.4	4.7	0.9
Choshi	Japan	35.73	140.87	35.2	19.4	5.7	0.4	2.2	13.5	10.7	5.6	1.4	0.4	4.6	0.9
Omaezaki	Japan	34.6	138.22	36.1	18.9	4.2	0.4	2.3	13.3	10.1	7.5	1.4	0.4	4.5	0.9
Nemuro	Japan	43.33	145.58	38.9	14.7	2.9	0.2	2.4	16.1	9.7	6.7	1.7	0.4	5.5	0.8
Agana Guam Mariana	Japan	13.48	144.8	36.1	19.5	4.2	0.5	2.2	12.7	10.1	7.8	1.3	0.4	4.3	0.8
Naha	Japan	26.2	127.68	36.1	19.6	4.2	0.4	2.3	13.9	10.5	5.7	1.4	0.4	4.7	0.8
Ishigakijima	Japan	24.33	124.17	34.2	18.3	4.4	0.4	2.1	13.0	9.9	10.6	1.3	0.4	4.4	0.8
Tanegashima	Japan	30.73	131	38.2	18.2	4.7	0.5	2.4	12.4	9.8	7.2	1.3	0.4	4.2	0.8
Chiang Mai Airport	Thailand	18.78	98.98	26.0	20.8	7.5	0.4	1.6	15.2	12.0	8.6	1.6	0.3	5.2	0.8
Penang	Malaysia	5.3	100.27	26.1	21.7	3.3	0.3	1.6	18.1	12.2	7.5	1.9	0.3	6.2	0.8
Bangkok	Thailand	13.73	100.57	25.9	21.0	4.8	0.3	1.6	17.5	12.2	7.9	1.8	0.3	6.0	0.8
Kota Kinabalu	Malaysia	5.93	116.05	27.6	20.4	3.2	0.3	1.7	17.1	11.5	9.5	1.8	0.3	5.8	0.8
Kota Bahru	Malaysia	6.17	102.28	27.9	21.6	3.4	0.4	1.7	17.8	12.1	6.1	1.9	0.3	6.1	0.8
Singapore Airport	Singapore	1.37	103.98	28.5	20.0	5.8	0.4	1.7	14.4	11.2	10.5	1.5	0.3	4.9	0.8
Science Garden	Philippines	14.63	121.01	27.7	20.0	4.0	0.4	1.7	16.8	11.5	9.4	1.7	0.3	5.7	0.7

Location	Country	Latitude	Longitude	Electrolyser OPEX [%]	Electrolyser CAPEX [%]	Hydrogen Storage CAPEX [%]	Hydrogen Storage OPEX [%]	Ammonia Synthesis OPEX [%]	Ammonia Synthesis CAPEX [%]	Operation & Maintenance [%]	Energy Curtailed OPEX [%]	Hydrogen Fuel Cell CAPEX [%]	Air Separation OPEX [%]	Air Separation CAPEX [%]	Water OPEX [%]
Kuching	Malaysia	1.48	110.33	28.9	21.6	6.8	0.4	1.8	14.7	11.9	6.3	1.5	0.3	5.0	0.7
Bukit Kototabang	Indonesia	-0.2	100.32	29.0	19.5	4.1	0.4	1.8	16.2	11.2	9.7	1.7	0.3	5.5	0.7
Jodhpur	India	26.3	73.02	21.2	21.8	2.2	0.2	1.3	19.9	12.6	10.7	2.1	0.2	6.8	1.0
New Delhi	India	28.58	77.2	21.1	22.8	2.3	0.3	1.3	20.7	13.1	8.1	2.2	0.2	7.1	1.0
Ahmedabad	India	23.07	72.63	21.2	22.7	3.2	0.3	1.3	20.3	13.2	7.8	2.1	0.2	6.9	0.9
Vishakhapatnam	India	17.72	83.23	21.4	23.2	7.1	0.3	1.3	17.4	13.3	7.2	1.8	0.2	5.9	0.9
Poona	India	18.53	73.85	21.8	22.9	3.7	0.3	1.3	19.9	13.2	6.9	2.1	0.2	6.8	0.9
Thiruvananthapuram	India	8.48	76.95	21.7	22.6	3.6	0.3	1.3	19.3	12.9	8.5	2.0	0.2	6.6	0.9
Santacruz Bombay	India	19.12	72.85	25.0	22.3	6.2	0.3	1.5	16.3	12.5	7.4	1.7	0.3	5.6	0.9
Madras	India	13	80.18	22.6	22.8	4.4	0.3	1.4	19.4	13.2	6.4	2.0	0.2	6.6	0.9
Goa	India	15.48	73.82	22.5	24.0	3.8	0.3	1.4	19.8	13.5	4.8	2.1	0.2	6.7	0.9
Nagpur Sonegaon	India	21.1	79.05	22.9	22.0	3.4	0.3	1.4	19.4	12.7	8.1	2.0	0.2	6.6	0.9
Sharura	Saudi Arabia	17.47	47.12	31.0	23.9	3.6	0.4	1.9	16.3	12.2	2.3	1.7	0.3	5.5	0.9
Wadi Al Dawaser	Saudi Arabia	20.5	45.2	32.1	21.8	2.9	0.4	2.0	15.8	11.3	5.5	1.6	0.3	5.4	0.9
Jeddah	Saudi Arabia	21.68	39.15	29.9	20.6	2.6	0.4	1.8	17.8	11.7	6.2	1.8	0.3	6.1	0.8
Masira	Oman	20.67	58.9	38.7	19.3	4.6	0.6	2.4	12.0	9.9	5.9	1.2	0.4	4.1	0.8
Madinah	Saudi Arabia	24.55	39.7	30.8	21.2	2.4	0.4	1.9	18.3	11.9	4.0	1.9	0.3	6.2	0.8
Al Ahsa	Saudi Arabia	25.28	49.48	35.3	19.7	3.5	0.5	2.2	13.7	10.3	7.5	1.4	0.4	4.7	0.8
Buraimi	Oman	24.23	55.78	31.6	20.5	2.5	0.4	1.9	17.5	11.5	5.2	1.8	0.3	6.0	0.8
Silifke	Turkey	36.38	33.93	27.6	19.3	4.7	0.4	1.7	17.4	11.7	8.5	1.8	0.3	5.9	0.8
Gaziantep	Turkey	37.08	37.37	27.3	18.5	5.1	0.4	1.7	17.0	11.5	10.0	1.8	0.3	5.8	0.8
Mugla	Turkey	37.2	28.35	26.5	19.9	5.8	0.4	1.6	18.2	12.4	6.2	1.9	0.3	6.2	0.7
Sonnblick	Austria	47.05	12.95	43.2	13.6	3.7	0.1	2.7	15.5	9.4	3.5	1.6	0.5	5.3	1.0
Malin Head	Ireland	55.37	-7.33	44.1	11.9	4.5	0.1	2.8	13.5	8.5	7.3	1.4	0.5	4.6	0.9
List	Denmark	55.02	8.42	39.1	13.4	12.0	0.2	2.4	13.4	10.7	1.7	1.4	0.4	4.6	0.9

Location	Country	Latitude	Longitude	Electrolyser OPEX [%]	Electrolyser CAPEX [%]	Hydrogen Storage CAPEX [%]	Hydrogen Storage OPEX [%]	Ammonia Synthesis OPEX [%]	Ammonia Synthesis CAPEX [%]	Operation & Maintenance [%]	Energy Curtailed OPEX [%]	Hydrogen Fuel Cell CAPEX [%]	Air Separation OPEX [%]	Air Separation CAPEX [%]	Water OPEX [%]
Lerwick	UK	60.13	-1.18	44.2	13.3	5.5	0.1	2.8	14.7	9.5	2.1	1.5	0.5	5.0	0.9
Dickson Island	Russian Federation	73.5	80.23	35.7	13.3	6.8	0.1	2.2	14.9	10.0	9.1	1.5	0.4	5.1	0.9
Skagen Fyr	Denmark	57.73	10.63	44.4	12.6	5.2	0.1	2.8	13.9	9.0	4.4	1.4	0.5	4.7	0.8
Aberporth	UK	52.13	-4.57	45.4	12.1	4.4	0.1	2.9	13.6	8.6	5.5	1.4	0.5	4.6	0.8
Faro	Portugal	37.02	-7.97	26.3	19.7	3.9	0.3	1.6	18.2	11.9	9.0	1.9	0.3	6.2	0.8
Guetsch	Switzerland	46.65	8.62	39.2	15.8	6.0	0.4	2.5	11.9	9.3	8.4	1.2	0.4	4.1	0.8
Valley	UK	53.25	-4.53	44.7	11.7	4.7	0.1	2.8	13.0	8.4	7.6	1.3	0.5	4.4	0.8
Cape Grim	Australia	-40.66	144.68	44.9	13.2	5.1	0.1	2.8	15.0	9.5	1.2	1.6	0.5	5.1	1.0
Willis Island	Australia	-16.3	149.98	46.5	13.1	2.3	0.1	2.9	15.1	8.8	3.0	1.6	0.5	5.1	1.0
Noumea	France	-22.28	166.45	39.7	18.4	5.3	0.5	2.5	11.9	9.8	5.4	1.2	0.4	4.1	0.8
Koumac	France	-20.57	164.28	29.5	20.7	3.0	0.4	1.8	17.7	11.8	6.2	1.8	0.3	6.0	0.8
Glenmore	Australia	-33.69	115.02	46.6	12.0	4.2	0.1	2.9	12.9	8.3	5.8	1.3	0.5	4.4	0.8
Wellington	New Zealand	-41.32	174.77	46.3	12.4	7.0	0.2	2.9	13.1	9.1	2.0	1.4	0.5	4.5	0.7
Carnarvon Airport	Australia	-24.88	113.67	42.0	16.3	3.8	0.6	2.6	10.7	8.5	9.6	1.1	0.4	3.6	0.8
Ouanaham	France	-20.77	167.23	34.3	18.6	6.9	0.5	2.1	12.3	10.4	8.4	1.3	0.4	4.2	0.7
Tennant Creek Airport	Australia	-19.63	134.18	40.1	18.6	3.2	0.5	2.5	13.2	9.8	5.1	1.4	0.4	4.5	0.7
Ils Des Pins Moue	France	-22.6	167.45	39.0	17.9	4.5	0.5	2.4	12.0	9.5	7.6	1.3	0.4	4.1	0.7

Appendix H

The following table presents the results from the IAPMT for the production of islanded 'green' ammonia production in the 2019 scenario by a multinational corporation. The results present the VRE mix and optimal plant design and operation.

Information about location					Decision variables			Resulting variables								Objective
Location	Country	Geographic region	Latitude	Longitude	Electrolyser rated power [MW]	HB & ASU rated power [MW]	Percentage of RE energy supplied by wind [%]	Percentage of RE rated power met by wind [%]	Supply energy profile Full Load Hours Equivalent	LCOE of energy supplied [$/MWh]	Supply energy curtailed [%]	Electrolyser load factor [%]	Haber-Bosch synthesis load factor [%]	Hydrogen storage size [t]	Electrolyser excess factor [%]	LCOA [$/t]
Arrecife Lanzarote	Spain	Northern Africa	28.95	-13.60	243	8.9	22	14	2,046	38	8	35	70	41	102	687
Casablanca	Morocco	Northern Africa	33.57	-7.67	227	12.6	0	0	1,825	32	18	34	43	44	32	757
Aswan	Egypt	Northern Africa	23.97	32.78	247	10.2	9	13	2,080	43	9	34	60	32	78	759
Mersa Matruh	Egypt	Northern Africa	31.33	27.22	188	12.9	53	49	1,958	47	10	44	47	22	7	779
El Kharga	Egypt	Northern Africa	25.45	30.53	279	14.4	0	0	2,132	41	6	32	43	22	42	796
Tunis	Tunisia	Northern Africa	36.83	10.23	212	12.1	1	1	1,726	35	23	34	42	32	28	798
Sidi Bouzid	Tunisia	Northern Africa	35.00	9.48	252	13.8	0	0	1,676	35	17	31	40	98	34	852
El Arish	Egypt	Northern Africa	31.12	33.75	272	14.7	0	0	1,910	46	10	31	41	27	36	877
El Natroon	Egypt	Northern Africa	30.40	30.35	257	14.1	0	1	1,834	48	12	32	42	24	35	896
Funchal	Portugal	Northern Africa	32.63	-16.90	260	13.5	0	0	1,482	46	16	30	41	66	41	940
Marion Island	South Africa	S-Saharan Africa	-46.88	37.87	170	11.6	99	96	4,626	32	0	55	59	62	8	552
Dakar	Senegal	S-Saharan Africa	14.73	-17.47	275	11.0	2	2	2,000	30	8	31	56	34	84	661
Gillot	France	S-Saharan Africa	-20.89	55.53	170	11.8	69	51	2,498	41	8	50	53	18	6	668
Garissa	Kenya	S-Saharan Africa	-0.47	39.63	281	11.8	1	2	1,885	32	7	31	53	48	75	697
Voi	Kenya	S-Saharan Africa	-3.40	38.57	267	13.4	1	1	1,872	32	10	32	45	25	46	706
Upington	South Africa	S-Saharan Africa	-28.43	21.27	239	13.2	0	0	1,771	33	14	34	43	20	33	729
Mombasa Airport	Kenya	S-Saharan Africa	-4.03	39.62	250	12.5	0	0	1,802	33	14	32	45	28	47	732
Beira	Mozambique	S-Saharan Africa	-19.83	34.85	262	13.5	0	0	1,714	34	11	32	44	20	42	739
Maun	Botswana	S-Saharan Africa	-19.98	23.42	238	12.8	0	0	1,692	35	15	33	44	17	37	748
Gough Island	UK	S-Saharan Africa	-40.35	9.88	181	10.7	79	58	2,322	46	8	47	59	74	24	753
Piura	Peru	Latin America	-5.17	-80.60	276	11.5	0	0	1,845	33	8	31	53	47	76	709
Punta Arenas	Chile	Latin America	-53.00	-70.85	191	12.2	98	94	3,328	39	8	45	51	99	15	720
Caracas Maiquetia	Venezuela	Latin America	10.60	-66.98	273	13.6	0	0	1,732	35	11	30	43	22	47	758
Ushuaia Airport	Argentina	Latin America	-54.80	-68.32	204	13.0	98	93	3,136	41	7	42	49	111	16	757
Petrolina	Brazil	Latin America	-9.38	-40.50	252	10.7	1	2	1,711	36	14	32	53	54	73	766

Information about location					Decision variables			Resulting variables								Objective
Location	Country	Geographic region	Latitude	Longitude	Electrolyser rated power [MW]	HB & ASU rated power [MW]	Percentage of RE energy supplied by wind [%]	Percentage of RE rated power met by wind [%]	Supply energy profile Full Load Hours Equivalent	LCOE of energy supplied [$/MWh]	Supply energy curtailed [%]	Electrolyser load factor [%]	Haber-Bosch synthesis load factor [%]	Hydrogen storage size [t]	Electrolyser excess factor [%]	LCOA [$/t]
Le Lamentin	France	Latin America	14.60	-61.00	286	10.8	5	5	1,751	41	7	30	57	44	94	770
Antofagasta	Chile	Latin America	-23.43	-70.43	250	13.1	0	1	1,648	37	15	32	43	37	40	797
Raizet	France	Latin America	16.27	-61.52	257	13.3	0	0	1,662	41	13	32	43	20	42	819
Brasilia	Brazil	Latin America	-15.78	-47.93	257	10.7	0	0	1,517	40	14	31	53	61	77	821
Mendoza Airport	Argentina	Latin America	-32.83	-68.78	228	12.6	0	0	1,579	38	20	33	42	29	33	827
Dodge City	USA	N. America	37.77	-99.97	164	11.3	61	46	2,276	39	11	50	53	24	7	668
Kahului	USA	N. America	20.90	-156.43	233	8.8	26	18	2,000	36	9	36	70	40	94	669
Lihue Kauai	USA	N. America	21.98	-159.35	152	10.4	67	50	2,315	39	14	53	56	28	7	674
Churchill	Canada	N. America	58.75	-94.07	179	12.0	81	60	2,342	44	8	48	52	51	9	729
Honolulu Oahu	USA	N. America	21.33	-157.92	233	9.7	21	18	1,777	41	12	35	61	25	77	739
New York	USA	N. America	40.65	-73.78	194	12.6	53	40	1,854	46	7	45	50	30	14	746
Inukjuak	Canada	N. America	58.45	-78.12	186	12.2	84	65	2,416	44	8	46	51	67	11	747
Tucson	USA	N. America	32.12	-110.93	245	13.7	0	0	1,808	34	14	33	41	24	31	759
Oklahoma City	USA	N. America	35.40	-97.60	189	12.5	51	40	1,894	45	11	44	49	27	11	761
Fort Worth	USA	N. America	32.83	-97.05	235	9.1	28	25	1,778	43	9	36	67	67	90	764
Kwajalein Island	Japan	Eastern Asia	8.73	167.73	156	11.0	71	54	2,568	30	12	53	54	21	4	562
Iwojima	Japan	Eastern Asia	24.78	141.31	179	12.4	67	54	2,290	33	8	48	50	22	7	609
Minamitorishima	Japan	Eastern Asia	24.30	153.97	139	9.9	62	51	2,218	34	17	55	57	13	4	611
Choshi	Japan	Eastern Asia	35.73	140.87	192	12.4	74	56	2,317	33	6	46	51	58	13	628
Nemuro	Japan	Eastern Asia	43.33	145.58	178	12.2	67	50	1,973	38	10	47	50	34	7	676
Naha	Japan	Eastern Asia	26.20	127.68	175	11.7	69	54	2,004	38	11	47	52	33	10	676
Ishigakijima	Japan	Eastern Asia	24.33	124.17	169	11.3	64	53	1,933	39	15	47	51	28	9	704
Omaezaki	Japan	Eastern Asia	34.60	138.22	178	12.2	54	44	1,810	41	12	46	49	34	8	717
Hachijojima	Japan	Eastern Asia	33.10	139.78	197	13.2	65	46	1,820	41	8	43	47	42	9	723
Tanegashima	Japan	Eastern Asia	30.73	131.00	177	12.3	63	49	1,775	42	12	46	49	27	6	729
Chiang Mai Airport	Thailand	S-Eastern Asia	18.78	98.98	261	10.9	0	0	1,727	35	13	31	53	66	76	764

Information about location					Decision variables			Resulting variables								Objective
Location	Country	Geographic region	Latitude	Longitude	Electrolyser rated power [MW]	HB & ASU rated power [MW]	Percentage of RE energy supplied by wind [%]	Percentage of RE rated power met by wind [%]	Supply energy profile Full Load Hours Equivalent	LCOE of energy supplied [$/MWh]	Supply energy curtailed [%]	Electrolyser load factor [%]	Haber-Bosch synthesis load factor [%]	Hydrogen storage size [t]	Electrolyser excess factor [%]	LCOA [$/t]
Penang	Malaysia	S-Eastern Asia	5.30	100.27	308	14.9	0	0	1,709	36	8	28	41	30	52	788
Bangkok	Thailand	S-Eastern Asia	13.73	100.57	293	14.1	0	0	1,695	36	9	29	43	46	53	790
Kota Kinabalu	Malaysia	S-Eastern Asia	5.93	116.05	330	12.2	0	0	1,547	39	6	26	51	76	99	831
Kota Bahru	Malaysia	S-Eastern Asia	6.17	102.28	340	15.7	0	0	1,523	40	5	26	40	40	59	847
Singapore Airport	Singapore	S-Eastern Asia	1.37	103.98	273	11.1	0	0	1,423	43	15	29	51	70	81	886
Science Garden	Philippines	S-Eastern Asia	14.63	121.01	305	14.9	0	0	1,439	42	11	27	39	41	50	894
Kuching	Malaysia	S-Eastern Asia	1.48	110.33	262	10.8	0	0	1,356	45	18	29	51	57	79	917
Bukit Kototabang	Indonesia	S-Eastern Asia	-0.20	100.32	285	13.9	0	0	1,310	47	15	28	40	42	51	953
New Delhi	India	Southern Asia	28.58	77.20	218	12.0	0	0	1,957	25	19	35	45	15	33	638
Jodhpur	India	Southern Asia	26.30	73.02	223	12.2	0	0	1,933	25	18	35	45	14	34	636
Vishakhapatnam	India	Southern Asia	17.72	83.23	244	10.7	0	0	1,869	26	15	32	52	53	67	656
Ahmedabad	India	Southern Asia	23.07	72.63	227	12.2	0	0	1,892	26	18	34	44	22	36	657
Thiruvananthapuram	India	Southern Asia	8.48	76.95	242	12.3	0	0	1,828	26	16	33	45	24	44	665
Poona	India	Southern Asia	18.53	73.85	226	12.0	0	0	1,796	27	19	33	44	23	38	678
Santacruz Bombay	India	Southern Asia	19.12	72.85	294	14.7	0	0	1,790	27	8	29	41	41	47	693
Madras	India	Southern Asia	13.00	80.18	268	13.4	0	0	1,711	28	11	31	44	40	47	693
Goa	India	Southern Asia	15.48	73.82	240	12.3	0	0	1,726	28	17	32	45	25	43	689
Nagpur Sonegaon	India	Southern Asia	21.10	79.05	252	13.3	0	0	1,665	29	14	32	43	25	39	702
Masira	Oman	Western Asia	20.67	58.90	144	10.3	69	59	2,291	41	20	51	52	27	3	735
Sharura	Saudi Arabia	Western Asia	17.47	47.12	271	11.4	0	0	2,240	39	6	32	54	25	74	741
Wadi Al Dawaser	Saudi Arabia	Western Asia	20.50	45.20	265	11.0	4	8	2,140	41	7	33	57	28	77	751
Jeddah	Saudi Arabia	Western Asia	21.68	39.15	249	10.4	4	7	2,093	42	10	33	58	33	76	773
Madinah	Saudi Arabia	Western Asia	24.55	39.70	250	10.5	3	10	1,932	46	10	33	57	56	76	831
Al Ahsa	Saudi Arabia	Western Asia	25.28	49.48	243	12.9	0	0	1,954	45	14	33	44	13	38	856
Silifke	Turkey	Western Asia	36.38	33.93	262	14.1	0	0	1,639	41	14	31	40	53	37	867

Information about location					Decision variables			Resulting variables								Objective
Location	Country	Geographic region	Latitude	Longitude	Electrolyser rated power [MW]	HB & ASU rated power [MW]	Percentage of RE energy supplied by wind [%]	Percentage of RE rated power met by wind [%]	Supply energy profile Full Load Hours Equivalent	LCOE of energy supplied [$/MWh]	Supply energy curtailed [%]	Electrolyser load factor [%]	Haber-Bosch synthesis load factor [%]	Hydrogen storage size [t]	Electrolyser excess factor [%]	LCOA [$/t]
Buraimi	Oman	Western Asia	24.23	55.78	270	14.1	0	0	1,929	46	9	32	43	22	41	856
Mugla	Turkey	Western Asia	37.20	28.35	231	13.2	0	0	1,647	41	20	32	40	47	29	891
Taif	Saudi Arabia	Western Asia	21.48	40.55	270	10.0	10	14	1,615	55	9	31	61	49	98	919
Sonnblick	Austria	Europe	47.05	12.95	152	10.5	92	75	3,995	30	3	59	63	43	6	518
List	Denmark	Europe	55.02	8.42	159	10.3	98	91	4,712	28	1	58	66	107	14	528
Malin Head	Ireland	Europe	55.37	-7.33	168	11.4	98	90	4,210	31	2	54	58	63	9	554
Dickson Island	Russian Federation	Europe	73.50	80.23	175	11.5	98	93	3,389	26	10	48	53	70	12	565
Lerwick	UK	Europe	60.13	-1.18	151	10.3	98	91	4,102	32	10	56	60	63	8	584
Skagen Fyr	Denmark	Europe	57.73	10.63	180	12.1	92	76	3,332	36	3	50	54	60	9	622
Aberporth	UK	Europe	52.13	-4.57	164	11.2	89	69	2,973	39	8	52	56	43	7	649
Guetsch	Switzerland	Europe	46.65	8.62	158	10.9	70	49	2,439	42	9	53	57	33	7	675
Valley	UK	Europe	53.25	-4.53	182	12.2	88	69	2,834	41	5	49	53	52	10	677
Belmullet	Ireland	Europe	54.23	-10.00	197	13.0	91	74	2,880	41	3	46	51	64	12	694
Cape Grim	Australia	Oceania	-40.66	144.68	144	10.0	100	100	5,637	28	0	64	68	44	6	473
Willis Island	Australia	Oceania	-16.30	149.98	137	9.8	99	99	5,115	30	7	63	65	38	3	519
Glenmore	Australia	Oceania	-33.69	115.02	187	10.6	97	93	3,834	40	4	48	61	93	29	677
Wellington	New Zealand	Oceania	-41.32	174.77	195	12.8	100	100	4,011	39	2	47	52	84	12	673
Carnarvon Airport	Australia	Oceania	-24.88	113.67	161	11.2	79	66	2,955	48	11	51	54	42	6	768
Noumea	France	Oceania	-22.28	166.45	242	9.4	32	22	1,773	47	7	36	67	47	88	775
Koumac	France	Oceania	-20.57	164.28	246	13.0	0	0	1,580	43	15	32	43	23	39	853
Cook	Australia	Oceania	-30.62	130.40	199	13.3	78	67	2,554	55	6	44	48	57	10	858
Ils Des Pins Moue	France	Oceania	-22.60	167.45	250	9.6	26	18	1,499	54	9	33	64	41	93	871
Geraldton Airport	Australia	Oceania	-28.78	114.70	180	12.3	64	53	2,307	59	10	46	50	44	8	899

Abbreviation: S-Saharan Africa – Sub-Saharan Africa; Lat. America – Latin America and the Caribbean; N. America – Northern America; S-Eastern Asia – South-Eastern Asia.

Appendix I

The following table presents the results from the IAPMT for the production of islanded 'green' ammonia production in the 2030 scenario by a multinational corporation. The results present the VRE mix and optimal plant design and operation.

Information about location					Decision variables			Resulting variables								Objective
Location	Country	Geographic region	Latitude	Longitude	Electrolyser rated power [MW]	HB & ASU rated power [MW]	Percentage of RE energy supplied by wind [%]	Percentage of RE rated power met by wind [%]	Supply energy profile Full Load Hours Equivalent	LCOE of energy supplied [$/MWh]	Supply energy curtailed [%]	Electrolyser load factor [%]	Haber-Bosch synthesis load factor [%]	Hydrogen storage size [t]	Electrolyser excess factor [%]	LCOA [$/t]
Arrecife Lanzarote	Spain	Northern Africa	28.95	-13.60	233	8.7	22	14	2,045	15	10	36	70	37	97	353
Aswan	Egypt	Northern Africa	23.97	32.78	221	9.8	7	10	2,103	15	14	36	58	21	65	374
Casablanca	Morocco	Northern Africa	33.57	-7.67	189	10.7	0	0	1,825	11	27	36	45	26	29	387
El Kharga	Egypt	Northern Africa	25.45	30.53	246	13.1	0	0	2,132	14	12	34	45	19	38	394
Mersa Matruh	Egypt	Northern Africa	31.33	27.22	185	8.4	23	20	1,864	18	19	41	65	26	61	402
Tunis	Tunisia	Northern Africa	36.83	10.23	185	10.7	1	1	1,726	12	29	36	44	33	27	413
El Arish	Egypt	Northern Africa	31.12	33.75	265	14.4	0	0	1,910	15	11	32	41	25	35	433
El Natroon	Egypt	Northern Africa	30.40	30.35	211	11.8	0	0	1,840	16	21	35	44	20	32	436
Sidi Bouzid	Tunisia	Northern Africa	35.00	9.48	148	9.8	0	0	1,676	12	41	37	40	26	11	454
Funchal	Portugal	Northern Africa	32.63	-16.90	270	13.9	0	0	1,482	15	14	30	41	68	43	477
Dakar	Senegal	S-Saharan Africa	14.73	-17.47	241	10.1	2	2	2,000	10	14	33	57	28	75	339
Marion Island	South Africa	S-Saharan Africa	-46.88	37.87	133	8.7	77	44	2,712	18	9	64	71	43	12	345
Garissa	Kenya	S-Saharan Africa	-0.47	39.63	207	9.8	1	2	1,886	11	21	35	54	25	56	354
Voi	Kenya	S-Saharan Africa	-3.40	38.57	203	10.7	0	0	1,875	10	23	35	48	16	40	362
Gillot	France	S-Saharan Africa	-20.89	55.53	204	8.3	33	19	1,911	17	10	40	73	27	81	359
Upington	South Africa	S-Saharan Africa	-28.43	21.27	205	11.5	0	0	1,771	11	21	36	45	16	31	371
Mombasa Airport	Kenya	S-Saharan Africa	-4.03	39.62	242	12.2	0	0	1,802	11	16	33	46	26	46	375
Beira	Mozambique	S-Saharan Africa	-19.83	34.85	225	12.1	0	0	1,714	11	18	34	45	17	37	375
Maun	Botswana	S-Saharan Africa	-19.98	23.42	216	11.8	0	0	1,692	11	20	35	45	17	35	378
Bloemfontein	South Africa	S-Saharan Africa	-29.10	26.30	268	14.3	0	0	1,676	12	10	31	41	27	38	395
Piura	Peru	Latin America	-5.17	-80.60	226	10.2	0	0	1,845	11	18	34	54	37	64	362
Caracas Maiquetia	Venezuela	Latin America	10.60	-66.98	222	11.6	0	0	1,732	11	21	33	46	17	41	383
Le Lamentin	France	Latin America	14.60	-61.00	210	9.1	3	4	1,752	14	21	35	58	31	69	386
Petrolina	Brazil	Latin America	-9.38	-40.50	193	10.2	0	0	1,730	11	27	35	47	20	38	388
Antofagasta	Chile	Latin America	-23.43	-70.43	193	10.6	0	0	1,652	12	27	35	46	29	34	408

Information about location					Decision variables			Resulting variables								Objective
Location	Country	Geographic region	Latitude	Longitude	Electrolyser rated power [MW]	HB & ASU rated power [MW]	Percentage of RE energy supplied by wind [%]	Percentage of RE rated power met by wind [%]	Supply energy profile Full Load Hours Equivalent	LCOE of energy supplied [$/MWh]	Supply energy curtailed [%]	Electrolyser load factor [%]	Haber-Bosch synthesis load factor [%]	Hydrogen storage size [t]	Electrolyser excess factor [%]	LCOA [$/t]
Raizet	France	Latin America	16.27	-61.52	215	9.5	2	3	1,638	15	21	34	56	43	66	412
Mendoza Airport	Argentina	Latin America	-32.83	-68.78	236	12.9	0	0	1,579	13	18	33	42	30	34	415
Brasilia	Brazil	Latin America	-15.78	-47.93	257	10.7	0	0	1,517	13	14	31	53	61	77	410
Cayenne-Rochea	France	Latin America	4.83	-52.37	204	10.7	0	0	1,663	13	27	34	45	23	39	423
Arica-Chacalluta	Chile	Latin America	-18.33	-70.33	262	13.7	0	0	1,503	13	15	30	41	38	41	435
Kahului	USA	N. America	20.90	-156.43	188	7.7	21	14	1,953	14	19	40	70	24	78	347
Lihue Kauai	USA	N. America	21.98	-159.35	196	8.4	29	17	1,794	16	15	40	68	24	70	362
Dodge City	USA	N. America	37.77	-99.97	185	8.4	22	13	1,829	15	19	40	65	31	62	365
Tucson	USA	N. America	32.12	-110.93	202	11.5	0	0	1,808	11	23	36	44	18	30	385
Honolulu Oahu	USA	N. America	21.33	-157.92	207	9.4	7	6	1,741	13	21	35	57	28	62	378
Las Vegas	USA	N. America	36.08	-115.17	192	11.0	0	0	1,793	11	26	36	45	22	28	391
Albuquerque	USA	N. America	35.05	-106.62	208	11.9	0	0	1,711	12	23	35	43	24	28	402
Fort Worth	USA	N. America	32.83	-97.05	173	7.8	17	15	1,748	16	25	40	65	34	64	399
Corpus Christi Airport	USA	N. America	27.77	-97.50	180	8.1	22	15	1,616	17	22	40	65	25	64	398
Hilo	USA	N. America	19.72	-155.07	207	9.3	0	0	1,537	13	25	34	53	37	63	411
Kwajalein Island	Japan	Eastern Asia	8.73	167.73	212	9.3	37	22	1,997	13	9	40	67	23	68	324
Minamitorishima	Japan	Eastern Asia	24.30	153.97	199	8.2	30	21	1,917	14	12	41	72	31	78	331
Iwojima	Japan	Eastern Asia	24.78	141.31	195	8.4	31	21	1,902	14	14	41	69	29	70	339
Choshi	Japan	Eastern Asia	35.73	140.87	210	9.1	31	17	1,666	15	13	38	65	39	70	367
Omaezaki	Japan	Eastern Asia	34.60	138.22	200	8.8	24	18	1,614	16	16	39	65	28	68	373
Nemuro	Japan	Eastern Asia	43.33	145.58	165	11.2	51	33	1,744	17	14	49	52	20	8	382
Agana Guam Mariana	Japan	Eastern Asia	13.48	144.80	209	8.5	19	16	1,551	16	17	37	66	28	81	381
Naha	Japan	Eastern Asia	26.20	127.68	224	9.8	27	16	1,534	16	13	36	60	30	68	386
Ishigakijima	Japan	Eastern Asia	24.33	124.17	185	8.1	23	16	1,613	15	22	39	64	28	67	383

Information about location					Decision variables			Resulting variables								Objective
Location	Country	Geographic region	Latitude	Longitude	Electrolyser rated power [MW]	HB & ASU rated power [MW]	Percentage of RE energy supplied by wind [%]	Percentage of RE rated power met by wind [%]	Supply energy profile Full Load Hours Equivalent	LCOE of energy supplied [$/MWh]	Supply energy curtailed [%]	Electrolyser load factor [%]	Haber-Bosch synthesis load factor [%]	Hydrogen storage size [t]	Electrolyser excess factor [%]	LCOA [$/t]
Tanegashima	Japan	Eastern Asia	30.73	131.00	205	8.7	28	18	1,452	18	15	38	66	33	74	392
Chiang Mai Airport	Thailand	S-Eastern Asia	18.78	98.98	206	9.3	0	0	1,727	12	24	35	54	46	62	388
Penang	Malaysia	S-Eastern Asia	5.30	100.27	224	11.6	0	0	1,709	12	21	33	45	21	42	394
Bangkok	Thailand	S-Eastern Asia	13.73	100.57	218	11.3	0	0	1,695	12	22	33	46	31	42	401
Kota Kinabalu	Malaysia	S-Eastern Asia	5.93	116.05	211	10.9	0	0	1,547	13	24	34	46	20	42	411
Kota Bahru	Malaysia	S-Eastern Asia	6.17	102.28	247	12.6	0	0	1,523	13	17	31	43	24	44	414
Singapore Airport	Singapore	S-Eastern Asia	1.37	103.98	214	9.6	0	0	1,423	14	26	32	51	39	64	432
Science Garden	Philippines	S-Eastern Asia	14.63	121.01	222	11.6	0	0	1,439	14	24	32	43	28	41	441
Kuching	Malaysia	S-Eastern Asia	1.48	110.33	267	11.3	0	0	1,356	15	17	29	49	52	74	447
Bukit Kototabang	Indonesia	S-Eastern Asia	-0.20	100.32	229	11.8	0	0	1,310	15	24	31	43	30	43	464
Jodhpur	India	Southern Asia	26.30	73.02	168	9.5	0	0	1,933	8	32	38	47	11	30	340
New Delhi	India	Southern Asia	28.58	77.20	189	10.7	0	0	1,957	8	26	37	46	12	30	338
Ahmedabad	India	Southern Asia	23.07	72.63	195	10.9	0	0	1,892	8	26	36	45	17	32	349
Vishakhapatnam	India	Southern Asia	17.72	83.23	204	9.5	0	0	1,869	9	24	35	53	39	58	347
Poona	India	Southern Asia	18.53	73.85	209	11.3	0	0	1,796	9	23	35	45	21	36	357
Thiruvananthapuram	India	Southern Asia	8.48	76.95	193	10.3	0	0	1,828	9	27	35	47	19	38	351
Santacruz Bombay	India	Southern Asia	19.12	72.85	214	9.7	2	7	1,704	11	22	34	54	37	62	365
Madras	India	Southern Asia	13.00	80.18	216	11.4	0	0	1,711	9	21	34	46	26	39	362
Goa	India	Southern Asia	15.48	73.82	240	12.3	0	0	1,721	9	17	32	45	24	43	362
Nagpur Sonegaon	India	Southern Asia	21.10	79.05	201	11.0	0	0	1,665	10	25	35	45	20	35	366
Sharura	Saudi Arabia	Western Asia	17.47	47.12	271	11.4	0	0	2,240	13	6	32	54	25	74	363
Wadi Al Dawaser	Saudi Arabia	Western Asia	20.50	45.20	232	10.4	2	4	2,182	14	14	34	55	19	64	368
Jeddah	Saudi Arabia	Western Asia	21.68	39.15	224	12.0	0	0	2,170	13	16	35	46	17	37	390
Masira	Oman	Western Asia	20.67	58.90	223	8.6	22	15	1,849	18	12	36	68	33	90	390
Madinah	Saudi Arabia	Western Asia	24.55	39.70	250	13.4	0	0	2,065	14	11	33	44	17	37	399

Information about location					Decision variables			Resulting variables								Objective
Location	Country	Geographic region	Latitude	Longitude	Electrolyser rated power [MW]	HB & ASU rated power [MW]	Percentage of RE energy supplied by wind [%]	Percentage of RE rated power met by wind [%]	Supply energy profile Full Load Hours Equivalent	LCOE of energy supplied [$/MWh]	Supply energy curtailed [%]	Electrolyser load factor [%]	Haber-Bosch synthesis load factor [%]	Hydrogen storage size [t]	Electrolyser excess factor [%]	LCOA [$/t]
Al Ahsa	Saudi Arabia	Western Asia	25.28	49.48	227	9.8	3	8	1,845	17	17	34	57	25	70	412
Buraimi	Oman	Western Asia	24.23	55.78	246	13.1	0	0	1,929	15	13	33	44	19	38	417
Silifke	Turkey	Western Asia	36.38	33.93	214	12.0	0	0	1,639	14	22	34	43	33	31	432
Gaziantep	Turkey	Western Asia	37.08	37.37	200	11.5	0	0	1,631	14	26	35	43	35	29	438
Mugla	Turkey	Western Asia	37.20	28.35	243	13.7	0	0	1,647	13	18	32	39	44	30	449
Sonnblick	Austria	Europe	47.05	12.95	138	9.7	83	56	3,320	16	7	63	65	23	4	318
Malin Head	Ireland	Europe	55.37	-7.33	125	8.8	81	46	2,610	18	13	64	67	30	5	355
List	Denmark	Europe	55.02	8.42	155	9.6	86	56	3,316	16	4	58	68	86	18	352
Lerwick	UK	Europe	60.13	-1.18	158	10.8	88	56	2,818	19	4	56	60	41	7	364
Dickson Island	Russian Federation	Europe	73.50	80.23	136	9.4	90	65	2,592	16	19	55	58	44	6	369
Skagen Fyr	Denmark	Europe	57.73	10.63	148	10.1	73	42	2,330	20	8	58	62	38	7	376
Aberporth	UK	Europe	52.13	-4.57	143	10.0	69	37	2,096	21	10	58	61	33	5	385
Faro	Portugal	Europe	37.02	-7.97	200	11.4	0	0	1,835	12	24	36	44	24	28	403
Guetsch	Switzerland	Europe	46.65	8.62	174	8.2	34	17	1,777	18	17	44	69	41	57	389
Valley	UK	Europe	53.25	-4.53	138	9.5	65	37	2,028	21	14	58	62	35	7	400
Cape Grim	Australia	Oceania	-40.66	144.68	137	9.6	95	82	4,848	16	2	66	69	33	5	310
Willis Island	Australia	Oceania	-16.30	149.98	136	9.8	85	67	4,054	18	6	64	66	15	2	323
Noumea	France	Oceania	-22.28	166.45	221	8.9	27	18	1,734	19	11	37	67	40	83	400
Koumac	France	Oceania	-20.57	164.28	241	12.7	0	0	1,580	14	16	33	43	22	39	418
Glenmore	Australia	Oceania	-33.69	115.02	151	10.1	68	46	2,716	23	10	55	60	33	10	411
Wellington	New Zealand	Oceania	-41.32	174.77	174	11.4	83	62	2,973	23	4	51	57	61	12	428
Carnarvon Airport	Australia	Oceania	-24.88	113.67	193	7.9	21	12	2,081	21	17	39	71	28	80	425
Ouanaham	France	Oceania	-20.77	167.23	228	9.4	6	7	1,461	18	18	33	58	53	79	447
Tennant Creek Airport	Australia	Oceania	-19.63	134.18	247	10.8	4	4	1,909	21	11	34	55	26	68	440

Information about location					Decision variables			Resulting variables								Objective
Location	Country	Geographic region	Latitude	Longitude	Electrolyser rated power [MW]	HB & ASU rated power [MW]	Percentage of RE energy supplied by wind [%]	Percentage of RE rated power met by wind [%]	Supply energy profile Full Load Hours Equivalent	LCOE of energy supplied [$/MWh]	Supply energy curtailed [%]	Electrolyser load factor [%]	Haber-Bosch synthesis load factor [%]	Hydrogen storage size [t]	Electrolyser excess factor [%]	LCOA [$/t]
Ils Des Pins Moue	France	Oceania	-22.60	167.45	225	9.4	18	13	1,456	20	15	35	61	35	76	439

Abbreviation:S-Saharan Africa – Sub-Saharan Africa; Lat. America – Latin America and the Caribbean; N. America – Northern America; S-Eastern Asia – South-Eastern Asia.